



Precambrian Geology  
**Wicklow Area**

Ontario Geological Survey  
Report 288

2001





Precambrian Geology  
**Wicklow Area**

Ontario Geological Survey  
Report 288

F.W. Breaks and R.H. Thivierge

2001

All publications of the Ontario Geological Survey and the Ministry of Northern Development and Mines are available for viewing and purchase at the following locations:

**Mines and Minerals Information Centre (MMIC)**  
**Macdonald Block, Room M2-17**  
**900 Bay Street**  
**Toronto, Ontario M7A 1C3**  
**Telephone: 1-800-665-4480 (toll free inside Ontario)**  
**(416) 314-3800**  
**Fax: (416) 314-3797**

**Mines Library**  
**933 Ramsey Lake Road, Level A3**  
**Sudbury, Ontario P3E 6B5**  
**Telephone: (705) 670-5615**

Purchases may be made only through:

**Publication Sales**  
**933 Ramsey Lake Road, Level A3**  
**Sudbury, Ontario P3E 6B5**  
**Telephone: (705) 670-5691 (local)**  
**Fax: (705) 670-5770**  
**E-mail: pubsales@ndm.gov.on.ca**

Use of Visa or Mastercard ensures the fastest possible service. Cheques or money orders should be made payable to the *Minister of Finance*.

### **National Library of Canada Cataloguing in Publication Data**

Breaks, F.W.

Precambrian geology, Wicklow area

(Ontario Geological Survey report, ISSN 0704-2582; 288)

Includes bibliographical references.

ISBN 0-7729-9514-1

1. Geology—Ontario—Wicklow Region. 2. Geology, Stratigraphic—Precambrian.  
I. Thivierge, R.H. (Robert Hamilton). II. Ontario Geological Survey. III. Title. IV. Series.

QE191.B73 2001

557.13'585

C2001-964002-1

Every possible effort has been made to ensure the accuracy of the information contained in this report; however, the Ontario Ministry of Northern Development and Mines does not assume any liability for errors that may occur. Source references are included in the report and users may wish to verify critical information.

If you wish to reproduce any of the text, tables or illustrations in this report, please write for permission to the Team Leader, Publication Services, Ministry of Northern Development and Mines, 933 Ramsey Lake Road, Level B4, Sudbury, Ontario P3E 6B5.

***Cette publication est disponible en anglais seulement.***

Parts of this report may be quoted if credit is given. It is recommended that reference be made in the following form:

Breaks, F.W. and Thivierge, R.H. 2001. Precambrian geology, Wicklow area; Ontario Geological Survey, Report 288, 107p.

Editors: Preliminary editing by Staff of Publication Services.  
Final compilation and edit by M.G. Easton.

# Contents

---

Explanatory Notes .....	ix
Abstract .....	x
Introduction .....	1
Access .....	1
Previous Geological Work .....	1
Present Geological Work .....	2
Field and Research Methods .....	2
Physiography .....	2
Acknowledgments .....	4
General Geology .....	5
Terminology .....	5
Rock Classification .....	5
Characteristic Accessory Minerals .....	5
Colour Index .....	5
Cataclastic Rocks .....	5
Metamorphic Grade .....	5
Migmatite Terminology .....	5
Geological Summary .....	5
Mesoproterozoic .....	10
Madawaska Highlands Gneissic Complex .....	10
Mafic to Intermediate Gneiss .....	11
Amphibolite Gneiss .....	11
Petrochemistry of the Amphibolite Gneiss .....	13
Tonalite-Quartz Diorite and Diorite-Quartz Diorite Gneisses .....	14
Felsic to Intermediate Gneiss .....	15
Modal Variation .....	17
Leucocratic to Mesocratic $\pm$ Hornblende-Biotite-Quartz-Plagioclase Gneiss .....	17
Clastic Metasedimentary Rocks of Madawaska Highlands Gneissic Complex .....	18
Distribution .....	18
Migmatization .....	18
Metasedimentary Metatexite .....	19
Paleosome .....	20
Leucosome .....	21
Modal Characteristics of Metasedimentary Paleosome .....	22
Homophanous and Nebulitic Metasedimentary Migmatite .....	22
Petrochemistry of Metasedimentary Rocks from the Madawaska Highlands Gneissic Complex .....	23
Hoare Lake Gneisses .....	24
Petrochemistry of the Hoare Lake Gneisses .....	26
Origin of the Hoare Lake Gneisses .....	27

Metasedimentary Rocks .....	28
Grenville Supergroup .....	28
Carbonate Metasedimentary Rocks .....	28
Clastic Metasedimentary Rocks .....	29
Mafic to Ultramafic and Related Tonalitic Plutonic Rocks .....	30
Structure .....	31
Petrology .....	31
Orthopyroxene-Bearing Metamorphic Segregations in Biotite-Hornblende Diorite .....	32
Petrochemistry of Mafic to Ultramafic and Related Tonalitic Plutonic Rocks .....	32
Rare Earth Element Geochemistry .....	33
Metagabbro .....	33
Anorthosite Suite Rocks .....	33
Metamorphosed Felsic to Intermediate Plutonic Rocks .....	34
Syenitic Suite Plutonic Rocks .....	34
New Carlow Syenite Complex .....	34
Corundum-Bearing Syenites .....	36
Petrochemistry of the New Carlow Syenite Complex .....	37
Rare Earth Element Geochemistry .....	39
Potassic Granitoid Suite .....	41
Structure .....	41
Petrology .....	41
Wicklow Granite .....	42
Tectonic Breccia .....	43
Petrochemistry of the Potassic Granitoid Suite .....	43
Sodic Granitoid Suite .....	44
Unmetamorphosed Felsic to Intermediate Plutonic Rocks .....	45
Potassic Granitoid Suite .....	45
Mafic Intrusive Rocks .....	46
Diabase .....	46
Cenozoic .....	46
Quaternary .....	46
Pleistocene and Recent .....	46
Metamorphism .....	47
Graphical Presentation of Metamorphic Mineral Assemblages .....	47
Madawaska Highlands Gneissic Complex .....	47
Grenville Supergroup .....	50
Retrograde Metamorphism .....	51
Structural Geology .....	52
Regional Tectonic Setting .....	52
Structural Domains .....	53
Detailed Structural Geology .....	56
Dikes .....	59
Faults and Joints .....	59
Summary of Structural Features .....	60

Economic Geology .....	61
Corundum .....	61
Hoover Mountain Deposit .....	61
Geology .....	61
Uranium .....	61
Dubblestein Occurrence .....	61
Geology .....	62
Mineralization .....	62
Thomas Occurrence .....	62
Geology .....	62
Mineralization .....	63
James Occurrence .....	63
Sulphide Mineralization .....	64
Molybdenum .....	64
Copper .....	64
Economic Evaluation of Granitic Pegmatites .....	64
Potassium Feldspar Geochemistry .....	64
Euxenite Mineral Geochemistry .....	65
Mineral Collecting .....	66
Recommendations for Future Mineral Exploration .....	67
Appendix 1. Modal Analyses .....	68
Appendix 2. Chemical Analyses .....	81
Appendix 3. Comparison with Literature .....	98
References .....	103
Metric Conversion Table .....	107

## FIGURES

1. Key map of the Wicklow area .....	1
2. Location of modally and chemically analyzed rock specimens and critical metamorphic minerals from the Wicklow area .....	3
3. Lithotectonic domains in the Bancroft–Barry’s Bay–Haliburton area .....	7
4. Quartz–total feldspar–mafics (QFM) modal variation of leucosome and paleosome from amphibolite gneiss and paleosome of diorite-quartz diorite gneiss .....	12
5. Total iron–magnesium–alkalis (FMA) plot of Wicklow area amphibolites .....	12
6. a) FeO(total)/MgO versus FeO (total) plot; b) FeO(total)/MgO versus SiO <sub>2</sub> plot for Wicklow area amphibolites .....	13
7. Silica versus total alkalis plot for amphibolites from the Wicklow area .....	14
8. Chondrite-normalized REE plots for amphibolites from the Wicklow area .....	14
9. Quartz–plagioclase–potassium feldspar (QPK) and quartz–total feldspar–mafics (QFM) modal variation of stromatic leucosome and coexisting paleosome from felsic to intermediate gneisses. ....	17
10. Ca versus Ca/Sr variation in high-grade clastic metasedimentary rocks and biotite gneiss paleosome from the Madawaska Highlands gneissic complex .....	18
11. Geological cross-section at Furz Mountain .....	19

12.	Quartz–total feldspar–mafic (QFM) modal variation of paleosome and leucosome from Wicklow area metasedimentary migmatites . . . . .	22
13.	K <sub>2</sub> O versus Na <sub>2</sub> O classification of high-grade clastic metasedimentary rocks and biotite gneiss from the Wicklow area . . . . .	23
14.	SiO <sub>2</sub> /Al <sub>2</sub> O <sub>3</sub> versus Na <sub>2</sub> O/K <sub>2</sub> O diagram for high-grade clastic metasedimentary rocks from the Wicklow area . . . . .	24
15.	Al–(Fe+Mg)–(Na+K+Ca) and Fe (total)–Mg–(Na+K) (FMA) ternary diagrams showing petrochemical variation of Wicklow area metasedimentary rocks and Hoare Lake cordierite-gedrite-hypersthene gneisses as compared to similar rocks from the literature . . . . .	24
16.	Detailed geology of part of the Hoare Lake gneisses . . . . .	25
17.	Modal variation of Little Papineau Lake plutonic complex plotted on quartz–total feldspar–mafic (QFM) and quartz–plagioclase–potassium feldspar (QPK) ternary diagrams . . . . .	31
18.	Total iron–magnesium–alkalis (FMA) variation of dioritic rocks from the Little Papineau Lake plutonic complex . . . . .	32
19.	Calcium–sodium–potassium (CNK) variation of dioritic rocks from the Little Papineau Lake plutonic complex . . . . .	32
20.	Chondrite-normalized REE plots for metagabbro, metadiorite and metaquartz diorite from the Little Papineau Lake plutonic complex . . . . .	33
21.	Quartz–plagioclase–potassium feldspar (QPK) modal variation of the New Carlow syenite complex . . . . .	36
22.	Harker diagrams illustrating petrochemical variation of selected major elements from rocks of the New Carlow syenite complex . . . . .	37
23.	Harker diagrams illustrating petrochemical variation of selected trace elements from rocks of the New Carlow syenite complex . . . . .	38
24.	Total iron–magnesium–alkalis (FMA) and calcium–sodium–potassium (CNK) variation of various petrographic phases from the New Carlow syenite complex . . . . .	39
25.	K/Rb relationships in various petrographic phases of the New Carlow syenite complex . . . . .	40
26.	K/Ba relationships in various petrographic phases of the New Carlow syenite complex . . . . .	40
27.	Chondrite-normalized REE plots of diorite, syenite, monzonite and corundum-enriched plagioclase from the New Carlow syenite complex . . . . .	40
28.	Modal variation of metamorphosed potassic granitoid suite rocks on a) quartz–total feldspar–mafic (QFM) ternary diagram, and b) quartz–plagioclase–potassium feldspar (QPK) ternary diagram . . . . .	42
29.	Chondrite-normalized REE plots for metamorphosed potassic granitoid rocks . . . . .	44
30.	Modal variation of unmetamorphosed potassic granitoid suite rocks in quartz–total feldspar–mafic (QFM) and quartz–plagioclase–potassium feldspar (QPK) ternary diagrams . . . . .	45
31.	AFM diagram depicting phase relations in high-grade assemblages developed in metasedimentary rocks . . . . .	50
32.	AFM diagrams depicting phase relations in granulite assemblages developed in metasedimentary rocks of the Madawaska Highlands gneissic complex. a) Assemblages containing potassium feldspar. b) Assemblages containing biotite as the sole K <sub>2</sub> O-bearing phase . . . . .	50
33.	Inferred <i>P–T</i> regional metamorphic condition in the Wicklow area . . . . .	51
34.	Map of structural trend surfaces in the Wicklow and adjacent areas . . . . .	back pocket
35.	Mineral lineation patterns in the Wicklow area, in relation to structural domains, and F <sub>3</sub> and later folds . . . . .	back pocket
36.	Lambert equal-area projection of contoured foliation and mineral lineation measurements . . . . .	56
37.	Lambert equal-area representation of fold data (F <sub>2</sub> axial planes and hinges; F <sub>3</sub> , F <sub>4</sub> hinges) . . . . .	56

38.	Lambert equal-area stereonet projections showing southeast-plunging D <sub>3</sub> folds coaxial with D <sub>2</sub> mineral lineations . . . . .	58
39.	Detailed geology of the Hoover Mountain corundum deposit . . . . .	back pocket
40.	Detailed geology of the western part of radioactive granite pegmatite dike, Thomas occurrence . . . . .	63
41.	Vertical variation of Ba, Cs, Rb, Sr and ratios Ba/Rb, K/Ba, K/Cs, K/Rb, Rb/Sr in blocky potassium feldspar from Dubblestein uraniferous granitic pegmatite . . . . .	65
42.	Sr versus Rb variation diagram for blocky potassium feldspar from the Dubblestein uraniferous granitic pegmatite . . . . .	66
43.	Na <sub>2</sub> O versus K/Cs diagram for blocky potassium feldspar from the Dubblestein and Thomas pegmatite occurrences . . . . .	66

## PHOTOS

1.	Coarse-grained to pegmatitic muscovite-biotite-magnetite-corundum plagioclase near the Hoover Mountain corundum deposit . . . . .	2
2.	Tectonic breccia of Wicklow granite . . . . .	2
3.	Typical exposure of felsic to intermediate gneiss at Yuill Lake . . . . .	16
4.	Metasedimentary protometatexite of granulite grade near McKenzie Lake . . . . .	20
5.	Metasedimentary metatexite near McKenzie Lake . . . . .	20
6.	Diablastic metapelite from metasedimentary migmatite near Papineau Lake . . . . .	21
7.	Homophanous metasedimentary migmatite of trondhjemite composition near South Papineau Lake Road . . . . .	22
8.	Metamorphic segregations containing orthopyroxene developed in metadiorite on Davis Island . . . . .	32
9.	Anorthositic gabbro in portion of a large inclusion contained within tectonic breccia of Wicklow granite . . . . .	34
10.	Very coarse feldspar porphyroblast displaying asymmetric “tails” near Balsam Lake . . . . .	54
11.	Highly porphyroblastic flaser-textured hornblende-biotite homophanous migmatite near Purdy . . . . .	54
12.	Abrupt truncation of folded layering within metatextitic metasedimentary migmatite near Maple Leaf . . . . .	55
13.	Early F <sub>2A</sub> folding of layering within a lens of amphibolitic gneiss from Madawaska Highlands gneissic complex . . . . .	55
14.	Typical F <sub>2</sub> disharmonic, asymmetric, nearly reclined folds with shallow-dipping axial planar fabric in biotite gneiss interlayered with granite sheets near Papineau Lake South Road . . . . .	57
15.	“Cascading folds” in biotite gneiss near Maynooth . . . . .	57
16.	Waterfalls on Papineau Creek controlled by prominent subhorizontally dipping joints in the Cardwell Lake granite . . . . .	60
17.	Longtime area resident, R. Armstrong, stands alongside the remnants of a mobile boiler, which was destroyed in a 1916 accident at the Hoover Mountain corundum deposit . . . . .	61
18.	Euhedral termination of a large blocky potassium feldspar crystal, which projects into the quartz-rich part of the core zone of the Dubblestein pegmatite . . . . .	62

## TABLES

1.	Classification and general features of metasedimentary migmatites from northern supracrustal domain, English River Subprovince . . . . .	6
2.	Table of lithologic units for the Wicklow area . . . . .	8

3.	Summary of tectonic features in the Wicklow and surrounding area .....	10
4.	Main rock types of the Hoare Lake gneisses .....	26
5.	Genetic classification of cordierite-orthoamphibole-bearing rocks and selected examples .....	27
6.	Petrologic units of the New Carlow syenite complex .....	35
7.	Metamorphic mineral assemblages from high-grade to granulite-grade Madawaska Highlands gneissic complex .....	48
8.	Metamorphic mineral assemblages from Grenville Supergroup rock types .....	49
9.	Classification of molybdenite mineralization in the Wicklow area .....	64

## **GEOLOGICAL MAP**

Map 2550	Precambrian Geology, Wicklow Area .....	back pocket
----------	---	-------------

## **CHART**

A.	Figures 34 and 35 .....	back pocket
----	-------------------------	-------------

# Explanatory Notes

1. Subsequent to the completion of this study, the terminology that pertains to the regional division of the Grenville Province has been revised. The reader is referred to the excellent and comprehensive publication by Easton (1992) for details on this division. The change in terminology that affects the Wicklow area is given below:

Terminology in this Report	Revised Terminology (Easton 1992)
Ontario Gneiss Segment	Central Gneiss Belt
Algonquin Domain	Algonquin Terrane
Central Metasedimentary Belt, Segment IVa	Central Metasedimentary Belt Boundary Zone (CMBBZ)
Grenville Supergroup, Segment IVb	Bancroft Terrane

2. All rare earth element patterns in this study have been derived by normalization with a composite of 12 chondritic meteorites (H. Wakita and D. Zellmar, unpublished data, quoted in Wakita, Rey and Schmitt (1971)).
3. The section on the structural geology has been written by the junior author and is based, in part, on his MSc thesis studies. The chapter is intended to be understandable in itself and therefore some minor repetitions of descriptions and observations made in the text preceding it were unavoidable.
4. A brief description of significant work done in the Wicklow area and its environs subsequent to the completion of this study (in 1985):

A current synopsis of the Grenville Province in Ontario, which updates “Regional Tectonic Setting”, can be found in Carr et al. (2000). In addition, White et al. (2000) provides a summary of the results of a Lithoprobe seismic reflection survey, which ran across the Central Metasedimentary Belt Boundary Zone, south through the Wicklow area along Papineau Lake.

U/Pb geochronology in the Barry’s Bay area establishes the following constraints on the timing of events in the Wicklow area:

- Orthogneisses near Bark Lake, roughly equivalent to map units 1 and 2 in the Wicklow area, were likely emplaced between 1420 and 1470 Ma (McMullen 1999).
- Regional metamorphism and active regional deformation occurred between 1055 and 1030 Ma (McEachern and van Breemen 1993; McMullen 1999).
- An age of approximately 990 Ma on a posttectonic pegmatite (McMullen 1999) effectively constrains the end of Grenvillian deformation in the region.

McMullen (1999) has also examined the structural and metamorphic history of the rocks both north of the Wicklow area and along Papineau Lake. The origin of the cordierite–gedrite gneisses at Hoare Lake has remained controversial. Peck and Valley (2000), using oxygen isotopic data, suggested that the protolith was a hydrothermally altered mafic volcanic rock that was subsequently subjected to upper amphibolite facies metamorphism. This interpretation differs considerably from that contained in this report.

5. Several field trip guidebooks cover the area immediately east, or north, of the Wicklow area and provide an opportunity to view rocks similar to those found in the Wicklow area. These include guidebooks by Appleyard and Stott (1975), Bartlett et al. (1983), Easton and Davidson (1994), and Carr and McMullen (2000).

# Precambrian Geology

## Wicklow Area

F.W. Breaks<sup>1</sup> and R.H. Thivierge<sup>2</sup>

<sup>1</sup>Geologist, Precambrian Geoscience Section, Ontario Geological Survey, Sudbury, Ontario

<sup>2</sup>Graduate Student, Carleton University, Ottawa, Ontario

Manuscript approved for publication and published with the permission of the Senior Manager, Precambrian Geoscience Section, Ontario Geological Survey.

---

## Abstract

---

Detailed 1:20 000 scale geological mapping coverage is presented for a 280 km<sup>2</sup> previously poorly known area situated approximately 20 km north of Bancroft.

The bedrock is of Proterozoic age. Most of the area is contained within the 1430±20 million-year-old Madawaska Highlands gneissic complex. This extremely complex gneissic mélange structurally underlies Grenville Supergroup supracrustal rocks which possibly date from 1286±15 Ma and are mainly composed of migmatized clastic metasedimentary rocks and felsic to intermediate gneiss. These 2 lithologic assemblages possibly contain the oldest rocks.

Mafic to intermediate gneiss, predominantly composed of layered amphibolite, is considerably less abundant and is enigmatic in origin. Rare, deformed, narrow, amphibolitic mafic dikes intrude metasedimentary migmatite and tonalite of the Indian Lake plutonic complex, however, it cannot be established whether such dikes are consanguineous with the amphibolitic gneiss.

Discrete plutonic masses, mainly composed of diorite-quartz diorite and ancillary tonalite-trondhjemite, are common. The largest single mass is the Little Papineau Lake plutonic complex, an irregular crescent-shaped mass, at least 19 km<sup>2</sup> in area, which is overprinted by the southeast-plunging Carlow synform.

Metamorphosed felsic to intermediate potassic rocks are widespread in the form of sheets and plutonic masses, and are compositionally distinct from partial melts derived from within the extensive metasedimentary migmatite. The largest masses are represented by the Wicklow granite and Cardwell Lake granite, which exhibit distinctively different structural trends. Sodic-suite rocks of this group are much less abundant and are mainly confined to the Indian Lake plutonic complex (tonalite-quartz diorite). This particular mass may constitute a less deformed equivalent of felsic to intermediate gneisses with which they are spatially associated.

Grenville Supergroup rocks are restricted to the core zone of the Carlow synform. They consist mainly of a 400 to 1200 m wide assemblage of marble, marble tectonic breccia, calc-silicate skarn, and rarer metapelite, psammitic metasedimentary rocks, quartzite, and possible para-amphibolite which envelops the New Carlow syenite complex. This plutonic mass comprises an interlayered assemblage of syenite, monzonite, plagiostenite, monzodiorite, diorite, quartz syenite and granite.

Structural evolution of the map area involved a complex, protracted tectonic history encompassing 4 recognizable regional folding events. The second or “typical Grenville” deformation event (D<sub>2</sub>), at about 1050 to 1100 Ma, imposed a very penetrative L–S fabric, strongly modifying earlier, rare, isoclinal, refolded D<sub>2A</sub> structures. D<sub>3</sub> structures are mainly evident as macroscopic southeast-plunging antiforms and synforms such as the Carlow syn-

form. D<sub>4</sub> structures are locally mesoscopic, east-trending, subhorizontal warping of gneissosity about shallow-plunging axes.

The metamorphic grade of the area varies from high grade to granulite grade. Rocks of the Madawaska Highlands gneissic complex contain sporadic “nodes” of intermediate-pressure orthopyroxene-bearing assemblages. Thus, it represents a terrane undergoing transition from high-grade to incipient granulite conditions. Maximum metamorphic conditions are deduced to be temperature = 770°C and load pressure = 8.5 kilobars. Grenville Supergroup metasedimentary rocks do not contain evidence of granulite conditions nor migmatization in compositionally favourable rock types and are deduced to have undergone regional metamorphism at somewhat lower *P-T* conditions.

Mineral exploration within the study area has been mainly desultory and directed only toward exploitation of the Hoover Mountain corundum deposit in 1916 and exploration of uranium-bearing granite pegmatites during the mid 1950s.

Surficial Pleistocene glacial deposits cover significant portions of the map area and mainly consist of fluvial outwash sands and gravels and ground moraine boulder till.

---

Breaks, F.W. and Thivierge R.H. 2001. Precambrian geology, Wicklow area; Ontario Geological Survey, Report 288, 109p.



# Introduction

The Wicklow area is bounded by latitudes 45°15'N and 45°22'30"N and longitudes 77°45'W and 78°00'W in Hastings County of southern Ontario (Figure 1). It encompasses an area of 280 km<sup>2</sup> and includes most of Wicklow Township, a significant part of southwestern Bangor Township, and considerably smaller portions of Carlow, Monteagle, Sabine, and Lyell townships. Maple Leaf, situated on Highway 62, represents the sole centre of population (approximately 100 persons). The villages of Maynooth, Purdy, Combermere and Lake St. Peter are situated proximal to the boundaries of the map area.

Mineral exploration has been desultory within the map area and was probably instigated with the discovery of corundum at the Burgess Mine, situated a short distance from the southeastern corner of the area in Carlow Township. In 1916, a small corundum deposit at Hoover Mountain was developed and represents the sole production of any mineral commodity within the map area to date. In the mid 1950s, considerable interest in uraniferous granitic pegmatites in the Bancroft region led to the discovery of 3 such pegmatites in the map area and some claim staking. To the writers' knowledge, no further exploration activity has resulted.

## ACCESS

Access to the area is via Highway 62 and 127, which, respectively, traverse the southwest and southeast corners of the map area. The Madawaska Highway, Little Papineau Lake Road and ancillary logging roads provide good access to a considerable portion of the western map area. The north-central and northeastern sections of the area are quite accessible by the West Papineau Lake–Centreview Road system which also includes an unnamed north-trending paved road yielding access to Mill Road and Bell Rapids. The New Carlow Road provides ingress into the extreme southern corner of the map area.

## PREVIOUS GEOLOGICAL WORK

Most of the area has remained unmapped subsequent to the reconnaissance investigations of Adams and Barlow (1910). Detailed coverage of Monteagle and Carlow townships by Hewitt (1954) at a scale of 1:31 680 partially overlaps the southeast corner of the map area. More recent 1:63 360 scale reconnaissance work by Lumbers and Vertolli (1980) extends mapping coverage to just within the

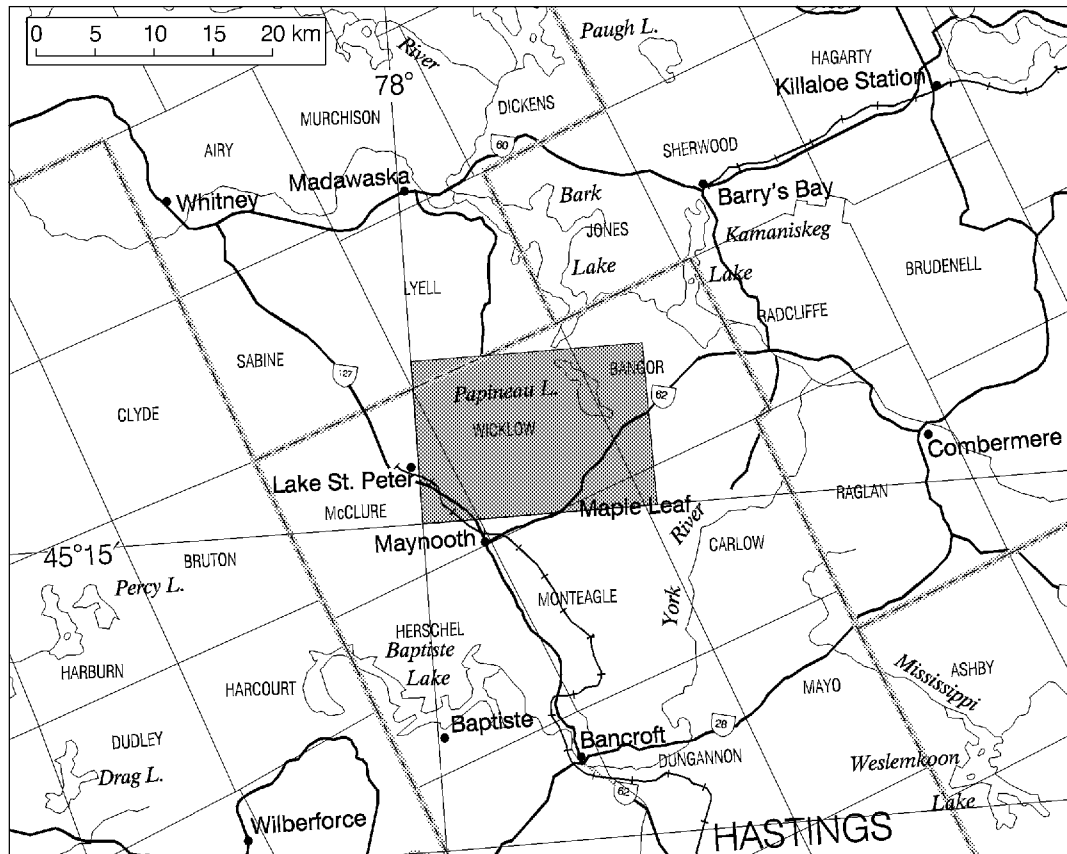


Figure 1. Location map for the Wicklow area.

eastern, northeastern and north-central limits of the map area.

Recent reconnaissance investigation of radioactive mineral occurrences in the Bancroft region has been published by Masson and Gordon (1981) and included the Dubblestein and Thomas uranium occurrences situated in the northeastern part of the area.

## PRESENT GEOLOGICAL WORK

This geological survey was undertaken during the summer of 1982, and resulted in publication of a 1:15 840 scale uncoloured preliminary map P.2614 (Breaks and Thivierge 1983) and a coloured 1:20 000 scale final map (Map 2550, back pocket).

The 1:15 840 scale field base maps were provided by the Cartography Section, Ministry of Natural Resources, Toronto, from Forest Resources Inventory sheets. Field data were plotted upon acetate overlays on vertical airphotos of the same scale. Geological data were obtained primarily via pace and compass traverses. Owing to the relatively poor rock exposure within most of the area, many traverses were routed in order to encounter all possible outcrops obvious on airphotos, rather than traverses strictly oriented normal to strike.

Geological research in the map area was undertaken by R.H. Thivierge (University of Ottawa) in the form of a MSc dissertation, and by W. Miller (Queen's University), who examined the unique gedrite-cordierite hypersthene gneisses near Hoare Lake as a subject of BSc thesis.

## FIELD AND RESEARCH METHODS

The vast majority of hand specimens collected during field mapping were slabbed by diamond saw and subsequently stained for potassium feldspar and plagioclase, according to well-known methods described by Bailey and Stevens (1960). This provided invaluable input regarding textural and compositional features of many rock units in the map

area. In addition, numerous modal analyses were conducted on stained rock slabs with aid of Mylar grids and a binocular microscope. The Mylar grids employed a choice of point spacings of 25 mm, 5 mm, 6 mm and 1.2 cm, and were interchanged according to the grain size of the rock slab in question. In the case of quickly discerning fine- to medium-grained hornblende from biotite during modal analyses, it was found that prolonged immersion (1 to 2 minutes) of HF-etched rock surfaces in a saturated sodium cobaltinitrite solution preferentially caused biotite to acquire a moderate yellow-green stain while hornblende remained unaffected. Geological units possessing very coarse grain size, such as coarse corundum-bearing syenites at Hoover Mountain (Photo 1), or a very coarse inclusion population, such as the granite tectonic breccia exposed on the Madawaska Highway (Photo 2), were modally analyzed utilizing a grid established by tape measure and employing a spacing established by dimension of the coarsest mineral size or inclusion.

In some cases, textural and compositional studies were enhanced by removal of obscuring rust coatings as effected by a dilute solution of oxalic acid. Treatment of moderately rusty covered exposures of the Hoare Lake cordierite-hypersthene-gedrite-garnet gneisses, for example, was particularly effective and yielded much information.

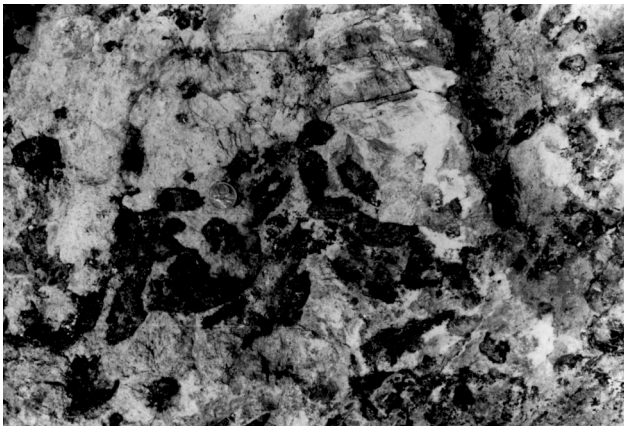
Unless otherwise stated, all assays and chemical analyses in this study were performed by the Geoscience Laboratory of the Ontario Geological Survey.

Locations of all modally and chemically analyzed samples are provided on Figure 2.

## PHYSIOGRAPHY

The map area is situated within the Madawaska Highlands of southern Ontario, and is characterized by relatively significant relief.

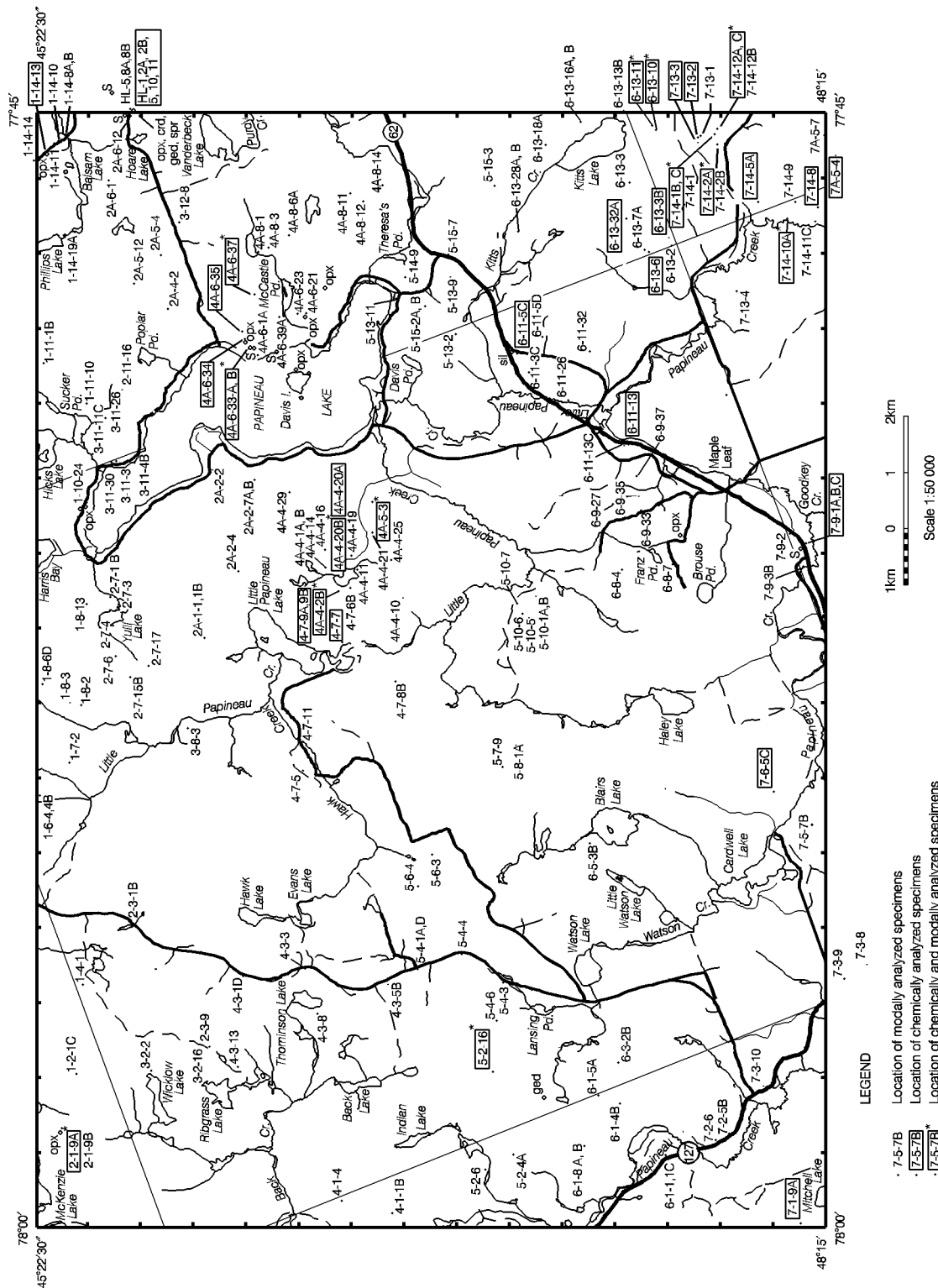
The highest elevations (about 530 m) occur in the west-central part of the map area at the site of an aban-



**Photo 1.** Coarse-grained to pegmatitic muscovite-biotite-magnetite-corundum plagiostenite situated about 65 m south of the Hoover Mountain corundum deposit. This exposure contains the highest modal abundance (19%) and coarsest corundum observed in the map area. Coin diameter is 2.3 cm.



**Photo 2.** Tectonic breccia of Wicklow granite, as exposed on Madawaska Highway in Concession XI, Lot 24, Wicklow Township. Note sharp truncation of gneissic layering in largest clast by foliated to gneissic fabric of granite matrix. Length of hammer approximately 0.3 m.



**Figure 2.** Location of modally and chemically analyzed rock specimens and critical metamorphic minerals from the Wicklow area. Abbreviations of critical metamorphic minerals: crd, cordierite; ged, gedrite; opx, orthopyroxene; S, sulphide minerals; sil, sillimanite; spr, sapphirine.

doned Ministry of Natural Resources fire lookout tower, and near the Little Papineau Lake Road on Concession VI, Lot 21, both in Wicklow Township. The lowest elevation is slightly less than 305 m at Papineau Creek where it crosses the southern map boundary. Thus, the overall relief is approximately 225 m. Local relief can approach 155 m, as between the summit of Furz Mountain (local name) and the surface of Papineau Lake. The relief of this specific area is particularly influenced by a prominent, vertically dipping north-northeast-trending fracture system which has contributed to the development of impressive cliffs (up to 64 m overall height) along the shoreline of Papineau Lake.

Most of the area is drained by the Papineau Creek system, which, in turn, empties into the York River beyond the limit of the map area. The local topography exhibits control both by bedrock structure and by various types of Pleistocene glacial deposits. Bedrock control is particularly obvious in several localities associated with macroscopic fold structures.

An arcuate drainage pattern involving Kitts Creek, Kitts Lake and part of Little Papineau Creek (downstream from its confluence with Kitts Creek) is demonstrative of bedrock control by the Carlow synform (*see* "Structural Geology"). This pattern is once again manifested 2.8 km northeast, as the southern shoreline of Papineau Lake and the incoming northeast- to east-trending drainage course of Little Papineau Creek describe a broad arc approximately bisected by the axial trace of the Carlow synform. Elsewhere in the Wicklow–Ribgrass–Thominson lakes area, the intersection of 2 major fracture sets has influenced the drainage effected by Back Creek. Dominant bedrock control here is the Wicklow antiform, a gently southeast-plunging macroscopic structure. A northwest- to north-trending, relatively linear fracture set approximately parallels the axial trace of this fold and is transected by a slightly curvilinear to pronouncedly arcuate fracture set oriented at high angles to this axial trace. Much of the upper portion of Little Papineau Creek and its tributaries, and much of the shoreline of Papineau Lake, exhibit strong linearity suggestive of fracture control.

In rare instances, plutonic bodies influence topography as exemplified by the late-tectonic Yuill Lake granite dike of the Hybla swarm. This 4.6 km long erosionally resistant dike has been partly responsible for forming the northeast-trending Hemlock Ridge. Several hills within the Little Papineau Lake plutonic complex relate to resistant knolls of diorite.

Pleistocene glacial deposits influence topography, drainage and outcrop distribution in several parts of the map area. The area in proximity to Blairs, Watson, Cardwell and Haley lakes, for example, features an extensive fluvial sand and gravel blanket, in many places interrupted by kettle and esker ridge deposits. In some cases, drainage is controlled by esker ridges, as exemplified by the stream between Blairs and Cardwell lakes.

Extensive Pleistocene surficial deposits cover most of the bedrock and approximately 30% of the map area contains virtually no outcrop. A large north-trending area of negligible rock exposure completely traverses the map area from beyond the headwaters of Little Papineau Creek southward toward Maple Leaf and Greenview.

## ACKNOWLEDGMENTS

Able assistance in the field was provided by C. Butler, G. Charlton and W. Miller. This study greatly benefited from discussions with B.O. Dressler, B.S. Brock, J. Vander Leeden, A. Davidson, H.D. Meyn, N.G. Culshaw, J.M. Moore, Jr. and W.K. Fyson, who also critically examined the "Structural Geology" section.

The writers are grateful to numerous residents of the area for assistance regarding access, mineral exploration activity and historical perspectives. Most notable here are R. Dubblestein and A. Dubblestein, R. Armstrong, E. Cragg, C. James, C. Ploughrite, and N. Baragar. Dr. G. Pollack of the Saskatchewan Mining and Development Corporation is gratefully acknowledged for use of microscope facilities in Saskatoon.

# General Geology

---

## TERMINOLOGY

In the following section, the geoscience terminology used in this study is defined.

## Rock Classification

Most metamorphosed and late-tectonic plutonic rocks were classified according to the system proposed by the International Union of Geological Sciences (IUGS) Subcommittee on the Systematics of Igneous Rocks (Streckeisen 1976). Minor departures were undertaken in the naming of relatively rare anorthosite suite rocks and some syenitic rocks. According to the IUGS classification, plagioclase-rich rocks, many of which are corundum bearing and genetically associated with the New Carlow syenite complex, would rigidly be termed anorthosites or gabbroids. The writers prefer to prefix these special syenitic rocks with “plagio” as in, for example, magnetite-muscovite-biotite-corundum plagiostenite found at the Hoover Mountain corundum deposit, in order to emphasize genetic connotation and consistency in map unit coding (*see* Map 2550, back pocket). Trondhjemite is used in this study in reference to a leucocratic to hololeucocratic tonalite with a colour index (CI) of 10 or less as defined by Streckeisen (1976). Anorthosite suite rocks were classified according to Buddington (1939), who defined anorthosite as a rock containing greater than 90% calcic plagioclase, and subdivided affiliated rocks according to colour index: gabbroic anorthosite (10 to 22.5), anorthositic gabbro (22.5 to 35) and gabbro (greater than 35).

High-grade metasedimentary rocks in the map area are separable with some difficulties into metawacke and metapelitic categories. In most cases, diagnostic minerals, such as cordierite and sillimanite, are lacking. In this study, an arbitrary division between these 2 categories was chosen at a colour index of 35, with metapelites exceeding this value.

## Characteristic Accessory Minerals

Characteristic accessory minerals occurring in abundances exceeding 1% are added to rock names in order of increasing relative abundance: for example, a hornblende-biotite tonalite contains biotite exceeding hornblende.

## Colour Index

Colour index (CI) refers to the sum of minerals containing significant levels of iron and/or magnesium and includes any of the following: biotite, hornblende, orthopyroxene, clinopyroxene, iron oxide, pyrite, cordierite, orthoamphibole, garnet and allanite. Classification of rocks according to colour index in this study follows the IUGS recommendations (Streckeisen 1976, p.24):

Hololeucocratic	0 to 5
Leucocratic	5 to 35
Mesocratic	35 to 65
Melanocratic	35 to 95
Ultramafic	95 to 100

## Cataclastic Rocks

In this study, the terms mylonite, protomylonite and cataclasite are used according to the classification of Higgins (1971, p.3).

## Metamorphic Grade

Division of metamorphic grade follows that proposed by Winkler (1979). Thus, the Wicklow area reflects metamorphic pressure–temperature conditions operative in the high-grade and regional hypersthene zones (granulite grade) as defined by Winkler (1979). Wherever possible, metamorphic assemblages are listed in order of relative increasing order of abundance.

## Migmatite Terminology

Metasedimentary migmatites are classified according to the scheme utilized by Breaks, Bond and Stone (1978), and Breaks and Bond (1993) to describe similar migmatites within the high-grade to granulite-grade terrane of the Archean English River Subprovince of northwestern Ontario. The classification and petrologic attributes of the main migmatite evolutionary stages are presented in Table 1.

## GEOLOGICAL SUMMARY

The map area is situated predominantly within the “Ontario Gneiss Segment” (Figure 3) of the Grenville Province (Wynne-Edwards 1972). A small portion of the transition zone between the Central Metasedimentary Belt and the Ontario Gneiss Segment is exposed in the core of the Carlow synform and is restricted to the southeast corner of the map area (Segment IVa of Wynne-Edwards 1972). The transition zone, according to Wynne-Edwards (1972), comprises supracrustal rocks of the Central Metasedimentary Belt locally admixed with migmatitic, gneissic rocks similar to those typifying the Ontario Gneiss Segment. In this study, the migmatitic gneissic rocks are grouped in the Madawaska Highlands gneissic complex that is equivalent to the Radcliffe hybrid gneiss as defined in Radcliffe Township and the western part of Brudenell Township (Hewitt 1954). A generalized succession of the rock types in the map area is given in Table 2 and is, in part, speculative owing to a paucity of geochronological work in the region.

The Madawaska Highlands gneissic complex, which structurally underlies supracrustal rocks of the Grenville Supergroup, probably contains the oldest crustal material in the area. This interpretation is based upon an age deter-

**Table 1.** Classification and general features of metasedimentary migmatites from the northern supracrustal domain, English River Subprovince.

Migmatitic Stage	Leucosome: Paleosome Ratio	Diagnosic Migmatitic Structure	General Processes Dominant	General Field Features
Protometatexite	< 0.1	Locally stromatic; sedimentary bedding or laminae may show preservation	Incipient 'selective' anatexis. Metamorphic differentiation may be important	Characterized by intercalated fine-grained wacke and medium- to coarse-grained porphyroblastic pelite components. Podiform and lentic potassic leucosomes exhibit confinement to pelitic horizons. Hydrothermal (quartz veins) mobilization may be important.
Metatexite	0.1 – 0.6	Stromatic and/or phlebitic	Local to moderate degree of anatexis	Mobilization developed <i>in situ</i> possess biotitic melanosomes along leucosome–paleosome interface. Mobilization (without melanosomes) also commonly injected along prevailing foliation or bedding surface of paleosome.
Inhomogeneous diatexite	0.6 – 0.9	Schollen structure especially characteristic. Locally schlieritic or nebulitic	Anatexis relatively extensive; mobilization essentially autochthonous	Repletion of disoriented paleosome + metatexite enclaves and melanosome clumps is diagnostic.
Homogeneous diatexite	>0.9	Homogeneous, usually massive. Locally schollen, schlieritic, or nebulitic, structures apparent	Very advanced fusion; mobilization probably allochthonous	Usually hololeucocratic and severely seriate. Rare more mafic variants (C1 15 – 30) may represent cases of complete anatexis effecting restitution of melanosome component into magmatic phase.

mination of 1430±20 Ma (Rb/Sr whole-rock isochron) by Bell and Blenkinsop (1980) near Barry’s Bay, north of the map area. This date not only provides the age of granulite metamorphism, but a minimum age for the clastic metasedimentary rocks and derived migmatites.

The clastic metasedimentary rocks comprise mainly metawacke and metapelite, and rare iron-rich pelites, the latter of which are characterized by high garnet and/or orthopyroxene contents. These rocks have been subjected to at least 2 episodes of metatexis, which have produced a pervasive stromatic structure characterized by distinctly trondhjemite to tonalite leucosome compositions. These migmatites are variably overprinted by porphyroblastic development of plagioclase, potassium feldspar and/or hornblende; recrystallization; and 4 periods of folding.

Age relations with other important lithologic assemblages, such as felsic to intermediate gneiss, less abundant mafic to intermediate gneiss, and sheets of metamorphosed granite, are enigmatic since all these major units demonstrate pervasive tectonic interleaving. At Furz Mountain, 200 m of metawacke and metapelite, the latter locally containing potassium feldspar-garnet-sillimanite-biotite-quartz-plagioclase associated with local sillimanite-bearing anatectic melt, are structurally underlain by at least 250 m of trondhjemitic to tonalitic orthogneiss and overlain by an erosionally truncated, mafic to intermediate gneiss of tonalite to quartz diorite composition.

Discrete masses of mafic to intermediate metaplutonic rocks of diorite-quartz diorite-tonalite-trondhjemite association are distributed widely, and probably intrude the migmatized clastic metasedimentary rocks, felsic to intermediate gneiss, and mafic to intermediate gneiss. The largest metaplutonic mass in the map area is represented by the Little Papineau Lake plutonic complex. Dioritic plutons such as this usually document a mafic to felsic lithologic fractionation pattern, which marks a general increase in quartz + plagioclase and a decrease in colour index as a function of decreasing relative age of rock type.

Anorthosite suite rocks are extremely rare within the area and occur as enclaves only. Primary layering is preserved in one enclave contained within the Wicklow granite.

Metamorphosed potassic granitoid suite rocks are ubiquitous and areally concentrated within 2 masses of significantly contrasting structural trends, which are reflective of the harbouring tectonic domains (*see* “Structural Geology”). The “Wicklow granite” is mainly composed of granite tectonic breccia that occupies the core zone of the southeast-plunging Wicklow antiform. The Cardwell Lake granite trends southwesterly and virtually normal to the Wicklow granite. Rocks of this group are entirely granite in composition and may be products of extensive partial melting of a tonalitic protolith. There is no demonstrable similarity between leucosome composition from metasedimentary migmatite belts and these granites, although the 2 groups are commonly spatially associated in a fortuitous manner.

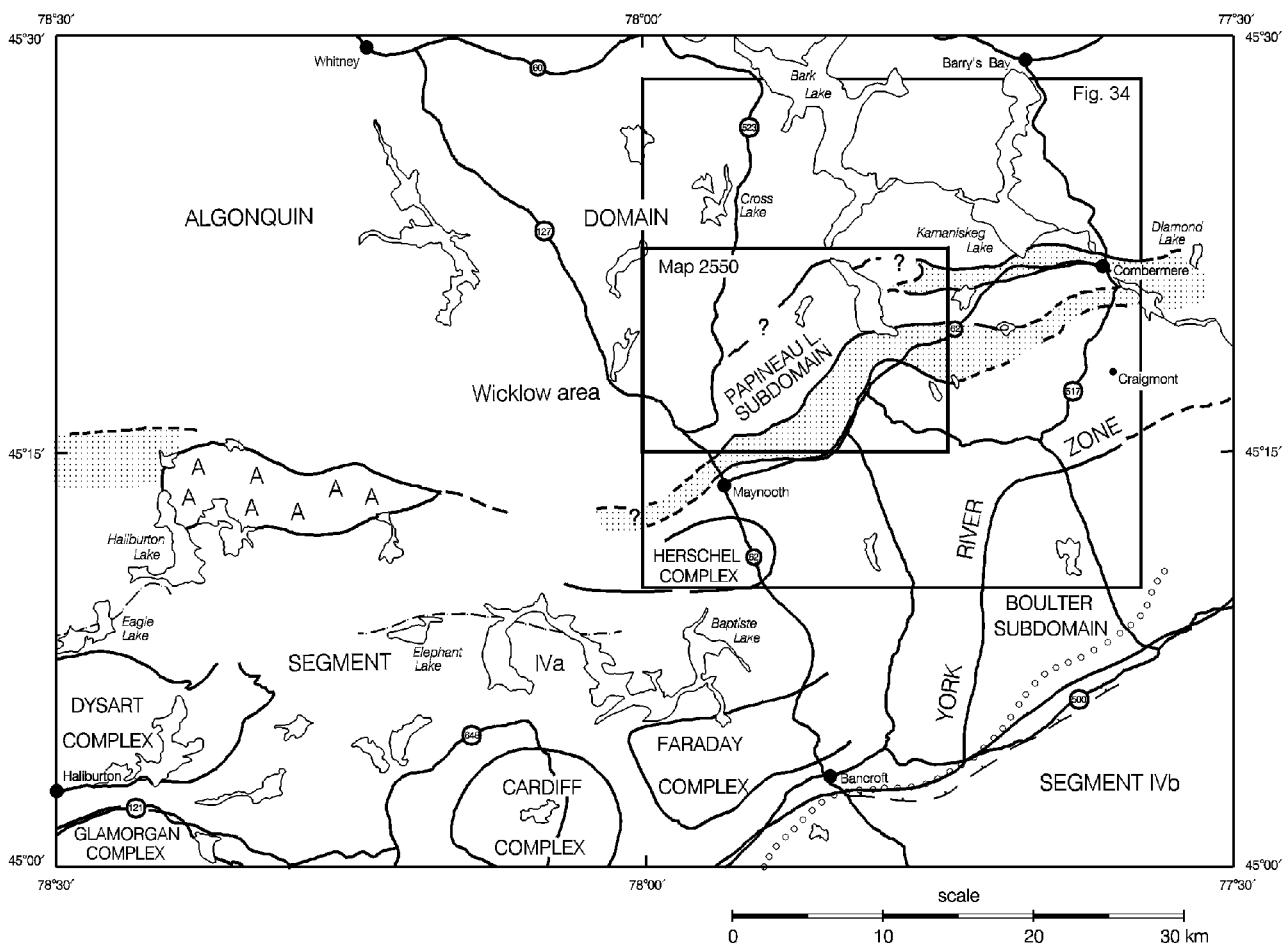
Metamorphosed sodic granitoid rocks, mainly of tonalite to quartz diorite and minor diorite compositions, are less common, being mainly confined within the Indian Lake plutonic complex. These rocks are probably a less deformed equivalent of felsic to intermediate gneisses with which there is a strong spatial relationship.

Unmetamorphosed felsic to intermediate plutonic rocks are areally miniscule and restricted to generally narrow, northeasterly trending granite pegmatite dikes of the Hybla pegmatite province. The 4.5 km by 240 m Yuill Lake dike is by far the largest dike. Modal variation on the quartz–plagioclase–potassium feldspar (QPK) ternary diagram (*see* Figure 30 in “Potassic Granitoid Suite” in “Unmetamorphosed Felsic to Intermediate Plutonic Rocks”) is virtually identical to that of metamorphosed granite.

Olivine diabase is extremely rare, found only as 2 narrow (1 to 3 m wide) dikes trending 105 to 205°.

Tectonic breccia, which is developed in several parts of the map area, appears as these main types: granite tectonic breccia (Wicklow granite), tonalite tectonic breccia, and metasedimentary migmatite tectonic breccia. Significantly, these rock types document that gneissosity and/or lineations, and metamorphic assemblages relating to a high-grade to granulite-grade tectonometamorphic event, clearly predate the event responsible for tectonic mobilization.

Grenville Supergroup rocks are confined to the southeastern corner of the map area. These rocks are probably somewhat younger than gneissic units of the Madawaska Highlands gneissic complex. The age of the contained su-



**Figure 3.** Lithotectonic domains in the Bancroft–Barry’s Bay–Haliburton area. Segment IVa and IVb of Wynne-Edwards’ (1972) Central Metasedimentary Belt belong to highlands and lowlands terrains, respectively. The highlands–lowlands boundary (solid line south of Bancroft) lies close to the sillimanite isograd (barbed line) of Divi (1972) and close to the approximate southern limit of the southeast-plunging mineral lineation (line of open circles). The Boulter metaplutonic-rich highlands subdomain lies south of the York River mylonitic-cataclastic zone. Gneiss and/or migmatite-cored complexes within Segment IVa are outlined and named. Within the poorly mapped Eagle Lake–Elephant Lake area, the known northern margins of calcareous metasedimentary belts are shown as dash-dot lines. The boundary of Segment IVa with the upper highlands Algonquin domain (Ontario Gneiss Segment) is considered as the southern margin of the high strain, relatively straight-trending migmatite zone (stippled) of the Papineau Lake subdomain around Maynooth. Note the large meta-anorthositic mass around Haliburton Lake (“A” letter pattern) lies along strike with a ductile, high-strain zone to the west, which underlies Segment IVa, and may be the source of meta-anorthosite slivers common to these high-strain zones (Davidson and Morgan 1980; A. Davidson, personal communication, 1982). Note also the apparent continuity eastward to the Papineau Lake subdomain, and the apparent merging of such zones further east around Combermere. The Wicklow map area (small box: Map 2550, back pocket) and the area of Figure 34 (larger box: Chart A, back pocket) are outlined.

**Table 2.** Table of lithologic units for the Wicklow area. Units are shown in order of tectonic affinity rather than strict chronological order; consequently, the unit order may vary slightly from that shown on Map 2550 (back pocket).

---

**CENOZOIC**

**QUATERNARY**

**RECENT**

Organic swamp and alluvial deposits

**PLEISTOCENE**

Boulder till ground moraine, fluvial sand and gravel

*UNCONFORMITY*

**PRECAMBRIAN**

**MESOPROTEROZOIC**

**Posttectonic Unmetamorphosed Plutonic Rocks**

**Mafic Intrusive Rocks**

Diabase dikes

*INTRUSIVE CONTACT*

**Felsic to Intermediate Plutonic Rocks**

Coarse-grained to pegmatitic biotite, magnetite-biotite, magnetite-allanite-biotite granite; muscovite-biotite granite pegmatite; aplite; granite pegmatite with quartz-rich core zones

*UNKNOWN CONTACT*

**Metamorphosed Felsic to Intermediate Plutonic Rocks (emplaced in Grenville Supergroup metasedimentary rocks)**

**Syenitic Suite Plutonic Rocks**

Diorite; monzodiorite; plagiostenite; syenite; monzonite; quartz syenite; quartz monzonite; granite; corundum-bearing plagiostenite

*INTRUSIVE CONTACT*

**Calcareous Metasedimentary, Associated Clastic and Derived Calc-Silicate Rocks (Grenville Supergroup)**

Marble; marble tectonic breccia; calc-silicate skarn; metapelite; psammitic metasedimentary rocks; quartzite; para-amphibolite

*TECTONIC CONTACT*

**MADAWASKA HIGHLANDS GNEISSIC COMPLEX**

**Metamorphosed Felsic to Intermediate Plutonic Rocks**

**Sodic Granitoid Suite**

Biotite and magnetite-biotite trondhjemite, hornblende-biotite and biotite-hornblende tonalite to quartz diorite; tonalite tectonic breccia

*INTRUSIVE CONTACT*

**Potassic Granitoid Suite**

Biotite, magnetite-biotite, hornblende-biotite granite; muscovite-biotite granite; allanite-biotite, magnetite-allanite-biotite granite; hybrid hornblende-biotite granite and quartz syenite associated with variably assimilated mafic inclusions; granite tectonic breccia

*UNKNOWN CONTACT*

**Anorthosite Suite Plutonic Rocks**

Anorthositic gabbro; gabbro; anorthosite

**Metamorphosed Mafic to Ultramafic and Related Tonalitic Plutonic Rocks**

Biotite-hornblende, hornblende-biotite diorite to quartz diorite; hornblende-biotite tonalite; magnetite-biotite to biotite trondhjemite; leucocratic hornblende-biotite diorite to quartz-diorite; diorite to quartz diorite gneiss; hornblende granite mobilizate hosted by diorite to quartz diorite; amphibolite layers and tectonized equivalents; hornblende; ultramafic rocks and tectonized equivalents; porphyroblastic gabbro; coronitic gabbro; amphibolite dikes

Table 2. Continued

## UNKNOWN CONTACT

**Clastic Metasedimentary Rocks and Derived Migmatite**

± Garnet-hornblende-biotite metawacke; ± garnet-potassium feldspar-hornblende-biotite metapelite; garnet-sillimanite-biotite metapelite; biotite-garnet-orthoamphibole-cordierite-orthopyroxene, and magnetite-biotite-garnet-orthopyroxene-plagioclase iron-rich metasedimentary rocks; protometatexite; metatexite; inhomogeneous diatexite; homogeneous diatexite; polyblastic (potassium feldspar, plagioclase, hornblende) metasedimentary migmatite; nebulitic to homophanous metasedimentary migmatite; metasedimentary migmatite tectonic breccia

± Garnet-hornblende-biotite metawacke; ± garnet-potassium feldspar-hornblende-biotite metapelite; garnet-sillimanite-biotite metapelite; biotite-garnet-orthoamphibole-cordierite-orthopyroxene, and magnetite-biotite-garnet-orthopyroxene-plagioclase iron-rich metasedimentary rocks; protometatexite; metatexite; inhomogeneous diatexite; homogeneous diatexite; polyblastic (potassium feldspar, plagioclase, hornblende) metasedimentary migmatite; nebulitic to homophanous metasedimentary migmatite; metasedimentary migmatite tectonic breccia

**Felsic to Mafic Gneiss**

Leucocratic biotite-quartz plagioclase gneiss; mesocratic hornblende-quartz-biotite plagioclase gneiss; mesocratic to melanocratic quartz-hornblende-plagioclase-biotite gneiss

**Felsic to Intermediate Orthogneiss**

Biotite trondhjemite to granodiorite gneiss with stromatic granite leucosome occasionally augmented by ancillary diorite, quartz diorite, or hornblende-biotite tonalite; foliated to gneissic biotite trondhjemite to granodiorite; biotite-hornblende and hornblende-biotite tonalite gneiss

**Intermediate to Mafic Orthogneiss**

Amphibolite gneiss; hornblende-biotite and biotite-hornblende quartz diorite to tonalite gneiss; diorite to quartz diorite gneiss

pracrustal rocks may approach the  $1286 \pm 15$  Ma age determination of Tudor Formation metavolcanic rocks situated near Bancroft (Silver and Lumbers 1966, age was originally reported as  $1310 \pm 15$  Ma, however,  $1286 \pm 15$  Ma is the corrected age when recalculated using current decay constants). However, no equivalents of these metavolcanic rocks were encountered within the study area.

The Grenville Supergroup rocks occur mainly within the core zone of the Carlow synform and consist of a thin assemblage of diverse metasedimentary rocks, which continuously mantle the New Carlow syenite complex. The rocks mainly consist of carbonate metasedimentary rocks in the form of marble, marble tectonic breccia, calc-silicate skarn, and subordinate clastic metasedimentary rocks such as metapelite, impure carbonate-bearing psammitic metasedimentary rocks, and rare quartzite with interbedded para-amphibolite.

Syenitic rocks, which postdate the Grenville Supergroup, form a complex assortment of quartz-bearing to quartz-undersaturated compositions which comprise at least 9 recognizable units, encompassing a wide compositional range in terms of quartz:plagioclase:potassium feldspar ratios. Rock compositions encountered are syenite, monzonite, plagiostenite, quartz syenite, monzodiorite and granite. The New Carlow syenite complex is most renowned for spectacular corundum-bearing plagiostenites. Relative age relations of most units of this plutonic mass are difficult to unravel due to tectonic interlayering, virtual obliteration of primary igneous textures, and relatively poor exposure.

Metamorphic assemblage data suggest the presence of 2 distinct  $P$ - $T$  domains within the map area. Mineral assemblages of rare metapelitic rocks in the Grenville Supergroup indicate  $P$ - $T$  progression into the second sillimanite zone in absence of partial melting. Thus, metamorphic conditions were approximately  $T = 625$  to  $725^\circ\text{C}$  and  $P = 1$  to 3 kilobars. Metamorphism in the Madawaska Highlands gneissic complex is considerably more severe, as indicated by widespread migmatization of clastic metasedimentary rocks and sporadic appearance of orthopyroxene. A critical textural observation at the unique Hoare Lake cordierite-gedrite hypersthene gneisses suggests metamorphic conditions of  $T = 730$  to  $790^\circ\text{C}$  and  $P$  less than 6 kilobars. This assemblage, in association with metastable enclaves of sillimanite ± spinel ± corundum mantled by cordierite and kyanite enclosed by sapphirine, implies that the peak of metamorphism probably occurred in the intermediate pressure granulite field with  $T = 770^\circ\text{C}$  and  $P = 8.5$  kilobars.

All rock types, with exception of posttectonic granite pegmatite dikes of the Hybla swarm and rare olivine diabase dikes, have endured tectonometamorphic transformations relating to a protracted tectonic history featuring at least 4 regional folding events (Table 3).  $D_1$  is characterized by high-grade metamorphic layering in rocks of the Madawaska Highlands gneissic complex. Early folding ( $D_{2A}$ ), evidenced as rare isoclinal refolded structures, is strongly modified by  $D_2$ , a strongly penetrative, second or "typical Grenville" deformation event at about 1100 to 1050 Ma. This episode, mesoscopically evident in asym-

**Table 3.** Summary of tectonic features in the Wicklow and surrounding area.

	Madawaska Highlands Gneissic Complex	Grenville Supergroup
	Diabase dike intrusion	
	Faulting	
	Jointing	
	Retrogression, stabilization	
	Pegmatite dike intrusion, mainly along NE trends	
Main “Grenvillian” or “Ottawan” orogeny	D <sub>4</sub> : E–W and (?) NE–SW low-amplitude, noncylindrical macroscopic folding (F <sub>4</sub> ) with shallow-plunging hinges	
	D <sub>3</sub> : Megascopic to macroscopic, disharmonic, open to tight, upright to steeply inclined southeast-plunging folding (F <sub>3</sub> ) coaxial with L <sub>2</sub> mineral lineation	
	D <sub>2</sub> : Penetrative, high-grade L–S metamorphic fabric (S <sub>2</sub> ) with NE trend and shallow SE dip, containing an essentially down-dip mineral lineation (L <sub>2</sub> ) Disharmonic, asymmetric, tight to highly isoclinal mesoscopic folding (F <sub>2</sub> ). Transposition, detachment or truncation structures. Basement reactivation, northwest-directed transport of upper surfaces. Granite ( <i>sensu stricto</i> ) migmatization	
		Alkalic magmatism Basaltic dike intrusion Intrusion of gabbroic and trondhjemitic plutons
		D <sub>1G</sub> : Development of stratiform foliation (S <sub>1G</sub> ) within Grenville Supergroup rocks
	— PRESUMABLE UNCONFORMITY —	
	Retrogression, stabilization	
	D <sub>2A</sub> : Folding (F <sub>2A</sub> ) of metamorphic layering (S <sub>1A</sub> )	
	D <sub>1A</sub> : Development of high-grade metamorphic layering (S <sub>1A</sub> ) within rocks of different origin in the Madawaska Highlands gneissic complex	

metric, tight isoclinal folds with strong northeast vergence, imposed a strong L-S fabric on a broadly northeast-striking, macroscopic, first-order, structural trend. All deformed rocks bear the legacy of this major deformation in the form of a penetrative, shallow to moderate, down-dip, southeasterly plunging lineation, the regional significance of which was first documented by Hewitt (1962). A third major folding event (D<sub>3</sub>) is represented by upright, southeasterly plunging, macroscopic folds exemplified by the Carlow synform and Wicklow antiform, and exhibit coaxiality with a penetrative mineral lineation. The fourth folding event (D<sub>4</sub>) involves upright to reclined, mesoscopic, east-striking, subhorizontal warping about shallowly plunging axes.

## MESOPROTEROZOIC

### Madawaska Highlands Gneissic Complex

Map units mentioned in this section refer to Map 2550 (back pocket).

A complex gneissic mélange composed mainly of a tectonic admixture of supracrustal rocks (predominantly represented by migmatized metasedimentary rocks, map unit 4), reworked plutonic rocks (felsic to intermediate orthogneiss, map unit 2), a less deformed diorite-quartz diorite-tonalite suite (map unit 6), in addition to felsic to

intermediate plutonic rocks consisting of sodic granitoid rocks (trondhjemite-tonalite-quartz diorite, map unit 10) and potassic granitoid rocks (solely composed of various types of metamorphosed granites, map unit 9). Mafic to intermediate gneiss (layered amphibolite, map units 1a, 1d), mesocratic to melanocratic biotite and hornblende-biotite quartzofeldspathic gneiss (map unit 3) and massive amphibolite enclaves (map units 6g, 1d) also occur, but only rarely achieve dominance at a given exposure. Amphibolite enclaves of unknown origin are ubiquitous within the Madawaska Highlands gneissic complex. A strong lineation and/or gneissosity pervades most of geologic units constituting this gneissic *mélange*, with exception of the Little Papineau Lake plutonic complex, which is relatively massive to poorly lineated. The Madawaska Highlands gneissic complex has an overall intermediate composition. Diorite, quartz diorite, tonalite, and derived orthogneisses, and metasedimentary migmatite of mainly intermediate composition predominate over felsic, and hololeucocratic to leucocratic, plutonic rocks, such as granite and trondhjemite.

In many instances, the degree of deformation and metamorphism relating to the Grenville orogenic event (1000 to 1050 Ma, Moore and Thompson 1980; Moore 1982) is so severe that the protolith of many gneisses cannot be recognized. Deformation and metamorphism obliterated all primary textures and structures, and tectonically reduced grain sizes, such that a wide range of rock types possess an approximately similar grain size. Pervasive recrystallization resulted in interlobate and polygonal granoblastic textures. Widespread anatexis affected compositionally favourable rock types.

## MAFIC TO INTERMEDIATE GNEISS (Map Unit 1)

This lithologic group (map units 1a, 1b, 1d, 1e) occupies only a small portion of the map area, and occurs as mappable units at 7 scattered localities, as listed below in order of relative decreasing areal extent:

1. immediately west of Vanderbeck Lake
2. northwest of Yuill Lake
3. northeast of Kitts Lake
4. immediately east of the southeast end of Cardwell Lake
5. between Balsam Lake and Mill Pond
6. on Madawaska Highway, 1 km west of Hawk Lake
7. 400 m south of Franz Pond

## Amphibolite Gneiss

In most cases, these map units (1a, 1d) are dominated by an amphibolite component interlayered on a centimetre to metre scale with ancillary volumes of white-weathering, medium- to coarse-grained biotite, hornblende-biotite, and biotite-hornblende trondhjemite to tonalite leucosome

(“amphibolite gneiss”). This mobilizate is an integral component of amphibolite gneiss throughout the map area and usually occurs interlayered in volumes of 20% or less. Amphibolite gneiss enclaves represent a very widespread minor rock type, occurring in minor proportions in virtually all other major rock types of the Madawaska Highlands gneissic complex.

This amphibolite paleosome is usually massive to weakly lineated. A weak to moderate foliation may be present if appreciable amounts of biotite are present.

Three main petrographic variants of these rocks were recognized in the field:

1. common amphibolite  
(hornblende + plagioclase assemblages)
2. biotite amphibolite
3. diopside amphibolite

Common amphibolites, which constitute most modal analyses listed in Appendix 1a, are very widespread and consist almost exclusively of hornblende and plagioclase. Biotite amphibolites are defined by an appreciable modal amount of biotite (8 to 22%, *see* specimens 2A-2-7A, 3-11-26 and 4A-4-25 *in* Appendix 1a). Diopside amphibolites are relatively rare and are characterized by a distinct greenish cast on fresh surfaces. In the only sample analyzed modally, diopside makes up 13% of the rock (*see* Appendix 1a).

Biotite occurs as thin subhedral laths in the size range 0.4 by 0.04 mm to 2.5 by 0.5 mm defining the foliation or as coarser grained porphyroblasts with diameters between 2 and 6 mm. Some biotite amphibolites may represent products of potassium metasomatism as suggested by the presence of randomly oriented, relatively late, porphyroblasts of biotite. This metasomatism may have resulted from potassium-bearing fluids, likely ingressed from metamorphosed potassic granitoid suite rocks (map unit 9), which commonly exhibit a close spatial relationship with the amphibolite enclaves. An example of porphyroblastic biotite amphibolite is situated in a Highway 127 roadcut 1 km northwest of the intersection with the Madawaska Highway (*see* specimen 7-2-5B *in* Appendix 1a). Metasomatism is also suggested by the presence of 5 to 10% potassium feldspar, a mineral usually absent, or present only in trace levels, in most amphibolites.

Clinopyroxene, sporadically accompanied by orthopyroxene in localized splotches and discontinuous layers within amphibolites, gives the rocks a variegated appearance. The pyroxene-rich domains are light green and contrast markedly against the dark green to black colour of the amphibolite host. Hornblende content decreases drastically from approximately 50% within the amphibolite host to 10% or less within the pyroxene-rich domains, suggesting that pyroxene in the light green domains developed via hornblende decomposition.

Accessory minerals in the amphibolites of the Wicklow area include opaque iron oxide, titanite, apatite, pyrrhotite, pyrite, and rare scapolite and epidote.

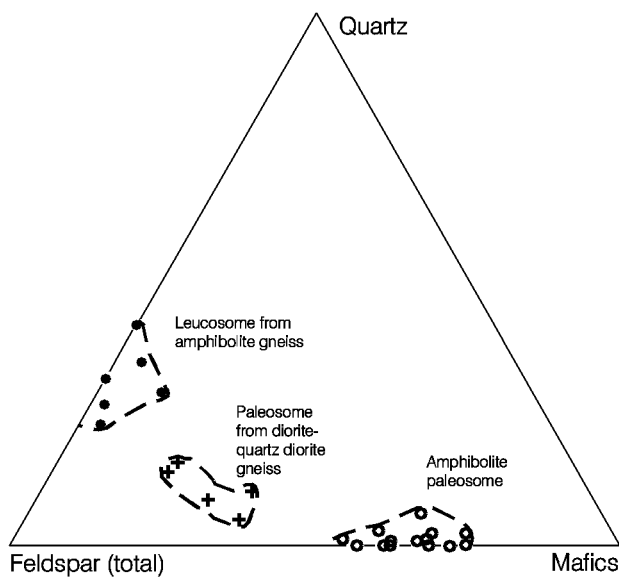
Colour index values of the amphibolite paleosome are generally quite high and modes plotted on Figure 4 define a field which is distinct from other mafic rocks, such as dioritic rocks (map unit 6), or paleosome from mafic to intermediate gneisses, that is, tonalite-diorite-quartz diorite gneissic suite (map unit 1b, *see* ensuing text; and *see* Figure 17 in “Petrology” of “Mafic to Ultramafic and Related Tonalitic Plutonic Rocks”).

Leucosomes developed within the amphibolites are generally hololeucocratic and trondhjemitic in composition (Appendix 1b) producing a well-defined field on Figure 4. Quartz contents are variable, but commonly approach and exceed 30%, a feature somewhat anomalous considering the relative paucity of quartz in the enclosing amphibolite paleosome.

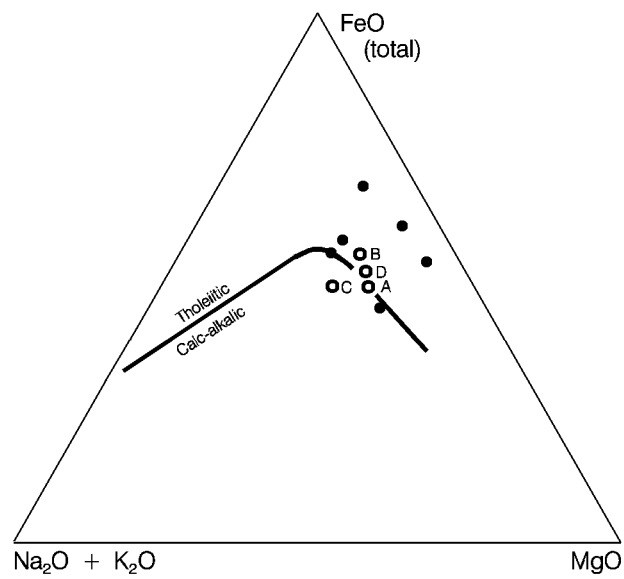
Amphibolite is also an important component in several exposures of tectonic breccia. Near Johnston Lake, rotated blocks of fine- to medium-grained, stictolitic diopside-garnet-biotite amphibolite (15 to 20%) are enclosed within poorly foliated, coarse-grained, biotite granite; the entire zone is at least 5 m in thickness. Protomylonite and mylonite textures are well developed in the granite host within 5 cm of the amphibolite inclusions. Quartz-rich biotite trondhjemite leucosome layers with 8 to 10 mm wide biotite-rich melanosomes are locally apparent within the amphibolite and are oblique to the foliation and gneissosity trends of the enclosing granite. This would seem to indicate that anatexis and high-grade metamorphism of the amphibolite blocks producing the leucosome-restite component predates the tectonic breccia event. This deduction has been supported in other tectonic breccia exposures within the area (*see* “Tectonic Breccia”).

Interesting stictolitic textures are well developed within the amphibolite blocks of this breccia exposure. These textures are characterized by 5 to 10 volume % of circular to elongate spots that are between 0.3 and 1.3 cm in diameter and contrast markedly against the dark biotite amphibolite host. The stictoliths, or flecks, were originated by porphyroblastic differentiation and are usually composed of a garnet (or rare diopside) core surrounded by a irregular shell of fine-grained, polygonal granoblastic plagioclase ranging from 0.5 to 1 mm in size. The garnets are usually ragged, xenomorphic, slightly poikilitic crystals with minor rounded inclusions of plagioclase, quartz and opaque iron oxide. They range in dimensions from 2 by 1.5 mm to 2 by 2.5 mm. Finer grained plagioclase (An<sub>60</sub>) varies between 0.15 by 0.17 mm to 0.6 by 1 mm grain dimensions. No quartz was observed within the outer plagioclase-rich shells of the stictoliths. Varied amounts of fine-grained, thin, subhedral biotite (1 to 5%), hornblende (1 to 5%), and opaque iron oxide (5 to 10%) occur within the outer shell. Hornblende exhibits a drastic decrease in both modal abundance and grain size compared with the amphibolite host (60% hornblende), suggesting that the development of the stictoliths was caused by metamorphic decomposition of hornblende.

The origin of the amphibolites is enigmatic. It is suspected that most are of mafic intrusive origin; however, severe tectonism has obliterated primary textures, structures and any critical crosscutting relations involving the major amphibolite units and various rock types enclosing them. In rare cases, interlayering with supracrustal rocks is apparent as at a Concession XII, Lot 23, Wicklow Township exposure on the Madawaska Highway. Here, a 3.5 to 6 m



**Figure 4.** Quartz–total feldspar–mafics (QFM) modal variation of leucosome and paleosome from amphibolite gneiss and paleosome of diorite-quartz diorite gneiss.



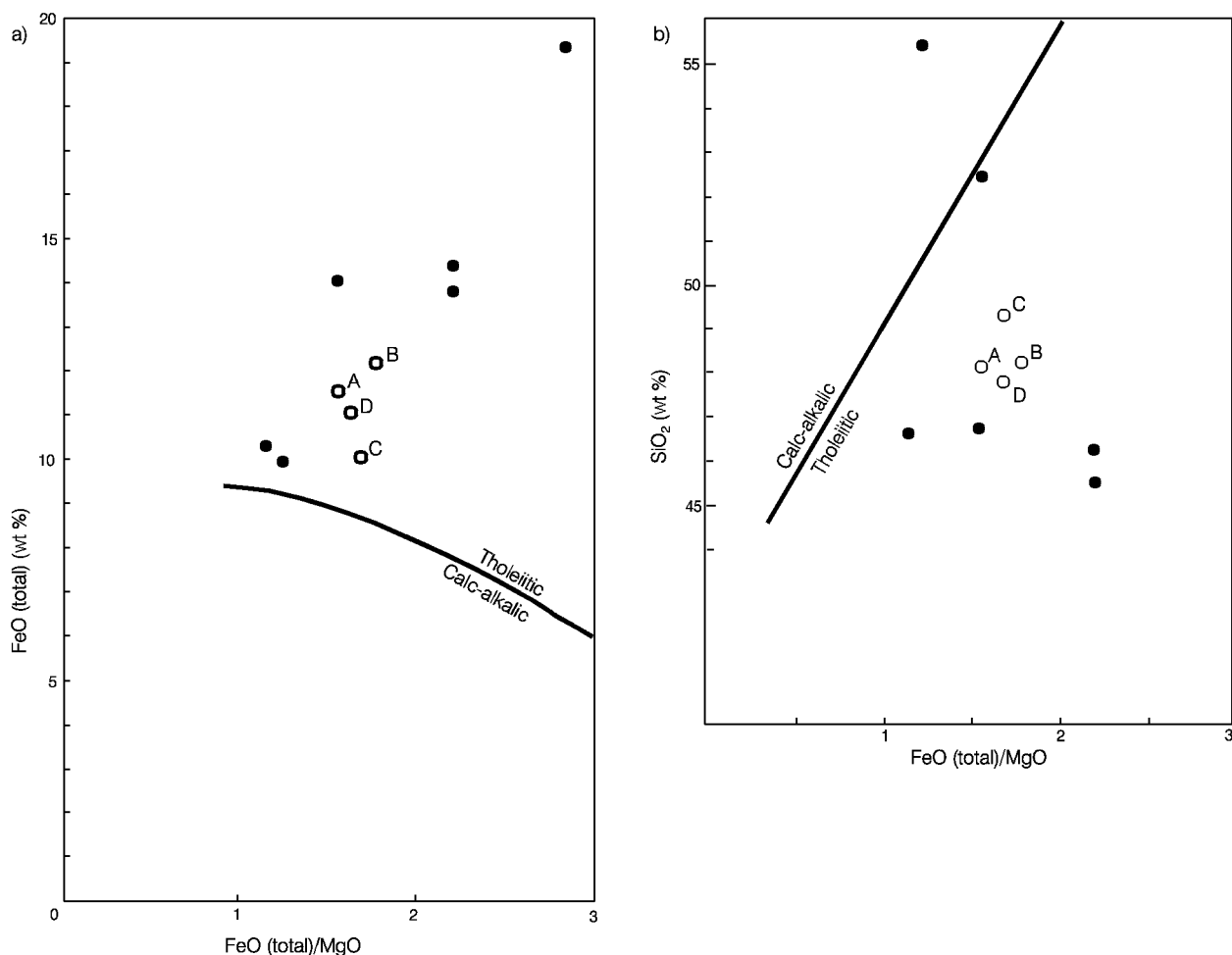
**Figure 5.** Total iron–magnesium–alkalis (FMA) plot (Irvine and Baragar 1971) of Wicklow area amphibolites. Analyses denoted by capital letter refer to Grenville Province amphibolites compiled in Appendix 3a.

wide metatextitic metasedimentary migmatite layer (20% of outcrop) is concordantly interlayered with fine-grained amphibolite containing 5 to 10% tonalitic leucosome. These relations, however, may be tectonic and do not necessarily imply a supracrustal origin for the amphibolite. A mafic metavolcanic origin can probably be ruled out since the nearest recognizable metavolcanic rocks are situated 18 km southeast of Maple Leaf in the Mallard Lake area (Hewitt 1955) and are probably of a younger geological age (Tudor Formation) than the amphibolite material of the Madawaska Highlands gneissic complex.

### PETROCHEMISTRY OF THE AMPHIBOLITE GNEISS

Four chemical analyses of amphibolite rocks from Wicklow area are presented in Appendix 2a and are compared, in Appendix 3a, with the mean values of amphibolites from the Grenville Province. Another 2 amphibolite specimens (HL-10, HL-11), contained within the unique Hoare Lake gneisses, were also analyzed (*see* Appendix 2e discussed in "Petrochemistry of the Hoare Lake Gneisses"). All analyses, except specimen 6-11-5D, plot within the tho-

leite field of the total iron–magnesium–alkalis (FMA) ternary diagram of Irvine and Baragar (1971) on Figure 5, and of the  $\text{FeO}_{\text{total}}/\text{MgO}$  versus  $\text{FeO}_{\text{total}}$  plot of Miyashiro (1974) on Figure 6a. This classification is also valid in the  $\text{FeO}_{\text{total}}/\text{MgO}$  versus  $\text{SiO}_2$  diagram of Miyashiro (1974) shown on Figure 6b. The only aberrant sample in the latter is specimen HL-10, which contains significantly higher  $\text{SiO}_2$  than the 5 other samples. Specimen 6-11-5D (*see* Appendix 2a) represents a diopside amphibolite dike which crosscuts syenitic dikes, both of which intrude carbonate-bearing psammitic metasedimentary rocks of the Grenville Supergroup. This amphibolite differs notably from the older amphibolites in the Madawaska Highlands gneissic complex. It contains less total Fe and more MgO (*see* Appendix 2a and Figure 5) with  $\text{SiO}_2$  and alkali levels being approximately similar. All amphibolite analyses differ from the average para-amphibolite of van de Kamp (1968). With the exception of the 2 amphibolites from the Hoare Lake gneissic suite, the analyses express an alkaline character on Figure 7, the  $\text{SiO}_2$  versus  $\text{Na}_2\text{O}+\text{K}_2\text{O}$  diagram of Irvine and Baragar (1971), as do all average Grenville amphibolite analyses listed in Appendix 3a.



**Figure 6.** a)  $\text{FeO}(\text{total})/\text{MgO}$  versus  $\text{FeO}(\text{total})$  plot, and b)  $\text{FeO}(\text{total})/\text{MgO}$  versus  $\text{SiO}_2$  plot for Wicklow area amphibolites. Analyses denoted by capital letters refer to Grenville Province amphibolites compiled in Appendix 3a. Both plots *after* Miyashiro (1974).

Most Wicklow area amphibolites, however, notably deviate from the various mean Grenville Province amphibolites (*see* Appendixes 2a and 3a, respectively) as indicated on the FMA,  $FeO_{total}/MgO$  versus  $FeO_{total}$  and  $SiO_2$  versus  $Na_2O+K_2O$  plots (*see* Figures 5, 6a and 7, respectively). This is possibly due to processes such as metasomatism and metamorphic differentiation.

Amphibolites of the study area, with the possible exception of biotite-rich amphibolites, for which no chemical analyses are presented here, chemically most closely resemble amphibolites derived from an igneous source. They are, therefore, interpreted as highly tectonized mafic dikes, and probably do not represent supracrustal rocks, since mafic metavolcanic rocks do not appear to be present in the Madawaska Highlands gneissic complex. Contrastingly, rare amphibolite dikes have been recognized in the area as, for example, within metasedimentary migmatite at Furz Mountain. This observation substantiates the authors' interpretation.

Amphibolites from the Madawaska Highlands gneissic complex all exhibit relatively flat, chondrite-normalized rare earth element (REE) patterns characterized by slight enrichment in light rare earth elements (LREE) over heavy rare earth elements (HREE) (Figure 8) as indicated by the low values and restricted range of  $La/Yb_N$  (2.2 to 6.1 in Appendixes 2a and 2e (*see* "Petrochemistry of the Hoare Lake Gneisses")). These rocks are enriched in total REE

(66 to 154 ppm) relative to chondrites, with enrichment factors of 26 to 82 times for La and 8 to 25 for Yb.

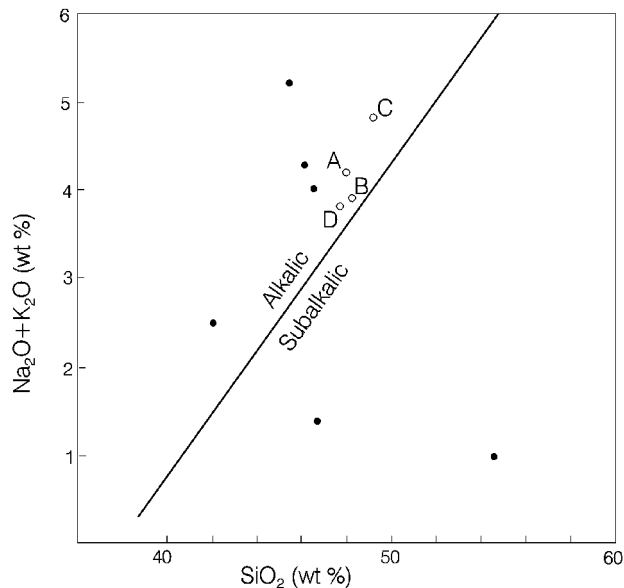
The dike cutting Grenville Supergroup metasedimentary rocks at locality 6-11-5D (*see* Figure 2) represents the most REE fractionated amphibolite, as indicated by the higher  $La/Yb_N$  ratio of 7.2.

Amphibolites from the Hoare Lake gneissic suite have lower total REE contents than the others, varying between 66 and 95 ppm. There may be slightly positive or negative europium anomalies ( $Eu/Eu^* 0.87$  to  $1.2$ ). Small negative anomalies characterize all other amphibolite analyses with  $Eu/Eu^*$  between 0.84 and 0.92.

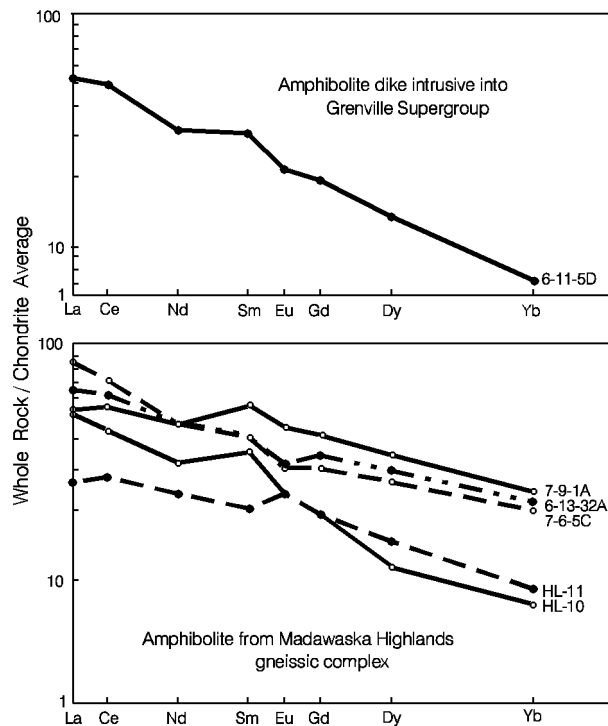
### Tonalite-Quartz Diorite and Diorite-Quartz Diorite Gneisses

Tonalite-quartz diorite-diorite gneissic (map units 1b, 1e) assemblages containing little amphibolite represent the other general type of mafic to intermediate gneiss unit within the map area and comprise 2 major variants:

1. hornblende-biotite and biotite-hornblende tonalite gneiss (CI 15 to 30) interlayered with subordinate biotite-hornblende diorite and white leucocratic to hololeucocratic granitoid leucosome and foliated hornblende-biotite trondhjemite (map units 1b).
2. diorite-quartz diorite gneiss (map unit 1e). Fine- to medium-grained biotite-hornblende and hornblende-biotite diorite and quartz diorite, inter-



**Figure 7.** Silica versus total alkalis plot (Irvine and Baragar 1971) for amphibolites from the Wicklow area. Analyses denoted by capital letters refer to Grenville Province amphibolites compiled in Appendix 3a.



**Figure 8.** Chondrite-normalized REE plots for amphibolites from the Wicklow area.

banded biotite trondhjemite, and medium- to coarse-grained deformed biotite granite.

These units are generally less abundant than the amphibolite-dominated mafic to intermediate gneiss. Rocks of map unit 1e, which are the most common of the 2 groups listed above, are well exemplified by an exposure on the extreme western point of the largest island in Balsam Lake. Quartz diorite gneiss here consists of 3 major components, intimately and regularly banded on a centimetre scale:

1. biotite-hornblende quartz diorite, fine grained
2. biotite trondhjemite, light grey (weathered surface), fine grained
3. hololeucocratic granite, medium- to coarse-grained, deformed, pervasively porphyroblastic with coarse augen-shaped potassium feldspar

This assemblage also contains small, dark green to black hornblende distributed in a train of highly flattened enclaves, fine-grained massive amphibolite and late-tectonic discordant hololeucocratic granite. It should be mentioned that one third of this outcrop on the south shoreline of the island in Balsam Lake is composed of homophanous meta-sedimentary migmatite (*see* "Metasedimentary Rocks").

Rocks of this group are especially common in the area north to northwest of Yuill Lake. Modal analyses of several diorite and quartz diorite paleosomes, presented in Appendix 1c, are mainly from this unit (specimens 1-6-4, 1-7-2, 1-8-2 and 1-8-3) and exhibit a distinctively lower colour index than paleosome from amphibolitic gneiss (*see* Figure 4).

Map unit 1b is less abundant than map unit 1e. Several exposures in the vicinity of the Madawaska Highway in Concession XII, Lot 22, Wicklow Township, can be regarded as typical. On the Madawaska Highway, approximately 3.5 km south from the north map boundary, a good outcrop of this gneiss is readily accessible. This lithologic assemblage consists of a interbanded, medium- to coarse-grained hornblende-biotite tonalite to quartz diorite, subordinate medium-grained biotite-hornblende diorite (30%) and coarse-grained leucocratic trondhjemite leucosome. Plagioclase and hornblende blastesis commonly affects these rocks.

White ovoid plagioclase and elongate subidiomorphic hornblende crystals achieve maximum dimensions of 10 by 13 cm and 3.8 by 7.7 cm, respectively. Plagioclase-rich, coarse-grained leucosome varies in quartz and colour index and is quartz diorite tonalite to trondhjemite in composition. It may be developed as irregular layers or as diminutive to extensive patches, the latter often enclosing rounded to agmatitic amphibolite and/or medium-grained diorite enclaves as within the aforementioned Madawaska Highway exposures. Scant enclaves of medium- to coarse-grained hornblende ultramafic rock are notable at this exposure.

## FELSIC TO INTERMEDIATE GNEISS (Map Unit 2)

This map unit occupies approximately 15 to 20% of the Madawaska Highlands gneissic complex, and occurs within several irregular belts of variable structural trend. It is interpreted in this study to predominantly represent migmatized metaplutonic rocks.

The most extensive belt containing these rocks trends south-southeast, 8 km from Wicklow Lake to Watson Lake. It structurally delineates a significant portion of the Wicklow antiform, being distributed along much of the eastern flank, the nose zone and part of western flanks near Back Lake.

This major belt of unit 2 rocks, between 1.3 and 2.8 km in width, may actually extend further south toward Cardwell-Haley Lakes area as suggested by small intermittent outcrops within this region of profuse glacial overburden. Its distribution is subsequently apparently severed by the southwest-trending straight gneiss tectonic domain (*see* "Structural Geology"). The belt may also coalesce with a narrow (280 to 800 m by 5 km) northeast-trending unit situated along a similarly trending portion of Little Papineau Creek, although interpretation is hampered once more by the Pleistocene glacial cover.

Other areas combining significant units of felsic to intermediate gneisses occur between Yuill Lake and Phillips Lake, in the Franz Lake-Brouse Pond area near Maple Leaf, in the Poplar Pond-Papineau Lake area, and in the vicinity of Furz Mountain.

In general, 2 lithologic groups can be recognized:

1. Trondhjemite to granodiorite gneiss: leucocratic  $\pm$  hornblende  $\pm$  diopside biotite trondhjemite and granodiorite paleosome (CI <10) with interlayered, relatively thin hololeucocratic to leucocratic biotite, biotite-hornblende, and hornblende-biotite granite leucosome (map unit 2a). Variants include: this gneissic type with ancillary diorite to quartz diorite (map unit 2b), or hornblende-biotite tonalite to trondhjemite (map unit 2c), and a relatively less gneissic variant of map unit 2a in which minor granite leucosome is apparent, causing a foliated to gneissic aspect to typical exposures. Amphibolite layers and enclaves may be present as a minor component within any of the above rock types.
2. Tonalite gneiss (map unit 2e): leucocratic biotite-hornblende and hornblende-biotite tonalite (CI 10 to 30) is interlayered with fine- to medium-grained biotite trondhjemite and fine-grained amphibolite. Lensoidal to stromatic leucocratic biotite and/or hornblende-bearing granite leucosome is responsible in part for the banding of these rocks. Massive, fine-grained amphibolite enclaves and layers are ubiquitous in both subgroups; however, these amphibolitic rocks rarely exceed more than 5%.

Many roadcuts exposing excellent outcrops of both general subgroups are situated along the Madawaska Highway, which trends approximately parallel to the Wicklow-Wat-

son lakes belt. Elsewhere, good exposures exist in the proximity of Franz Lake. The best exposures for further detailed section study are situated along the northwestern and western faces of Furz Mountain.

Stromatic migmatite structures prevail within both groups, marked by pervasive interlayering of paleosome and leucosome components (millimetre to centimetre spacing). Grey weathered surfaces of the trondhjemite to tonalite paleosome contrasts with the moderate to deep pink colouration of granite leucosomes. The leucosome component commonly constitutes 20 to 30% of a given gneissic exposure, and, in many cases, the diagnostic stromatic aspect is rendered cryptic or even obliterated by severe extension, isoclinal folds (with highly appressed limbs, and axial planes parallel to layering), later granitoid injection, and overprinting by porphyroblastesis (potassium feldspar, plagioclase and hornblende). In rare cases, thin (<5 mm) biotite-rich, fine- to medium-grained melanosome selvages are preserved along the paleosome-leucosome interface, for instance, in a hornblende-biotite tonalite gneiss exposed along the power line about 240 m southeast of the Highway 127–Madawaska Highway junction. However, in most instances, this component has been obliterated.

A characteristic exposure showing the diversity of the trondhjemite-tonalite gneisses is located at Yuill Lake (map unit 2e). As partly portrayed in Photo 3, a complexly interbanded suite of the following rock types was noted in this exposure:

1. hornblende-biotite tonalite, foliated, medium grained
2. biotite trondhjemite, relatively massive, fine grained, medium-grey on weathered surface
3. magnetite-biotite trondhjemite, fine to medium grained, with local coarse potassium feldspar porphyroblast and leucosome patches
4. amphibolite gneiss (<5%), fine- to coarse-grained amphibolite with rare 1 by 1 cm diopside porphyro-



**Photo 3.** Typical exposure of felsic to intermediate gneiss at Yuill Lake. Length of hammer about 0.3 m.

blasts interlayered with thin hololeucocratic white trondhjemite leucosomes

5. hornblende-garnet-biotite metasedimentary rock, fine to coarse grained, porphyroblastic (garnet, plagioclase)

This exposure clearly demonstrates the complexity and probable protracted evolutionary history implicit in many of the gneissic assemblages of the map area. Early isoclinal folding of trondhjemite leucosome layering within the amphibolite host is evident immediately right of the hammerhead in Photo 3. A later event of broad, open, S-type folding with west-plunging fold axes is superimposed over the early layer-normal compression event. These structural events are postdated by a coarse-grained, magnetite-biotite granite dike, obvious in the upper right-hand corner of Photo 3. Besides late to posttectonic granite dikes (map unit 11), scarce fine-grained biotite granite dikes (map unit 9d) were the only rocks types younger than the felsic to intermediate gneisses. A roadcut on the Madawaska Highway in Concession X, Lot 26, Wicklow Township, exposes a 0.6 to 1.2 m wide dike of biotite granite in sharp contact with deformed hornblende-biotite granite leucosome which may contain allanite within a hornblende-biotite tonalite gneiss. The granite dike itself exhibits a very subtle biotite lineation coaxial with regional lineation patterns and minor fold axes, suggesting an emplacement prior to cessation of the 1000 to 1050 million-year-old Grenville tectonometamorphic event.

Age relations with units other than the aforementioned granite dikes are dubious since all attendant geologic units display tectonic concordancy with the felsic to intermediate gneisses. This relationship can be seen on a Madawaska Highway roadcut in Concession IX, Lot 26, Wicklow Township, in which grey biotite trondhjemite gneiss paleosome (CI 5 to 10) containing 20 to 30% contorted layers of hornblende-biotite granite is broadly interlayered with fine- to medium-grained, weakly foliated hololeucocratic granite. The latter rock contains trace quantities of muscovite, biotite and allanite along with relatively large amphibolite enclaves.

In rare cases, calc-silicate skarn assemblages are locally contained within felsic to intermediate gneiss, for example, approximately 840 m southwest of Moore’s Pond. Here, a grey biotite trondhjemite gneiss with 20% medium- to coarse-grained, pink, hololeucocratic granite leucosome layers contains very local domains with the skarn assemblage diopside + hornblende + phlogopite + calcite + tremolite and possibly scapolite. Diopside nodules up to 5 cm across and containing at least 90% diopside with minor hornblende and phlogopite are also notable in the gneisses at this outcrop and appear to be related to a deformed granitic pegmatitic mass nearby.

Ultramafic enclaves are present in rare instances, such as on a small island immediately west of Davis Island in which 5 by 10 cm dark green enclaves contain the assemblage plagioclase + garnet + phlogopite + diopside.

## Modal Variation

In Appendix 1d, modal analyses of stromatic leucosomes and adjoining paleosome host components from typical felsic to intermediate gneissic rocks are presented. These data show a generally significant increase in quartz, potassium feldspar content and lower colour index of the leucosome relative to the paleosome, as also shown on the quartz–plagioclase–potassium feldspar (QPK) and quartz–total feldspar–mafic (QFM) ternary diagrams in Figure 9. The leucosome component is almost invariably hololeucocratic and granitic in composition. Although data are limited, the granitic compositions of these thin stromatic leucosomes are very similar to that of the more extensive sheets of metamorphosed potassic granitoid suite (map unit 9), possibly suggesting a common origin. Note also the general compositional disparity between leucosomes developed in felsic to intermediate gneisses compared with those derived in migmatized metasedimentary rocks (cf. Figure 9 with Figure 28 in “Petrology” of “Potassic Granitoid Suite”).

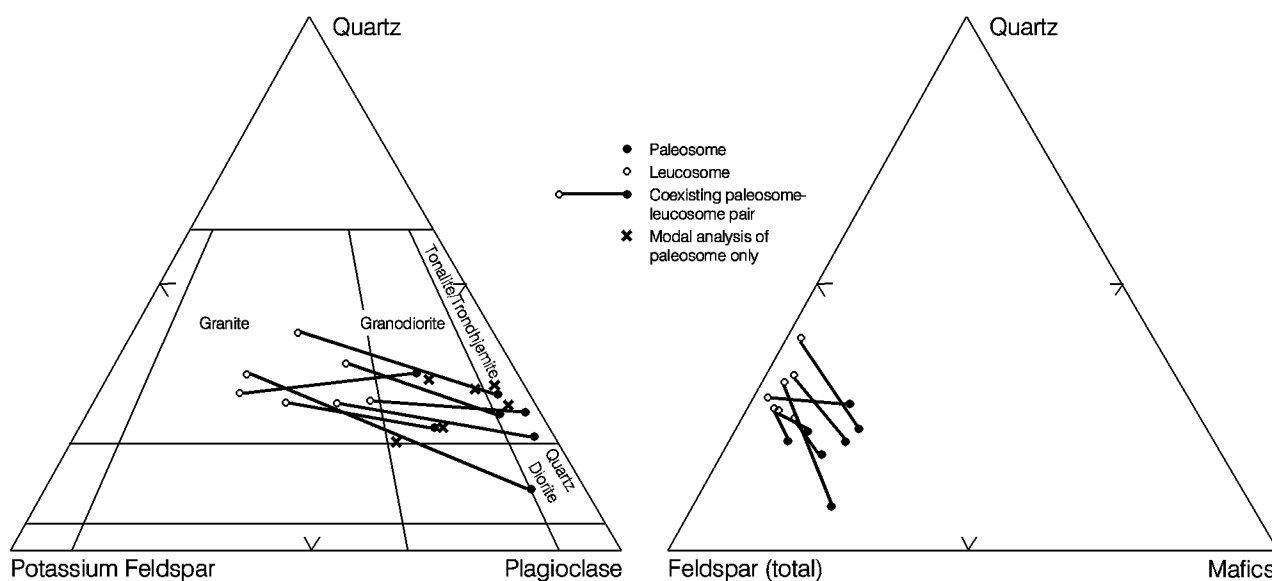
Modal variations of paleosome components from felsic to intermediate gneisses are presented in Appendix 1e. Paleosome compositions exhibit a relatively even split between granodiorite and trondhjemite fields when the additional data from Appendix 1c are plotted on the QPK plot (see Figure 9). An exception is specimen 5-8-1A (see Appendix 1d), which plots in the quartz diorite field. The colour index range of the paleosome is relatively small. Most specimens have colour indices between 10 and 23 as indicated on the QFM plot (see Figure 9).

## LEUCOCRATIC TO MESOCRATIC ± HORNBLende-BIOTITE-QUARTZ-PLAGIOCLASE GNEISS (Map Unit 3)

Gneiss of this category (map units 3b, 3c) is restricted mainly to exposures along Highway 127. An excellent roadcut is situated immediately north of Maynooth at a point where the Canadian National Railway tracks cross Highway 127. Layers of biotite-rich mesocratic (CI 40 to 60) migmatitic gneiss (map unit 3b) are usually less than 1 m thick and contain layered to podiform pink syenite to quartz syenite leucosome. The paleosome is fine to medium grained, and exhibits a well-developed lepidoblastic texture. These rock units possibly represent highly strained metamorphic derivatives of pelitic clastic metasedimentary rocks. A sedimentary origin is difficult to prove here since these units are complexly interleaved with a wide variety of contrasting rock types, a situation which differs from metapelites occurring in belt-like associations as with map unit 3.

In Appendix 2b, 3 chemical analyses of biotite-rich paleosome from this gneiss group are presented. Comparison with metasedimentary analyses in Appendixes 1f and 2c demonstrates a closer affiliation to metapelites than metawackses. However, some marked differences can be noted. The  $\text{Na}_2\text{O}/\text{K}_2\text{O}$  and  $\text{Al}_2\text{O}_3/\text{Na}_2\text{O}$  ratios are very similar to various metapelites in Appendix 2c, although absolute  $\text{Al}_2\text{O}_3$  contents are generally lower.

Concentrations of certain trace elements are greater in biotite gneiss (see Appendix 2b) compared with metasedimentary rocks in Appendixes 2c and 2d; for instance, Ba



**Figure 9.** Quartz–plagioclase–potassium feldspar (QPK) and quartz–total feldspar–mafic (QFM) modal variation of stromatic leucosome and coexisting paleosome from felsic to intermediate gneisses.

(3550 to 4310 ppm) and Sr (910 to 1390 ppm) and less commonly Cr (91 to 361 ppm) and Ni (96 to 220 ppm). The Ca/Sr ratios, in particular, are markedly lower in the gneiss than in the metasedimentary rocks. They are, on average, approximately one third that of metawackes or metapelites from the Wicklow area, and serve as the most useful discriminatory inter-element ratio (Figure 10). Calcium contents of the gneisses are markedly higher than in either metawacke or metapelite and serve as a distinguishing geochemical criterion.

## CLASTIC METASEDIMENTARY ROCKS OF THE MADAWASKA HIGHLANDS GNEISSIC COMPLEX (Map Unit 4)

### Distribution

The high- to granulite-grade, migmatized metasedimentary rocks of map unit 3 underlie much of the map area in proximity to Papineau Lake, and comprise a major portion of the Madawaska Highlands gneissic complex. These rocks are distributed mainly within a 10 km wide, complexly shaped belt which generally strikes west to southwest, and are interlayered with various other units of the gneissic complex. Regionally, these metasedimentary rocks extend beyond the eastern map limits toward Kamaniskeg Lake and Combermere (R.H. Thivierge, unpublished data, 1983; G.M. Stott, OGS, personal communication, 1983).

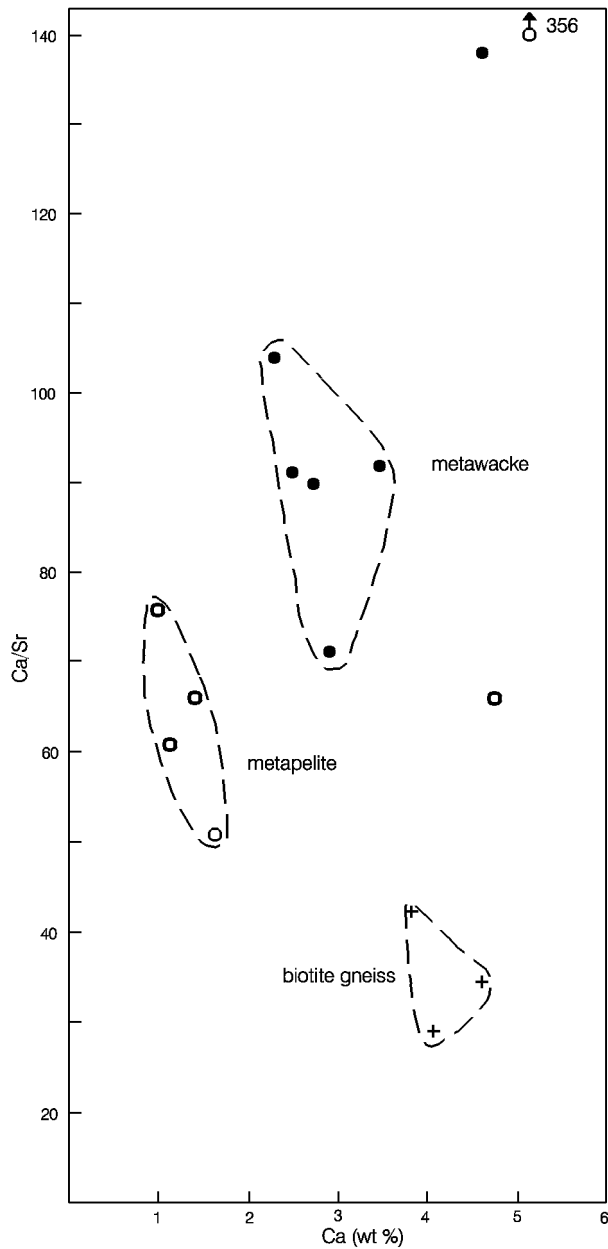
A major bifurcation probably occurs just beyond the eastern map limits, manifesting in a 1 to 1.3 km wide secondary belt trending west to southwest toward Cragg Pond, past Maple Leaf, before extending beyond the southern map limits near the Goodkey Creek–Papineau Creek confluence. Deflection in the trend of this belt is related to folding from the Carlow synform. Several secondary indentations are due to the intrusion of potassic granitoid rocks (map unit 9) like those immediately north-northwest of Davis Falls (Papineau Creek). A second, major, 1.3 to 2.7 km wide arm of the metasedimentary belt commences in the Phillips–Balsam lakes area and extends westward, possibly across the entire map area, through the northern part of Papineau Lake and thence between Yuill and Little Papineau lakes toward Little Papineau Creek. This metasedimentary belt may ultimately connect with similar migmatitic metasedimentary rocks in the Wicklow Lake–Moore Creek–McKenzie Lake area.

Less extensive occurrences of migmatitic metasedimentary rocks are exposed in the Indian–Back lakes area, proximal and immediately north of Mitchell Lake, north of Yuill Lake, within Little Papineau Lake plutonic complex near Moore’s Pond (local name), on Concession VII, Lots 18 to 20 in Wicklow Township near Little Papineau Lake Road, and as innumerable, local, centimetre- to metre-thick layers within felsic to intermediate gneissic suites as best seen in the Franz Pond area.

The thickness of the metasedimentary belts can only be estimated in one locality, that is, along the northwest face of Furz Mountain (local name) where approximately 50 m of sillimanite-garnet-biotite-potassium feldspar, and garnet-biotite, and hornblende-biotite metapelites are intercalated within trondhjemitic-tonalitic and mafic to intermediate gneisses (Figure 11).

### Migmatization

The metasedimentary rocks of the Madawaska Highlands gneissic complex differ from their Grenville Supergroup counterparts by displaying widespread evidence of migmatization. Metasedimentary migmatites in the map



**Figure 10.** Ca versus Ca/Sr variation in high-grade clastic metasedimentary rocks and biotite gneiss paleosome from the Madawaska Highlands gneissic complex.

area were classified according to the scheme utilized by Breaks, Bond and Stone (1978) to describe similar migmatites within the high-grade to granulite-grade terrane of the English River Subprovince of northwestern Ontario (see Table 3). As defined in the terminology section of this study, protometatexite and metatexite migmatite stages were most widely developed, whereas diatexite (map unit 4g) is only scantily apparent and is not an important map unit.

## Metasedimentary Metatexite

In their most pristine condition, metatexites are typified by 10 to 20% podiform and/or stromatically disposed, generally medium- to coarse-grained sodic granitoid leucosome hosted within fine- to medium-grained garnet-quartz-biotite-plagioclase and hornblende-quartz-biotite-plagioclase metapelitic paleosome. The best examples are situated in the McKenzie Lake area (Photos 4 and 5) and near Indian Lake (Concession VIII, Lot 31, Wicklow Township).

The protometatexite shown in Photo 4 occurs within a small domain showing transition from high to granulite metamorphic grade characterized by a breakdown of hornblende in the presence of quartz. Small, medium- to coarse-grained pods of trondhjemite leucosome contain stable orthopyroxene and magnetite (see specimen 2-1-9 in Appendix 1g), whereas, 120 m to the northwest, similar trondhjemite pods contain only hornblende and minor biotite as the stable mafic minerals.

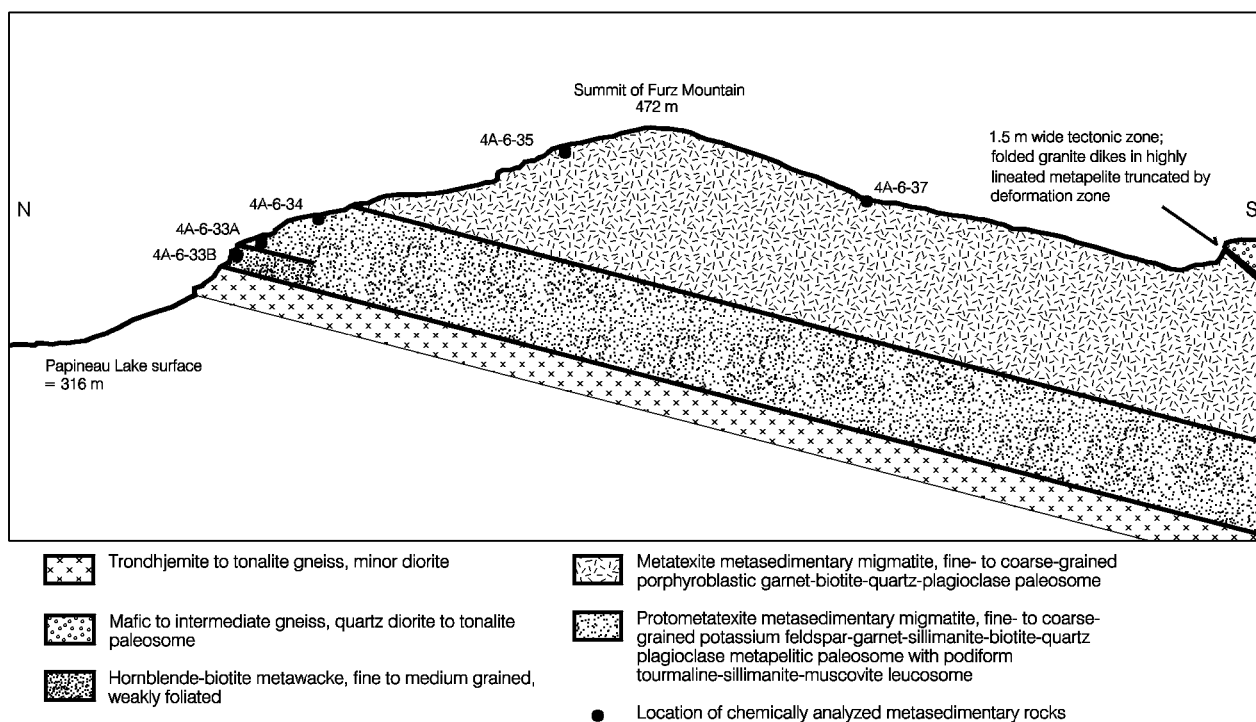
Several minor plutonic rocks intrude the metasedimentary sequence within the area; they are amphibolitized

layers and tectonized equivalents of possible former mafic dikes (map unit 6g), foliated biotite and hornblende-biotite granite (map units 9a, 9e), late-tectonic granite dikes (map unit 11), rare diabase dikes (map unit 12), and quartz veins.

Enclaves containing skarn assemblages occurring within the metasedimentary migmatite sequence are rare and of very localized extent. Diopside-scapolite marbles were encountered in roadcuts very near Balsam Lake. Diopside-rich stictolithic skarns are developed on the second largest island in Balsam Lake. Enigmatic mafic gneiss (map units 1a, 1d) also occurs locally within the metasedimentary rocks. The mafic gneiss tends to be more extensive than the mafic dikes as observed in the area southwest of Balsam Lake, and immediately east of Kitts Lake–Kitts Creek where a narrow, 3 km long unit occurs.

Smaller amphibolitic enclaves are relatively widespread in metasedimentary migmatite. Volumetrically, however, they comprise only a few percent of a given exposure. Quite possibly, these rocks represent severely tectonized, transposed mafic dikes because they are petrographically quite similar to deformed but continuous amphibolite dikes exposed near the summit of Furz Mountain and in the Centreview area.

Primary sedimentary structures and textures have been pervasively obliterated owing to the severity of tectonic deformation, high- to granulite-grade regional metamorphism and attendant blastesis, leucosome generation, and recrystallization processes. Possible bedding was encountered at one exposure situated on Highway 62, 1.8 km southwest of Maple Leaf. An enclave of metasedimentary



**Figure 11.** Geological cross-section at Furz Mountain, looking east, with locations of chemically analyzed metasedimentary rocks (see Appendixes 1f, 2c and 2d).

rock is contained within coronitic metagabbro and exhibits intercalated 5 to 10 cm wide fine-grained biotitic meta-wacke and thinner 2.5 cm wide medium-grained biotite-rich metapelitic layers which plausibly could be mimetic after original sedimentary bedding.

### Paleosome

Metasedimentary paleosomes are generally fine- to medium-grained, leucocratic to mesocratic rocks which typically weather light buff to locally rusty brown. More than one half of the modally analyzed specimens presented in Appendix 1f are mesocratic, although the colour index range is quite wide (15.8 to 59.4).

These rocks are usually lepidoblastic. Quartz lenses, which typically are 5 to 15 cm in length and 3 to 5 mm in width, may give the rock a banded appearance.

Advanced blastesis can destroy the usual fine- to medium-grained, biotite-dominant paleosome texture and render recognition of the rocks as clastic metasedimentary rocks difficult. The blastesis progressively converts the original metasedimentary rocks into an inequigranular, fine- to coarse-grained rock containing up to 40% phenoblasts that consist of plagioclase, and less commonly of potassium feldspar and hornblende (Photo 6). Allanite also occurs as phenoblasts (up to 8 by 10 mm), but only rarely.

The metatexites are commonly diablastic containing idiomorphic to subidiomorphic plagioclase and potassium feldspar. These minerals are commonly in the 1 to 3 cm diameter range and may be equant, elongate, ovoid, augen or sigmoidal in shape. Colouration of plagioclase can be semivitreous to opaque white, light orange, or faintly mauve. Potassium feldspar is usually light pink. The pronounced variability in appearance of metasedimentary metatexite as caused by advanced blastesis and deformation, can be comprehended by comparing medium-grained

paleosome of Photos 4 and 5 with the blastesis-dominated examples in Photo 6.

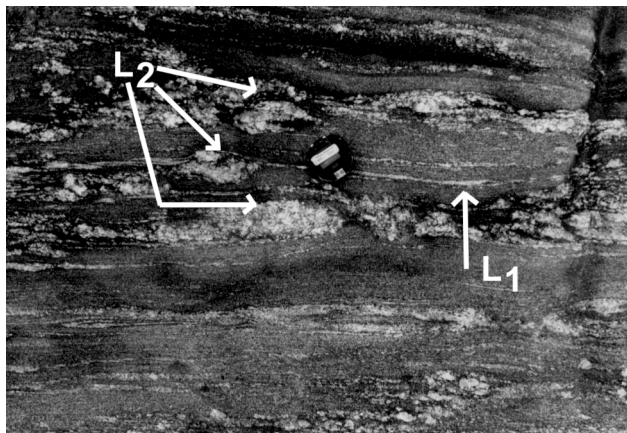
The development of porphyroblasts in metasedimentary migmatites is widespread, although it should be noted that greatest intensity of porphyroblastesis occurs proximal to tectonic zones of high strain as observed near the east shoreline of Papineau Lake in Concession X, Lot 3, in Bangor Township. Crystallization of porphyroblastic minerals may have, in part, been instigated by high strain developed within tectonic zones and thus appearance of such minerals on a great scale may potentially serve as an additional criterion to delineate such zones. It is interesting to note that other workers, such as A. Davidson and N.G. Culshaw, have observed a similar relationship between intense porphyroblastic crystallization and proximity of tectonic zones in several other areas of the Grenville Province (A. Davidson, N.G. Culshaw, Geological Survey of Canada, personal communication, 1983).

Quartz and plagioclase of the paleosome are granoblastic and typically in the 1 to 3 mm diameter range. They are rarely poikilitic, and usually relatively strain free. In a few places, undulose extinction and bent twin lamellae in plagioclase are notable. Biotite forms thin, subhedral, oriented laths typically measuring 0.8 to 1 mm by 0.1 to 0.2 mm and is mainly responsible for the pronounced lepidoblastic texture of the paleosome. Some samples that have a relatively high colour index and significant quantities of hornblende or sillimanite (*see* specimens 2A-2-4 and 4A-6-33A, respectively, in Appendix 1f) are somewhat nematoblastic.

Garnet is not very common in the paleosome of the rocks described here. In certain areas, however, for instance on Furz Mountain, garnetiferous rocks occur. Also, the unique gedrite-cordierite-hypersthene-garnet gneisses of possible metasedimentary affiliation near Hoare Lake, and some metasedimentary migmatites in the



**Photo 4.** Metasedimentary protometatexite of granulite grade at Concession I, Lot 28, Lyell Township near McKenzie Lake. Close-up of trondhjemite podiform leucosome indicates presence of coarse-grained dark orthopyroxene (in left centre of the photo). Coin has a diameter of 1.7 cm and marks the position of orthopyroxene-potassium feldspar-hornblende-quartz-biotite-plagioclase metapelitic paleosome.



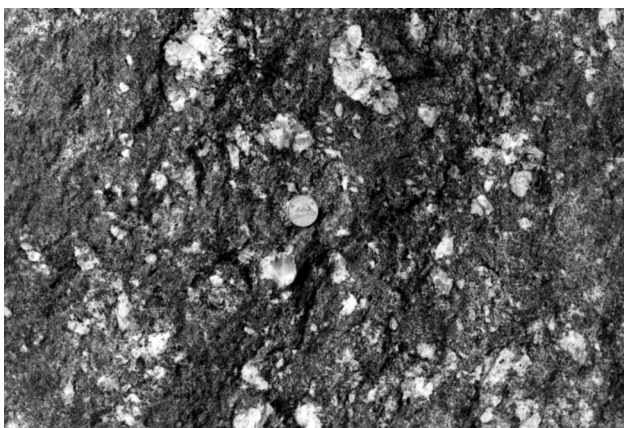
**Photo 5.** Metasedimentary metatexite on Concession I, Lot 27, Lyell Township near McKenzie Lake. Note the two distinct generations of leucosome as designated by L<sub>1</sub> (early leucosome, arrows) and L<sub>2</sub> (later leucosome generation). Toward the lower left-hand corner, isoclinal folding of L<sub>1</sub> can be seen.

Centreview–Balsam Lake area, contain significant amounts of garnet (maximum of approximately 17%, *see* specimen 4A-6-21 *in* Appendix 1f, from Furz Mountain). Garnet is typically red-brown, ovoid to rounded in shape, and commonly in the 3 to 7 mm diameter range. Extremely large poikiloblastic subidiomorphic garnets with diameters in the 3 to 5 cm range occur in unique iron-rich magnetite-biotite-garnet-orthopyroxene-plagioclase  $\pm$  quartz metapelites located on Concession VII, Lot 4, in Bangor Township south of McCastle Pond (*see* specimen 4A-6-21 *in* Appendix 1f). Garnet locally deflects the foliation surfaces that are primarily defined by biotite, and less commonly by accompanying hornblende and sillimanite. No pre-tectonic mineral fabric was observed within any of the garnet porphyroblasts examined in thin section. The main poikiloblastic inclusions within garnet are drop-like quartz (0.1 to 0.25 mm diameter) and plagioclase (0.2 to 0.4 mm diameter). Biotite and sillimanite may also occur, but are not common.

In several places, garnet probably grew at the expense of biotite as garnet poikiloblasts were noted to be surrounded by a thin 1 to 2 mm wide shell of polygonal granoblastic plagioclase and very minor biotite and iron oxide. An obvious depletion of biotite has developed within these leucocratic coronas as more biotite is present in immediate unaffected paleosome.

Hornblende is a common accessory mineral in the metasedimentary paleosome, and usually is present as subidiomorphic to xenomorphic grains in the 1 to 3 mm size range. Phenoblasts are less common and have been observed in sizes up to 0.7 by 1.5 cm.

Potassium feldspar is a widespread mineral in high-grade metasedimentary rocks although modal amounts are usually relatively low, very often less than 10%. This mineral is similar in size and shape to quartz and plagioclase. The general absence of aluminosilicates contacting potassium feldspar grains substantiates that most of the potassium feldspar originated by metamorphic reactions other



**Photo 6.** Diablastic metapelite from metasedimentary migmatite near eastern shore of Papineau Lake on Concession X, Lot 3, Bangor Township. Porphyroblasts consist of xenomorphic to subidiomorphic plagioclase and ancillary potassium feldspar. Diameter of coin is 2 cm.

than muscovite + quartz =  $\text{Al}_2\text{SiO}_5$  + potassium feldspar + vapour or melt. Much of the potassium feldspar could very well have been inherited as an original detrital phase, however, the absence of conglomeratic units renders it impossible to demonstrate whether detritus of potassic granitoid suite rocks was involved in the formation of the rocks.

Sillimanite is relatively rare, occurring in only 3 localities: on Furz Mountain (*see* specimen 4A-6-33A *in* Appendix 1f), proximal to the Hoare Lake gneisses at Centreview, and at an aforementioned roadcut on Highway 62, 1.8 km southwest of Maple Leaf. It occurs as robust, idiomorphic, vitreous white needles commonly in train-like aggregates, and comprises up to 15% as in the potassium feldspar-garnet-sillimanite-biotite-quartz-plagioclase metapelites on Furz Mountain. Maximum dimensions for sections normal to the *c* axis are 2.6 by 2.9 mm. Dimensions parallel to the mineral lineation rarely exceed 0.5 by 1 cm. The fine-grained, fibrolite form of sillimanite was not encountered within the study area. Sillimanite may be locally poikiloblastic, containing sparse quantities of rounded inclusions of quartz and zircon.

Additional accessory minerals are iron oxide, apatite, allanite, pyrite, zircon and tourmaline. Anhydrous iron oxide is by far the most common accessory mineral making up from <1 to 5% of the rocks. Apatite and zircon are relatively widespread as well, although generally very scarce within a given thin section. Apatite is commonly rounded to rarely euhedral hexagonal and is in the 0.4 to 0.6 mm diameter range.

Diminutive zircons are nearly a universal trace accessory in metasedimentary paleosome in the map area. This mineral, typically in the size range 0.04 to 0.18 mm, usually occurs as well rounded circular to elongate crystals and is the only mineral phase showing evidence of detrital origin.

## Leucosome

The leucosome component typically is a medium-grained, white-weathering, sodium-rich granitoid rock which falls into trondhjemite-tonalite or plagioclase-rich portion of the granodiorite fields (*see* Figure 28a *in* “Petrology” of “Potassic Granitoid Rocks”). Ubiquity of these rock compositions has also been verified by extensive hand specimen and some outcrop feldspar staining studies. At many outcrops, as near Davis Falls (local name) on Papineau Creek and in the Centreview area, a distinctive lustrous green colouration is evident on fresh surfaces, possibly due to extensive saussuritization of plagioclase. Textures vary from allotriomorphic-granular to interlobate-granoblastic. Accessory minerals include biotite, hornblende, magnetite, diopside and orthopyroxene, but most commonly consist solely of biotite.

In relatively weakly deformed rocks, for instance, near McKenzie Lake in the northwestern corner of the study area, evidence for 2 leucosome-forming events was observed (*see* Photo 5). Both leucosomes are of trondhjemitic composition. The first leucosome-forming event (L-1) is characterized by relatively thin, fine-grained, granoblastic

tic layers, which locally exhibit intense isoclinal folding. This early leucosome markedly contrasts against the more voluminous stromatic to podiform, medium- to coarse-grained trondhjemite leucosome (L-2) formed during a later metamorphic episode. L-1 leucosomes are locally deflected around L-2 leucosome pods, as can be seen immediately right of the coin in Photo 5.

### Modal Characteristics of Metasedimentary Paleosome

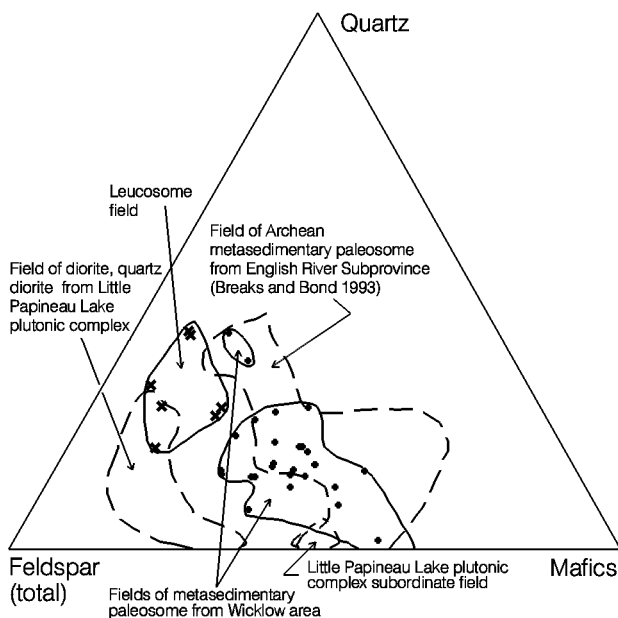
In Appendix 1f, 26 modal analyses of paleosome variants encountered within the study area are listed. These data are plotted on a QFM diagram (Figure 12), which documents a rapid decrease in quartz content with increasing colour index for the metasedimentary paleosome. Some compositional similarity is shared with Archean clastic metasedimentary rocks from the high-grade to granulite-grade northern supracrustal domain of the English River Subprovince as studied by Breaks and Bond (1993). Approximately 70% of the Grenville Province metasedimentary paleosome samples fall within the Archean metasedimentary field. It should be noted that the Archean field is somewhat more extensive than the field occupied by the Wicklow area metasedimentary rocks within the QFM ternary plot. A major difference not shown on this diagram is the common presence of hornblende in these Grenville Province metasedimentary rocks, a mineral virtually absent from metawackes and metapelites of the Archean rocks, which probably can be attributed to a relatively higher calcium content of the Wicklow area metasedimentary units. Metasedimentary rocks from the study area contain more quartz and less total feldspar for a given colour index value

than the diorite, quartz diorite, tonalite, and trondhjemite of the Madawaska Highlands gneissic complex (see Figure 12).

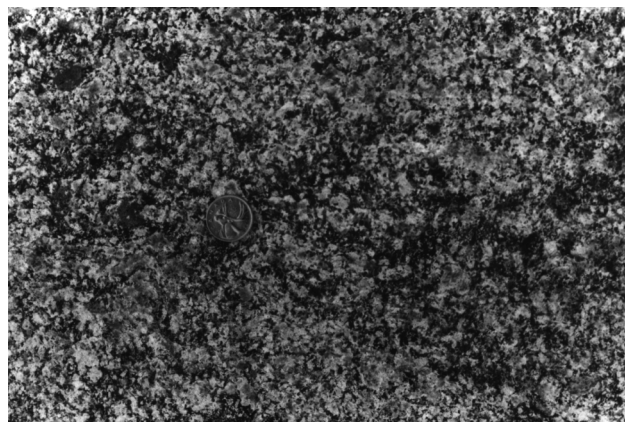
### Homophanous and Nebulitic Metasedimentary Migmatite

These rocks are essentially confined to a narrow 240 to 500 m wide unit trending from the eastern map limits at Purdy, west toward Theresa’s Pond (local name) and Davis Pond. Through advanced paleosome blastesis, an increase in leucosome volume and tectonic reduction in the grain size of stromatic leucosome, metasedimentary metatexite can be converted into nebulitic and homophanous migmatite as described by Mehnert (1971, p. 40-42). During the process, the petrographic characteristics of paleosome and leucosome components become progressively “blurred”. Homophanous migmatites (map unit 4m) represent the most difficult evolutionary stage to recognize, since, in these rocks, the blastesis has created a homogeneous to vaguely banded “plutonic” appearing rock (Photo 7). Nebulitic migmatites also contain a significant amount of granitoid material, but, more commonly, exhibit biotite mafic schlieren, and relatively resistant biotitic paleosome layers.

In some homophanous migmatites, as exposed near Purdy on Highway 62, a vague banding is evidence of the original stromatic layering. The leucosome component of the homophanous migmatites differs drastically in terms of modal QPK contents from the metamorphosed potassic granitoid suite rocks (map unit 9) even though these 2 lithologic groups commonly show a close spatial relationship, as seen in the Theresa’s Pond area (see Appendix 1g; see also Figure 28 and Appendixes 1n, 1o and 1p in “Petrology” of “Potassic Granitoid Suite”). The mineralogy, that is, the trondhjemite character of the homophanous migmatites, is identical with the stromatic leucosome of metasedimentary metatexites.



**Figure 12.** Quartz–total feldspar–mafics (QFM) modal variation of paleosome and leucosome from Wicklow area metasedimentary migmatites, and comparison to Archean metasedimentary migmatite paleosome from the English River Subprovince.



**Photo 7.** Homophanous metasedimentary migmatite of trondhjemite composition near South Papineau Lake Road, Concession X, Lot 3, Bangor Township. Vague clots of metasedimentary paleosome can be seen, however, blastesis has increased the grain size of these scarce nebulitic paleosome remnants to closely match that of the leucocratic parts of this rock. Diameter of coin is 2.3 cm.

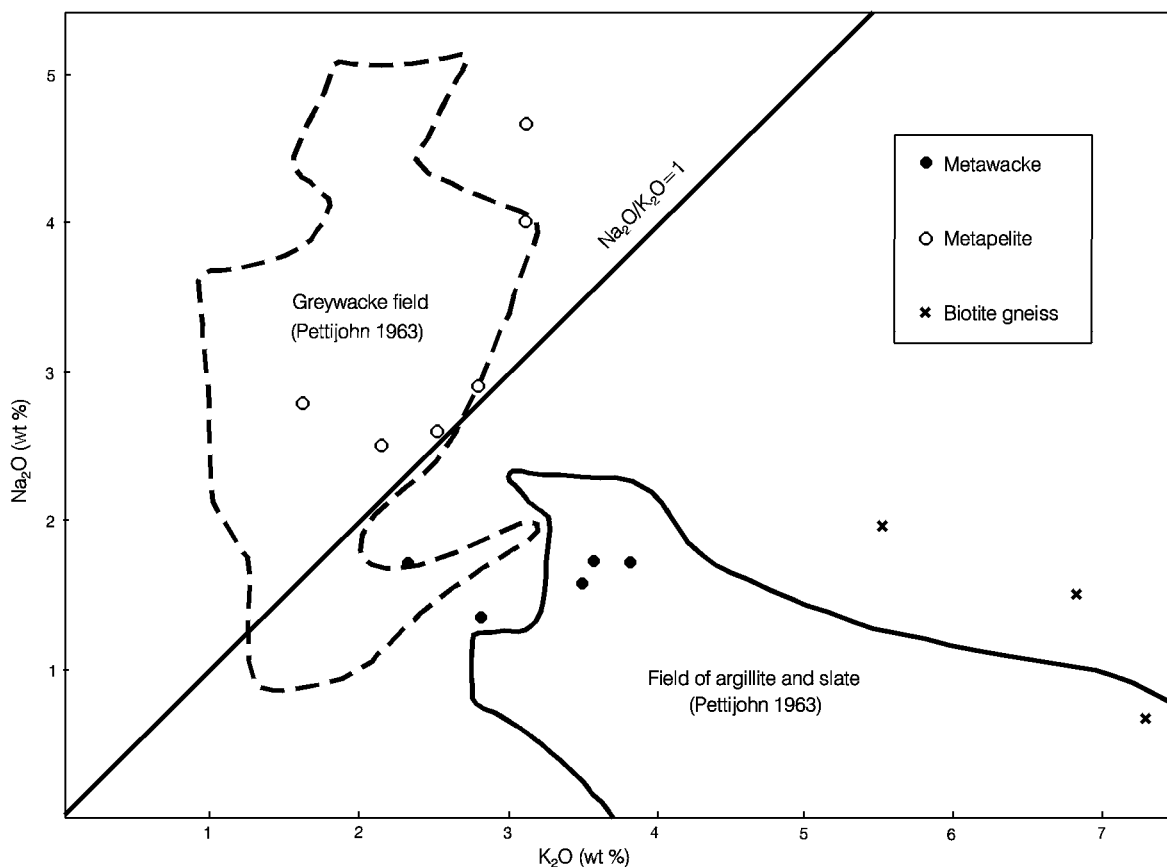
## Petrochemistry of Metasedimentary Rocks from the Madawaska Highlands Gneissic Complex

Eleven clastic metasedimentary rock samples from the Madawaska Highlands gneissic complex have been analyzed for major and selected trace elements. The chemical analyses are listed in Appendixes 2c and 2d. Chemical classification of these rocks has been attempted in Figures 13 and 14, utilizing the  $K_2O$  versus  $Na_2O$  and  $SiO_2/Al_2O_3$  versus  $Na_2O/K_2O$  plots, respectively, of Pettijohn (1963), bearing in mind that Na and K, in particular, may be susceptible to mobilization under conditions of diagenesis, metamorphic differentiation (development of plagioclase, potassium feldspar and hornblende porphyroblasts) and anatexis. The authors tried to minimize the influence of the latter 2 effects as much as possible by selecting relatively homogenous fine-grained samples, which are relatively devoid of anatectic products, as represented by the trondhjemite leucosome. The  $SiO_2/Al_2O_3$  versus  $Na_2O/K_2O$  diagram is useful in testing chemical maturity of sandstones, according to Pettijohn, Potter and Siever (1972). High-grade clastic metasedimentary rocks from the Wicklow area (see Appendixes 1f and 1g) plot almost entirely in the greywacke field (see Figure 14). Although this diagram suggests that clastic metasedimentary rocks are of the im-

mature greywacke type association, no chemical discrimination between greywacke and pelitic compositions is possible for the Wicklow rocks.

According to Pettijohn (1963), excess of Na over K represents one of the prime geochemical characteristics of metawackes. Contrastingly, Na:K ratios of metapelites (mudstones, slates, argillites) usually fall below one. Most samples can be classified as either metawacke or metapelite (see Figure 13). Obvious sillimanite-garnet-biotite metapelites (see specimens 4A-6-33A, 4A-6-34 in Appendix 2c) plot outside Pettijohn's metapelite field and fall within and near the boundary of the low Na/K end of his greywacke field. Other disparities relate to rocks containing very high  $K_2O$  contents. This can be seen, in Appendix 2b, in analyses of biotite gneisses, which contain  $K_2O$  contents between 5.5 and 7.3%. These rocks all have probably endured chemical changes during deformation and metamorphism.

Exotic analytical results (specimens 7-9-1C and 7-9-2) were omitted in the computation of average metawacke and metapelite compositions in Appendix 3b. Pettijohn (1957, p. 509) suggested the  $Al_2O_3/Na_2O$  ratio as a useful index of metasandstone maturity. Possible metawackes from the map area listed in Appendix 2d exhibit a restricted range in  $Al_2O_3/Na_2O$  ratios with the average value of 5.2 very close to Pettijohn's greywacke average of



**Figure 13.**  $K_2O$  versus  $Na_2O$  classification of high-grade clastic metasedimentary rocks and biotite gneiss from the Wicklow area. Greywacke and argillite-slate fields are drawn on the basis of data plotted in Figures 2 and 3 of Pettijohn (1963, p.58).

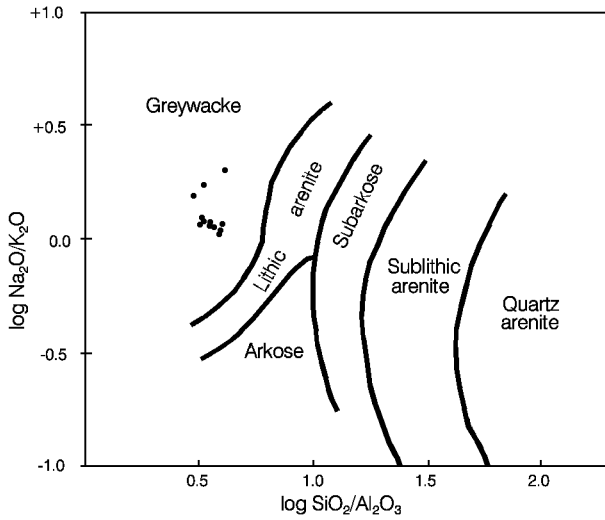
4.8. Contrastingly, the probable metapelites (see Appendix 1g) display a considerably wider range (8.4 to 20.5) with a significantly higher average (10.4).

On the FMA diagram (Figure 15), the Wicklow-area clastic metasedimentary rocks overlap with Archean counterparts from the English River Subprovince, although a tendency toward higher total iron contents can be noticed in rocks of the map area. Also notable is the slight to moderate Mg enrichment in the biotite gneisses of map unit 3.

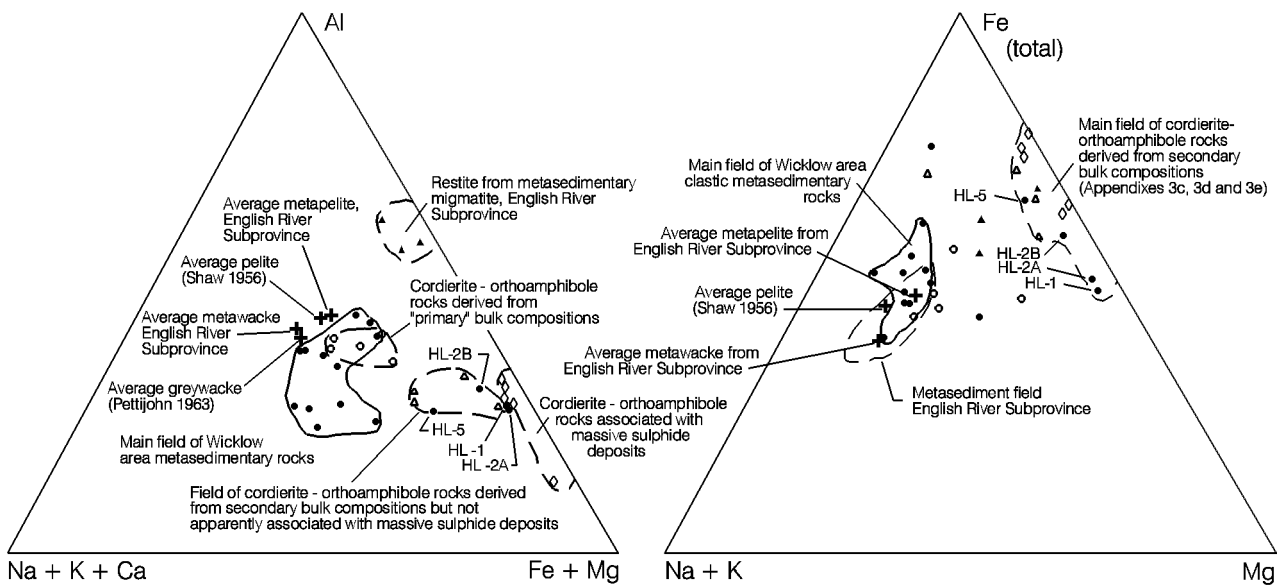
In Appendix 3b, mean bulk compositions of average Wicklow-area metawackes and metapelites are compared with those of similar rocks from the literature. The average metawackes from the Wicklow area are notably lower in SiO<sub>2</sub> and enriched in Al<sub>2</sub>O<sub>3</sub>, CaO, Fe<sub>total</sub> and TiO<sub>2</sub> compared to Archean counterparts and the average greywacke of Pettijohn (1963). Levels of Na<sub>2</sub>O and K<sub>2</sub>O are approximately similar. The average Wicklow metapelite exhibits higher SiO<sub>2</sub>, TiO<sub>2</sub>, and CaO and lower Al<sub>2</sub>O<sub>3</sub>, Na<sub>2</sub>O, and K<sub>2</sub>O contents than rocks of either mean Archean or Proterozoic metapelitic compositions. The apparent depletion of CaO in both metasedimentary groups from the study area is modally reflected by widespread hornblende, a mineral that is commonly absent from Archean metasedimentary rocks such as those from the English River Subprovince (Breaks and Bond 1993). On the Ca versus Ca/Sr plot (see Figure 10), one can discriminate between metawacke, metapelite and the enigmatic biotite-rich gneisses (map unit 3), although additional data are needed to more confidently define the 3 fields.

### Hoare Lake Gneisses

These gneisses are part of the Madawaska Highlands gneissic complex, are enclosed by high-grade migmatized pelitic metasedimentary rocks of the Centreview area, and underlie only a very small portion of the map area. They are of considerable interest to metamorphic petrologists, however, owing to the unique coexistence of gedrite, hypersthene and cordierite. These intermediate-pressure granulite-grade rocks also contain metastable traces of kyanite, sillimanite and sapphirine. The gneisses are exposed in 9 small outcrops traceable over a strike length of about



**Figure 14.** SiO<sub>2</sub>/Al<sub>2</sub>O<sub>3</sub> versus Na<sub>2</sub>O/K<sub>2</sub>O diagram for high-grade clastic metasedimentary rocks from the Wicklow area (after Pettijohn, Potter and Siever 1972, p.62).



**Figure 15.** Al-(Fe+Mg)-(Na+K+Ca) and Fe (total)-Mg-(Na+K) (FMA) ternary diagrams showing petrochemical variation (weight percent) of Wicklow area metasedimentary rocks and Hoare Lake cordierite-gedrite-hypersthene gneisses as compared to similar rocks from the literature. Symbols: •, Wicklow area clastic metasedimentary rocks including Hoare Lake gneisses, the latter denoted by HL-1, HL-2A, HL-2B, HL-5; ○, cordierite-orthoamphibole rocks derived from “primary” bulk compositions; ◇, cordierite-orthoamphibole rocks associated with volcanogenic massive sulphide deposits; △, cordierite-orthoamphibole rocks derived from secondary bulk compositions, but not apparently associated with massive sulphide deposits; ▲, restite (garnet-plagioclase-sillimanite-cordierite-quartz) from metasedimentary migmatite of the English River Subprovince.

240 m and width of 200 m. Extension of these gneisses beyond the eastern map area limits is quite possible. Intercalation of several rock types is notable and is shown on a detailed map of one of the outcrops (Figure 16). These units (*see* Figure 16) are discussed in this section of the study. The area underlain by these gneisses has been mapped in detail by Miller (1983) who delineated 6 distinct interlayered rock units (Table 4). With the exception of the amphibolite layers, these rock units are variably affected by weathering. Garnet-rich restite units are most notably weathered and it is virtually impossible to collect fresh material.

Unit 4d, Map 2550, which corresponds to gneiss unit 5 (*see* Table 4) represents the main occurrence of hypersthene, cordierite and gedrite. This unit is restricted to 4 outcrops, which mostly exhibit a relatively fresh mauve-brown to brown-black colouration depending upon local proportions of cordierite, hypersthene and gedrite. As

shown on Figure 16, these rocks exhibit an irregular, 4 to 6 cm wide, mineralogical layering defined by a diffuse physical separation of the major megascopic mineral assemblages:

1. biotite + plagioclase + quartz + garnet
2. biotite ± garnet + plagioclase + cordierite + gedrite + hypersthene

This banding is clearly truncated by 0.5 to 1 m wide, irregular masses of medium- to coarse-grained, quartz-rich mobilizate composed of the assemblage: gedrite + biotite + plagioclase + cordierite + garnet + quartz. This particular mobilizate is readily discernable by its coarse grain size, euhedral plagioclase megacrysts and clear, indigo-blue, coarse anhedral cordierite which locally is 10 by 15 cm in size. Tonalitic mobilizate compositions also exist (gneiss unit 4A *in* Figure 16 and Table 4); however, these appear to be mainly restricted to interlayering with amphibolite, plagioclase-quartz-garnet-biotite restite (gneiss unit 3 *in* Fig-

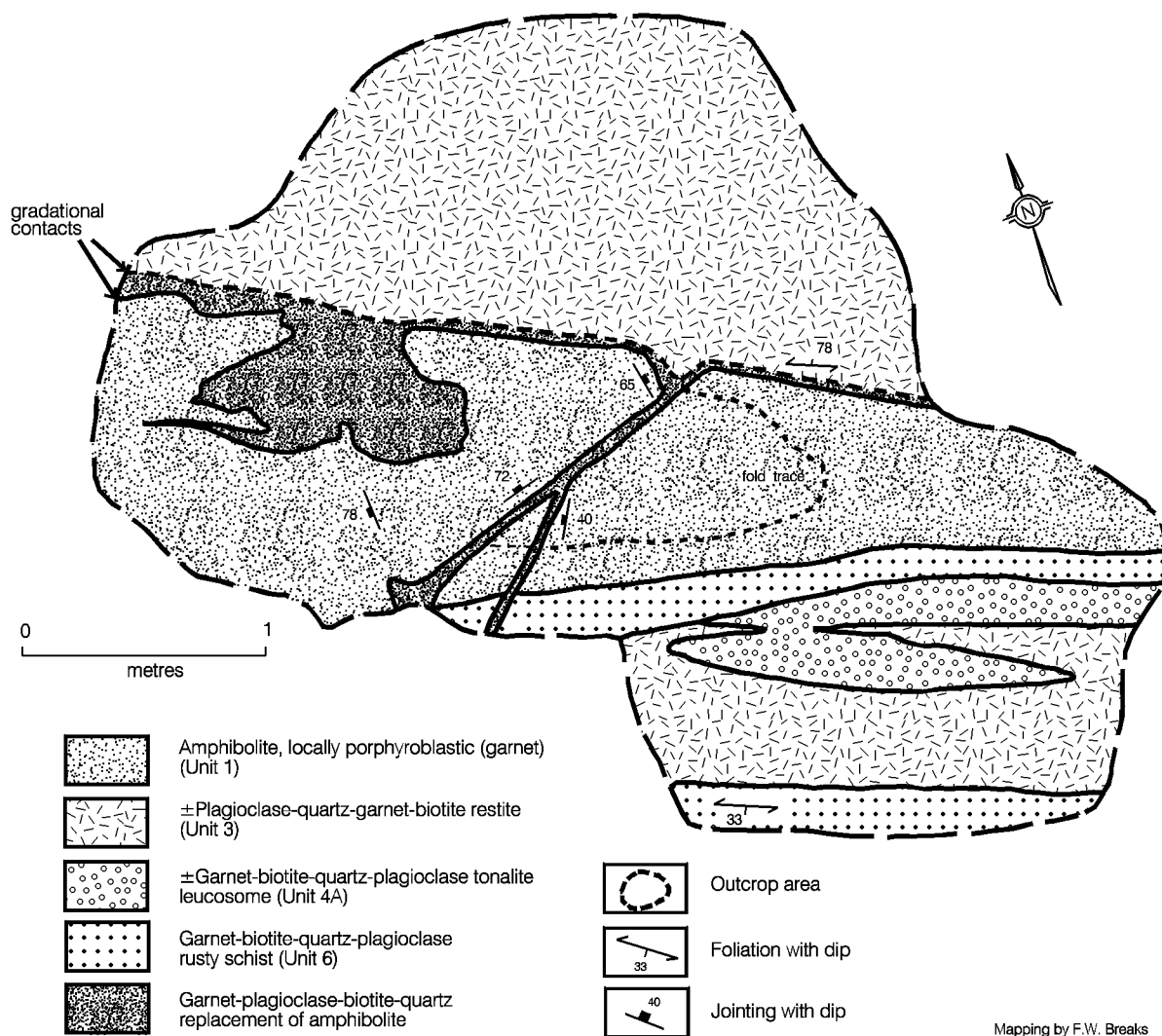


Figure 16. Detailed geology of part of the Hoare Lake gneisses.

**Table 4.** Main rock types of the Hoare Lake gneisses.

Unit Number	Lithology	Specimen Number in Appendixes 1h and 2e	Comments
Unit 1	Amphibolite layers, fine to medium grained, locally porphyroblastic (garnet), 0.5 to 2 m width, vaguely folded	HL-10, HL-11	Local replacement by garnet-plagioclase-biotite-quartz orthopyroxene
Unit 2	± Biotite-garnet-quartz-orthopyroxene-plagioclase quartz diorite, maple-brown weathered surface, >1 m width	HL-5	
Unit 3	± Plagioclase-quartz-garnet-biotite restite, medium to coarse grained	HL-8A	
Unit 4A	± Garnet-biotite-quartz-plagioclase tonalite leucosome, white weathering, leucocratic, allotriomorphic to hypidiomorphic granular, medium to coarse grained	HL-8B	Diffusely interspersed throughout Unit 3 as lenses and pods. May also contain quartz-rich layers.
Unit 4B	Mobilizate assemblages orthoamphibolite-orthopyroxene-cordierite-garnet-quartz-plagioclase occur in 1 to 2 cm wide layers in Unit 5, medium to coarse grained; white weathering	HL-2B	
Unit 5	± Biotite plagioclase orthoamphibole-cordierite-orthopyroxene gneiss, medium to coarse grained, melanocratic, granoblastic to nematoblastic	HL-1, HL-2A	Main unit containing cordierite and orthoamphibole.
Unit 6	Garnet-biotite-quartz-plagioclase schist, rusty weathering, well foliated		

ure 16 and Table 4), and rusty almandine-biotite schist (gneiss unit 6 in Figure 16 and Table 4).

Gedrite is mainly confined within large, dark, brown-black, irregular clot-like aggregates up to 3.5 by 11 cm that contrast with the mauve-brown colouration of the encompassing finer grained cordierite-hypersthene-rich domains. These clots consist essentially of coarse, fibrous, subhedral, dark, black-brown gedrite with individual crystals measuring up to 0.7 by 3 cm.

Cordierite is generally anhedral, light mauve on clean weathered surfaces, and falls mainly into a 1 by 1 mm to 6 by 8 mm size range. Texturally, it occurs in 2 situations. First, it occurs as medium-grained crystals disseminated uniformly with orthopyroxene of approximately similar size.

The second textural variant of cordierite forms lensoidal polycrystalline aggregates measuring up to 1 by 4.2 cm contained within domains defined by high abundance of coarse, fibrous gedrite. The lensoidal cordierites actually form a complex symplectite with sillimanite, spinel and rare corundum. The latter 3 minerals always occupy the central confines of lensoidal cordierite aggregates and probably represent metastable relicts with respect to gedrite, hypersthene, biotite and garnet, which occur adjacently. The sillimanite-spinel-corundum cores (up to 1.2 cm by 0.4 cm) are conspicuous on clean weathered surfaces. They exhibit a faint green colour, which can be related to the scant quantities of green to dark green, fine-grained, glossy, anhedral spinel. Spinel is largely enclosed within the coarsely crystallized sillimanite; however, it may be distributed along the contacts between cordierite and sillimanite.

Garnet is usually medium- to coarse-grained, nonpikilitic, subhedral to anhedral, equant to ovoid, deep red-brown, and generally ranges in size from 2 to 6 mm, and locally up to 0.7 by 1.6 cm. In gneiss unit 3 (see Figure 16 and Table 4), this mineral is anhedral and occurs in masses of fine- to medium-grained biotite or in quartz masses, accounting for about 30% of the mode (Appendix 1h). Scant, fine-grained intergrowths of sapphirine completely mantling kyanite have been recognized microscopically by Miller (1983) and apparently are only contained within garnet.

Amphibolite layers locally exhibit a partial genetic connection in derivation of hypersthene-bearing assemblages as documented on Figure 16. This is revealed by embayments into amphibolite layers that contain the replacement assemblages garnet + plagioclase + biotite + quartz + orthopyroxene and plagioclase + biotite + quartz + orthopyroxene. A transgressing vein (see Figure 16) that bifurcates seems to imply a metamorphic reaction involving hornblende decomposition, such as, hornblende + garnet = orthopyroxene + plagioclase + H<sub>2</sub>O (de Waard 1965). These veins contain fine-grained iron oxide + orthopyroxene + plagioclase (An<sub>45</sub>) in which an apparent disappearance of hornblende in the host is evident over a 4.5 to 5 mm interval. The presence of an amphibolite protolith, however, does not explain the presence of the additional phases cordierite and gedrite, nor the significant masses of garnet and quartz-rich mobilizate developed in gneiss units 4B and 5 (see Figure 16 and Table 4).

**PETROCHEMISTRY OF THE HOARE LAKE GNEISSES**

Analyses of 4 of the main units comprising the Hoare Lake gneissic assemblage are presented in Appendix 2e. Ged-

**Table 5.** Genetic classification of cordierite-orthoamphibole-bearing rocks and selected examples.

---

I)	Primary bulk composition (no chemical modification required). A unique clastic metasedimentary rock relatively low in alkalis and enriched in MgO: Yellowknife area, Slave Province (Kamineni 1973); Pistil Ogo, Lizard, Cornwall, England (Tilley 1937); Kragere district, Norway (Brøgger 1934).
II)	Secondary bulk compositions (modification developed at chemical syn- to postlithification, but prior to medium- to high-grade metamorphism)
A.	Metasomatic alteration of mafic to intermediate metavolcanic rocks.
1.	Association with volcanogenic massive sulphide ore deposits of various ages: Coronation Mine, Ontario (James, Grieve and Pauk 1978); Amulet Mine, Noranda, Quebec (Wilson 1941; de Rosen-Spence 1969); Gullbridge copper deposit, Newfoundland (Upadhyay and Smitheringale 1972).
2.	No apparent association with volcanogenic massive sulphide ore deposits: Aulanko area of Finland (Simonen 1948); Yalwal, New South Wales, Australia (Vallance 1967); Kenidjack, Cornwall, England (Tilley 1935).
B.	Derivation of restite bulk compositions via anatexis. Alkali depletion related to physical removal of leucosome systems from zone of anatexis: general theory (Grant 1968); Fishtail Lake area, Ontario (Lal and Moorhouse 1969); Hoare Lake gneisses, Bangor Township, Ontario (this study).
C.	Metamorphism of aluminous, (Fe+Mg)-enriched, alkali-depleted paleosols (theoretical possibility, but no known examples in literature).

---

rite-hypersthene-cordierite-mafic mineral-rich rocks are interpreted as restite. Analyses of specimens HL-1 and HL-2A exhibit the same strong depletion of Na<sub>2</sub>O, K<sub>2</sub>O and CaO reported in the literature from various other occurrences of cordierite-orthoamphibole-bearing rocks (Appendixes 3c and 3d). Pronounced enrichment in total Fe and Mg is such that the restite component plots near the Fe<sub>total</sub>-Mg sideline (*see* Figure 15), and exhibits the highest Mg/(Fe+Mg) ratio when compared to any similar rock from the literature, including those from nearby Fishtail Lake (Lal and Moorhouse 1969, p.157). Brown-weathering biotite-garnet-orthopyroxene quartz diorite (specimen HL-5) contains significantly higher CaO, similar total Fe, and significantly lower MgO than the restite.

On the Al-(Fe+Mg)-(Na+K+Ca) ternary diagram (*see* Figure 15), restite compositions (specimens HL-1, HL-2A) from Hoare Lake gneisses express a closer similarity to various dealkalized cordierite-orthoamphibole rocks from the literature, particularly those values shown in Appendix 3c.

Analyses of specimens HL-1 and HL-2A indicate that these rocks may represent an anatectic, metasedimentary restite. The composition of this restite, however, is considerably different from similar restites derived in low-pressure, high- to granulite-grade metasedimentary migmatite belts such as the northern supracrustal domain of the English River Subprovince (Breaks and Bond 1993). Three analyses from the latter, shown in Appendix 3e, plot considerably removed from Hoare Lake restite compositions (*see* Figure 15). Such compositional disparity may relate to the higher pressure conditions of granulite-grade metamorphism and higher calcium contents in the metasedimentary progenitor of the Hoare Lake restite.

Rare metasedimentary rocks exhibiting slight to moderate enrichment in MgO, and generally relatively low K<sub>2</sub>O, may crystallize cordierite + orthoamphibole metamorphic assemblages without apparently requiring modification of the original bulk composition through dealkalization processes. These rocks, for example, occur in the Slave Province (Kamineni 1973), the Lizard area of Cornwall, England (Tilley 1937), the southern coast of Norway

(Brøgger 1934, 1935), and at Tarklahti, in the Orijarvi area of Finland (Eskola 1914; Appendix 3f).

### ORIGIN OF THE HOARE LAKE GNEISSES

Cordierite + orthoamphibole-bearing rocks appear to represent a polygenetic group as inferred by such studies as Eskola (1914, 1933), Tilley (1935, 1937), Vallance (1967), Lal and Moorhouse (1969), Grant (1968), Upadhyay and Smitheringale (1972) and de Rosen-Spence (1969). This apparently restricted metamorphic association is governed by a peculiar mafic bulk composition having very low contents of Na, K and Ca, and relatively high Al, Fe and Mg. This is indicated mineralogically at Hoare Lake by a paucity of plagioclase and biotite, and an absence of potassium feldspar in the main unit containing coexisting cordierite + gedrite + hypersthene. Based on available literature, the authors attempted a genetic classification of cordierite-orthoamphibole rocks (Table 5). These unique mineralogical assemblages characterize either peculiar and rare magnesium-rich, alkali-deficient metasedimentary rocks, or a variety of protoliths that endured through secondary dealkalization.

In view of the strong metasedimentary context of the Hoare Lake occurrence, that is, the presence within the central confines of an extensive metasedimentary migmatite belt, in addition to granulite metamorphic conditions, it seems plausible that mechanism similar to the anatectic model proposed by Grant (1968) may have been operative. This is particularly convincing in terms of lensoidal to podiform leucosome, which coexists with 2 types of restite assemblages (gneiss units 3 and 5). In both cases, characteristic metamorphic minerals, such as garnet, cordierite, hypersthene and gedrite, which developed in the leucosome component, are also stable within the enclosing and more voluminous restite. An origin as metasomatically altered metavolcanic rocks overprinted by later low- to high-grade regional metamorphism has been proposed or inferred in the Coronation Mine area of Manitoba (Froese 1969), in the Noranda area (de Rosen-Spence 1969) and at the Gullbridge copper deposit in Newfoundland (Upadhyay and Smitheringale 1972). This phenomenon is effectively ruled out for the Hoare Lake gneisses since mafic metavol-

canic rocks are entirely absent from the local geologic record.

Certain cordierite-orthoamphibole rocks discussed in the literature appear to represent distinct, peculiar metasedimentary compositions as was remarked on by Tilley (1937) in his investigations in the Cornwall region of England: "The fine banding of the anthophyllite-cordierite rocks with layers of contrasted composition, their field relations, and their general petrography make it evident that they represent genuine sedimentary types." Rocks of this type (*see* Appendix 3f) plot in a relatively restricted field on both the AFM and Al-(Fe+Mg)-(Na+K+Ca) diagrams (*see* Figure 15), partially overlapping with analyses of metasedimentary rocks from the study area. However, a purely sedimentary origin of various units of Hoare Lake gneisses must be ruled out except possibly for the rusty-weathering biotite-rich schist (gneiss unit 6 in Figure 16). Great compositional differences exist between cordierite-anthophyllite rocks deduced to represent unadulterated metasedimentary rocks from gneisses of a highly mafic character, such as specimens HL-1 and HL-2A from gneiss unit 5 of the Hoare Lake gneissic suite. In addition, structures such as the fine sedimentary banding of the type noted by Tilley (1937) are not observable in unit 5 of the Hoare Lake gneisses.

Two REE analyses of the interpreted mafic-rich restite (gneiss unit 5) are given in Appendix 2e (specimens HL-1 and HL-5). These rocks exhibit the most depleted REE compositions in the Wicklow area, with total REE contents less than 16 ppm and probable very flat chondrite patterns ( $La/Yb_N = 0.7$  to  $2.2$ ). Lanthanum is only enriched by 6 times relative to chondrite, and ytterbium between 2.7 and 8 times chondrite. However, due to the fact that analytical sensitivity limits were recorded for Ce, Nd and Sm, it was not possible to construct meaningful chondrite plots for gneiss unit 5.

The degree of REE depletion, evidenced in the gedrite-cordierite-hypersthene mafic-rich unit, lends further credence to the authors' interpretation that these rocks represent anatectic residua.

The rare earth element characteristics of Hoare Lake amphibolites (gneiss unit 1) are similar to that of amphibolite elsewhere in the Madawaska Highlands gneissic complex and are thus all compared earlier in "Petrochemistry of the Hoare Lake Gneisses".

To summarize, the authors believe that the Hoare Lake gneisses originated from a pelitic protolith. Extensive partial melting followed by removal of most of the granitic melt by a tectonic filtering process could account for the peculiar mineralogy of the rocks. The filtering process would tend to concentrate the heavier mafic residue enriched in iron, magnesium and aluminum, and deplete sodium, potassium and calcium, which is paramount in order to crystallize cordierite- and gedrite-bearing assemblages. Minor amphibolitic layers also reacted to granulite-grade regional metamorphic conditions manifested as a local de-

composition reaction of hornblende (reaction possibly accompanied by garnet) that produced orthopyroxene-bearing assemblages lacking cordierite.

## Metasedimentary Rocks (Map Unit 5)

### GRENVILLE SUPERGROUP

Grenville Supergroup rocks are confined to the core zone of the Carlow synform. A 280 m long exposure on Highway 62 near Davis Falls (Papineau Creek) reveals tectonic interleaving of Grenville Supergroup metasedimentary rocks and structurally underlying migmatized metasedimentary rocks of the Madawaska Highlands gneissic complex. This constitutes the sole exposure in the study area where such relations are revealed.

This metasedimentary association is almost entirely restricted to the outer periphery of the New Carlow syenite complex, defining an arc varying between 400 and 1200 m in breadth. Rock types encountered consist of a relatively diverse and commonly interbedded assemblage of carbonate metasedimentary rocks (marble (map units 5b, 5c), marble tectonic breccia (map unit 5a) and calc-silicate skarn (map units 5h to 5v)), and clastic metasedimentary rocks (psammitic metasedimentary rocks (map unit 5e), pelitic metasedimentary rocks (map unit 5f), and rare interbedded quartzite-para-amphibolite (map units 5d and 5g)).

### CARBONATE METASEDIMENTARY ROCKS

Marbles, derived tectonic breccia, and various calc-silicate skarns represent the most prevalent rock types within this supracrustal sequence. Most exposures are friable weathering and rusty coloured, in part due to the common presence of accessory pyrite and/or pyrrhotite. Clean white-grey weathered surfaces reveal a massive to locally laminated to very thinly bedded (0.5 to 2.0 cm thickness), medium- to coarse-grained, granoblastic rock, consisting of quartz + scapolite + diopside + carbonate or quartz ± phlogopite + graphite + diopside + carbonate assemblages.

In most instances, carbonate constitutes approximately 80 to 90% of the visually estimated mode.

Marble tectonic breccia was mapped in localities within a restricted area: along a prominent scarp trending 015° and parallel to Little Papineau Creek immediately upstream from the bridge crossing of the New Carlow Road; along a nearby paved road that is a cutoff section of Highway 62; and one occurrence 300 m east of Kitts Lake. These rocks consist of rounded to angular fragments and disrupted layers of brown-weathering biotite quartzofeldspathic paragneiss and local quartz-rich fragments. The quartz-rich clasts significantly protrude on weathered surfaces, are usually subrounded, and range in size from 2 by 3 cm to 24 by 43 cm. The matrix of these contains mineral assemblages identical to that of nonbrecciated marbles.

Calc-silicate skarn assemblages derived from these marble units are widespread. Mineralogically, they are quite diverse. In this study, an attempt was made to characterize the various skarns (map units 5h to 5v) as a possible aid in deciphering regional metamorphic patterns. These rocks probably bear a genetic relationship to the New Carlow syenite complex, as most intense development of calc-silicate skarn appears to occur within approximately 100 m of the outer contact and within numerous enclaves scattered in relatively small quantities throughout the syenite. The following mineral assemblages have been observed by the authors in skarns of the present area.

*Tremolite-Bearing Skarns:*

tremolite + calcite + phlogopite + hornblende + diopside  
(map unit 5h)

talc + quartz + tremolite + calcite + diopside  
(map unit 5j)

*Diopside- and/or Actinolite-Bearing Skarns:*

quartz + plagioclase + diopside + actinolite ± pyrite  
± phlogopite ± titanite (map unit 5q)

quartz + calcite + diopside + scapolite (map unit 5p)

actinolite + diopside ± titanite (map unit 5s)

plagioclase + diopside (map unit 5v)

*Hornblende-Bearing Skarns:*

hornblende + diopside ± epidote ± quartz ± plagioclase  
(map unit 5n)

quartz + plagioclase + hornblende (map unit 5m)

garnet + hornblende + plagioclase (map unit 5u)

*Augite-Bearing Skarns:*

augite + garnet + scapolite + plagioclase (map unit 5t)

Assemblages containing tremolite and talc are relatively rare. A good exposure, containing these minerals coexisting with diopside, albite, phlogopite, carbonate, quartz and minor pyrrhotite, is located on Highway 62, 1.1 km northeast of the Little Papineau Creek bridge.

Boudins of this coarse-grained assemblage are contained within rusty-weathering, fine- to medium-grained graphite-diopside laminated marble, siliceous fine- to coarse-grained porphyroblastic (potassium feldspar) ± plagioclase-quartz-potassium feldspar psammitic metasedimentary rocks, fine- to medium-grained porphyroblastic (garnet) and lepidoblastic graphite-garnet-quartz-potassium feldspar-biotite-plagioclase metapelite. Tremolite was also found within calc-silicate enclaves hosted in felsic to intermediate gneiss near Moore's Pond. Garnet-bearing skarns are also rare, with the most impressive example exposed along the previously mentioned portion of Highway 62 and near Grover Mountain (local name). Large masses consisting of xenomorphic, coarse-grained garnet are associated with scapolite, plagioclase and local augite. A veined appearance at the exposure is due to the presence of fibrous scapolite within a pseudo-breccia network.

Actinolite-rich skarns occur at several localities in the New Carlow syenite complex. On the northwest face of Hoover Mountain (Concession XVI, Lot 4, Bangor Township), a 20 by 30 m wide zone of quartz-phlogopite-actinolite skarn is composed mostly of medium- to coarse-grained actinolite (90%). A zone of comparable size and mineralogy with additional subordinate phases of scapolite and diopside occurs near the extreme southeastern map corner in Lot 4, Concession XIV, of Bangor Township.

## CLASTIC METASEDIMENTARY ROCKS

Clastic metasedimentary rocks of the Grenville Supergroup (map units 5d, 5e, 5f, 5g) are considerably less abundant than the carbonate metasedimentary rocks. They are composed of sillimanite ± garnet-graphite-potassium feldspar-biotite-plagioclase metapelite (map unit 5f), carbonate- and/or scapolite-bearing psammitic metasedimentary rocks (map unit 5e), quartzite (map unit 5d) and para-amphibolite (map unit 5g). No preservation of sedimentary textures was observed in the field or microscopically.

Metapelites are fine- to medium-grained, equigranular to porphyroblastic, light brown-weathering, non-migmatitic rocks. They may be compositionally banded in a cryptic manner. This banding can only be discerned by feldspar staining. Bands 3 to 5 cm in thickness, showing enrichment in potassium feldspar (*see* specimen 6-13-16A *in* Appendix 1i) alternate with plagioclase-dominated bands containing very sparse potassium feldspar (*see* specimen 6-13-16B *in* Appendix 1i). The plagioclase-rich layers contain significantly larger amounts of quartz and plagioclase, and smaller amounts of biotite and graphite (*see* Appendix 1i). An average modal composition of these pelitic metasedimentary rocks is probably approached by specimen 6-11-26 (*see* Appendix 1i).

Ovoid- to augen-shaped, red-brown, garnet poikiloblasts up to 3 by 5.5 mm, occur in a few places, where they constitute approximately 5% of the pelitic metasedimentary rocks, for example, on Highway 62, 1.3 km northeast from the Little Papineau Creek bridge. A portion of this pelitic rock (25 to 30%) is composed of thin subhedral laths of biotite (0.6 by 0.1 mm) and minor graphite (0.06 by 0.02 mm to 6.5 by 0.2 mm size range), which form a well-developed lepidoblastic fabric. Several coexisting metamorphic assemblages were documented in these pelitic rocks:

1. graphite + sillimanite (robust prisms) + garnet + quartz + potassium feldspar + biotite + plagioclase (An<sub>33</sub>)
2. graphite + potassium feldspar + quartz + biotite + plagioclase (An<sub>45</sub>)
3. biotite + graphite + titanite + hornblende + quartz + plagioclase (An<sub>57</sub>)

Psammitic metasedimentary rocks are of relatively widespread distribution. These consist of biotite + plagioclase + quartz + potassium feldspar assemblages, which are fine to coarse grained, porphyroblastic, well foliated to mylonitic, hololeucocratic and white weathering.

The considerable degree of strain imposed upon the Grenville Supergroup metasedimentary rocks is most ap-

parent within these more competent siliceous metasedimentary layers. In particular, sigmoidal potassium feldspar porphyroblasts up to 2 by 3 cm exhibit the same sense of apparent rotation as in the various underlying gneisses of the Madawaska Highlands gneissic complex. Mylonitic textures are particularly well developed in these hololeucocratic rocks.

Carbonate-scapolite-bearing psammitic metasedimentary rocks are well exposed in 2 localities: in roadcuts on Highway 62 adjacent to Davis Falls, and near Grover Mountain on Concession III, Lot 4, Wicklow Township. The psammitic metasedimentary rocks are laminated to very thinly bedded (0.5 to 2 cm) and record at least 2 folding events, 3 periods of dike emplacement, and overprinting by porphyroblasts and skarn assemblages. In thin section, they are very finely laminated, with compositional banding defined by 0.5 to 1 mm wide biotite-, scapolite- and carbonate-rich layers. The rocks are polygonal granoblastic with most grains in the 0.5 to 1 mm diameter size range.

Interlayered with these metasedimentary rocks are fine- to coarse-grained, hornblende-rich, garnet-plagioclase metasandstones.

Interbanded quartzite and thin (3 to 5 cm) para-amphibolite were encountered in one exposure within the Grenville Supergroup on Concession III, Lot 4, Bangor Township. The para-amphibolite layers are fine to medium grained, and moderately foliated due to preferred orientation of thin subhedral biotite laths, which account for about 18% of the mode (*see* Appendix 1i). Quartzite layers, up to 1 m in thickness, contain approximately 85% coarse-grained quartz and ancillary levels of medium- to coarse-grained plagioclase, potassium feldspar, biotite and titanite (*see* Appendix 1i). Except for the different geological setting, the para-amphibolite compares relatively well with several biotite amphibolites from the Madawaska Highlands gneissic complex (*see* Appendixes 1a and 1i).

## Mafic to Ultramafic and Related Tonalitic Plutonic Rocks (Map Unit 6)

Rock types of this group (map units 6b to 6m) occur widely within the Madawaska Highlands gneissic complex. Diorite and quartz diorite are particularly common, occurring not only within relatively large metaplutonic complexes such as in the Little Papineau Lake–Moore’s Pond area, but also as an ancillary component in the aforementioned mafic to intermediate and felsic to intermediate gneisses.

Discrete masses of diorite and consanguineous tonalitic rocks were delineated within 4 parts of the map area:

1. Little Papineau Lake–Moore’s Pond–south Papineau Lake area (Little Papineau Lake plutonic complex)
2. Ribgrass–McKenzie lakes area

3. southwestern corner of the map sheet, approximately paralleling Highway 127 and mostly in McClure Township
4. south of Indian Lake (Indian Lake plutonic complex)

The Little Papineau Lake plutonic complex is by far the largest diorite intrusion within the map area, although it should be mentioned that the full extent of similar rocks in the Ribgrass Lake area is not presently known and could very well continue significantly beyond the northwestern boundary of the map area. The Little Papineau Lake plutonic complex appears to describe an irregular crescent shape with a maximum breadth of 6.6 km. From a midpoint at Moore’s Pond, the complex tapers 4.2 and 5.8 km southwest and east, respectively. The complex covers a total area of approximately 21 km<sup>2</sup>.

The moderate concavity of the south to southwestern contact of this complex and, to a lesser extent, of the northern contact, is related to the macroscopic folding influence of the Carlow synform. A significant northwest-trending lobe may extend to Hawk Lake, where similar dioritic rocks are exposed; this interpretation is highly tenuous due to a large intervening tract of Pleistocene glacial cover. Such an extension would, however, be structurally compatible and conformable with adjacent southeast-plunging major units, such as granite tectonic breccia (map unit 9g) which cores the Wicklow antiform.

The third significant mass is situated mainly within McClure Township and, albeit more irregular than the other major dioritic units, also conforms to the southeast trend of the surrounding structural domain. It may be possible that this mass constitutes the mafic core zone of a tonalite-quartz diorite-diorite plutonic complex (Indian Lake plutonic complex). Diorite is a common, but minor, intrusive unit within encircling foliated and/or lineated felsic to intermediate plutonic rocks of this complex (map units 10a, 10c), although it cannot be proven that these 2 assemblages are consanguineous.

Several smaller diorite-quartz diorite masses are contained within the map area: 600 m east of McCastle Pond, 560 m north of Wicklow Lake, in the Poplar Pond area, 420 m southeast of Franz Pond, immediately north of the Hawk Lake, and on Davis Island (Papineau Lake). Several of the largest masses display gradation into diorite-quartz diorite gneiss, particularly within zones of apparent constriction. Examples are observed near the eastern end of the Little Papineau Lake plutonic complex proximal to Theresa’s Pond, and at the pronounced narrowing of the McClure Township mass, as exposed along Highway 127 immediately south of the Papineau Creek bridge. Because of their spatial relationship with the lesser deformed rock types, these gneissic zones were grouped within map unit 6, “metamorphosed mafic to ultramafic and related tonalitic plutonic rocks”.

Excellent exposures of such diorite to quartz-diorite gneiss can be examined along Highway 127 and between Papineau Lake and Theresa’s Pond.

Large enclaves of other rock types occur on a local scale and consist of felsic to intermediate gneiss, metasedimentary migmatite, and potassic granitoid suite rocks, as in the Moore's Pond area. Two separate units of metasedimentary metatexite with dimensions 1.6 km by 600 m and 400 by 320 m were delineated in this area and could represent roof pendants. Mappable sheets of metamorphosed potassic granitoid rocks (map units 9d, 9e) are also contained within the central confines of the Little Papineau Lake plutonic complex, as can be seen at the outlet of Moore's Pond.

## STRUCTURE

These plutonic rocks are relatively massive to moderately foliated. Hornblende lineations are well developed in the gneissic equivalents, and poorly or not developed in the more massive rocks. Foliate structures are most apparent within biotite-bearing phases (map units 6c, 6d, 6e). Gneissosity is locally defined by planar, discontinuous layers and irregular pods of light to medium pink, coarse-grained, hololeucocratic granite which locally constitutes 5 to 10% of the diorite. Medium- to coarse-grained subidiomorphic hornblende porphyroblasts are commonly associated with these anatectic mobilizates and almost invariably congregate along the diffuse boundary between the diorite to quartz diorite paleosome with the leucosome.

## PETROLOGY

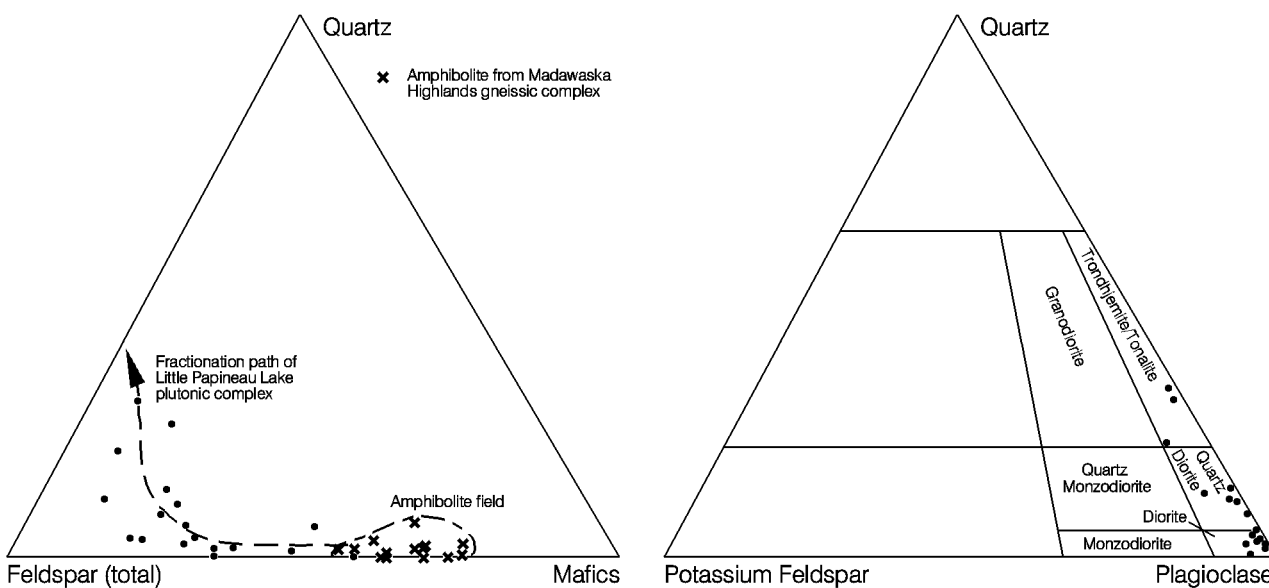
Most of the dioritic plutonic complexes in the study area are petrologically similar, and the following section is largely based on observation from the Little Papineau Lake plutonic complex which contains the best exposures of such plutonic rocks. This mass consists of an apparently comagmatic gabbro-diorite-quartz diorite-tonalite-trond-

hjemite suite, which illustrates a trend of decreasing colour index (CI) with decreasing relative age (Figure 17).

Biotite-hornblende diorite and rarer hornblende-biotite diorite are the dominant rock types (CI 18 to 56, Appendix 1j). Quartz diorites are considerably less abundant, probably composing 5 to 10% of the plutonic complex. Hornblende:biotite ratios are listed in Appendix 1j. A more restrictive range in CI for quartz diorite relative to the diorites is exhibited (usually 11 to 27, with one specimen reaching an extreme of 48). Plagioclase contents increase with decreasing CI as shown on the QFM diagram in Figure 17, and maximum levels of 73 to 76% occur within the quartz diorite field (*see* specimens 4-7-9B, 4-7-11 and 4A- 4-1B *in* Appendix 1j).

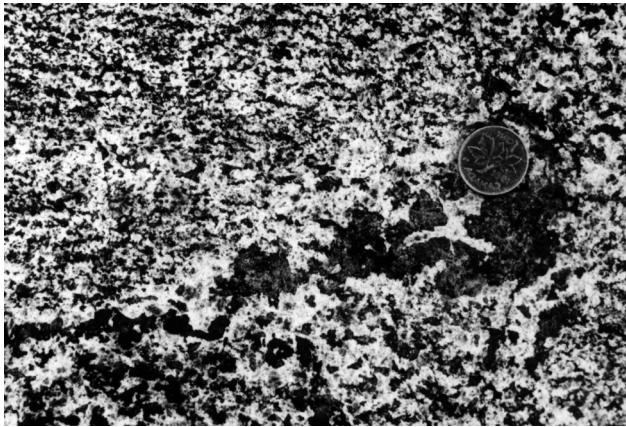
Trondhjemite and tonalite contain 20 to 28% quartz and represent maximum contents of quartz attained in the fractionation trend shown on Figure 17.

Diorite and quartz diorites (map units 6c, 6d and 6m) usually exhibit interlobate granoblastic textures. Hornblende or biotite rock varieties are somewhat nematoblastic or lepidoblastic. Very commonly, a variegated "salt and pepper" texture is apparent on clean weathered surfaces of massive exposures. Plagioclase of oligoclase composition, (maximum size 1.5 by 3 mm), quartz (maximum size 1.2 by 2.6 mm), and hornblende (maximum size 1.5 by 3.7 mm) are all xenomorphic and nonpoikilitic. Biotite is the only subidiomorphic mineral and occurs in all rock types as fine- to medium-grained subhedral laths (0.15 by 0.7 mm to 0.2 by 1.2 mm in size). Minor potassium feldspar is commonly present and is commonly located along plagioclase grain contacts. Accessory minerals include apatite, opaque iron oxide, apatite, titanite, epidote, and zircon, as listed in approximate order of decreasing abundance.



**Figure 17.** Modal variation of Little Papineau Lake plutonic complex plotted on quartz-total feldspar-mafics (QFM) and quartz-plagioclase-potassium feldspar (QPK) ternary diagrams, also showing on the QFM diagram, for comparison, amphibolite from the Madawaska Highlands gneissic complex.

Leucocratic biotite-hornblende quartz diorite and tonalite (map units 6m and 6k) occur as local intrusive masses and dikes and postdate the diorite rocks. Many good exposures occur along and near the eastern shoreline of Little Papineau Lake, in the Moore's Pond area, and near Hawk Creek in vicinity of its confluence with Little Papineau Creek. The rocks are poorly foliated to massive, medium grained and commonly possess a porcelaneous, white, weathered surface. The rock texture is interlobate granoblastic, and all major minerals (quartz, plagioclase, hornblende) are xenomorphic. Only biotite is idiomorphic and ranges between 0.25 by 0.04 mm and 2 by 0.2 mm in size. Interlobate granoblastic texture is a subdivision of granoblastic texture (Spry 1969) and contrasts with the polygonal granoblastic variant.



**Photo 8.** Metamorphic segregations containing orthopyroxene developed in metadiorite on Davis Island. Diameter of coin is 1.85 cm.

### Orthopyroxene-Bearing Metamorphic Segregations in Biotite-Hornblende Diorite

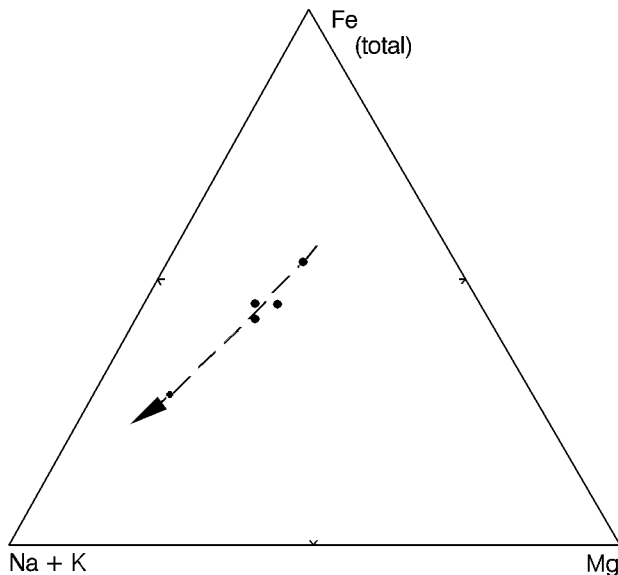
On Davis Island in Papineau Lake, metamorphic, anatectic segregations in biotite-hornblende diorite contain dark, elongate (2.6 by 15 cm) to ovoid (14 by 21 cm) masses that usually consist of an orthopyroxene and/or diopside core discontinuously mantled by hornblende (Photo 8). Boundaries with the diorite host are usually diffuse. Orthopyroxene is also contained within larger irregular aggregates up to 7.8 by 10 cm near the cottage at the southeastern tip of Davis Island.

The diorite host is medium grained, slightly linedated and is postdated by dikes, listed below in order of decreasing relative age:

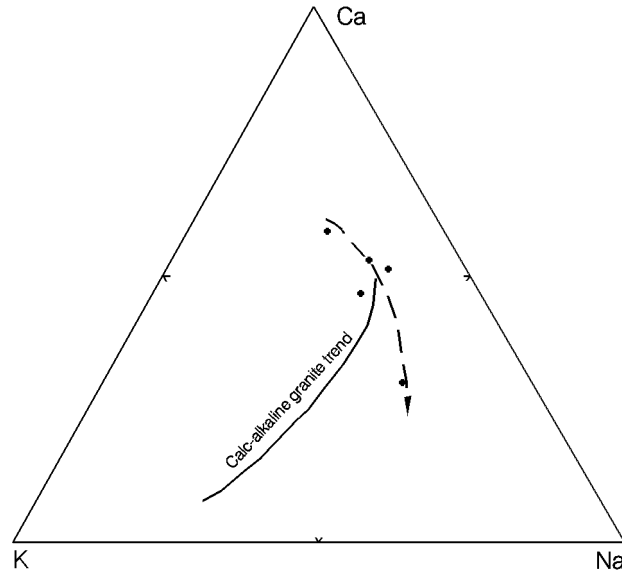
1. hololeucocratic trondhjemite, fine grained, deformed
2. leucocratic magnetite-biotite and allanite-magnetite biotite granite, medium to coarse grained, deformed
3. hololeucocratic granite, coarse grained to pegmatitic, posttectonic

### PETROCHEMISTRY OF MAFIC TO ULTRAMAFIC AND RELATED TONALITIC PLUTONIC ROCKS

Appendix 2f presents 5 analyses of typical rock types from the Little Papineau Lake plutonic complex. These analyses, plotted on FMA and Ca-Na-K (CNK) variation diagrams (Figures 18 and 19, respectively), indicate a fractionation trend marked by a continuous increase of Na and decrease in total Fe, Mg and Ca. K<sub>2</sub>O values (1.43 to 2.28%) define a flat trend versus increasing SiO<sub>2</sub>. There is no pronounced K<sub>2</sub>O depletion in specimen 4A-5-3, possi-



**Figure 18.** Total iron-magnesium-alkalis (FMA) variation of dioritic rocks from the Little Papineau Lake plutonic complex.



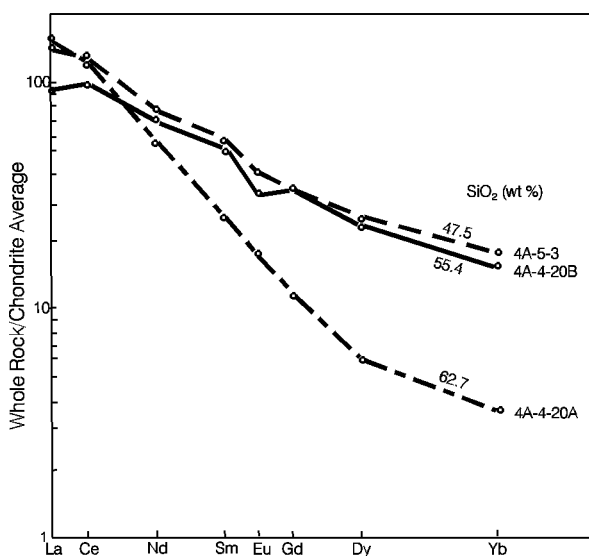
**Figure 19.** Calcium-sodium-potassium (CNK) variation of dioritic rocks from the Little Papineau Lake plutonic complex. Solid line represents the calc-alkaline granite trend of Nockolds and Allen (1953).

bly the least fractionated rock. Specimen 4A-4-20A, a hornblende-biotite quartz diorite, represents the most fractionated rock as indicated by the relatively high  $\text{SiO}_2$ ,  $\text{Na}_2\text{O}$ , Rb; low  $\text{Fe}_{\text{total}}$ , Mg, Ca, Sr, Ba values; and the K/Rb and Ca/Sr ratios. Some of the rocks contain 18 to 20%  $\text{Al}_2\text{O}_3$  and probably are plagioclase-rich cumulates. This is also suggested by several modal analyses in Appendix 1j in which plagioclase accounts for approximately 70 to 75% of the mode.

The regular decrease of  $\text{TiO}_2$ ,  $\text{FeO}_{\text{total}}$ , MgO and CaO, and the increase of  $\text{Na}_2\text{O}$  versus  $\text{SiO}_2$  (not illustrated in this study), in addition to the smooth trends on the QFM diagram in Figure 17, suggest that the rocks were formed by fractional crystallization of a gabbroic melt (Barker and Arth 1976). The smooth  $\text{SiO}_2$  trend noted above would be yet more convincing if chemical analyses of rare quartz-rich trondhjemites, as exemplified by specimens 4-7-6B and 4-7-8B (*see* Appendix 1j), were available.

### Rare Earth Element Geochemistry

Chondrite-normalized REE patterns for 3 typical rock types from the Little Papineau Lake plutonic complex are shown on Figure 20. These exhibit moderate fractionation patterns featuring enrichment of LREE over HREE, with total REE contents varying between 200 and 249 ppm (*see* Appendix 2f). Gabbro and diorite show a flatter trend relative to quartz diorite with  $\text{La}/\text{Yb}_\text{N}$  ranging from 5.3 to 9.3 and accompanied by small negative Eu anomalies ( $\text{Eu}/\text{Eu}^* = 0.77$  to  $0.92$ ). Fractionation in the quartz diorite (*see* specimen 4A-4-20A *in* Appendix 2f) is much more pronounced, evidenced by the considerably greater  $\text{La}/\text{Yb}_\text{N}$  ratio of 43.3, absence of an Eu anomaly, and lower total REE.



**Figure 20.** Chondrite-normalized REE plots for metagabbro, metadiorite and metaquartz diorite from the Little Papineau Lake plutonic complex.

## METAGABBRO

Metagabbro is relatively rare within the study area (map units 6b, 6c). The most noteworthy exposure occurs along Highway 62, 1.8 km southwest of Maple Leaf. Otherwise, these rocks occur mainly as enclaves in some deformation zones described in “Tectonic Breccia”. The Highway 62 exposure consists of coronitic metagabbro, interlayered wacke-pelitic metasedimentary rocks, sillimanite- and garnet-bearing metapelites, biotite-magnetite-plagioclase-hornblende-quartz-garnet iron-rich siliceous metasedimentary rocks, and several generations of granitic dikes. The metagabbro is medium to coarse grained, melanocratic and porphyroblastic. A spotted appearance is evident on weathered surfaces due to complex symplectites composed of diopside phenoblasts (up to 4.5 by 7 mm) mantled by fine-grained plagioclase. Microscopically, the coronas surrounding these coarse diopsides can be seen to consist of 2 parts:

1. a thin inner shell (0.2 to 0.75 mm width) of graphic quartz-hornblende
2. an outer shell of fine- to medium-grained, polygonal granoblastic aggregate of plagioclase ( $\text{An}_{38}$ ), 0.5 to 4 mm in width

The large diopside core is poikiloblastic with 5 to 10% quartz and opaque iron oxide inclusions that are oriented parallel to the prismatic cleavages of the pyroxene.

Plagioclase-rich, porphyroblastic gabbro enclaves were also observed in metasedimentary migmatite, for instance, on Concession V, Lot 4, Wicklow Township, 1.2 km southwest of Davis Pond. Here, a 4 by 7 m sized inclusion of garnet-biotite-hornblende metagabbro occurs that is moderately lineated and medium to coarse grained. It contains 15 to 20% circular to irregularly elongate domains that consist of about 80% plagioclase and subordinate garnet, magnetite and biotite. These domains are 3 by 3 mm up to 6 by 9 mm, and are difficult to observe on fresh or slab cuts. Weathering or mild etching with HF acid facilitates megascopic study.

## Anorthosite Suite Rocks (Map Unit 7)

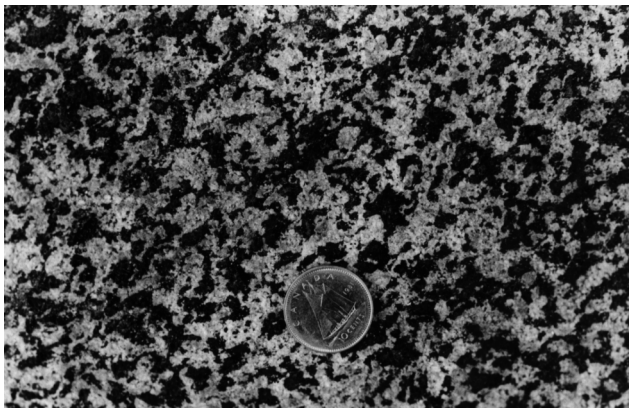
Members of the anorthosite suite (map units 7a, 7c) are very restricted in distribution and occur only as recrystallized, deformed enclaves in 3 localities as coded on Map 2550 (back pocket). A relatively large enclave (>10 m in size) is contained within a prominent southeast-plunging granite tectonic breccia which occupies much of the core zone of the Wicklow antiform. The main rock type of the enclave is a diopside-hornblende metagabbro (Photo 9) that is interlayered with thin 4.5 to 6.5 cm thick bands of fine-grained anorthosite.

The metagabbro (*see* Photo 9) is a vaguely lineated, medium grey to faint green-grey weathering, fine- to coarse-grained, mesocratic rock composed of irregular, black, mafic clots often interconnected in an anastomosing network. The clots, which measure up to 0.8 by 2.5 cm, are a thoroughly recrystallized polygonal granoblastic aggre-

gate of strain-free hornblende, locally coexisting with an irregular core zone of dark green diopside. The matrix, which constitutes about 57% of the rock (Appendix 1k), consists almost solely of fine-grained polygonal granoblastic plagioclase (An<sub>62</sub>) and minor fine-grained opaque iron oxide. At the same locality, irregularly shaped enclaves of hornblendite also occur that may represent tectonically decimated layered ultramafic rocks.

At a second locality (that is, roadside outcrops immediately north of Balsam Lake), gabbro and anorthositic gabbro enclaves occur within fine- to medium-grained, hornblende-biotite, migmatized metasedimentary rocks and are veined by granitic pegmatite. The gabbro is medium grained, mesocratic, and moderately hornblende nematoblastic. Plagioclase (An<sub>72</sub>), the only other significant mineral phase, comprises about 52% of the mode (*see* Appendix 1k) and exhibits well-developed polygonal granoblastic textures. Minor amounts of diopside are intergrown with hornblende. Rounded zircons (0.1 by 0.2 mm) occur as rare accessory minerals within hornblende, and have imposed well-developed pleochroic halos upon the host. The third exposure of anorthosite suite rocks is situated about 680 m northwest of Cragg Pond. Here, enclaves of anorthositic gabbro, similar to the Balsam Lake unit, are enclosed within foliated biotite granite.

The 2 enclaves of anorthositic gabbro situated within the western part of the map area, near Cragg Pond and in the Wicklow antiform, may have been tectonically scavenged from a larger plutonic mass. A relatively extensive anorthosite body, which has an easterly termination in Bruton Township, 10 km to the west of the Wicklow area (*see* Figure 3), has been delineated by A. Davidson (Geological Survey of Canada, personal communication, 1982). It is believed to represent the source for the tectonic enclaves described here.



**Photo 9.** Anorthositic gabbro in portion of a large inclusion contained within tectonic breccia of Wicklow granite in Concession XIII, Lot 27, Wicklow Township. Diameter of coin is 1.7 cm.

## Metamorphosed Felsic to Intermediate Plutonic Rocks

### SYENITIC SUITE PLUTONIC ROCKS (Map Unit 8)

#### New Carlow Syenite Complex

Intruding the Grenville Supergroup metasedimentary package is a complex assemblage of quartz-bearing to undersaturated syenitic rocks referred to, in this study, as the New Carlow syenite complex. This mass is very poorly exposed in the study area. Pleistocene glacial deposits cover most of the western flanks of the complex in the Greenview area.

The syenitic rocks are exposed intermittently over 6.5 km from Grover Mountain to the extreme southeastern corner of the map area. Hewitt (1955) previously examined most exposures in Carlow Township and part of Belot Mountain in Bangor Township. The northwest termination, most of the northeastern and part of the northwestern flanks of the complex were not defined until the present study. On Hewitt's Map 1954-3 (Hewitt 1955), several integral rock types of the complex appear as amphibolite, paragneiss and hybrid granite gneiss (for example, on Belot Mountain), which were reinterpreted in the present study.

Enclaves of garnet-biotite-quartz-feldspathic metasedimentary rocks are present in places, as for instance, on Concession XIV, Lot 3, Bangor Township.

Petrologically renowned for spectacular corundum-bearing pegmatites and related rocks, the syenite complex constitutes a very complicated, generally interlayered, variably metamorphosed, and deformed plutonic assemblage composed of at least 9 discernable rock types (Table 6) encompassing a wide compositional range (Figure 21).

Petrologic features of the major rock types are summarized in Table 6 and modal analyses given in Appendix 11. Relative age relations are difficult to discern for most rock types listed in this table due to the tectonic concordance imposed by deformation events, virtual obliteration of primary igneous textures, and relatively poor exposure. The earliest intrusive unit may be the diorite to monzonite (unit NCS-1), if a trend of mafic to felsic geochemical fractionation played an important role in the evolution of the diverse lithologic assemblage. These equigranular mafic rocks are usually well foliated and/or lineated, fine to medium grained, contain hornblende in excess of biotite, and contain considerable anhedral to subhedral apatite (up to 5%), titanite (up to 3%), and opaque iron oxide. The latter mineral is frequently enclosed by a thin shell of titanite. Unit NCS-1 is postdated by scarce, narrow dikes of coarse-grained titanite-augite syenite (unit NCS-5) and fine-grained, recrystallized, hololeucocratic syenite (possibly unit NCS-2). Small, fine-grained amphibolite enclaves may also be locally apparent as on Concession XIV, Lot 3,

Table 6. Petrologic units of the New Carlow syenite complex.

Unit Number	Lithology	Petrologic Features <sup>1</sup>	Examples in Appendixes 1l, 1m, 2g, 2h, and 2i	Comments
NCS-1	Titanite-biotite-hornblende diorite to monzodiorite ± iron oxide	Well foliated and/or lineated, fine to medium grained. Colour Index 30–50. Black to brown-black.	7-14-2A, 6-13-3B, 7A-5-3, 7-13-3, 7-14-2, 7-14-5A, 7-14-8, 7-14-10A	Widespread in Hoover Mountain area. Finer grained highly recrystallized units may be confused for clastic metasedimentary rocks.
NCS-2	Muscovite ± magnetite ± biotite-augite syenite	Weakly foliated, fine to medium grained. Colour Index <20. Faint orange-pink, maple brown.	6-13-32 6-13-7A 7-14-10B	Most widespread in Grover Mountain area. Occurs also as rare, deformed, thin exocontact dikes in carbonate-scapolite-biotite laminated to very thinly bedded psammitic metasedimentary rocks here.
NCS-3	Muscovite-magnetite-biotite-plagioclase syenite	Massive to weakly foliated, fine to medium grained. Colour Index <20. Grey white, and locally buff coloured.	6-11-3C 7-14-12B	Occurs as small exocontact lenses (up to 200 by 600 m) in Grenville Supergroup metasedimentary rocks. Also prominent at the Hoover Mountain corundum deposit, where it encloses the main corundum ore horizons.
NCS-4	Titanite-augite syenite to monzonite	Massive to vaguely foliated and lineated, coarse grained to pegmatitic. Colour Index <10. Moderately to intensely recrystallized. Light to moderate pink to maple brown.	6-13-10, 6-13-11, 6-13-13B, 7-13-1, 7-14-9, 7-14-11C, 7A-5-7	Mainly developed on Hoover Mountain.
NCS-5	Titanite-augite syenite to quartz syenite	Massive, medium to coarse grained. Colour Index <10. Moderate pink and white.	7-14-2B, 6-11-13C	Occurs as narrow, internal dikes postdating unit NCS-1 and as exocontact dikes postdating skarn assemblages.
NCS-6	Quartz-bearing syenitic rocks. Biotite, biotite-magnetite, magnetite-augite granite, quartz syenite and quartz monzonite	Massive to weakly lineated. Colour Index <10. Moderate to deep pink or light to moderate maple brown.	6-13-6, 6-13-30, 7-13-4, 6-13-7A, 7-13-2	
NCS-7	Corundum ± muscovite-biotite plagiostenite	Well foliated, fine to medium grained. Colour Index 20–30. Corundum locally <1%. White to light grey.	7-14-1C	Relatively rare lithology found only at small corundum showing 60 m southwest of the Hoover Mountain corundum deposit (Figure 39, back pocket).
NCS-8	Muscovite-magnetite-biotite-corundum plagiostenite to monzodiorite	Massive, medium to coarse grained. Colour Index <10. Corundum content 4–19%. White to faint pink white.	7-14-1, 7-14-12A, 7-14-12C	Main corundum-bearing unit at Hoover Mountain.
NCS-9	Magnetite-muscovite-corundum biotite plagiostenite	Massive, medium grained. Colour Index 5–10. Corundum content <6%. White to light grey.	7-14-1B	Relatively rare lithology gradational into unit NCS-8 at small corundum occurrence 60 m southwest of the Hoover Mountain deposit.

<sup>1</sup>Colours given on weathered surfaces only

Bangor Township. Unit NSC-1 is also abundant and inter-layered with unit NSC-2 in an area of relatively good exposure near Grover Mountain.

Exocontact syenitic dikes were mapped in 3 localities, that is, near Grover Mountain (Concession III, Lot 4, Wicklow Township), on Highway 62 near Davis Falls, and 2.5 km along Highway 62 from Davis Falls. Only a narrow (2.5 cm) deformed dike of fine- to medium-grained augite syenite emplaced in very thinly bedded, fine-grained carbonate-scapolite-biotite metasandstone at the first locality bears a resemblance (unit NSC-2) to internal intrusive phases of the New Carlow syenite complex. The other dikes, which are also deformed, consist of hololeucocratic sphene and sphene-augite syenite to quartz syenite. Only a single dike of fine-grained diopside amphibolite definitely postdates the latter type of exocontact syenitic intrusions as observed at the Grover Mountain locality. No syenitic dikes related genetically to the New Carlow syenite complex have yet been observed to postdate rocks of the Madawaska Highlands gneissic complex. This includes exposures such as at Davis Falls, where these gneissic rocks and Grenville Supergroup rocks are closely juxtaposed.

Dark green and locally moderate yellowish green augite is the characteristic accessory mineral on units NCS-2, NCS-4 and NCS-5, and is confined to the most potassic rocks. This mineral forms anhedral to subhedral stubby prisms varying from 1 by 1 mm to 1.5 by 3.5 cm in size and makes up 4 to 13% in the rocks. Parts of pyroxene cross-sections are notable in places on slab surface. On feldspar-stained slab surfaces, augite is commonly seen to be separated from potassium feldspar by thin, continuous, wispy 1 to 3 mm wide shells and irregular bands (0.6 to 1.1 cm width) of fine-grained, polygonal, granoblastic plagioclase. Similar plagioclase also occurs as irregular clots up

to 0.6 by 1.7 cm. Dark brown euhedral to subhedral sphene (1 by 1 mm to 0.5 by 1 cm size range) is commonly associated with augites.

Unit NSC-4 is usually massive and coarse grained; however, relatively intense recrystallization and deformation have produced a variant with weak foliation due to relatively penetrative, wispy plagioclase banding, as in specimens 7-14-11C, 7-14-5A and 6-13-10. These bands enclose augen-shaped to ovoid potassium feldspar megacrysts which may reach 2 by 3 cm in size. These megacrysts are characterized by very ragged contacts which possibly were caused by extensive, strain-instigated, grain-boundary migration. Augite megacrysts are also enveloped by potassium feldspar, but are notably less coarse in grain size vis-à-vis augites in relatively massive counterparts.

Quartz-bearing granitoids (unit NCS-6) account for a very small portion of the New Carlow syenite complex, and possibly may represent the most geochemically fractionated compositions. These rocks are widely scattered in terms of both locality and composition. Small exposures are found 0.6 km west of Kitts Lake; on Belot and Hoover Mountains; and at the western limit of exposure for the complex on Concession XIV, Lot 4, Bangor Township near Papineau Creek. Granites represent the most common compositional class (see Figure 21). Quartz syenite and quartz monzonite are less common.

Several units of the New Carlow syenite complex, such as units NCS-1, NCS-2 and highly recrystallized variants of unit NCS-4, locally exhibit a distinctive maple brown colouration on weathered surfaces. Such rocks commonly are strongly weathered, which is most intense on topographic highs such as Belot Mountain where many outcrops consist of maple brown sandy *grus*. In many cases, unit NCS-4 also tends to produce a rough surface due to protruding potassium feldspar megacrysts and rare coarse-grained quartz combined with pock-marked, recessive, mechanically weathered augite.

**CORUNDUM-BEARING SYENITES  
(Map Units 8d, 8e, 8f, 8g, 8h and 8j)**

Rocks of this group (units NCS-7, NCS-8 and NCS-9) are situated at 3 closely spaced localities on Hoover Mountain (see Figure 39 in "Economic Geology"). Relationship with other units of the New Carlow syenite complex is largely enigmatic due to the paucity of outcrops in this area. These rocks are definitely interlayered with unit NCS-2, the buff-coloured syenite of Hewitt (1955, p.34), at the Hoover Mountain corundum deposit, and proximally surrounded by massive coarse-grained titanite-augite syenite (unit NCS-4), and medium-grained titanite-biotite-hornblende monzodiorite (unit NCS-1). The main corundum-bearing unit (unit NCS-8) is a medium- to coarse-grained, vaguely foliated to pegmatitic, white-weathering hypidiomorphic-granular plagiostenite to leucocratic monzodiorite. Modal variation is limited (Appendix 1m; see Figure 21). These rocks differ considerably in modal composition with potassic members of the New Carlow syenite complex.

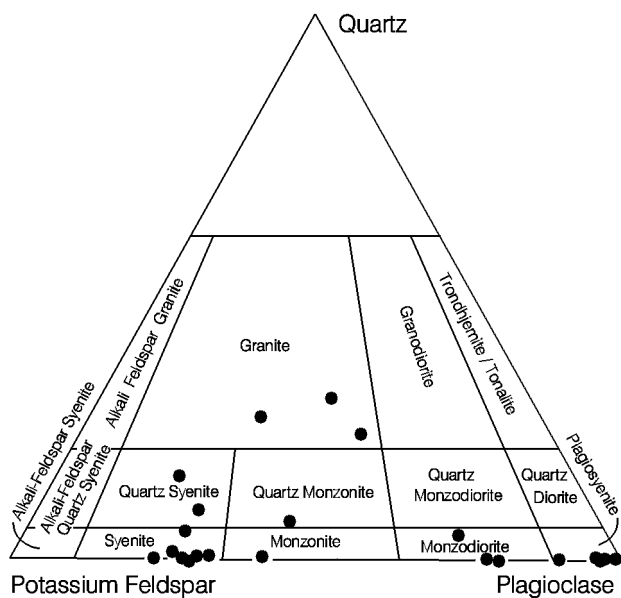


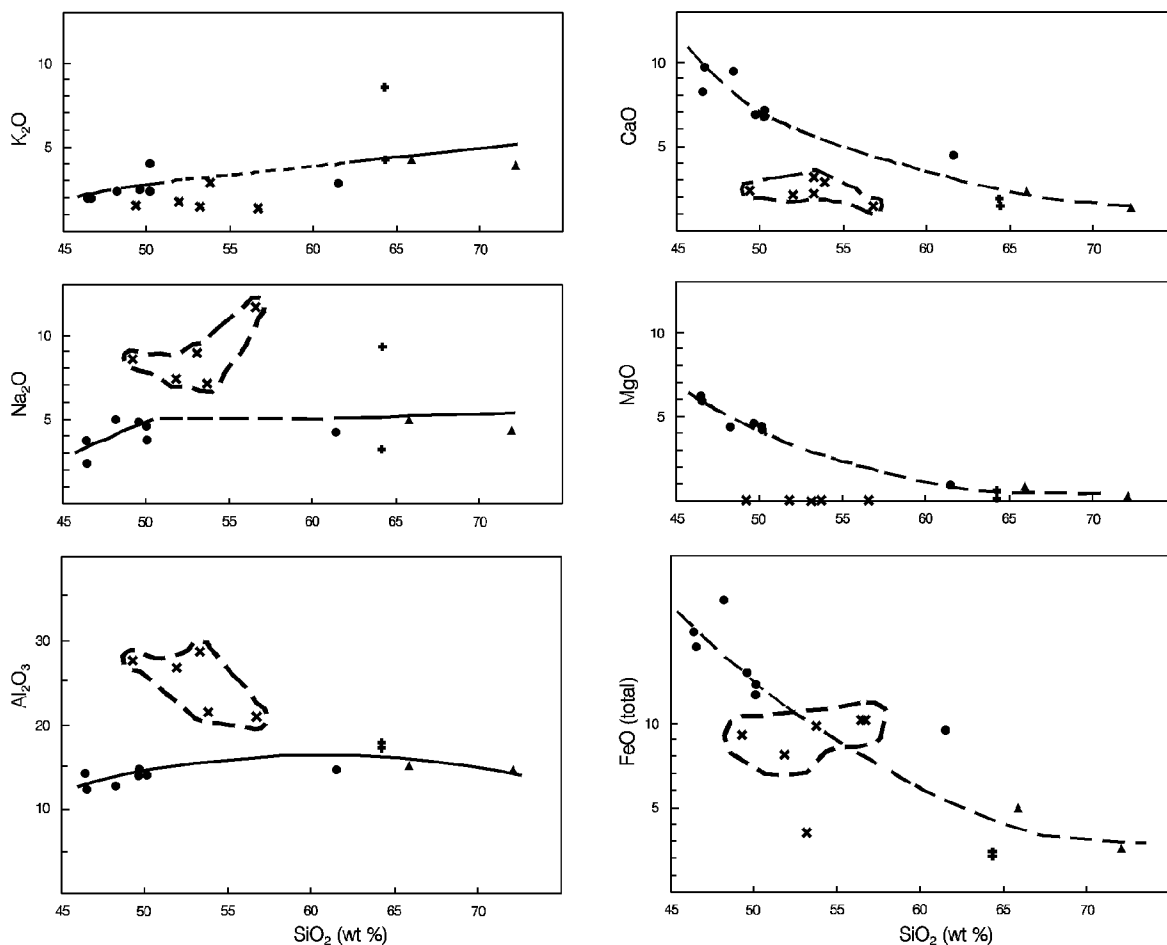
Figure 21. Quartz–plagioclase–potassium feldspar (QPK) modal variation of the New Carlow syenite complex.

Corundum, typically deep brown to bronze coloured, occurs as euhedral, barrel-shaped, hexagonal dipyrnidal crystals up to 5 by 15 cm in size on exposures similar to that shown in Photo 1. Most commonly, however, corundum is subhedral, showing incomplete crystallographic development on prismatic sections and sections normal to the *c* axis. The bronze colour on slab surfaces is mainly observed on sections parallel to (0001) and is probably caused by the reflection of light on fine lamellar twinning planes (1102) and (0112). Thin, irregular, 1 to 3 mm wide light green shells of secondary muscovite commonly completely mantle corundum. Corundum modally constitutes between 4 and 19% of the rock.

Other corundum-bearing syenites are relatively minor and include biotite plagiосyenite (unit NSC-7) and magnetite-muscovite-corundum-biotite plagiосyenite (unit NSC-9). The latter grades into and is compositionally similar to coarse-grained corundum plagiосyenite (see Appendix 1m). Unit NSC-7 contains more biotite and minor corundum. Corundum in both units is generally finer grained than in the coarse corundum plagiосyenite to monzodiorite (unit NSC-8), with an observed size range of 1 by 1 mm to 0.7 by 1.1 cm.

## PETROCHEMISTRY OF THE NEW CARLOW SYENITE COMPLEX

In Appendixes 2g, 2h and 2i, 16 chemical analyses of most rock types listed in Table 6 are presented. The corundum-bearing syenites are characterized by the low contents of SiO<sub>2</sub>, Nb, Y, Sc and an excess of Al<sub>2</sub>O<sub>3</sub>. All rock types of this complex appear to define relatively consistent fractionation trends on most Harker diagrams (Figures 22 and 23). When curves are constructed on a basis of chemical variation in rocks exclusive of the corundum-bearing plagiосyenites, the uniqueness of these latter rock types becomes more apparent. In particular, CaO, Na<sub>2</sub>O, MgO and Al<sub>2</sub>O<sub>3</sub> contents of the corundum-bearing syenites plot in an area considerably removed from the general fractionation curves (see Figure 22). MgO is extremely depleted in the corundum-bearing syenites, ranging from 0.85 to below detection limits. The low MgO values in rocks containing SiO<sub>2</sub> comparable to diorites and monzodiorites of this complex are one of the major geochemical characteristics of the corundum-bearing syenites. The FMA variation diagram (Figure 24) suggests an apparent fractionation trend from rocks enriched in Fe and Mg toward increasing Na+K levels, of which the highest relative values are contained within the quartz-bearing phases (unit NCS-6).



**Figure 22.** Harker diagrams illustrating petrochemical variation of selected major elements from rocks of the New Carlow syenite complex. Symbols represent samples from the following units: •, NCS-1; x, NCS-7, NCS-8, NCS-9; ▲, NCS-6; +, NCS-4.

Geochemical trends on a CNK diagram (*see* Figure 24) are less obvious.

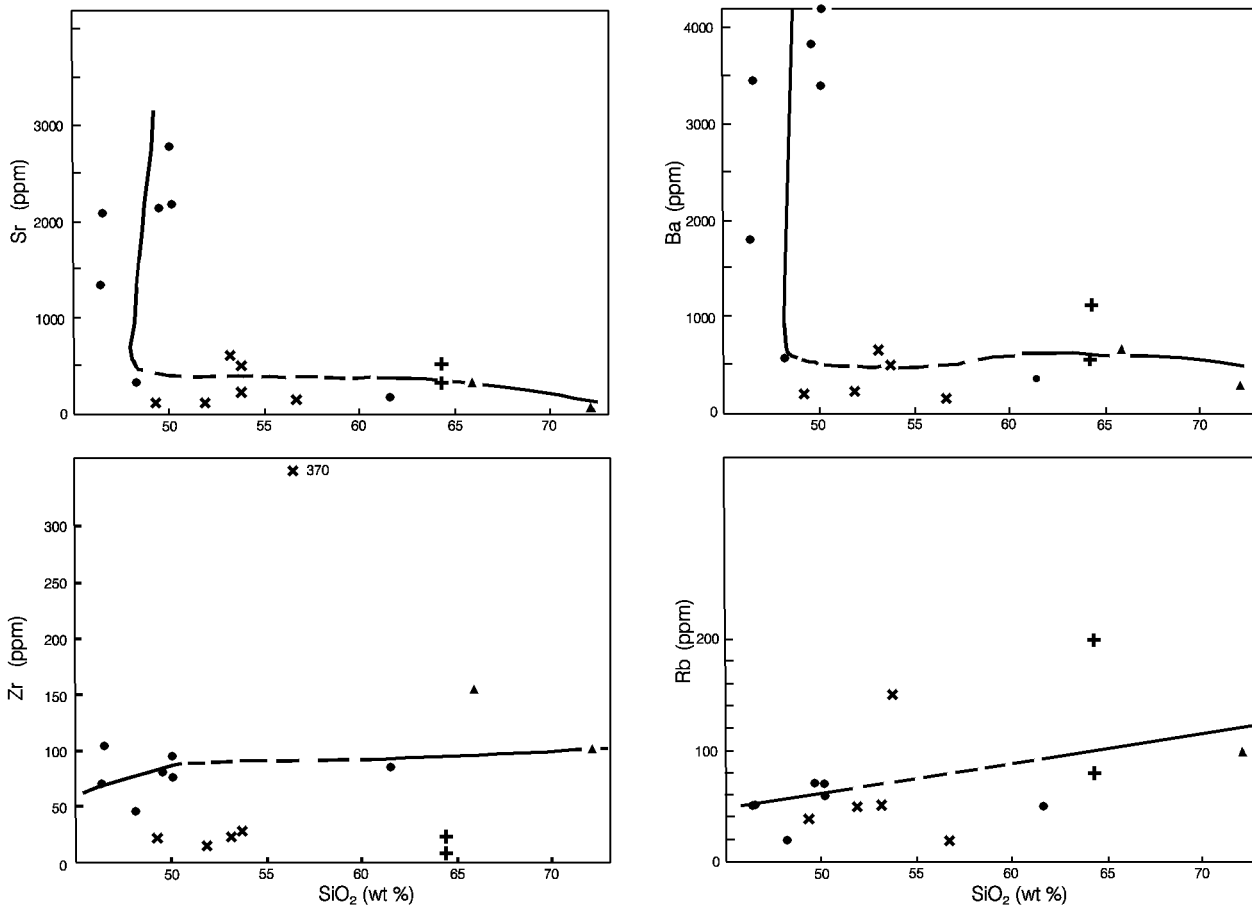
Dioritic rocks appear to represent the most “primitive” composition in the New Carlow syenite complex, as suggested by generally highest total Fe as FeO, MgO, and CaO (*see* Figure 24 and Appendix 2g) and tendency toward lowest SiO<sub>2</sub> levels. This is also expressed by the extremely high Ba (360 to 6054 ppm) and Sr (185 to 2770 ppm), and lowest average K/Ba (19) and highest average K/Rb (512) ratios. No excess Al<sub>2</sub>O is notable in any diorite or monzodiorite analysis in Appendix 2g.

The behaviour of Sr and Ba versus SiO<sub>2</sub> is somewhat anomalous (*see* Figure 23), and trends here are marked by a rapid decline of these elemental abundances between SiO<sub>2</sub> levels of 45 and 52%. At successively higher SiO<sub>2</sub> concentrations, levels of Sr and Ba remain relatively low. Very few granitic rocks contain levels of Sr and Ba at the SiO<sub>2</sub> values observed in many of the diorites from New Carlow syenite complex. Such levels of Sr and Ba concentration are only rarely attained in geological materials, some examples of which are deep sea calcareous pelagic sediments (2075 ppm Sr; Turekian and Kulp 1956), deep sea clays (up to 4160 ppm Ba; Fischer and Puchelt 1972), and some nepheline syenites. Miaskitic nepheline syenite on Stjer-

noy, north Norway, (Heier 1964) exhibits mean values of Ba comparable to diorite of the New Carlow syenite complex, but contains Sr levels approximately twice as high. Nepheline syenites at Blue Mountain, Ontario, are relatively depleted in Sr and Ba, containing quite high K/Ba and K/Rb ratios (Heier 1965), which do not compare favourably with the Stjernoy or New Carlow syenitic rocks.

The K/Rb and K/Ba ratios of the Stjernoy syenites and diorites from the New Carlow syenite complex demonstrate a closer similarity. However, phases of the latter complex, exclusive of the diorite, show a trend toward lower K/Rb ratios in the range of most crustal materials (Figure 25). The K/Ba ratios show a strong increase from 8 to 67 (Figure 26). The other syenitic phases plotted on this diagram mostly plot near the average crustal ratio of 65.

The origin of various rocks comprising the New Carlow syenite complex is not readily explicable. The high corundum content of 4 to 19% demands special conditions of formation that normally appear in differentiating syenitic magmas which are devoid of this mineral. All petrographically defined phases, exclusive of those containing corundum, apparently delineate a typical fractional crystallization sequence. The high Sr and Ba contents, particularly those of the diorites, could either indicate a relatively



**Figure 23.** Harker diagrams illustrating petrochemical variation of selected trace elements from rocks of the New Carlow syenite complex. Symbols represent samples from the following units: •, NCS-1; ×, NCS-7, NCS-8, NCS-9; ▲, NCS-6; +, NCS-4.

primitive syenitic magma type (Heier 1964) or represent crustal contamination. If contamination was an important factor, a trend toward lower K/Rb ratios should be noticeable. At Stjernoy, Heier (1965) argued to the contrary since K/Rb ratios there remain uniformly high (K/Rb = 484 to 802). Assimilation of aluminous metasedimentary rocks may constitute one process in which  $\text{Al}_2\text{O}_3$ , Sr and Ba contents of a fractionating diorite-syenite magma were sufficiently modified to allow crystallization of the corundum-bearing phases and is the explanation favoured in this study.

Several phases of the New Carlow syenite complex exhibit a slight enrichment in tin, relative to the Clarke value of 1 ppm. Most notable here are phases from units NCS-3, NCS-4, NCS-6, NCS-7 and NCS-8, in which Sn collectively ranges between 3.9 and 8.7 ppm, and could relate to crustal contamination through metapelitic rocks in which Sn is commonly enriched (shale average = 6 ppm Sn, Turekian and Wedepohl 1961).

### RARE EARTH ELEMENT GEOCHEMISTRY

Seven REE analyses from the New Carlow syenite complex are given in Appendixes 2g, 2h and 2i, with chondrite-normalized patterns shown on Figure 27. The rock types analyzed (units NCS-1, NCS-4, NCS-8) exhibit 3 distinct REE patterns, which become progressively more fractionated as total REE contents decrease. Systematic variation in total REE,  $\text{La}/\text{Yb}_N$  or  $\text{Eu}/\text{Eu}^*$ , however, is not clearly correlative with increasing  $\text{SiO}_2$  content.

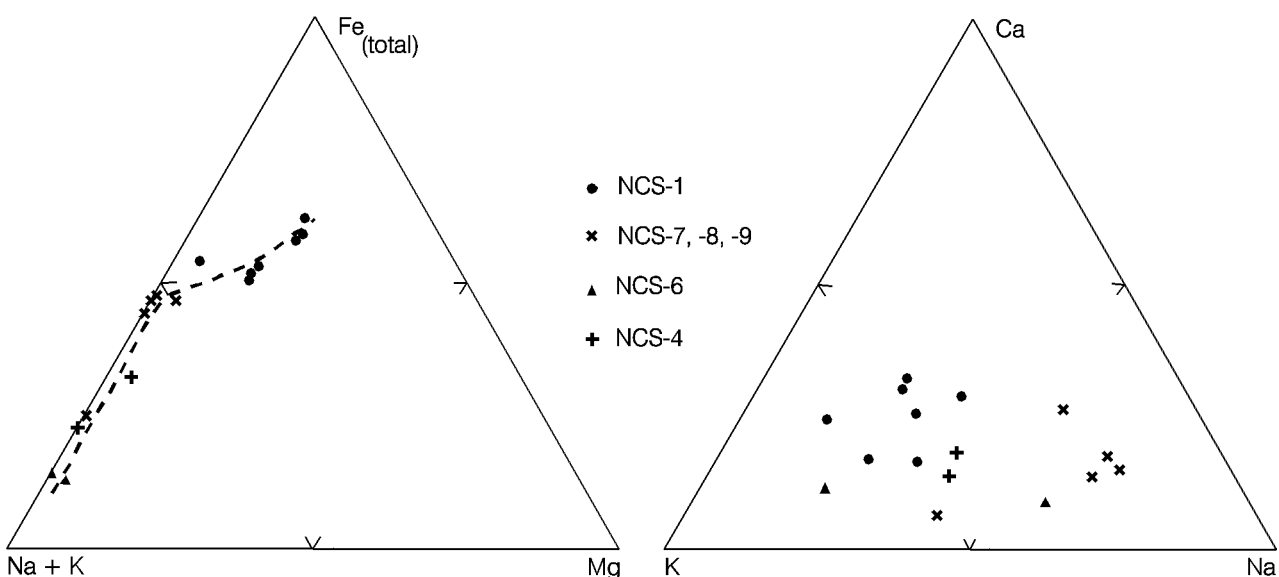
Diorites (unit NCS-1) and augite syenite to monzonite (unit NCS-4) exhibit overlapping ranges for total REE contents and flat chondrite patterns relative to corundum-enriched plagiostenite (unit NCS-8). However, some distinct differences are also discernable. The diorites ( $\text{REE} =$

351 to 672 ppm) exhibit small negative Eu anomalies ( $\text{Eu}/\text{Eu}^* = 0.82$  to  $0.89$ ) relative to unit NCS-4, where prominent negative anomalies are evident ( $\text{Eu}/\text{Eu}^* = 0.35$  to  $0.46$ ).  $\text{La}/\text{Yb}_N$  ratios of unit NCS-1 range between 4.3 and 20.8 and, with the exception of specimen 7-14-2, are considerably higher than unit NCS-4 values ( $\text{La}/\text{Yb}_N = 3.0$  to  $5.9$ ). Similarly, the chondrite patterns of specimen 7-14-2 and unit NCS-4 are striking, apart from the obvious difference in  $\text{Eu}/\text{Eu}^*$  ratios.

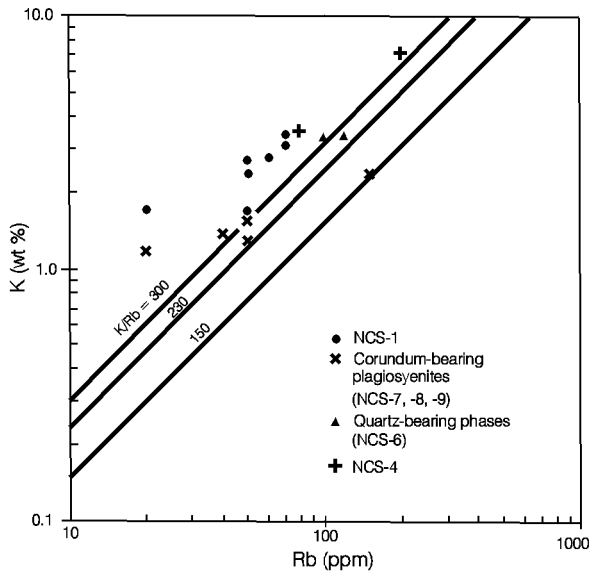
Corundum-enriched plagiostenite (unit NCS-8), as exemplified by typical ore material from the Hoover Mountain corundum deposit, has the most fractionated REE pattern determined for the New Carlow syenite complex. This is revealed by the large  $\text{La}/\text{Yb}_N$  ratio of 1.1 which features drastic depletion of HREE ( $\text{Yb} = 0.45 \times$  chondrite) relative to LREE ( $\text{La} = 32 \times$  chondrite). Presence of a moderate positive Eu anomaly ( $\text{Eu}/\text{Eu}^* = 1.57$ ) is a further unique feature.

Syenites and monzonites (unit NCS-4) could conceivably be generated by partial melting of a quartz-poor, feldspathic protolith such as the spatially related diorites (unit NCS-1).

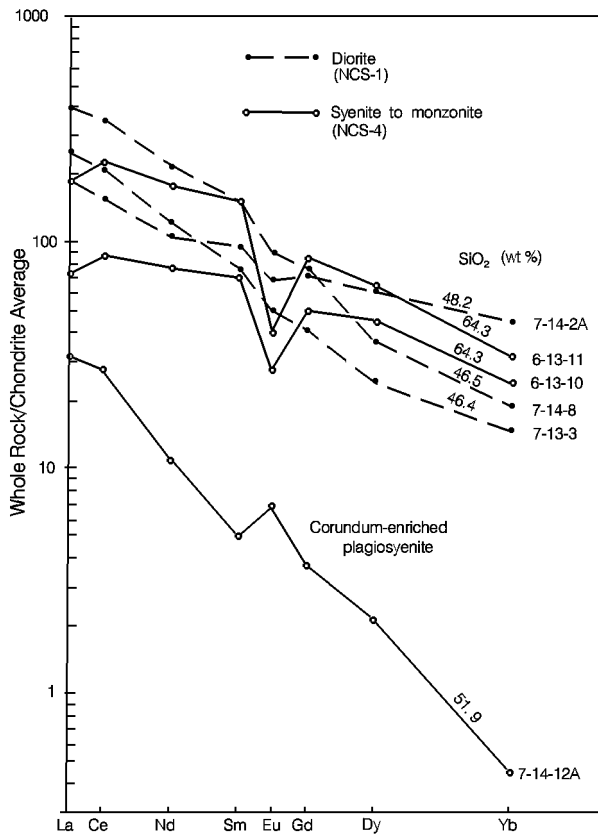
Since the diorites commonly contain potassium feldspar (*see* Appendix 11), a ready source of potassium (2.01 to 4.06%  $\text{K}_2\text{O}$ ) (*see* Appendix 2g) could be available and, under conditions of incipient anatexis, a quartz-poor, potassium feldspar-enriched melt phase should be expected. However, the much lower barium contents in the syenites and monzonites (unit NCS-4: average 840 ppm Ba) (*see* Appendix 2h) relative to the diorites (unit NCS-1: average 2780 ppm Ba) (*see* Appendix 2g), in particular, pose a problem to this model since most barium is probably contained within potassium feldspar and the resulting melt phase should correspondingly have relatively low barium.



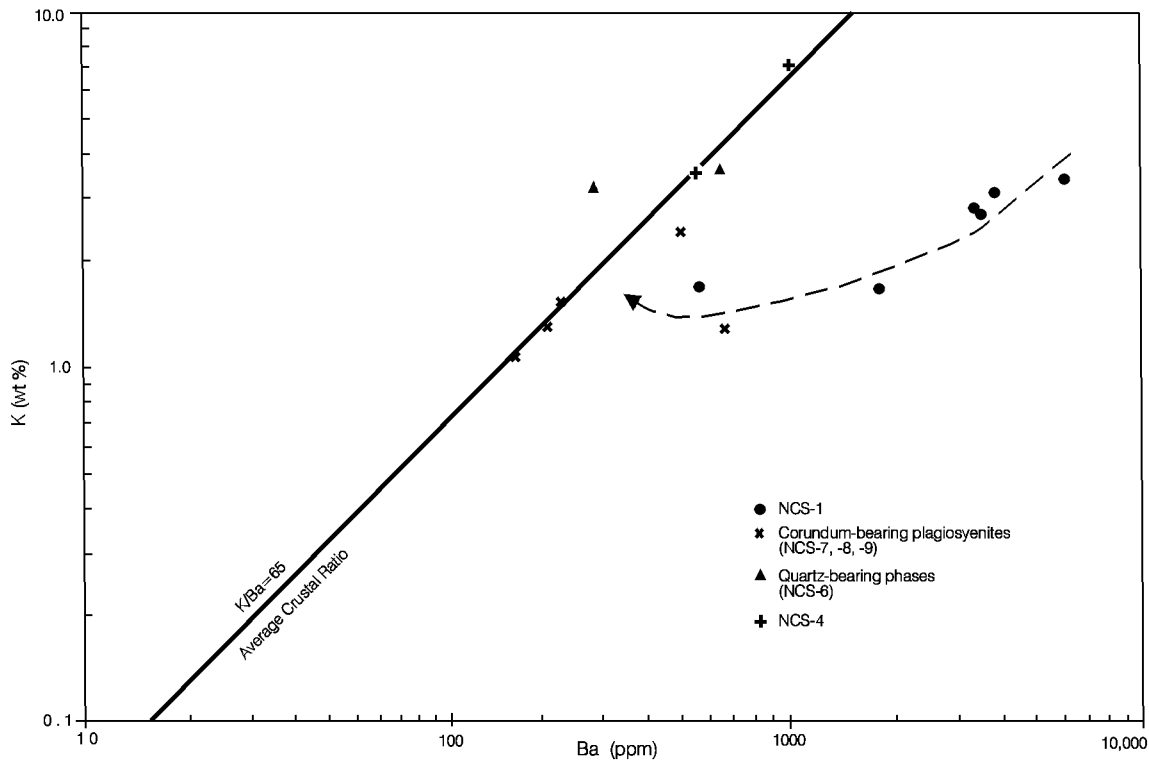
**Figure 24.** Total iron–magnesium–alkalis (FMA) and calcium–sodium–potassium (CNK) variation of various petrographic phases from the New Carlow syenite complex.



**Figure 25.** K/Rb relationships in various petrographic phases of the New Carlow syenite complex. Range and mean K/Rb ratios for crustal materials from Taylor (1965).



**Figure 27.** Chondrite-normalized REE plots of diorite, syenite, monzonite and corundum-enriched plagiосyenite from the New Carlow syenite complex.



**Figure 26.** K/Ba relationships in various petrographic phases of the New Carlow syenite complex.

## Potassic Granitoid Suite (Map Units 9a to 9g)

Rocks of this group occur within all map units of the Madawaska Highlands gneissic complex. The great majority of them, however, are confined to 2 relatively large masses:

1. the Wicklow granite, a granite tectonic breccia occupying the core zone of the southeast-plunging Wicklow antiform
2. a southwest-trending unit intermittently exposed between Franz Pond area and Cardwell Lake

Less extensive, mappable units were delineated between Davis Pond and Theresa's Pond (possibly extending to Purdy); and in the vicinity of Little Papineau Lake Road about 3.5 km east of its junction with the Madawaska Highway.

At these less extensive occurrences, the rocks form sheet-like, erosionally resistant cappings on many hills, as, for example, immediately northeast of Theresa's Pond, near McCastle Pond, and 3 km north of Maple Leaf. The maximum or average thickness of such sheets is not known. Geological age of the metamorphosed granites is unknown; however, their emplacement may predate the Grenville Supergroup as suggested by their absence within such supracrustal rocks. The aforementioned 2 larger masses have differing structural trends, relatable to their occurrence in contrasting structural domains (*see* "Structural Geology").

### STRUCTURE

These rocks are generally medium grained and moderately foliated, and in a few places, are gneissic. The gneissic banding is defined by discontinuous, 0.5 to 1 cm thick hololeucocratic, medium-grained, plagioclase-quartz-potassium feldspar layers alternating with more mafic, fine- to medium-grained quartz-biotite-hornblende-plagioclase bands. Thin bands rich in quartz may also contribute to the gneissosity. The rocks may also be vaguely lineated, the lineation being defined by ribbon-like trains of biotite and rarer hornblende prisms. Quartz rodding may also define a lineation. At several outcrops, the influence of mild cataclasis has led to development of protomylonite textures featured by coarse-grained, augen- to sigmoidal-shaped potassium feldspar and rare plagioclase porphyroclasts embedded within a fine- to medium-grained matrix. This matrix, in places, exhibits localized quartz banding and streaky biotite-rich aggregates. Maximum dimensions of potassium feldspar and plagioclase porphyroblasts are 2.2 by 1.5 cm and 1 by 1.5 cm, respectively. Good examples of the blastomylonites were encountered along Highway 127 about 0.8 km northwest of the junction with the Madawaska Highway (Concession V, Lot 3, McClure Township), near an unnamed road about 1.2 km north-northwest of its termination near Maple Leaf (Concession III, Lot 11, Wicklow Township), and 1.2 km west of Indian Lake (Range 50, McClure Township).

### PETROLOGY

The rocks of map units 9a to 9g are almost entirely granite in composition (Figures 28a and 28b; Appendixes 1n, 1o and 1p). They are moderate to deep pink due to a large proportion of potassium feldspar. A few approach quartz syenite composition (*see* Figure 28b). A hololeucocratic to very leucocratic aspect of these metamorphic granites is another notable idiosyncrasy. On Figure 28a, it can be observed that relatively few samples exceed a colour index of 10 and approximately one half of the population is hololeucocratic. Potassium feldspar, quartz and plagioclase form an interlobate granoblastic, commonly seriate texture and are ubiquitous within the metamorphosed granites. Biotite is the most abundant accessory mineral and occurs as slender to stubby subhedral laths. Allanite is a euhedral to subhedral accessory mineral. It exhibits hematitic halos and radial fracturing within host minerals. In some cases, allanite prisms define a lineation within granite sheets, such as that interleaved within diorite gneiss on Highway 127, located 1 km northwest of the Madawaska Highway junction. This was also noted in more vaguely lineated magnetite-allanite-biotite granite exposed at the western end of Davis Island in Papineau Lake. Allanite may make up 5% of the granite. Allanite-rich granites commonly are characterized by deep red-brown, medium-grained spots set in a deep pink granitic matrix. An outcrop showing well-developed allanite spots is located on Highway 127 as mentioned above. Hornblende is relatively scarce, occurring only in a narrow east-trending 100 to 320 m wide granite unit in the Davis Pond-Theresa's Pond area. It is xenomorphic and makes up between 0.2 and 2.3% of the rock (*see* Appendix 1n). Hornblende may, however, be quite abundant locally in zones surrounding partially assimilated mafic inclusions, for instance, near the outlet of Davis Pond. Here, the hornblende formed by a reaction between the granite melt and amphibolitic enclaves that resulted in rocks of quartz-poor biotite-hornblende, allanite-biotite-hornblende and hornblende syenite, monzonite, and monzodiorite compositions (map unit 9c). Accessory minerals are opaque iron oxide, pyrite, hematite, muscovite and zircon.

Several petrologic variants were delineated within the broad metamorphosed potassic granitoid suite of rocks (map units 9a to 9g). A distinctive, mauve-coloured hololeucocratic, fine- to medium-grained granite was encountered in many localities. It is characterized by minor fine- to medium-grained muscovite. An easily accessible outcrop of this rock is located on Highway 127 about 1.8 km north-northwest from Maynooth, where, as in most exposures, it represents a minor component of the outcrop. As a dominant unit, it was only encountered in a Madawaska Highway roadcut, 3 km north of the Little Papineau Lake Road junction. These granites appear to form sheets that are between 1 and 10 m thick. Deep red-brown hematitic halos, measuring 1 by 1 mm to 4 by 5 mm on surfaces normal to foliation, are developed around fine-grained, disseminated allanite, and characterize some exposures of these granites as within the aforementioned Madawaska Highway roadcut.

The granites grouped as map units 9a to 9g are interpreted to be magmatic in origin. The common concordance with enclosing units is possibly tectonic in origin. In one rare instance, however, a slight discordancy between a 0.5 to 1 m wide muscovite-magnetite granite and steeply dipping metasedimentary migmatite host was observed in an outcrop about 120 m southwest of the Highway 62 junction with the South Papineau Lake Road and suggests an emplacement of the granite as a dike. Modal proportions of quartz-plagioclase-potassium feldspar compare well (*see* Appendix 1o and Figure 28b) to other coarser grained granites within the study area.

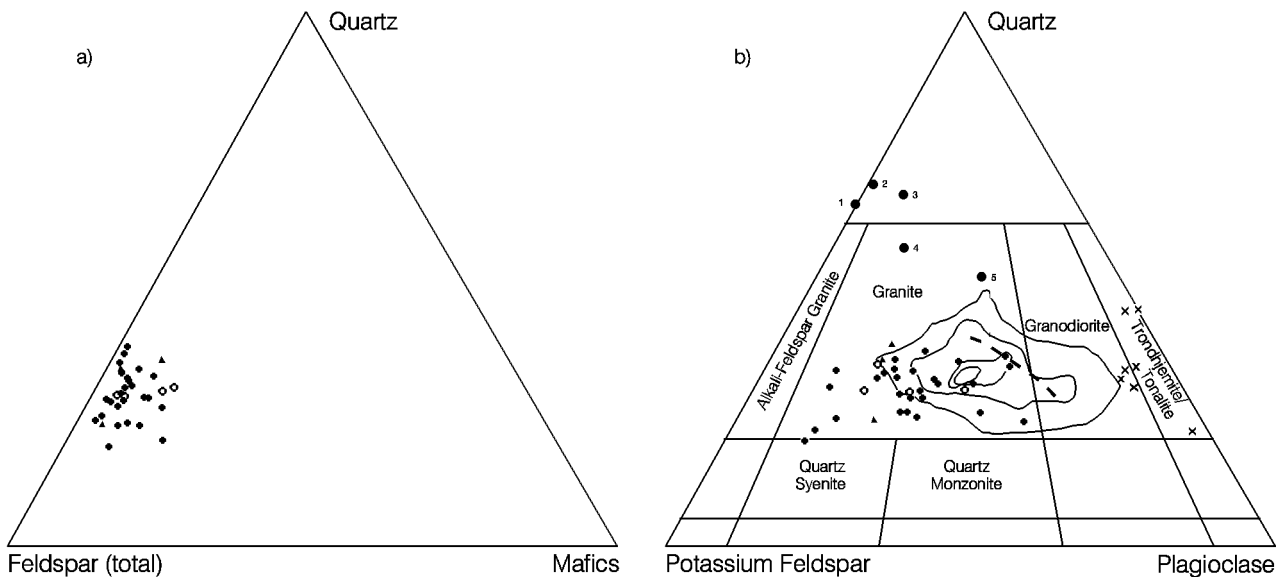
**Wicklow Granite**

This 7.5 km elongate granite unit represents the most extensive such mass delineated within the study area and is structurally controlled. It is largely confined to the Wicklow antiform core zone and is very poorly exposed. The best outcrops are situated on the Madawaska Highway. The width of the Wicklow granite ranges between 1.2 and 1.7 km in the northern part (Wicklow-Thominson lakes area) and, southward, it thins rapidly before disappearing near Lansing Pond.

Most of the pluton consists of granite tectonic breccia, and is intruded by previously described hololeucocratic to leucocratic, fine- to medium-grained, muscovite-allanite-magnetite granite. The best exposure is an extensive roadcut on the Madawaska Highway at a point between Thominson and Evans lakes. Here, angular to rounded megaclasts (*see* Photo 2) constitute between 30 and 35% of the

rock and are enclosed within a coarse-grained, foliated, biotite to hornblende-biotite granite matrix. A modal analysis of a typical granite tectonic breccia is presented in Appendix 1p. Clasts here consist of fine- to medium-grained biotite-hornblende ± diopside diorite (foliated and gneissic), amphibolite (fine grained and massive), biotite trondhjemite (gneissic) and relatively rare metasedimentary metatextite and pink to white calcite-scapolite-diopside calc-silicate skarn. Rarer fragment types include anorthosite suite rocks described previously. The amphibolite clasts vary in appearance from those illustrating excellent agmatitic structures (with sharp inclusion boundaries) to well-rounded inclusions with local 0.5 to 1 cm wide biotite-rich halos, which probably originated via reaction with a fluid-rich phase. Several of these amphibolite clasts have been assimilated by the granite to the extent that the granite matrix has locally been converted into a hybrid, quartz-depleted, hornblende diorite and monzodiorite. Some fragments, such as the largest shown in Photo 2, exhibit an abrupt truncation of gneissic layers by the foliation of the enclosing granite. This fragment contains prograde diopside and possible orthopyroxene of granulite-facies metamorphic grade. Isoclinal folds in some clasts show the same relationship, strongly suggesting a high-grade tectonometamorphic event prior to the tectonic mobilization and granite emplacement episode responsible for development of the breccia.

Modally, the granite matrix (*see* Appendix 1p and Figure 28b) is similar to other metamorphosed granites of the study area. Quartz content is relatively constant. The po-



**Figure 28.** Modal variation of metamorphosed potassic granitoid suite rocks on a) a quartz-total feldspar-mafics (QFM) ternary diagram, and b) a quartz-plagioclase-potassium feldspar (QPK) ternary diagram. Symbols for rocks and sources used in a) and b): •, metamorphosed granites, this study; ▲, metamorphosed hololeucocratic muscovite-bearing granites, this study; ○, matrix of tectonic breccia, Wicklow granite, this study; ×, leucosome from metasedimentary migmatite, this study. In addition, for b): ●, modal analyses of arkoses from the literature: 1, sparagmite, Precambrian, Norway (Barth 1938, p.60); 2, arkose, Precambrian (Jotnian), Satakunta, Finland (Simonen and Kuovo 1951); 3, pale arkose, Triassic, Connecticut (Krynine 1950, p.85); 4, red arkose, Triassic, Connecticut (Krynine 1950, p.85); 5, average of 24 arkoses, Eocene-Oligocene, Santa Ynez Mountains, California (van de Kamp, Leake and Senior 1976). Contours represent modal analyses of 260 thin sections of granites from the eastern United States. Contours more than 0, 2, 5, and 7% (0.25% contour from Chayes 1952, p.42). Dashed line represents the locus of ternary minima and eutectics from 0.5 to 5 kilobars water vapour pressure (Luth, Jahns and Tuttle 1964).

tassium feldspar:plagioclase ratio varies from 1 to 2.8. Accessory minerals are biotite, hornblende, allanite and rare pyrite. Local porphyroblasts of plagioclase and potassium feldspar may be present. Potassium feldspar porphyroblasts are more abundant and are up to 7.5 by 14 cm in size.

The compositional variations of the metamorphosed granites of the map area are portrayed on quartz–plagioclase–potassium feldspar (QPK) and quartz–total feldspar–mafics (QFM) ternary diagrams (*see* Figure 28). All samples are granitic in composition and are characterized by an overall wide range in potassium feldspar:total feldspar ratios. Chayes (1952) demonstrated that crystal–liquid equilibria is an important controlling factor in the evolution of many granitic masses and documented that the modal analyses of granites from the eastern United States cluster relatively closely on a QPK diagram (*see* Figure 28b). The main concentration trend of the Chayes contours approximately parallels the locus of isobaric minima and eutectics in the haplogranite system ( $\text{SiO}_2\text{-KAlSi}_3\text{O}_8\text{-NaAlSi}_3\text{O}_8\text{-H}_2\text{O}$ ), otherwise known as the low-temperature “thermal valley”. This comparison of the haplogranite system with Chayes’ results must be viewed as approximate, since minor amounts of albite will be finely intergrown with potassium feldspar and not accounted for in the modal analyses. Approximately 60% of the metamorphosed granites from the study area fall within Chayes’ contours, although no distinct clustering is evident proximal to the low-temperature cotectic portion of the diagram. The granitic rocks in the study area, therefore, do not appear to represent minimum melt composition. Most rocks, instead, show a trend toward increasing potassium feldspar content, and may represent products of relatively extensive partial melting in the source region. Obvious magmatic rocks, such as the unmetamorphosed subsolvus granite pegmatite dikes of the Hybla swarm, interestingly exhibit an identical trend, with only one sample falling close to the low-temperature thermal valley (*see* Figure 28b) as traced between 0.5 and 5 kilobars  $P_{\text{H}_2\text{O}}$ .

Leucosome compositions from metatexitic and homophanous metasedimentary migmatites fall into a distinctively different field within Figure 28b, and bear no resemblance to metamorphosed granites. Fine-grained, recrystallized granites (*see* Appendix 1o) may be inadvertently classified as arkose. No modal similarity, however, exists between any of the study area granites and various arkoses from the literature as indicated on Figure 28b.

### Tectonic Breccia

In this study, the tectonic breccias were classified according to their matrix and, thus, have been listed in several legend subdivisions:

1. granite tectonic breccia (map unit 9g)
2. tonalite tectonic breccia (map unit 10e)
3. metasedimentary migmatite tectonic breccia (map unit 4n)

The breccias are characterized by diagnostic features, listed as follows:

1. intense diastrophism in metasedimentary migmatite and biotite quartzofeldspathic gneiss
2. rootless intrafolial folds
3. rotation of fragments as indicated by pre-existing gneissosity and lineation within the clasts at various athwart positions in relation to the enclosing matrix foliation
4. truncation of planar fabric containing prograde granulite-facies and high-grade metamorphic assemblages within relatively mafic fragments by foliation of enclosing host medium
5. presence of protomylonite to mylonite textures
6. leucosome-melanosome migmatitic couplets in metapelitic fragments, situated at an abrupt angle with the fabric of the matrix. Observations 4 and 6 document that tectonic mobilization developed late in the tectonometamorphic history of the area and after a high-grade to granulite-facies anatexis event.

Granite tectonic breccia, by far the most common breccia, occupies a significant portion of the Wicklow granite and is also known to occur 200 m southeast of Johnson Lake and very near the outlet of McCastle Pond. These occurrences have already been described (*see* “Metamorphosed Felsic to Intermediate Plutonic Rocks”, and “Mafic to Intermediate Gneiss”).

Tectonic breccias containing a tonalitic matrix occur in 2 localities: near the northwestern map area corner in Concession I, Lot 24, Lyell Township, and 0.8 km southwest of Furz Mountain summit in Concession VII, Lot 3, in Bangor Township. These rocks contain 10 to 20% linedated fragments of medium-grained diorite and/or amphibolite embedded within a foliated to gneissic hornblende-biotite tonalite host. The diorite clasts are up to 1 by 1.3 m in size. The lineation within the clasts trends at various angles to the enveloping foliation surfaces as at the Furz Mountain occurrence.

Breccias contained within metasedimentary migmatites are also rare, are exposed in a few small outcrops in the Centreview area (Concession VIII, Lot 8, Bangor Township), and contain large diopside-bearing metagabbro clasts.

### PETROCHEMISTRY OF THE POTASSIC GRANITOID SUITE

Nine major and trace element analyses representative of the metamorphosed potassic granitoid group appear in Appendix 2j. Rocks from this group exhibit relatively little variation in terms of major element chemistry, which is most apparent for  $\text{SiO}_2$  (69.9 to 76.9%),  $\text{Al}_2\text{O}_3$  (12.2 to 15.4%),  $\text{K}_2\text{O}$  (4.17 to 6.53%),  $\text{Na}_2\text{O}$  (1.44 to 2.97%) and total Fe as  $\text{Fe}_2\text{O}_3$  (0.99 to 4.54%). Calcium contents are mostly quite similar to the average alkali granite (Nockolds 1954, p.1012) and average low-calcium granite (Turekian and Wedepohl 1961, p.188). On a Ca–Na–K (CNK) diagram (*see* Figure 19), the alkalic chemistry of these rocks is also indicated by a distinct clustering beyond the calc-alkalic igneous trend of Nockolds and Allen (1953).

On Figure 28b, Barth mesonormative proportions of quartz, albite and orthoclase of Wicklow-area metamorphosed granites have been plotted in the haplogranite system ( $\text{SiO}_2\text{-NaAlSi}_3\text{O}_8\text{-KAlSi}_3\text{O}_8\text{-H}_2\text{O}$ ) and compared to 507 contoured granite analyses from the literature. Most analyses from the map area lie outside this contoured field and only one sample falls on the locus of ternary minima or eutectics, that is, low-temperature trough for the haplogranite system. Instead, the observed distribution of Wicklow-area granites suggests a  $\text{K}_2\text{O}$  and  $\text{SiO}_2$  enrichment relative to most minimum-melt granitic compositions. This scatter in normative compositions renders it difficult to envisage minimum melt crystal-liquid equilibria as a relevant controlling factor in the petrogenesis of Wicklow-area granites, and corroborates observations previously made on the basis of modal variation.

In the analyses listed in Appendix 2j, trace element variation is greatest for Ba (800 to 1710 ppm), Zr (45 to 475 ppm), Sr (155 to 440 ppm) and total REE (389 to 1459 ppm). Rubidium (80 to 170 ppm) is more restricted; however, in most analyzed specimens, this element is depleted relative to K, as all but 2 specimens exceed the crustal K/Rb upper limit of 300 (Taylor 1965). Ratios of K/Ba indicate a slight depletion of Ba relative to the crustal average of 65.

All specimens exhibit similar, strongly fractionated, chondrite-normalized REE patterns showing moderate to pronounced depletion of HREE relative to LREE (Figure 29). Lanthanum ranges from 89 to 386 ppm, representing

an enrichment relative to chondrites between 262 and 1135 times chondrite. Ytterbium (0.6 to 4.7 ppm), on the other hand, exhibits a much more restricted range of enrichment (2.7 to 21.4 $\times$  chondrite). Degree of fractionation, as expressed by the chondrite-normalized La/Yb<sub>N</sub> ratio, is particularly high for specimens 3-11-4B, 4-3-15B and 7-2-6, where ratios vary between 53 and 193 (see Appendix 2j). The remaining specimens show more moderate La/Yb ratios (15 to 36).

All granites contain negative Eu anomalies, featured by Eu/Eu\* between 0.29 and 0.72. The most pronounced Eu anomalies occur in granites with highest total REE (see specimens 4-3-15B, 7-2-6 and 7-6-4B in Appendix 2j). There is a tendency for a decrease in total REE contents and an increase in Eu/Eu\* with increasing  $\text{SiO}_2$  content.

Maximum total REE levels (1459 ppm in specimen 7-2-6, see Appendix 2j) are contained within allanite-bearing granite on Highway 127. This substantial content is mainly composed of LREE (1435 ppm) and probably relates to the presence of allanite, which preferentially partitions LREE over HREE from the melt into allanite due to its very high distribution coefficients (Henderson 1984, p.26).

### Sodic Granitoid Suite (Map Units 10a to 10c)

These rocks are mainly confined to the Indian Lake plutonic complex. This is a tonalite-quartz diorite-diorite meta-plutonic association and trends southeasterly, parallel to

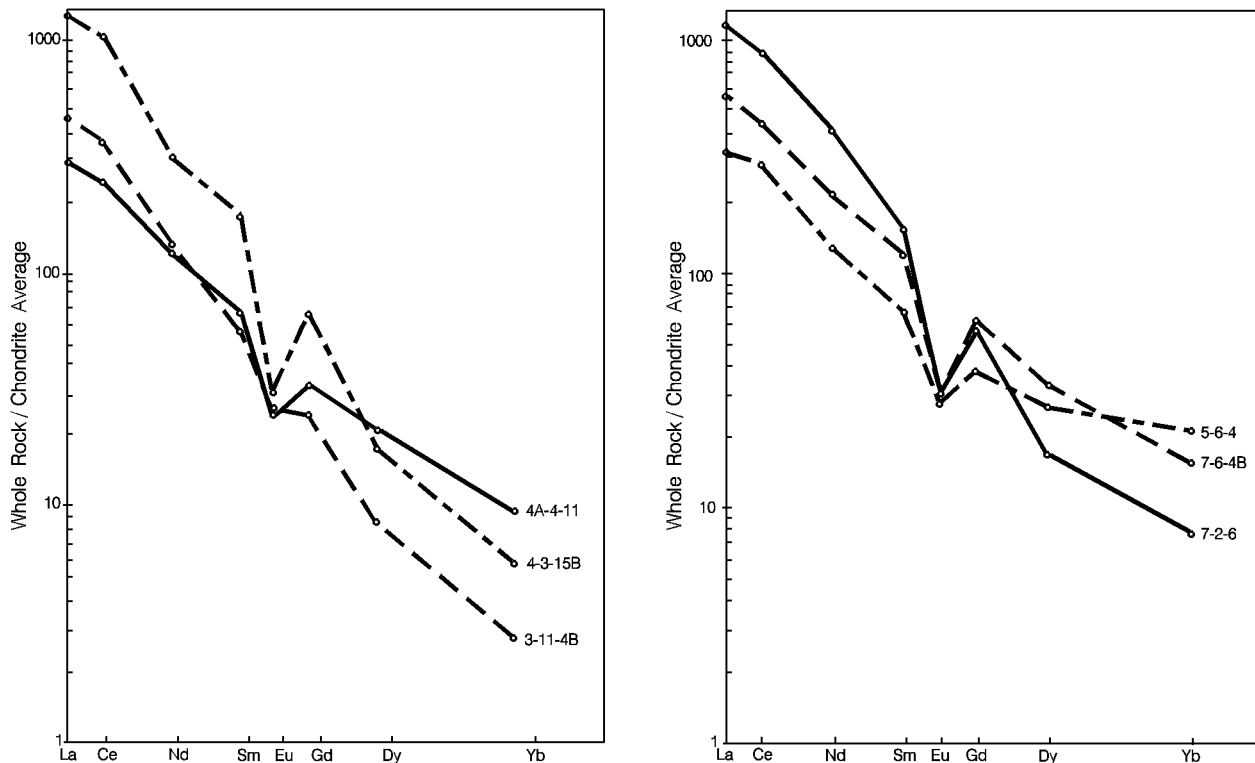


Figure 29. Chondrite-normalized REE plots for metamorphosed potassic granitoid rocks from the Wicklow area.

the McClure–Wicklow township boundary between Indian Lake and the Madawaska Highway, for a distance of about 5.4 km. The width of the complex is consistently about 2.5 km. A branch of this complex extends beyond the western map area limits, identical rock types were encountered at the village of Lake St. Peter, just west of the map area.

A strong hornblende lineation pervades most parts of the Indian Lake plutonic complex and may be accompanied by weak to moderate foliations. This foliation is defined by the preferred orientation of biotite. All rock types have been recrystallized and exhibit interlobate granoblastic textures.

Dominant rock types are light grey-weathering biotite, hornblende-biotite, and biotite-hornblende tonalite to quartz diorite. Subordinate diorite also occurs. Modal analyses of typical rock types of this complex are given in Appendix 1q. Good exposures of quartz diorite to tonalite are located on Range 31, McClure Township, very near the boundary with Wicklow Township and at the termination of a hunting club access road which commences at Highway 127 near the Papineau Creek bridge. These exposures contain 10 to 20% inclusions of medium-grained, lineated, biotite-hornblende diorite, concordant to subtly discordant boudinaged amphibolite dikes, and thin (1 to 2 cm) white hololeucocratic, fine- to medium-grained trondhjemite veins.

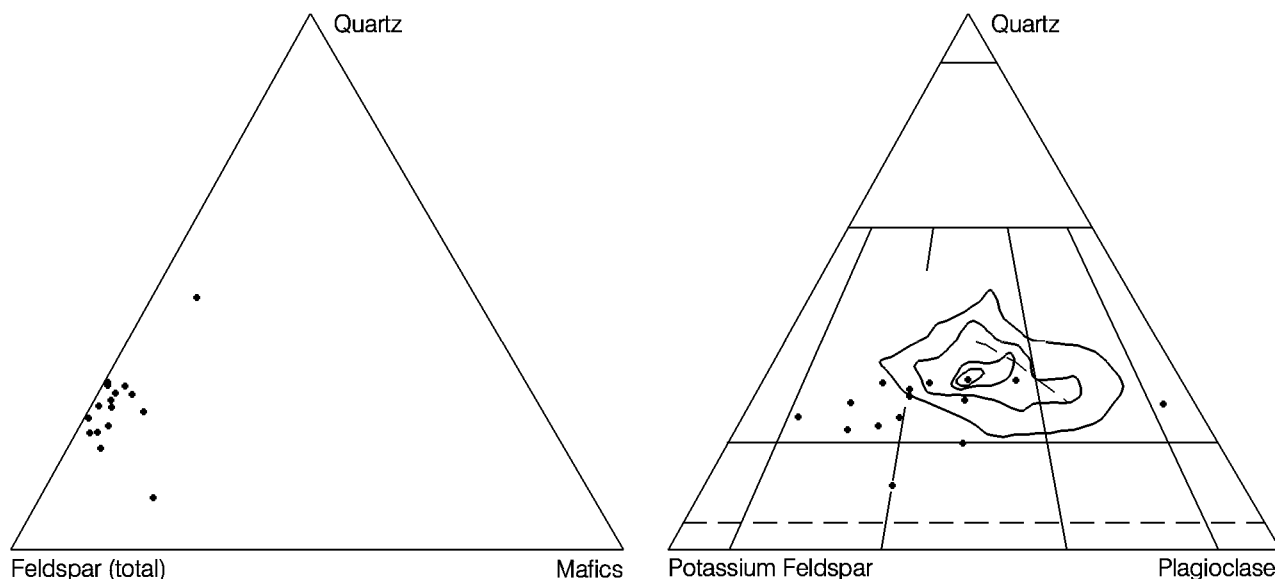
Trondhjemitic-tonalitic metaplutonic rocks commonly occur elsewhere within the study area, in most places as inclusions within metasedimentary migmatite, dioritic metaplutonic rocks, metamorphosed granites, and felsic to intermediate gneisses. Their relationship with the felsic and intermediate gneisses, as in the Brouse Pond area, may simply point out that the tonalitic-quartz diorite metaplutonic rocks are less deformed equivalents of such gneisses.

## Unmetamorphosed Felsic to Intermediate Plutonic Rocks (Map Unit 11)

### POTASSIC GRANITOID SUITE

Dikes of the posttectonic Hybla granite pegmatites (map units 11a to 11f) extend across the northwestern part of the map area and trend between 040 and 060°. Besides rare diabase dikes, these rocks represent the only rocks that escaped the main effects of the Grenville orogeny in the area. Most dikes are in the 0.5 to 3 m width range. Contacts of the dikes with host rocks are invariably sharp and vertical to subvertical. The 4.5 km by 240 m Yuill Lake granite pegmatite-aplite dike is, by far, the largest Hybla dike in the area. It has a steep, slightly curvilinear northwest contact, which strikes 045°. Wider dikes may exhibit a discontinuous quartz-rich core zone that completely encloses homogeneous euhedral blocky potassium feldspar megacrysts. The largest examples of these crystals measure 3.5 m in diameter as encountered on Balsam Lake (*see* “Dublestein Occurrence” in “Economic Geology”). Such coarse grain sizes are very exceptional as most dikes rarely exceed a 5 to 20 mm grain-size range. These large feldspar, coarse albite, and accessory biotite crystals are usually euhedral. Otherwise, these rocks exhibit an inequigranular, allotriomorphic-granular texture. Aplite-pegmatite layering is relatively rare and was only observed within the Yuill Lake dike.

Modal analyses of several posttectonic dikes are presented in Appendix 1r. Compositional variation is portrayed on QFM and QPK diagrams (Figure 30). A compositional variation quite similar to that of a metamorphosed potassic granitoid suite is apparent, excluding 2 extreme rock samples. Specimen 5-6-3 is likely part of a quartz-rich



**Figure 30.** Modal variation of unmetamorphosed potassic granitoid suite rocks in quartz–total feldspar–mafic (QFM) and quartz–plagioclase–potassium feldspar (QPK) ternary diagrams. On the QPK diagram, contours represent modal analyses of 260 thin sections of granites from the eastern United States. Contours more than 0, 2, 5, and 7% (0.25% contour from Chayes 1952, p.42). Dashed line represents the locus of ternary minima and eutectics from 0.5 to 5 kilobars water vapour pressure (Luth, Jahns and Tuttle 1964).

core zone and specimen 1-2-1C is of a rare albitic trondhjemite composition.

Most rocks are hololeucocratic as indicated on a QFM diagram (*see* Figure 30). Accessory minerals in the granitic dikes are biotite, magnetite, allanite, titanite, muscovite, apatite and rare zircon in approximate order of decreasing abundance. Most of these constituents are euhedral to subhedral, with the exception of magnetite, which occurs as coarse, irregular, anhedral, locally spectacular aggregates up to 5 by 8 cm. Sphene-bearing pegmatitic dikes were only noted in the extreme southwestern corner of the map area, where such examples are exposed along Highway 127. Euhedral allanite, which is usually glossy black on fresh surface, and weathers to a khaki brown, is a very common mineral in posttectonic granite pegmatites of the area. The largest crystal measured 1 by 2.3 cm on outcrop surface.

## Mafic Intrusive Rocks (Map Unit 12)

### DIABASE

Narrow, massive, fine-grained to aphanitic diabase dikes (1 to 3 m width) were found at 2 localities, that is, on Madawaska Highway at the previously mentioned “type” outcrop for granite tectonic breccia of the Wicklow granite, and very near the northeastern shoreline of Papineau Lake on Concession X, Lot 2, Bangor Township. These 2 dikes have attitudes of 110/43S and 100/90, respectively. The rocks are dark grey on a fresh surface. Minor sulphide minerals, such as pyrrhotite, commonly form films along fractures and weather rusty brown.

## CENOZOIC

### Quaternary

#### PLEISTOCENE AND RECENT

Surficial glacial deposits cover large portions of the map area, particularly in the western third of the area. Extensive north-south oriented glaciofluvial till, and scarcer ground moraine boulder till, completely transgresses the map

sheet (*see* Map 2550, back pocket). Other, less extensive, areas dominated by glacial deposits are situated east of Maple Leaf and Greenview and along Papineau Creek in the southwestern corner of the map area. Locally, these deposits may have considerable thickness, as documented in Greenview. On a farm in this area, approximately 90 m of overburden was encountered prior to intersecting bedrock while drilling a well.

The map area has not received detailed or reconnaissance Pleistocene geological mapping. A large area immediately south of the map area has been surveyed by Barnett and Leyland (1981), who considered that the glacial deposits are of probable Wisconsinan age. Direction of ice movement, as ascertained by drumlinoidal ridges and glacial striae within the map area, averaged about 196°. Ground moraine, boulder-till deposits are relatively older, based on exposures such as on the Greenview Road south of Maple Leaf, where outwash sands overlie boulder till. Boulder till covers extensive parts of the map area. Boulder tills occupy topographically elevated areas, as in the northwest corner, east of Hawk and Evans lakes; between the western shore of Papineau Lake and the higher ground between Johnson, Yuill and Little Papineau lakes, and Moore’s Pond. Much of the Centreview area is also covered with boulder till. Good roadcuts can be examined along the Centreview Road immediately west of Hoare Lake.

Sporadic, very large, erratic blocks are notable in the map area; for example, 1.8 km northwest of Little Papineau Lake, where the largest single boulder measured 3 by 3 by 10 m: a boulder of allanite-magnetite-biotite granite, petrologically identical to the Yuill Lake dike. Smaller erratic blocks occur in many areas of boulder till, for example, the higher ground immediately east of the erratic pile described above.

Fluviatile deposits, the most abundant glacial unconsolidated sediments in the area, are mainly represented by outwash sand and gravel deposits, which occupy extensive areas and are locally pitted with kettle depressions as in the Blairs-Haley lakes area. Groups of esker ridges occur in the Blairs-Little Watson-Cardwell lakes area, and at the western map boundary trending parallel to the Papineau Creek.

# Metamorphism

Most of the study area is underlain by high-grade metamorphic rocks using the definitions of Winkler (1979). Locally, however, hypersthene zone (granulite-grade) rocks occur. These orthopyroxene-bearing assemblages are apparently confined to local “nodes”, as a continuous distribution in the field is not observed. These “nodes” were encountered at 7 localities, which are predominantly concentrated within the northeastern portion of the map area approximately bounded by Papineau Lake, the Wicklow–Bangor Township boundary, Highway 62, and northeastern map boundaries (*see* Figure 2). The largest “nodes” occur at Davis Island (240 m diameter) and near Hoare Lake (200 by 240 m). Thus, the study area has a metamorphic pattern that characterizes it as high grade that locally achieves granulite-facies conditions.

Selected coexisting metamorphic mineral assemblage data and corresponding rock types are listed within Tables 7 and 8. Orthopyroxene is generally restricted to rocks of mafic bulk compositions such as amphibolite, diorite, quartz diorite and pelitic metasedimentary rocks. It only rarely appears in rocks of more felsic compositions such as trondhjemite.

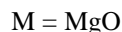
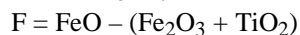
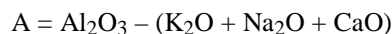
The most petrographically interesting appearance of orthopyroxene is in association with gedrite + garnet + cordierite + biotite (*see* “Hoare Lake Gneisses”). This unique assemblage (*see* Table 7) probably documents that granulite metamorphism in the area occurred under intermediate pressures (Green and Ringwood 1967). Evidence for this interpretation are the metastable cordierite-sillimanite-spinel domains described in detail in the ensuing text. Although no stable aluminosilicates appear to coexist with the Hoare Lake gneiss assemblages, it is probable that the prograde metamorphic event engendering these unique mineral assemblages occurred within  $P$ – $T$  confines of the sillimanite field. This interpretation is substantiated by robust sillimanite occurring in garnet-sillimanite-quartz-biotite-plagioclase metapelite on the Centreview Road about 125 m west of the orthopyroxene-bearing gneisses.

## GRAPHICAL PRESENTATION OF METAMORPHIC MINERAL ASSEMBLAGES

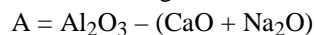
Compatible, limiting metamorphic mineral assemblages mainly from metasedimentary rocks listed in Tables 7 and 8 are shown schematically in 2 modifications of the AFM projection of Thompson (1957) from the AKFM tetrahedron (Figures 31 and 32). This projection is a graphic reduction of the 10 component system  $\text{SiO}_2$ - $\text{Al}_2\text{O}_3$ - $\text{FeO}$ - $\text{Fe}_2\text{O}_3$ - $\text{MgO}$ - $\text{TiO}_2$ - $\text{CaO}$ - $\text{Na}_2\text{O}$ - $\text{K}_2\text{O}$ - $\text{H}_2\text{O}$ , based on the assumptions of silica saturation (presence of quartz), that plagioclase is of constant composition, that magnetite and ilmenite are present, and that  $P$ ,  $T$  and  $P_{\text{H}_2\text{O}}$  were constant.

The 2 modified projections relate to presence or absence of potassium feldspar. Many high-grade metasedi-

mentary rocks of the Wicklow area contain this mineral and, hence, it has been employed as a projection point in the AKFM tetrahedron, as initially devised by Rheinhardt (1968). The components of the projection are arranged as follows:



However, some rocks do not contain potassium feldspar, such as  $\text{K}_2\text{O}$ -impoverished metawackes and certain dealcalized rocks (Hoare Lake gneissic suite). These rocks cannot be represented on the above ternary diagram. Therefore, another modification of the AFM diagram devised by Froese (1963, 1969, 1972, 1978) was used. It employs plagioclase as the projection point, since it is present in almost all rocks containing no potassium feldspar. Components were arranged as follows:



Based on published experimental data and field and microscopic studies, it appears that there are some differences between the metamorphic conditions responsible for the mineral assemblages in the rocks of the Grenville Supergroup and those represented by the Madawaska Highlands gneissic complex. Therefore, these 2 lithological groups will be discussed separately.

## MADAWASKA HIGHLANDS GNEISSIC COMPLEX

This metamorphic domain (*see* Table 7) differs from the Grenville Supergroup in containing intermediate-pressure granulite-grade assemblages in addition to trondhjemite-tonalite anatectic melt systems developed within the clastic metasedimentary belts of wacke-pelite composition. The specific assemblage potassium feldspar (perthite) + garnet + sillimanite + biotite + quartz + plagioclase ( $\text{An}_{32}$ ) in association with irregular pods of sillimanite-bearing leucosome, as on Furz Mountain, indicates temperatures greater than  $665^\circ\text{C}$  and pressures exceeding 3 kilobars. The invariant point of pertinence to these temperature and pressure value estimates is defined by the intersection of the curve muscovite + quartz = aluminosilicate + potassium feldspar + vapour (Althaus et al. 1970) with the curve albite + muscovite + quartz +  $\text{H}_2\text{O}$  = melt +  $\text{Al}_2\text{SiO}_5$  (Storre and Karotke 1971).

The upper limits of metamorphic conditions are inferred from the mineral assemblages encountered in the Hoare Lake gneisses. The deduction is based on the critical textural–mineralogical relations of metastable sillimanite and spinel, which are completely enveloped by cordierite, which, in turn, is enclosed mostly by gedrite. Similar coronas were reported from other metamorphic terranes by Heitanen (1959), Vernon (1972) and Robinson and Jaffe (1969).

**Table 7.** Metamorphic mineral assemblages from high-grade to granulite-grade Madawaska Highlands gneissic complex.

Metamorphic Grade	Lithology	Metamorphic Assemblage <sup>1</sup>	Retrogressive Mineral(s)	
<b>High Grade</b>	Metawacke	± Fe-oxide + bt + grt + qtz + hbl + pl (An <sub>45</sub> )	Muscovite replacing biotite and plagioclase	
	Metawacke	kfs + grt + bt + qtz + pl		
	Metapelite	± grt + hbl + kfs + qtz + bt + pl		
	Metapelite	± kfs + Fe-oxide + hbl + qtz + bt + pl		
	Metapelite	kfs + qtz + pl + bt		
	Metapelite	grt + hbl + qtz + pl + bt		
	Metapelite	Fe-oxide + grt + bt + pl (An <sub>38</sub> )		
	Metawacke	± hbl + Fe-oxide + ttn + qtz + bt + pl		
	Metapelite	Fe-oxide + sil + grt + qtz + bt + pl		Chlorite, muscovite replace biotite; Incipient to moderate sericitization of plagioclase
	Anatectic pods in metapelite	Fe-oxide + Perthite + grt + sil + bt + qtz + pl (An <sub>32</sub> )		
	Metawacke	Fe-oxide + ged + bt + qtz + pl (An <sub>28</sub> )		
	Iron-rich metasediment	bt + Fe-oxide + pl + hbl + qtz + grt		
	Metapelite	± ep ± ttn ± Fe-oxide + hbl + qtz + pl (An <sub>27</sub> ) + bt		
	Metapelite	di + pl + qtz + bt		
	Calc-silicate skarn	hbl + di + scp + pl (An <sub>34</sub> ) + qtz		
	Calc-silicate skarn	hbl + ttn + c + scp + di		
	<b>High Grade</b>	Amphibolite	qtz + di + hbl + pl (An <sub>54</sub> )	Local chlorite replacement of biotite
		Amphibolite	ttn + di + qtz + pl (An <sub>36</sub> ) + hbl	
Amphibolite		Fe-oxide + bt + pl (An <sub>34</sub> ) + hbl		
Amphibolite		bt + hbl + Fe-oxide + grt + pl (An <sub>60</sub> )		
Amphibolite		± qtz + Fe-oxide + ttn + bt + hbl + pl		
Metagabbro		bt + di + hbl + pl (An <sub>38</sub> )		
Metagabbro		± Fe-oxide + bt + grt + hbl + pl		
Diorite		kfs + Fe-oxide + qtz + bt + hbl + pl (An <sub>28</sub> )		
Quartz diorite		Fe-oxide + kfs + hbl + qtz + bt + pl		
Tonalite		hbl + kfs + bt + qtz + pl		

<sup>1</sup> Listed in order of increasing abundance (abbreviations at end of table)

In the Hoare Lake area, cordierite ± spinel ± corundum probably formed at the expense of sillimanite, gedrite, with, or in the absence of, quartz. Robinson and Jaffe (1969) have described similar cordierite-rimmed enclaves containing sillimanite, kyanite, staurolite, spinel and bytownite in cordierite-gedrite gneisses interbedded within the Ammonoosuc Volcanics of Middle Ordovician age at Richmond, New Hampshire. These aluminous enclaves developed according to 2 major reactions defined by Robinson and Jaffe (1969):

- 1) quartz + gedrite + aluminosilicate = cordierite
- 2) gedrite + aluminosilicate = cordierite + corundum

In the New Hampshire and Hoare Lake rocks, gedrite is never observed in contact with aluminosilicate minerals. The great similarity in textures of the Hoare Lake rocks with several of those documented in great detail by Robinson and Jaffe (1969), and the observation that these enclaves only occur within coarse gedrite-rich patches as at

Hoare Lake and at Fishtail Lake, Ontario (Lal and Moorhouse 1969, p.151) suggests a common metamorphic reaction and lends some weight to the model derived by Robinson and Jaffe (1969).

These authors explained the observed reactions by assuming a breakdown of the high-pressure assemblage of gedrite + aluminosilicate + quartz because of a decrease in load pressure due to tectonic uplift and/or rapid erosion. Cordierite, having been formed according to the reactions above, may completely enclose one of the reacting minerals, sillimanite, and, in doing so, curtails the reaction from achieving completion. Corundum, as seen in reaction 2 above, is formed from quartz-free assemblages only.

Reaction 1 of Robinson and Jaffe (1969) can be approximated experimentally by the reaction aluminum enstatite + sillimanite + quartz = cordierite (Schreyer and Yoder 1964, p.304; Newton, Charlu and Kleppa 1974) and is plotted in Figure 33. Intersection of the lower and upper curves of Greenwood (1963) with the kyanite–sillimanite

Table 7. Continued

Metamorphic Grade	Lithology	Metamorphic Assemblage	Retrogressive Mineral(s)
<b>Granulite Grade</b>	Trondhjemite	Fe-oxide + opx + bt + qtz + pl	
	Metagabbro	qtz + opx + bt + di + hbl + pl	
	Quartz diorite	Fe-oxide + bt + opx + di + pl (An <sub>35</sub> , antiperthite)	
	Amphibolite dike	qtz + opx + pl	
	Metapelite	opx + Fe-oxide + kfs + hbl + qtz + pl (An <sub>33</sub> ) + bt	
	Anatectic pods in preceding metapelite assemblage	hem + opx + kfs + bt + qtz + pl	
	Anatectic pods in diorite	± qtz + di + opx + pl (An <sub>33</sub> )	Hornblende thinly mantles coarse diopside and/or
		± qtz + Fe-oxide + hbl + pl + opx	Orthopyroxene polycrystalline aggregates
	Iron-rich metasediment	qtz + Fe-oxide + bt + grt + opx + pl (An <sub>35</sub> )	
	Lenoid pods in amphibolite	qtz + Fe-oxide + opx + hbl + di + pl (An <sub>42</sub> )	
<b>Granulite Grade</b>	<b>Hoare Lake gneisses</b>		
	Amphibolite layers	± opx + Fe-oxide + qtz + pl + hbl	
	Scalloped replacement zones in amphibolite	qtz + bt + grt + opx + pl	
	Transgressing 2 to 3 cm wide veins in amphibolite	Fe-oxide + opx + pl (An <sub>45</sub> )	
	Quartz diorite layers	± Fe-oxide ± bt + grt + qtz + opx + pl (An <sub>50</sub> )	
	Garnet-quartz restite	± pl + bt + grt + qtz	
	Cordierite-orthoamphibole-orthopyroxene restite	grt + qtz + pl (An <sub>40-44</sub> ) + bt + oam + opx + crd qtz + pl (An <sub>34</sub> ) + bt + oam + crd + opx qtz + pl (An <sub>33</sub> ) + bt + grt + crd + opx qtz + pl (An <sub>33</sub> ) + bt + oam + grt spl + sil + crd (small metastable enclaves in gedrite-rich domains) spr + ky (small metastable enclaves in garnet-rich domains)	

Abbreviations: An Anorthite

<i>bt</i>	<i>Biotite</i>	<i>grt</i>	<i>Garnet</i>	<i>ky</i>	<i>Kyanite</i>	<i>spr</i>	<i>Sapphirine</i>
<i>crd</i>	<i>Cordierite</i>	<i>ged</i>	<i>Gedrite</i>	<i>oam</i>	<i>Orthoamphibole</i>	<i>scp</i>	<i>Scapolite</i>
<i>di</i>	<i>Diopside</i>	<i>hem</i>	<i>Hematite</i>	<i>opx</i>	<i>Orthopyroxene</i>	<i>sil</i>	<i>Sillimanite</i>
<i>ep</i>	<i>Epidote</i>	<i>hbl</i>	<i>Hornblende</i>	<i>pl</i>	<i>Plagioclase</i>	<i>spl</i>	<i>Spinel</i>
<i>Fe-oxide</i>	<i>Opaque iron oxide</i>	<i>kfs</i>	<i>Potassium feldspar</i>	<i>qtz</i>	<i>Quartz</i>	<i>ttn</i>	<i>Titanite</i>

Table 8. Metamorphic mineral assemblages from Grenville Supergroup rock types.

Metamorphic Grade	Lithology	Assemblage
High Grade	Metapelite	gr + qtz + kfs + bt + pl (An <sub>47</sub> )
	Metapelite	gr + sil + grt + bt + kfs + qtz + pl (An <sub>32</sub> )
	Metapelite	± gr ± bt + ttn + qtz + hbl + pl (An <sub>57</sub> )
	Marble	di? + Fe-oxide + qtz + tlc + c
	Marble	± pl ± scp + qtz + di + phl + c
	Marble	ttn + qtz + di + scp + c
	Siliceous carbonate metasediment	c + qtz + scp + bt + pl
	Calc-silicate skarn	qtz + hbl + pl + grt + scp
	Calc-silicate skarn	± pl + act + ttn + qtz + di
	Amphibolite dike	qtz + di + hbl + pl (An <sub>32</sub> )

Abbreviations: An Anorthite

<i>act</i>	<i>Actinolite</i>	<i>Fe-oxide</i>	<i>Opaque iron oxide</i>	<i>kfs</i>	<i>Potassium feldspar</i>	<i>scp</i>	<i>Scapolite</i>
<i>bt</i>	<i>Biotite</i>	<i>grt</i>	<i>Garnet</i>	<i>phl</i>	<i>Phlogopite</i>	<i>sil</i>	<i>Sillimanite</i>
<i>c</i>	<i>Carbonate</i>	<i>gr</i>	<i>Graphite</i>	<i>pl</i>	<i>Plagioclase</i>	<i>tlc</i>	<i>Talc</i>
<i>di</i>	<i>Diopside</i>	<i>hbl</i>	<i>Hornblende</i>	<i>qtz</i>	<i>Quartz</i>	<i>ttn</i>	<i>Titanite</i>

boundary of Holdaway (1971) suggests metamorphic conditions characterized by a temperature of 730 to 790°C and a load pressure of about 6 kilobars. The peak metamorphic conditions prior to unloading are deduced to have been

around the kyanite–sillimanite boundary, that is,  $T = 770^\circ\text{C}$  and  $P = 8.5$  kilobars. This is petrographically deduced from metastable inclusions of sapphirine mantling kyanite, with both minerals entirely contained within garnet.

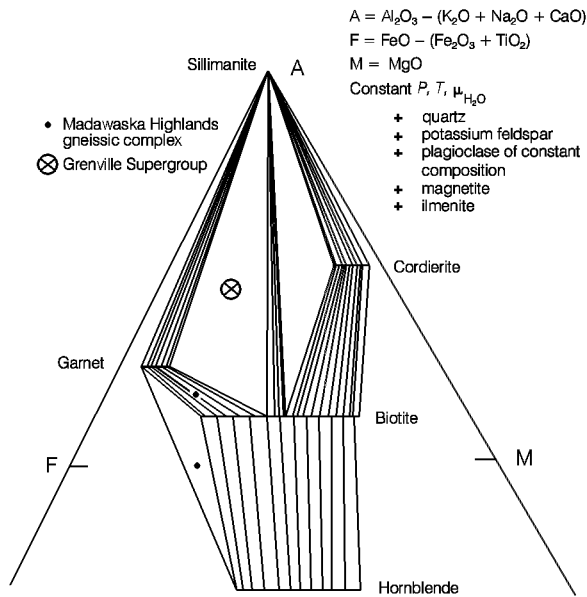
Somewhat higher temperatures than  $770^\circ\text{C}$  possibly prevailed. The reaction hornblende + quartz = orthopyroxene + clinopyroxene + plagioclase + vapour (Binns 1969), can be observed locally in amphibolite, for example, near Franz Pond. This pressure-nonspecific reaction characterizes temperatures of about  $810^\circ\text{C}$ .

## GRENVILLE SUPERGROUP

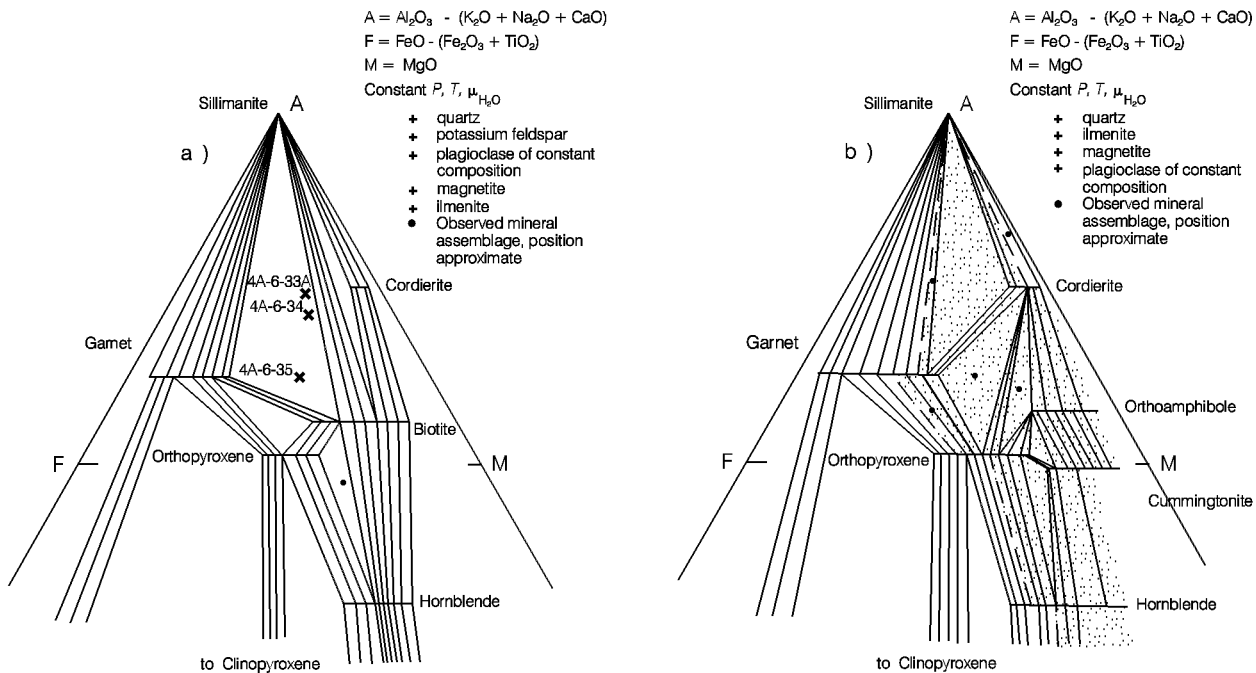
Metamorphism of rocks of the Grenville Supergroup has occurred under conditions distinct from those of the Madawaska Highlands gneissic complex.

Rare Grenville Supergroup metapelites were metamorphosed under pressure of less than 3 kilobars. This is indicated by metapelites characterized by the presence of sillimanite and potassium feldspar and the absence of anatectic melts (see Table 8). These observations indicate metamorphic temperatures above the divariant reaction muscovite + quartz =  $\text{Al}_2\text{SiO}_5$  + potassium feldspar + vapour, but below the curve of minimum melting (see Figure 33), which also constrains pressure to less than 3 kilobars (see Figure 33).

These observations suggest metamorphic conditions under which the Grenville Supergroup rocks of the present



**Figure 31.** AFM diagram depicting phase relations in high-grade assemblages developed in metasedimentary rocks of the Wicklow area.



**Figure 32.** AFM diagrams depicting phase relations in granulite assemblages developed in metasedimentary rocks of the Madawaska Highlands gneissic complex. a) Assemblages containing potassium feldspar. b) Assemblages containing biotite as the sole  $\text{K}_2\text{O}$ -bearing phase. Diagram (a) is after Rheinhardt and Skippen (1970). Diagram (b), including stippled area which indicates biotite coexistence, is from Froese (1978). Bulk compositions of sillimanite metapelites containing potassium feldspar are placed on (a). Analyses for specimens 4A-6-33A, 4A-6-34 and 4A-6-35, shown in (a), are in Appendixes 1f and 2c, respectively. These may possibly be in granulite grade as crosscutting mafic dykes which contain orthopyroxene.

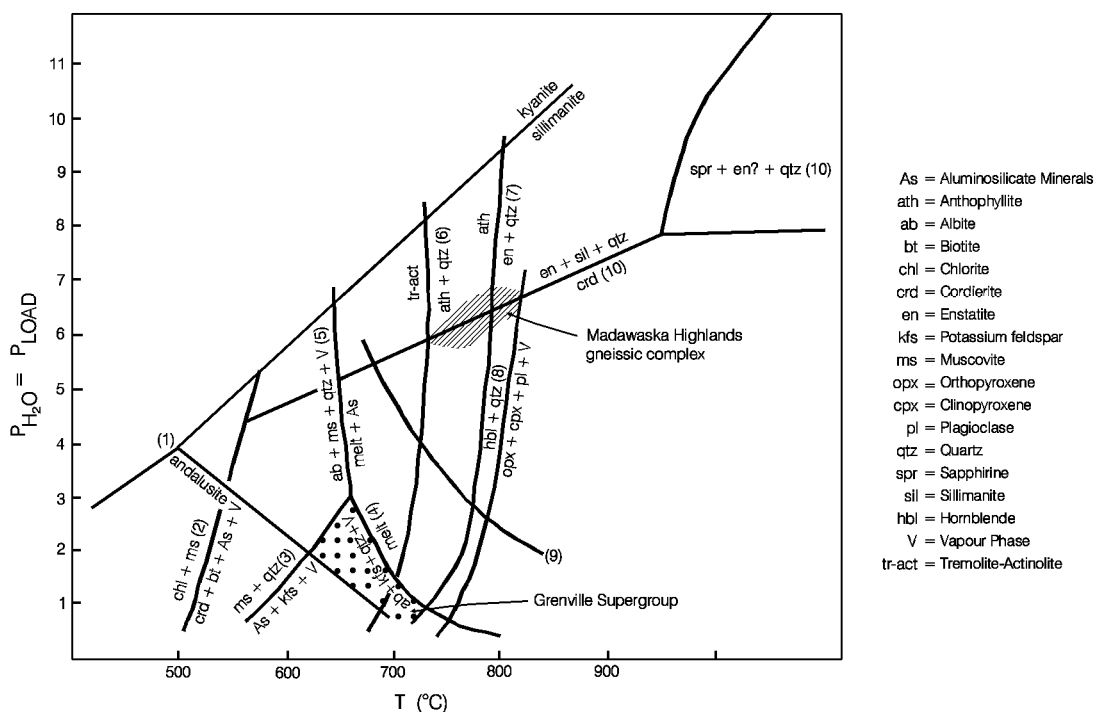
area were formed as follows:  $T = 625$  to  $725^{\circ}\text{C}$ ;  $P = 1$  to 3 kilobars (see Figure 33). These temperature values are considered to be maximum estimates, as common graphite in the metapelites probably had the effect of reducing reaction temperatures (for details, see Kerrick 1972).

In summation, the observed metamorphic mineral assemblages appear to indicate 2 distinct metamorphic domains within the study area. Juxtaposition of the lower  $P$ - $T$  Grenville Supergroup rocks over highly migmatized, higher  $P$ - $T$  Madawaska Highlands gneissic complex rocks infers, then, that horizontal tectonics occurred posterior to the regional metamorphism. This conclusion is substantiated by observations in tectonic breccia zones contained within the higher  $P$ - $T$  metamorphic domain. In these breccia zones, fragments occur that exhibit an older, tectonic-

prograde metamorphic texture truncated by a later fabric of the breccia matrix.

## RETROGRADE METAMORPHISM

In the map area, retrograde minerals are restricted to zones of obvious fluid ingress, that is, joint surfaces and fault zones. Many rock fractures, particularly in the southwestern corner of the area, exhibit epidote and/or hematite coating. Narrow, late-stage faults show moderate chlorite and/or sericite replacement of biotite. Thin mantling of orthopyroxene and diopside megacrysts by hornblende indicates local retrogression of granulite assemblages, particularly those developed within anatectic melts, such as on Davis Island in Papineau Lake. Incipient to moderate sericitization of plagioclase is another effect of retrograde metamorphism.



**Figure 33.** Inferred  $P$ - $T$  regional metamorphic condition in the Wicklow area in terms of experimentally calibrated reactions: 1, aluminosilicate system (after Holdaway 1971); 2, Hirschberg and Winkler (1968); 3, Althaus et al. (1970); 4, Merrill, Robertson and Wyllie (1970), and Tuttle and Bowen (1958); 5, Storre and Karotke (1971); 6, 7, Greenwood (1963); 8, Binns (1969); 9, Binns (1969), beginning of melting curve for quartz-bearing amphibolite and hornblende pyroxene gneiss; 10, Newton, Charlu and Kleppa (1974).

# Structural Geology

## REGIONAL TECTONIC SETTING

The Bancroft district embraces contrasting highland–lowland terranes (Hewitt 1956, 1962) whose elements reflect a complex and protracted tectonic evolution of a basement and cover series of rocks, which have suffered a Mesoproterozoic period of intense deformation and metamorphism.

Wynne-Edwards (1972) outlines 3 broad lithotectonic segments in this district (*see* Figure 3): 1) a reworked highland basement complex comprising the Ontario Gneiss Segment (the Algonquin Domain in Figure 3); 2) a transitional highland zone, north and west of Bancroft, involving mixed basement and cover rocks, comprising Segment IVa of the Central Metasedimentary Belt; and 3) a lowland cover succession (Grenville Supergroup) southeast of Bancroft, comprising carbonate- and volcanic-rich rock Segment IVb of the Central Metasedimentary Belt.

The northern highlands area (*see* Figure 3) is underlain by the Algonquin Domain of the Ontario Gneiss Segment (Davidson and Morgan 1980) within which two-pyroxene granulite facies is shown to be regionally widespread (Fraser, Heywood and Mazurski 1978; Davidson et al. 1979). Whole-rock Rb/Sr analysis of granulite-grade paragneiss from the Barry's Bay area (Bell and Blenkinsop 1980) suggests a metamorphic age of  $1430 \pm 20$  Ma, considered to be in general agreement with other values reported from the Ontario Gneiss Segment. Lumbers (1980, 1982) regards this region, at least in its eastern portion from Bark Lake to the Ottawa River, to involve various "anorthosite suite" orthogneisses, which he collectively names the "Algonquin batholith". High-grade metamorphism, in part retrogressive, is apparent in some regions of the Algonquin Domain (Davidson and Morgan 1980).

Other crustal domains in the western Ontario Gneiss Segment (Davidson, Culshaw and Nadeau 1982) are lithologically and metamorphically distinct, and display deformation patterns with prominent northeast and northwest trends, which structurally succeed each other generally in a southeast direction. Domains are outlined by high-strain "tectonite zones", considered to be very ductile loci of mobility between tectonically interleaved crustal segments. The internal structure of the various domains suggests truncation patterns generally to one side across tectonite zones: northeast-trending domains truncate domains on their northwest sides, whereas northwest-trending domains truncate underlying domains on their northwest sides as well as along their flanks. Asymmetric small-scale structures (sigmoidal feldspar augen, rotated tectonic gneiss inclusions) commonly imply that northwest-trending domains display macroscopic folds essentially coaxial with the penetrative southeast-plunging mineral lineation, which also passes continuously through northeast-trending domains.

Whereas Wynne-Edwards (1972) regards northwest trends within the Ontario Gneiss Segment as reflecting "Hudsonian" structures, it is clear from the evidence given

by Davidson and co-workers, as well as that presented later here, that these are in regional interplay with northeast trends and have a common geometric fabric element in the southeast-plunging lineation. Such a fabric is critical for regional correlation of deformational style (Park 1969).

In the Hastings Basin (Segment IVb), Grenville Supergroup carbonate rocks underlie the terrain around Bancroft and overlie and interfinger with volcanic rocks further southeast. These rocks were deposited ca. 1300 million years ago and postdate an inferred period of basement stabilization in the highlands (J.M. Moore, Jr., personal communication, 1983).

The Wicklow map area straddles the interpreted boundary between lithotectonic segments 1 and 2, which lie within the Haliburton–Hastings–Madawaska highlands region (Hewitt 1956, 1962), and are dominated by grey quartzofeldspathic gneiss and migmatite of high-grade, and locally granulite-grade, metamorphism. Segment IVa is primarily defined by Wynne-Edwards (1972) in the Glamorgan and Cardiff areas west of Bancroft, where northernmost Grenville Supergroup rocks, including important suites of alkalic gneiss, envelop domal masses of "grey gneiss" and migmatite considered to represent a possibly contiguous remobilized basement in mantled gneiss domes. Many such domal masses are broadly northeast trending and inclined away from the lowlands region. Wynne-Edwards (1972) extends the segment northeastward through the Bancroft area as far as the Ottawa River, and includes in it the southern portion of Hewitt's highlands region, presumably as a transitional lithotectonic zone where folded belts and enclaves of Grenville Supergroup rocks are intermixed with more typical "grey gneiss" of the highlands. On this basis, the northern margin of Segment IVa is here considered to extend northeastward of Maynooth, roughly parallel to Highway 62, and contain the Grenville Supergroup rocks and syenitic gneiss exposed in the southeastern part of the Wicklow map area (*see* Figure 3 and "Structural Domains").

Lumbers (1978, 1980, 1982) suggests that the Grenville Supergroup unconformably overlies Algonquin-region rocks with a continuous, basal coarse clastic ("arkosic") sequence, extending northeastward through Maynooth, Combermere and Golden Lake to the Ottawa River. He considers local "pebbly to bouldery" units to reflect direct erosion of their underlying basement and/or reworking of an arkosic regolith. This unit is claimed to display a facies change upward into progressively carbonate-rich rock units. A similar basal clastic sequence is proposed by Bright (1979, 1980) as the Anstruther Lake Group of "coarsely recrystallized, migmatitic arkose and arenite", which mantles the Cardiff dome and forms a belt running easterly through South Elephant Lake and Baptiste Lake in the Bancroft area. The concept of a basal arkosic sequence to the Grenville Supergroup has influenced regional summaries of economic mineral distribution (Masson and Gordon 1981; Carter, Colvine and Meyn 1980; Storey and Vos 1981).

Significant belts of alkalic gneiss in the Bancroft district, including nepheline- and corundum-bearing varieties, parallel the northwestern margin of the Central Metasedimentary Belt and are restricted in occurrence to highlands Segment IVa. An important nepheline syenite suite, showing igneous textures, yields a U/Pb zircon age of  $1225 \pm 3$  Ma and whole-rock Rb/Sr crystallization ages of  $1187 \pm 56$  and  $1164 \pm 26$  Ma, and may have formed in a continental rifting environment (Miller and Gittins 1982). Stable sialic basement to the Grenville Supergroup was, thus, seemingly present at least as far southeastward as the lowland boundary. The “rifting event” occurred during or subsequent to most major trondhjemite intrusions related to the Elzevirian orogeny, and long before such plutons were uplifted and eroded to contribute clasts within the unconformable Flinton Group (ca. 1080 to  $1050 \pm 25$  Ma) (Moore and Thompson 1980).

The original relationships between basement and cover are highly modified by regional ductile deformation of complex style, which, in both highlands and lowlands, is portrayed by “D<sub>2</sub>” (with respect to the Grenville Supergroup) metamorphic fabrics and metamorphic ages from ca. 1050 to at least 1000 Ma. This corresponds to the “main” Grenvillian or “Ottawan Orogeny” (Moore 1982; Moore and Thompson 1980; *see also* Bell 1981), which is possibly related to collision of continental fragments (Moore 1982). Adams and Barlow did not identify the original nature of the basement to the cover sequence, evidence of it being “everywhere torn to pieces by the granitic intrusions of the Laurentian granites” (Adams and Barlow 1913, p.36), whose “enormous development” has arched the cover concomitant with “a second factor in the form of a tangential pressure, acting . . . in a general northwesterly and southeasterly direction” (Adams and Barlow 1910, p.16) which they relate to a northeast-trending orogenic belt.

Within the highlands region, the D<sub>2</sub> deformation is characterized by a penetrative L–S fabric with a mineral lineation plunging uniformly southeast at shallow angles, regardless of variations in the strike of the foliation (e.g., Hewitt 1962). The foliation is a composite S<sub>1</sub>–S<sub>2</sub> fabric where S<sub>1</sub> is commonly defined by earlier metamorphic segregation layering tightly to isoclinally folded about S<sub>2</sub> surfaces. Foliation generally dips shallowly southeastward, but also curves in strike from northeast to northwest outlining later major southeast-plunging folds (Figure 34, back pocket). These folds constitute another ubiquitous characteristic of the highlands region. Within the lowlands, the predominant D<sub>2</sub> mineral lineation trends northeast or southwest at a high angle to that in the highlands, and lies within moderately to steeply dipping, northeast-striking foliation surfaces.

With regard to the structural transition from lowlands (Segment IVb) to highlands (Segment IVa), Hewitt (1956, 1962) considered broad southeast-dipping mylonite zones to separate the 2 terranes. He also postulated (Hewitt 1956) that a marked northward increase in metamorphic grade, indicated by a sillimanite-garnet gneiss zone east of Bancroft, represents a “frontal zone of dynamic metamor-

phism” between lowlands and highlands. However, Best (1966) showed that the mylonitic rocks occur within the highlands quartzofeldspathic gneiss, and do not, themselves, constitute an abrupt break. Best (1966) suggested a progressive change in D<sub>2</sub> structural character from lowlands to highlands that involves tightening of folds and rotation of axial lineations into a down-dip direction (southeast) of maximum extension. On statistical grounds, Divi (1972) and Divi and Fyson (1973) demonstrated a similar progressive rotation of axial lineations from low-plunging, northeast-southwest axes with small rake angles within the foliation in the lowlands, to southeast-plunging lineations with large rake angles (that is, approximately down-dip) in the highlands. This transition is displayed in Figure 3 as the southern limit of the southeast-plunging lineation, and roughly parallels the physiographic highlands boundary suggested by Hewitt (1956) and the sillimanite isograd at the lowlands margin (Divi 1972). Quartz microfabric data from Segment IVa of the highlands suggest that the penetrative southeast-plunging lineation within an L–S fabric locally reflects northwest-directed ductile thrusting (Culshaw 1982; Culshaw and Fyson 1981, 1982). Consequently, it is probable that many of the elongate northwest-inclined gneiss core complexes, such as the Glamorgan and Dysart complexes, constitute nappe-like folds (N.G. Culshaw, personal communication, 1982) within Segment IVa.

Pillowed mafic metavolcanic rocks occur within a marginal highlands subdomain around Boulter, which is dominated by large gabbroic and trondhjemitic plutons (*see* Figure 3). This subdomain is transitional in the sense that the rock association is typical of the lowland Elzevirian orogeny, yet structural features are present, in the form of southeast-plunging lineation and folding, indicative of highlands (i.e., basement-dominated?) terrane. However, it is perhaps significant that the Boulter highlands subdomain passes through an arcuate zone along the York River, which locally contains mylonitic and cataclastic rocks (R.R. Miller, personal communication, 1982; B.S. Brock, personal communication, 1983; R.H. Thivierge, unpublished data, 1983) only along which, and north of which, occurs alkalic gneiss in disposition with quartzofeldspathic gneiss, which is more typical of highlands Segment IVa.

## STRUCTURAL DOMAINS

With respect to the map pattern of the composite foliation (S<sub>1</sub>, S<sub>2</sub>) surfaces in the Wicklow and surrounding area (*see* Figure 34, back pocket), 3 structural domains are recognized from north to south: 1) the interior Algonquin Domain, 2) the Papineau Lake subdomain of the Algonquin Domain proper, which together constitute the Madawaska Highlands gneissic complex, and 3) Segment IVa of the Central Metasedimentary Belt.

The Papineau Lake subdomain defines a broad belt of relatively straight-trending gneiss striking generally northeastward and dipping at shallow to moderate angles southeast. It extends diagonally across the Wicklow map area from Maynooth through Cardwell, Papineau and Purdy lakes to the Madawaska River south of Combermere. It is

approximately 6 km wide in its central portion around Papineau and Purdy lakes and thins considerably to about 2 km wide, both eastward near Combermere and westward near Maynooth. The Papineau Lake subdomain contains rocks similar to those of the interior Algonquin Domain, including varieties of layered grey quartz-plagioclase gneiss and biotitic ( $\pm$  garnet-sillimanite) migmatite, partly of sedimentary origin, as well as a significant mass of poorly layered to massive metadiorite, the Little Papineau Lake stock (*see* Map 2550, back pocket). Both regions display local hypersthene within mafic rocks, and rarely contain Grenville Supergroup rock types. The Madawaska Highlands gneissic complex is largely equivalent to Hewitt's (1955) Radcliffe hybrid gneiss east of Combermere, which also contains granulite-grade rocks (Brock 1982). Carbonate-rich, quartzitic and other layered metasedimentary rocks of Segment IVa, lying south of Highway 62, display high-grade metamorphism.

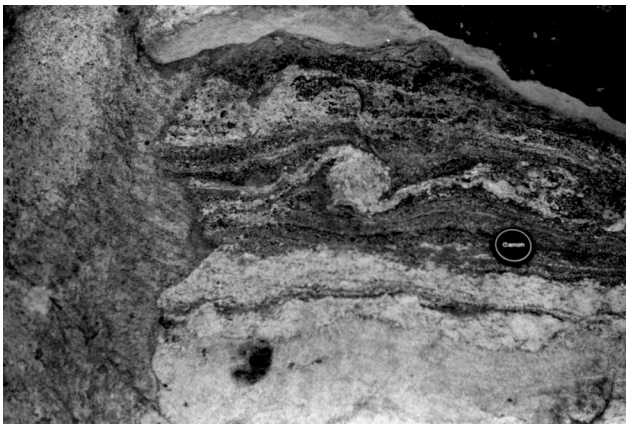
Domains to either side of the straight-trending region are dominated by macroscopic, shallow southeast-plunging folds, which are roughly spaced about 2 to 5 km apart. These folds generally abut or die out against the Papineau Lake subdomain and hence aid in outlining it. One major southeast-plunging structure, the Carlow synform, and a few smaller open folds affect rocks in the central Papineau Lake subdomain. Of particular note, the penetrative southeast-plunging mineral lineation is coaxial with such folds (*see* "Detailed Structural Geology") and passes uniformly through the straight-trending and other domains (Figure 35, back pocket).

Very coarse ovoid feldspar porphyroblasts occur in many places and within different rocks, and display generally recrystallized sigmoidal tails, which signify ductile tectonic transport (Photo 10). These may be isolated or occur within seams of granitoid leucosome. In the few places where such asymmetric porphyroblasts are well exposed, the deduced tectonic overriding is of upper layers toward the northwest along the lineation direction. In contrast,

little or no asymmetry is observed when viewed down-plunge. These features indicate that, at least locally, the mineral lineation represents the direction of tectonic transport and thus is likely an extension direction. Feldspar and quartz crystals, which appear to have grown during the latest metamorphism, commonly mask the apparent asymmetry of many porphyroblasts within the Madawaska Highlands gneissic complex.

Marginal zones of the Papineau Lake subdomain are distinguished from most of its interior portion by displaying some combination of the following: 1) representing the relatively straight-trending outer boundaries against which southeast-plunging folds abut; 2) being conspicuously rich in pink, prekinematic to synkinematic granite displaying lenticular, stromatic and nebulitic migmatite structure, and/or containing abundant ovoid to rhomboid feldspar augen; 3) displaying generally intense ductile deformation with isoclinal asymmetric folding, transposition and detachment structures, which contribute to a locally heterogeneous tectonic admixture of rocks; and 4) containing "fragmental gneiss", that is, tectonic breccia, in which detached or isolated blocks of more mafic rock are enveloped by relatively felsic gneiss and show truncated or discordant internal gneissosity (*see* Photos 2 and 11). In some outcrops, biotitic migmatite with abundant feldspar porphyroblasts shows a swirly to nebulitic layering suggestive of highly ductile flow, and contains fragments or lenticular masses of metagabbro, anorthositic metagabbro, or rarer meta-anorthosite (*see* Photo 11). The rock types forming these fragments do not constitute mappable bodies in the area and are generally restricted to the marginal zones of the Papineau Lake subdomain. It is tempting to regard these as exotic fragments derived from deeper crustal regions along zones of significant ductile displacement.

The southern marginal zone forms a continuous belt 1 to 3 km wide (*see* Figure 35, back pocket) and underlies and delimits Segment IVa, roughly along Highway 62 east of Maynooth. Commonly, the granitoid component of the



**Photo 10.** Very coarse feldspar porphyroblast displaying asymmetric "tails" indicative of clockwise rotation with well-banded, fine-grained biotite gneiss. At this locality, immediately east of Balsam Lake, the rocks are affected by a later macroscopic  $F_4$  fold and hence geographic sense of rotation is misleading. Note crosscutting, fine-grained tonalitic dike to the left.

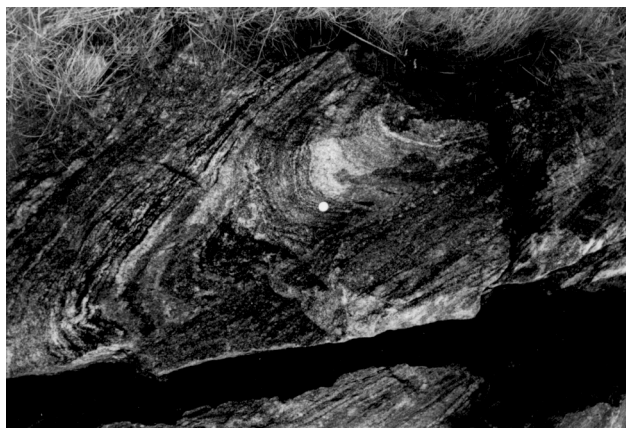


**Photo 11.** Highly porphyroblastic flaser-textured hornblende-biotite homophanous migmatite on Highway 62 at Purdy. Note the streaky layering suggestive of very ductile flow which encloses an exotic metagabbroic fragment containing an older, oblique internal foliation. These fragments document transposition parallel to the enveloping layering which dips southward to the right.

migmatites prevails, and may be mapped on a small scale, such as south of Papineau Lake and southeast of Cardwell Lake. The northern marginal zone is best defined in the Purdy Lake–Kamaniskeg Lake area (Thivierge 1982), where it is 1 to 1.5 km wide and dips fairly consistently at about 15 to 25° to the south. It is traceable sporadically westward into the Wicklow map area, at least to the north end of Papineau Lake, where later folds influence its distribution. Poor outcrop exposure makes an extension further westward speculative. It is continuous eastward through Combermere to the Diamond Lake area, where similar rocks with meta-anorthositic fragments occur (B.S. Brock, personal communication, 1983). Form lines suggest a pattern in which the 2 marginal zones merge near Diamond Lake, and perhaps also at Maynooth.

One group of tectonic fragments, composed of metamorphosed diopside-bearing pyroxenite, occurs sporadically within both marginal zones, but more prevalently in the southern zone. If the pyroxenite is considered to be a “skarn”-type metamorphic product, it may have been derived from carbonate supracrustal rocks, perhaps of relatively proximal origin compared to the meta-anorthositic fragments.

In some outcrops within or near these marginal zones, abrupt truncation of gneissic layering is observed between rocks for which no significant ductility contrast is apparent (Photo 12). Davidson, Culshaw and Nadeau (1982) and Schwerdtner and Mawer (1982) describe identical structures, which may represent intense transposition of asymmetrically folded layering. Other truncations occur in which ductility contrasts are more apparent (e.g., see Photo 2), but the truncation is commonly of upper limbs of tight  $D_2$  folds (cf. Photo 13). This truncation pattern at outcrop scale is similar to the megascopic truncation pattern between lithotectonic domains of the western Ontario Gneiss Segment (Davidson, Culshaw and Nadeau 1982) in that the structurally upper portions (i.e., southeastward) of the domains are commonly the truncated sides.



**Photo 12.** Abrupt truncation of folded layering within metatextitic metasedimentary migmatite on Highway 62, 2 km northeast of Maple Leaf. This indicates internal discordance between rocks of identical composition and texture. Note truncation of upper fold surface subparallel to the axial trace.

Of particular note, the basal coarse clastic sequence of Lumbers (e.g., 1980, 1982), in the authors' opinion, is not convincingly such, but corresponds in distribution to marginal zones of the Papineau Lake subdomain. The “pebbly to bouldery units”, although locally observed to develop, in part, from underlying rocks, are best explained as representing various stages of tectonic disaggregation rather than as relict primary depositional features. No “facies change” upward into carbonate units is observed. These units are instead quite similar to straight-trending, high-strain “tectonite zones” of Davidson, Culshaw and Nadeau (1982). Many rock types correspond to their descriptions of so-called “tectonoclastic gneiss” (see Photo 2), “augen mylonite” (see Photo 11) and “tectonite gneiss” (see Photo 12) and are interleaved macroscopically. Similar rock types were apparently first recognized in the studies of Adams and Barlow (1910, 1913). Adams and Barlow observed intimate relationships between granite migmatization and an accompanying later penetrative deformation. They suggested that slow, uniform movement of the invading “granite magma” within the basement and lower cover sequence enhanced an overall plasticity, and that continued tectonic movements upon cooling resulted in progressive stages of gneissic structure ranging from “fluidal” porphyroblastic (feldspar) textures to lenticular and fragmental “protoclastic” textures and “thinly foliated” banded gneiss.

It must be noted that several features which contribute to distinguishing the marginal zones are also present in rocks throughout the Madawaska Highlands gneissic complex. For example, the interior Papineau Lake subdomain includes rocks with generally lower degrees of granite migmatization, which form lithologically more coherent low-dipping belts of metasedimentary migmatite and masses of veined metadioritic rock, as well as areas with rocks and structures similar to the features outlined. Leucosomal material may also be largely derived *in situ* as suggested locally (e.g., muscovite-sillimanite leucogranite



**Photo 13.** Early  $F_{2A}$  folding of layering within a lens of amphibolitic gneiss from Madawaska Highlands gneissic complex exposed on Highway 62 at Oram Park in Bangor Township. This fold has been refolded at high angle by an  $F_2$  fold of regional type. Note the upper limb truncated by porphyroblastic gneiss. View is to the south, down-dip with respect to the enveloping gneiss.

pods within biotite-sillimanite-garnet metasedimentary migmatite at “Furz Mountain” northeast of Davis Island on Papineau Lake; patchy or dispersed hypersthene-hornblende-plagioclase leucosome within foliated metadiorite on Davis Island). The distinction for the marginal zones is mainly on the combination of features which suggest active high-strain zones, generally with prominent migmatization and/or blastesis, in a ubiquitously ductile tectono-metamorphic scenario with local sigmoidal kinematic indicators showing northwest-directed overriding along the direction of mineral lineation.

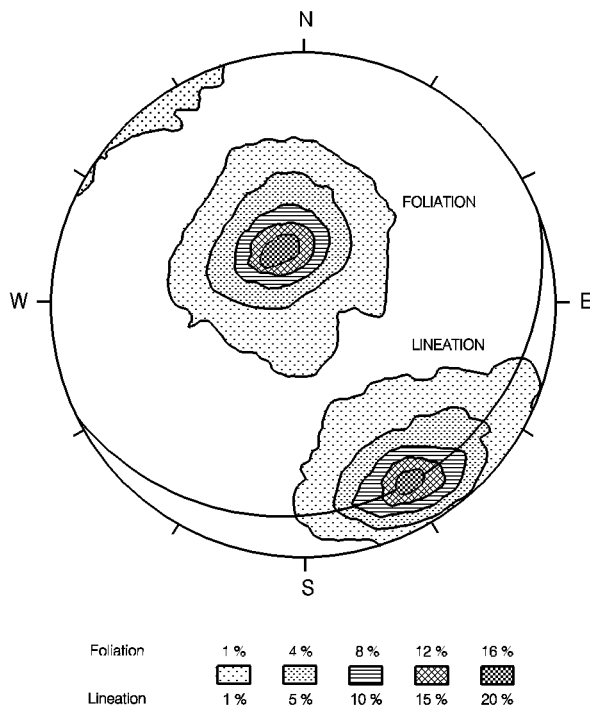
The interpretation of the northwestern margin of the Central Metasedimentary Belt (i.e., the northern margin of Segment IVa) is consistent with recent studies along the same margin north and southwest of Haliburton (Davidson and Morgan 1980; Schwerdtner and Mawer 1982), which suggests that a similar high-strain, relatively straight-trending zone (“tectonite zone”) underlies the arcuate Eagle Lake marble belt (see Figure 3). The zone appears to be a continuous structure from the Koshlong Lake shear zone (Schwerdtner and Mawer 1982) in the south into the Halls Lake–north Kennisis Lake–north Haliburton Lake areas (A. Davidson, Geological Survey of Canada, personal communication, 1982). It is apparently continuous along strike from here through an unmapped region into the Papineau Lake subdomain, which also continues eastward into the Diamond Lake area beyond Combermere (B.S. Brock, personal communication, 1983). This zone

would then constitute a major zone of ductile displacement between the Central Metasedimentary Belt and the Algonquin Domain of the Ontario Gneiss Segment, and basement cover relations of the Grenville Supergroup are consequently cryptic.

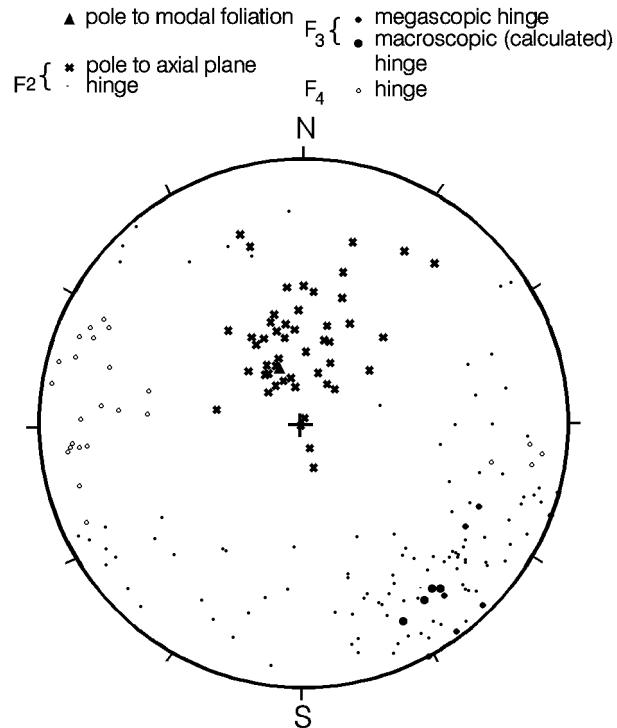
## DETAILED STRUCTURAL GEOLOGY

At least 4 regional folding events can be recognized in the Wicklow area (see Table 3). The first 2 are observed mainly at mesoscopic (outcrop) scale and no macroscopic structures are yet known that could be related to them.

Some rocks of the Madawaska Highlands gneissic complex display structures of 1, and possibly 2, deformation events which supracrustal rocks of the Grenville Supergroup do not reflect. An early high-grade metamorphic layering ( $S_{1A}$ ), presumably of tectonic origin ( $D_{1A}$ ), is, in many places, polymigmatitic in the sense of containing 2 or more stromatic leucosomes. Polysomal grey gneiss may indicate several early periods of leucosome development within basement rocks that are absent from cover rocks (e.g., Appleyard 1974; Appleyard and Stott 1975; Francoeur 1975), but it is cautioned that relations may be ambiguous and leucosome fractions may be of restricted origin dependent upon specific bulk compositions. It is tempting, however, to relate the metamorphic layering to a broadly “Elsonian” granulite-facies event within the Algonquin region, based on a  $1430 \pm 20$  Ma age determination



**Figure 36.** Lambert equal-area projection of contoured foliation (total 1524) and mineral lineation (total 425) measurements from Wicklow and the adjacent areas. The cyclographic trace shown is of the modal foliation, corresponding to a pole to foliation maximum at 19%. Note that lineation contours define a partial great circle along this plane, and the lineation maximum is close to down-dip.

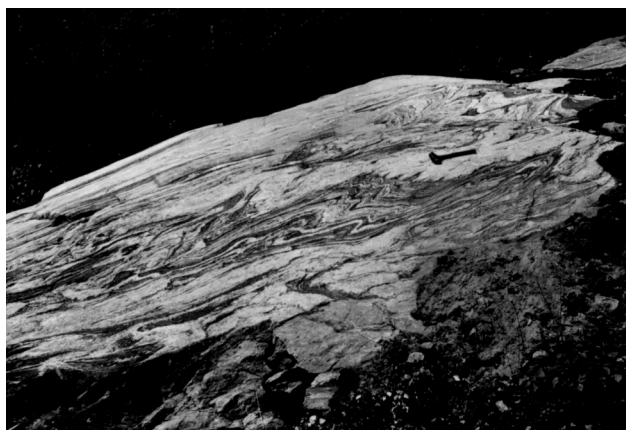


**Figure 37.** Lambert equal-area representation of fold data ( $F_2$  axial planes and hinges;  $F_3$ ,  $F_4$  hinges). Note that many  $F_2$  axial planes lie close to the modal foliation for the area, and that most  $F_2$  hinges are coaxial with  $F_3$  hinges (compare with Figure 36, mineral lineations). Macroscopic  $F_3$  hinges are the same as those shown in Figure 38.

(Rb/Sr whole-rock isochron) obtained by Bell and Blenkinsop (1980) from near Barry's Bay. Earliest folding of this layering (during  $D_{2A}$ ) is rarely identifiable, except in some nose regions of subsequent, regionally dominant folds (*see* Photo 13), where the original geometry and orientation are greatly modified.

Compositionally layered rocks of the Grenville Supergroup do not display an early high-grade metamorphism, although they contain an early stratiform foliation ( $S_{1G}$ ) largely in conformity with the later regional foliation ( $S_2$ ). The significance of early folds found in one locality marginal to the New Carlow syenite complex (Lot 3, Concession 2, Wicklow Township) refolded by regionally dominant folds is not understood and, thus, comparison cannot be confidently made with those in the Madawaska Highlands gneissic complex.

Virtually all rocks in the area are affected by regional ductile deformation that produced the penetrative L–S fabric. This deformation corresponds to the “main” Grenvillian or “Ottawan Orogeny” (about 1050 to at least 1000 Ma) (Moore 1982; Moore and Thompson 1980). Foliation is composite ( $S_1$  and  $S_2$ ) and is parallel to layering within both Madawaska Highlands gneissic complex and Grenville Supergroup rocks, except in the nose areas of  $F_2$  folds, where the  $S_2$  foliation, defined by mafic and felsic aggregates, is axial planar and crosscuts folded  $S_1$  fabrics and layering. Foliation surfaces generally trend northeastward, where not affected by later folding, and mineral extension lineations are uniformly southeast-plunging (Figure 36). As shown by a net projection, the modal foliation for the Wicklow area strikes  $066^\circ$  and dips  $19^\circ$  southeast (*see* Figure 36). The net projection shows that mineral lineations lie on a partial great circle which coincides with the modal foliation surface. The modal lineation plunges  $19^\circ$  toward  $150^\circ$ . This is at a rake of  $84^\circ$  southeast within the modal plane of the foliation, which is essentially down-dip.



**Photo 14.** Typical  $F_2$  disharmonic, asymmetric, nearly reclined folds with shallow-dipping axial planar fabric in biotite gneiss interlayered with granite sheets on Highway 62 near Papineau Lake South Road. Folds are coaxial with mineral lineation and express vergence to northeast (left to right). Note presence of an upper enveloping surface nearly axial planar to the folds and flame structures and detached fold limbs in the centre. View is westward, slightly oblique to up-plunge.

$F_2$  folds are typically very tight to isoclinal, disharmonic and asymmetric (Photos 14 and 15). Owing to the isoclinal nature of these folds, axial planes generally are subparallel to fold limbs or enveloping gneissosity surfaces. Orientations of mesoscopic  $F_2$  axial planes are shown on Figure 37, where it is apparent that they coincide with the dominant foliation in the area. Fold axes are commonly parallel to the mineral lineation and many are reclined folds, but they also vary considerably in plunge with a general spread within the modal foliation surface from northeast–southwest to southeast (*see* Figure 37). The problem of mineral lineations indicating extension parallel to fold axes is discussed by Hobbs, Means and Williams (1976, p.283–288). A likely explanation for the variable orientation is that  $D_2$  involved not only generation of new folds in the area, perhaps trending northeast–southwest, but also rotation of older elements along  $D_2$  axial surfaces, into an overall conformity with the southeast-plunging extension lineation. It is noteworthy that the variation in orientation shown by the fold axes is similar to that shown by fold axes and parallel lineations in the lowlands supracrustal domain (Segment IVb) to the southeast (Divi 1972).

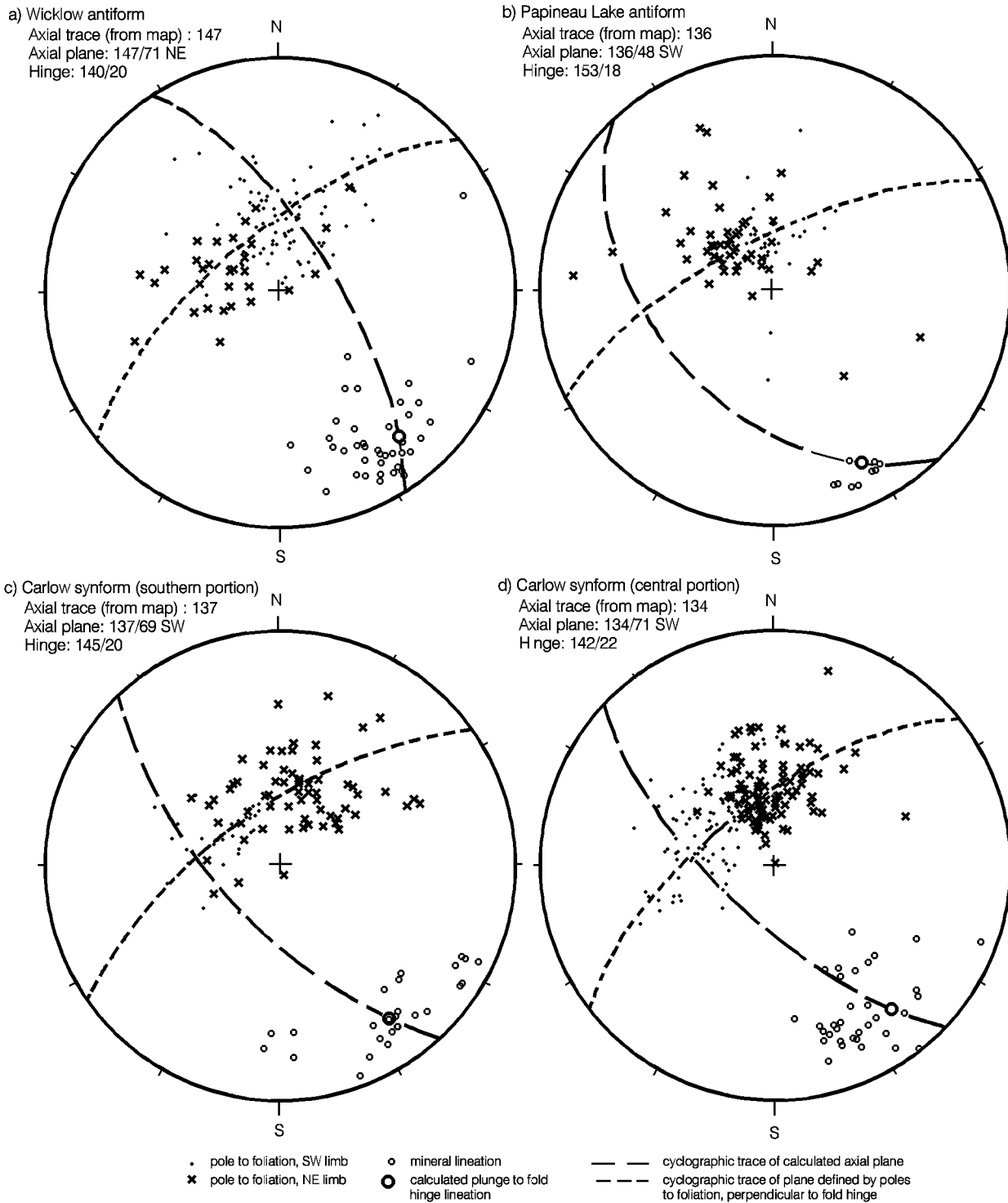
Southeast-plunging macroscopic  $D_3$  structures, which fold the  $D_2$  fabric and yet are essentially coaxial with the  $L_2$  mineral lineations, constitute an ubiquitous characteristic of the highland region in the Bancroft district. All  $D_3$  folds are typically disharmonic, open to tight, and gently plunging. Several structures display curvilinear to off-stepped axial traces owing to the disharmonic nature of folding (e.g., Wicklow antiform, Carlow synform). Axial planes are steep to inclined. Calculated plunges of several  $F_3$  folds are shown on Figure 38, and are compared with  $L_2$  mineral lineations found within them. There is strong agreement between the two and this coaxial relationship suggests an intimate tectonic evolution from  $D_2$  deformation penetrative at outcrop scale to  $D_3$  deformation reflected by map-scale open folds.



**Photo 15.** “Cascading folds” in biotite gneiss on Highway 127, 7 km northwest of Maynooth, displaying northeast vergence (left to right). Note incipiently to moderately developed axial planar transposition of asymmetrically folded layering. Some abruptly truncated limbs are obvious in area below the Brunton compass. View is to southeast, approximately down-plunge.

In the Glamorgan–Cardiff area of Segment IVa, southeast-plunging structures are expressed mainly by northwest-trending belts of Grenville Supergroup rocks between relatively rigid gneiss-cored structures (N.G. Culshaw, personal communication, 1982) which influence

their disposition. South of the Wicklow map area, a similar style may be present in that the folds occur between the metaplutonic Boulter subdomain and a large, poorly known oval structure south of Maynooth (*see* Figure 34, back pocket). Within the interior Algonquin Domain



**Figure 38.** Lambert equal-area stereonet projections showing southeast-plunging D<sub>3</sub> folds coaxial with D<sub>2</sub> mineral lineations. a) Wicklow antiform; b) Papineau Lake antiform; c) Carlow synform (southern portion in Segment IVa); d) Carlow synform (central portion in southern marginal zone of Papineau Lake subdomain).

around the Wicklow area, these trends form prominent structural and aeromagnetic patterns, which generally appear to abut against the northern marginal zone of the Papineau Lake subdomain (*see* Figure 34, back pocket) as best exemplified by the Bangor antiform, northeast of the map area (R.H. Thivierge, personal communication, 1982). At least 9 large structures of this type are evident in Figure 34 (back pocket), which, from west to east, are named the Indian Lake synform, Wicklow antiform, Hawk Lake synform, (?) Cross Lake antiform, Carlow synform, Papineau Lake antiform and complementary synform, Bangor antiform, Kamaniskeg Lake synform, and an unnamed, but apparently very large, antiform east of Combermere.

South of the Papineau Lake zone, Segment IVb also contains southerly plunging D<sub>3</sub> structures which similarly abut against it. Perhaps of some significance, an antiform in Monteaule Township, south of the Wicklow area, appears to splay outward at the southern marginal zone and tightens in a southerly direction. A southeastward tightening is also observed for folds of the interior Algonquin Domain as they approach the northern marginal zone. Large antiformal structures (the Wicklow and Bangor antiforms) show a considerable tightening southeastward as they approach the northern margin of the Papineau Lake subdomain, whereas large synformal structures, such as the Kamaniskeg Lake synform, display a progressive opening. This geometrical pattern could suggest that antiforms are either highly attenuated or possibly truncated at the marginal zone. As this marginal zone is the lower or northwest side of the northeast-trending Papineau Lake subdomain, the structural pattern is reminiscent of the apparent truncations between crustal segments in the western Ontario Gneiss Segment (Davidson, Culshaw and Nadeau 1982).

It should be stressed that the Algonquin region is only known at reconnaissance scale (Lumbers 1980, 1982) and portions remain unmapped to date. For example, the axial trace of the Cross Lake antiform is speculative and not shown on Figure 34 (back pocket). A prominent aeromagnetic and topographic lineament, the Cross Lake lineament, appears to lie subparallel to a possible axial trace of the antiform, although not necessarily conforming with it in position. Aeromagnetic trends may locally coincide with F<sub>3</sub> axial traces and/or inflection traces of fold limbs (as exemplified in the Wicklow antiform and Kamaniskeg Lake synform). However, available trends in the Cross Lake area suggest that an antiformal structure tightens in a southeasterly direction.

Northwest of Papineau Lake, near Yuill Lake in the Wicklow area, structural trend surfaces suggest that an antiformal structure trending southeastward from Cross Lake is refolded at a very high angle to produce a chain of non-cylindrical structures.

Only the Carlow synform appears to be traceable through the Papineau Lake subdomain and into Segment IVa. Asymmetric parasitic folds to the Carlow synform are found on both limbs (the Papineau Lake antiform on the northeastern limb with "S" style; and "Z" style folds on the southwestern limb), which are generally of mesoscopic to intermediate (i.e., several outcrop) scale. Northwest along

the axial trace of the synform, the structure tightens at the margin of Segment IVa and opens within the southern marginal zone of the Papineau Lake subdomain. An area here is very open and no reliable axial trace can be drawn. It seems to be continuous northward with the synformal structure west of Papineau Lake, but it is also possible that these are different folds. It appears that certain structural features of the Papineau Lake zone mitigated against the development of F<sub>3</sub> folds within it, at least on the scale of the observed spacing for F<sub>3</sub> folds within the interior Algonquin Domain and Segment IVa.

A fourth deformational event with respect to the Grenville Supergroup, D<sub>4</sub>, is defined by east-trending folds in the northeastern map area, especially at Balsam Lake, and possibly by southwest-trending folds in the Yuill Lake area (*see* Figure 34, back pocket). These fold the D<sub>2</sub> mineral lineation and parts of D<sub>3</sub> folds. Many of these folds are noncylindrical, upright to steeply inclined, and of low amplitude. Wavelengths are in the order of one hundred to several hundred metres. In the former area, asymmetric minor folds found on north-dipping limbs plunge shallowly toward the west (*see* Figure 37). Although the map-scale folds in both areas show contrasting orientations, this may not preclude that they represent the same fold generation. Elsewhere in the map area, this folding is portrayed by outcrop-scale warps and undulations of gneissosity. These too are low amplitude, noncylindrical structures with subhorizontal roughly east-west plunges.

## Dikes

Late planar to curvilinear pegmatite dikes and quartz veins appear to postdate all folding events. Although variable orientations occur, the majority of pegmatites and, to a lesser extent, quartz veins trend northeasterly (generally 040 to 060°) and dip moderately to steeply southeast. These orientations correspond very well to regional dike trends, including the Hybla-type dikes of Monteaule Township (Storey and Vos 1981).

Unmetamorphosed diabase dikes occur in 2 known localities: at the northeast end of Papineau Lake, and along the Madawaska highway southwest of Evans Lake. Both trend west-northwest and the one at Papineau Lake dips steeply northward. These are presumably fracture-controlled intrusions of the post-Precambrian Ottawa-Bonnechere fault system, occurring near its southwestern margin.

## Faults and Joints

No major brittle-type faults are defined in the map area. Minor brittle faults locally displaying cataclasis are found in several roadcuts in the western Wicklow area; they are variable in attitude, although some strike northeast to north-northeast with moderate to shallow dips southeastward. No senses of displacement have been determined.

Joints mainly correspond to 2 prominent regional sets, although several other sets are locally discernable. The prominent sets are both subvertical and include planar fractures, which are commonly 5 m or more long and coated by epidote, hematite and chlorite. One set strikes

northeastward (generally 030 to 050°) and corresponds in orientation with some pegmatite intrusions. The other strikes northwestward (generally 315 to 335°). Both are closely parallel to topographic lineaments, especially along the shores of Bark, Papineau and Kamanisseg lakes. Locally, they feature intense epidotized and hematized fracture zones. The northwest-striking set may incorporate fractures associated with normal faulting in the Ottawa–Bonnechere graben, but the map area is to the west of westernmost faults of that system (*see* Appleyard and Stott 1975).

Subhorizontally dipping joints are particularly prominent in metamorphosed potassic granitoid suite rocks. This is especially striking in the Cardwell Lake granite where waterfalls are controlled by these joints (Photo 16).

## SUMMARY OF STRUCTURAL FEATURES

Basement-cover relationships of the Algonquin Domain (Ontario Gneiss Segment) and the Grenville Supergroup (Segment IVa of the Central Metasedimentary Belt) are not considered to be directly observable in the fashion outlined by Lumbers (1980, 1982), but are indeed cryptic and have perhaps involved a form of preferential granite migmatization along a “front”, which included both basement and cover in the manner suggested by Appleyard (1974). Whether or not a “coarse basal arkosic sequence” contributed to preferential migmatization remains largely speculative.

An interplay of northeast-striking foliation and southeast-plunging lineations with coaxial southeast-plunging major folds (reflecting D<sub>2</sub> and D<sub>3</sub> deformation) is suggested to constitute the major “Grenvillian” tectonic framework modifying the basement–cover relations. Regions with major southeast-plunging F<sub>3</sub> folds abut against the relatively straight northeast-trending Papineau Lake subdomain on either side, and signify that the F<sub>3</sub> folding

died out in the zone though the coaxial lineation crosses it. Granitoid and porphyroblastic migmatites, particularly in the marginal zones of the Papineau Lake straight zone, show many features of ductile tectonic fragmentation and mobility and, in some cases, northwestward transport can be inferred. The features described at all scales are similar to those in a region of extensive northwest-directed ductile thrusting described by Davidson, Culshaw and Nadeau (1982).

The southern margin of the Papineau Lake zone apparently constitutes a regional zone of ductile mobility and is correlative both eastward and westward with similar zones which are considered to represent the northernmost limit of the Grenville Supergroup.

Later folding and faulting is of a minor scale in the area. All rocks were subsequently subjected to late pegmatite dike intrusion, mainly along northeast trends, fracturing, and local diabase intrusion along west-northwest trends.



**Photo 16.** Waterfalls on Papineau Creek controlled by prominent subhorizontally dipping joints in the Cardwell Lake granite.

# Economic Geology

Mineral exploration within the map area has been largely confined to 2 general time periods and commodities: 1) ca. 1900 to 1916: corundum-bearing syenites, and 2) mid 1950s: uranium-bearing granitic pegmatites.

All known mineral occurrences are described in the ensuing section including mineralization encountered by this survey. No documented mineral exploration has occurred within the map area subsequent to the brief period of uranium exploration activity. The numbers following the deposit names in this section correspond to the property and occurrence numbers on Map 2550 (back pocket).

## CORUNDUM

The discovery of corundum by W.F. Ferrier of the Geological Survey of Canada in 1897 in the New Carlow area (Hewitt 1954), adjacent to the southeast corner of the study area, led to the establishment of a flourishing local abrasives industry. The development of the Burgess and Craigmont corundum deposits stimulated relatively intense exploration in the general region. Many occurrences were discovered in the New Carlow area in the early 1900s, including a small deposit within the map area at Hoover Mountain (Hewitt 1955) (Figure 39, back pocket).

### Hoover Mountain Deposit (4)

A small, but undocumented, quantity of corundum ore was mined at Hoover Mountain in 1916. This ore was probably hand-sorted on site and transported a short distance to the Burgess Mine for milling (R. Armstrong, resident and former prospector, New Carlow, personal communication, 1982). The property was possibly worked by Manufacturer's Corundum Company, contemporaneously active at the Burgess Mine, although Hewitt (1955, p.34) makes no mention of the developer involved. Operations at Hoover Mountain ceased in September of 1916 due to an accident involving the explosion of a steam boiler and dynamite (Photo 17), which resulted in the loss of several buildings and one workman's life (R. Armstrong, personal communication, 1982).

## GEOLOGY

A 0.7 to 1 m wide zone of coarse-grained to pegmatitic muscovite-magnetite-biotite-corundum syenite, averaging approximately 6% corundum was mined within a shallow trench 63 m long, 7 to 14 m wide, and having a maximum depth of 3.1 m (*see* Figure 39, back pocket); this horizon is within a buff to reddish coloured, medium-grained magnetite-biotite syenite. The rock is equigranular, allotriomorphic granular and poorly foliated. It has a mafic mineral content of approximately 10 to 15% and does not contain any megascopic corundum.

Euhedral to subhedral translucent corundum is also contained within a small outcrop containing similar syenite situated approximately 60 m southwest of the main de-

posit (*see* Figure 39, back pocket). Concentrations of up to 19% spectacularly developed corundum were observed on slabs cut from loose rock, which apparently came from a shallow blast pit at this occurrence. Corundum crystals, which achieve maximum dimensions of 5 by 15 cm, are usually bronze coloured. Corundum may be partially mantled and embayed by anhedral magnetite. Fine-grained greenish muscovite may also mantle corundum, forming thin shells that possibly originated via alteration processes. A medium- to coarse-grained muscovite-corundum-biotite syenite also occurs at this occurrence and obviously grades into the coarsest corundum-bearing unit. Modal percentage of corundum here is less than 5%.

## URANIUM

Uranium mineralization is confined to 3 occurrences located in the Balsam Lake area, and is hosted in late potassic pegmatites within metasedimentary migmatite. These radioactive pegmatites, known as the Dubblestein, Thomas and James occurrences, were evaluated during the 1950s (for references, *see* below). The mineralization at that time was deemed to be sporadic and uneconomic. The radioactive pegmatites appear to belong to the Hybla feldspar and rare element pegmatite province outlined by Storey and Vos (1981), although the tentative limits of this province were not extended northward to encompass this map area by these authors.

### Dubblestein Occurrence (1)

This uraniferous pegmatite is located on the north shore of Balsam Lake about 800 m west of the Centreview-Kamanisseg Lake Road and represents the coarsest potassic pegmatite observed within the map area. It consists of a 22° north-dipping, zoned pegmatite sheet that is at least 6.5 m in thickness and approximately 30 m in strike length. Ten claims covering the mineralization and surrounding area were staked by E. Dubblestein in 1955. Ensuing development work comprised 107 m (352 feet) of diamond drilling



**Photo 17.** Longtime area resident, R. Armstrong, stands alongside the remnants of a mobile boiler, which was destroyed in a 1916 accident at the Hoover Mountain corundum deposit.

and blasting (Geological Survey of Canada, Radioactive Resources Division, File 31 F/5-3). Recent evaluations of this occurrence were undertaken by Paulter (1980) and Masson and Gordon (1981).

## GEOLOGY

The pegmatite is mainly hosted by highly deformed, diastatic, migmatized clastic metasedimentary rocks. These host rocks are fine to coarse grained, with sparse ovoid plagioclase and potassium feldspar porphyroblasts with maximum diameters of 3 to 4 cm. The metasedimentary rock contains 10 to 20% deformed hololeucocratic granitoid mobilizate. Interlayered fine- to medium-grained amphibolite represents a minor component of the host rock. Also within the surrounding rocks are skarns, as observed on a nearby island in Balsam Lake. Here, a diopside-rich gneiss exhibiting a stictolithic texture is developed in the form of diopside-rich clots mantled by plagioclase. This skarn assemblage is interlayered within metasedimentary migmatite, deformed coarse-grained biotite-quartz monzonite and fine-grained amphibolite.

The pegmatite is zoned as previously documented by Paulter (1980) and Masson and Gordon (1981). The zonation is as follows: 1) border zone: graphic intergrowth of quartz and potassium feldspar about 1 m in width; 2) intermediate zone: mainly homogeneous blocky potassium feldspar, quartz and coarse-bladed biotite aggregates (this zone is about 2 m in thickness); 3) core zone: enriched in milky quartz with local isolated blocky potassium feldspar (Photo 18) (this zone ranges in width from 0.5 to at least 3.5 m).

There is an overall increase in grain size toward the core zone. Potassium feldspar crystals in the border zone are about 10 by 14 cm in comparison to the blocky potassium feldspar crystals, which are up to 1.36 m in diameter, and are in contact with the quartz-rich core zone.

## MINERALIZATION

Radioactive mineralization is very sporadic and usually localized within, and proximal to, large bladed biotite ag-



**Photo 18.** Euhedral termination of a large blocky potassium feldspar crystal (marked by hammer), which projects into the quartz-rich part of the core zone of the Dubblestein pegmatite.

gregates. These randomly oriented aggregates are developed within the intermediate zone and achieve maximum dimensions of 0.2 by 1.4 m. As shown by Paulter (1980), these biotite aggregates may be hosted entirely by large blocky potassium feldspar, by graphic quartz-potassium feldspar or by block quartz. In the latter case, a delicate intergrowth of quartz and biotite is notable.

Euxenite forms euhedral to subhedral, tabular to rectangular crystals and appears to represent the main radioactive mineral phase. This mineral ranges in size from 1 by 1 mm to tabular crystals with maximum dimensions of 0.9 by 2.4 by 4.4 cm, and tends to occur along the contact of coarse biotite crystals with potassium feldspar or quartz. Local concentrations of euxenite (up to 15%) have caused intense radioactive damage to adjacent potassium feldspar crystals especially, as shown by radial fracture patterns and pronounced hematization. Euxenite also occurs as euhedral mineral inclusions in all the major pegmatite-forming minerals, suggesting an early paragenesis. Masson and Gordon (1981) report the presence of pyrochlore which contained 1.5%  $U_3O_8$  and 0.8% Th. However, mineral analyses obtained by E. Dubblestein in 1955 reveal somewhat higher  $U_3O_8$  concentrations of 6.36 and 8.63%, which probably relate to the presence of euxenite and approximate the  $U_3O_8$  contents of analyzed material in this study. Isometric crystals of pyrochlore were not encountered in this study at the Dubblestein pegmatite.

Two grab samples of radioactive pegmatite submitted by E. Dubblestein in 1955 to the Ontario Department of Mines registered 0.02 and 0.11%  $U_3O_8$  with high trace levels of Ce, Nb, Th and Zr (E. Dubblestein, prospector, Timmins, personal communication, 1982).

## Thomas Occurrence (2)

The Thomas radioactive pegmatite is exposed on the south shore of Balsam Lake approximately 300 m due west from the Centreview-Kamanisseg Lake Road. The property was probably discovered by E. Dubblestein, who, in 1955, submitted material to the Lakefield Research Limited laboratories for analysis (Masson and Gordon 1981, p.31). A.C. Thomas investigated the uraniumiferous mineralization at depth with 9 diamond-drill holes in 1958, which varied between 9.1 and 18.3 m in length. No significant extension of mineralization to depth was established by the drilling program (Geological Survey of Canada, Radioactive Resource Division, File 31 F/5-3).

## GEOLOGY

This pegmatite is generally conformable and is contained in east-striking metasedimentary migmatites and minor interlayered amphibolite similar to those exposed at the nearby Dubblestein radioactive pegmatite. The pegmatite is exposed approximately for 60 m and varies in width from 0.5 to 2 m. In contrast to the Dubblestein pegmatite, contacts of the Thomas pegmatite are relatively steep, dipping between 67 and 80° south (Figure 40).

## MINERALIZATION

The most intense radioactivity occurs near the western limit of the exposure (*see* Figure 40). In this area, the pegmatite appears to interdigitate with the host metasedimentary migmatite, in addition to displaying local flexures in strike. The pegmatite is rudimentarily zoned, containing a discontinuous, irregular quartz-rich core. This quartz-rich zone contains local crystals of albite and blocky potassium feldspar, the latter measuring up to 10 by 30 cm. Along the northern part of the pegmatite, there is a 0.5 to 1 m wide magnetite-biotite granite pegmatite characterized by intergrowths of quartz and potassium feldspar with biotite and magnetite contents of approximately 5 and 1%, respectively. Surrounding most of the quartz-rich core zone is a 0.3 to 1.5 m wide coarser unit consisting mainly of blocky potassium feldspar and albite. This unit appears to become progressively enriched in albite in a westerly direction. In the vicinity of the aforementioned joint-controlled flexure, the rock type could be termed an albite-rich syenite. Maximum radioactivity occurs here. This area exhibits prominent hematization and highest contents of coarse anhedral magnetite (5 to 10%) and euhedral allanite (5%). Allanite forms euhedral crystals up to 20 mm by 1.3 cm enclosed in all major pegmatite-forming minerals and usually weath-

ers to a rusty brown to light khaki colour. Fresh surfaces of crystals not totally replaced by metamict products are glossy black. Hematization is almost always developed adjacent to allanite, especially when this mineral contacts coarse albite crystals. Analysis of allanite indicated 55 ppm  $U_3O_8$  and 2030 ppm Th, according to Masson and Gordon (1981, p.31).

Small cavities up to 6 by 12 cm are locally evident in the albite syenite unit and contain euhedral crystal aggregates of potassium feldspar, muscovite books, and anhedral grey calcite. Fine-grained, light-greenish muscovite may be found distributed along hairline fractures.

A sample from the radioactive zone was taken by Masson and Gordon (1981, p.29) and registered 540 ppm  $U_3O_8$  and 1.7% Th, suggesting the presence of thorite.

### James Occurrence (3)

This uranium occurrence was discovered by C.B. James, who staked 10 claims in 1955 (C.B. James, resident, Centreview, personal communication, 1982). The exact location of this occurrence is not known to the authors; however, according to C.B. James, it is apparently a short distance west of a small unnamed lake near the western limits of his farm. Five grab samples were submitted to the Ontario De-

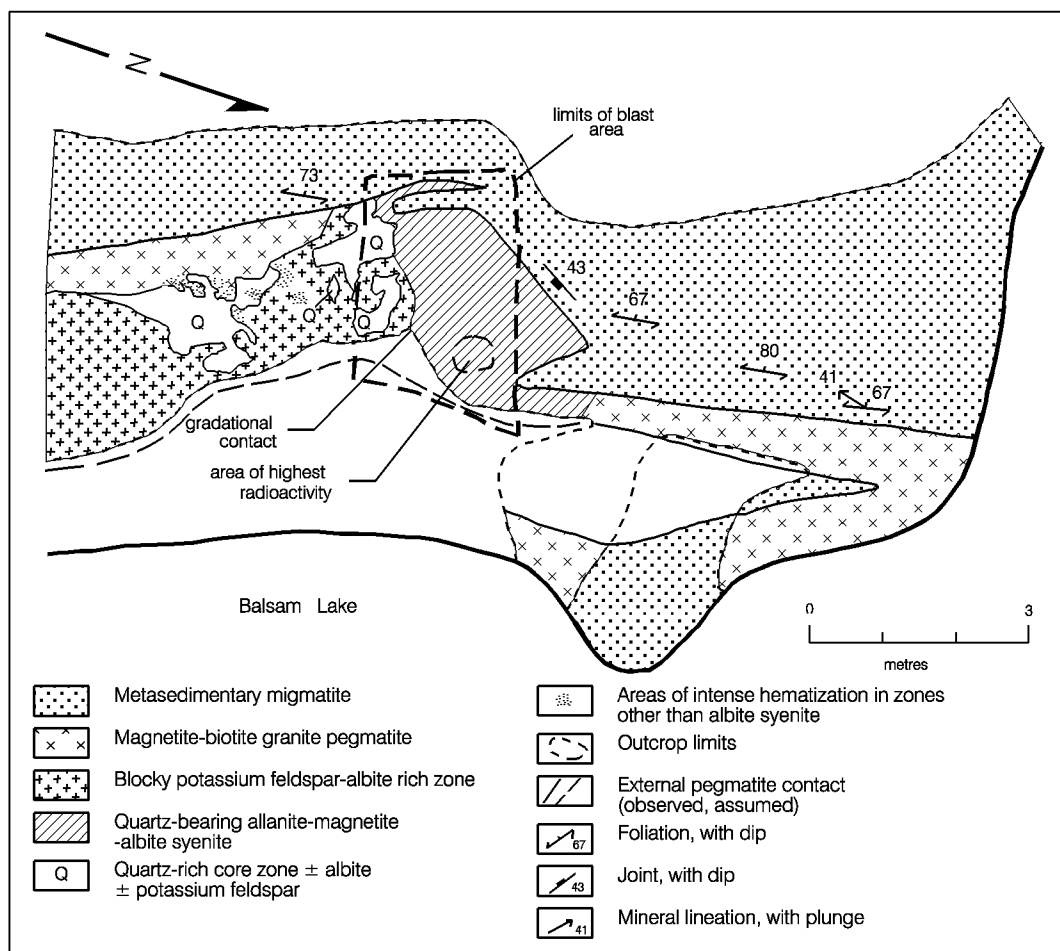


Figure 40. Detailed geology of the western part of radioactive granite pegmatite dike, Thomas occurrence.

**Table 9.** Classification of molybdenite mineralization in the Wicklow area.

---

I.	Metasedimentary Migmatite Association:
1.	in fine- to medium-grained garnet-biotite metawacke paleosome and related quartz-rich leucosome pods on western shoreline of Papineau Lake. Molybdenite in paleosome occurs as linear aggregates up to 6.5 by 0.5 cm.
2.	in medium-grained nebulitic leucosome on largest island in Balsam Lake. MoS <sub>2</sub> grains up to 1 by 2 cm within a 10 by 58 cm area.
II.	Granite Dike Association:
1.	in zoned granite dike emplaced in coronitic metagabbro on Highway 62, 1.7 km southwest of Maple Leaf. MoS <sub>2</sub> grains up to 2.1 by 2 cm are principally confined to an outer quartz-rich portion of 20 cm wide dike associated with possible ankerite, biotite, pyrite, and meager apatite. Medium-grained MoS <sub>2</sub> is contained within a fine-grained biotite granite core zone. Massive coarse-grained pyrrhotite with minor pyrite and chalcopyrite occurs in central parts of the same dike system elsewhere in this exposure.
2.	in pyrite-bearing granite dike in roadcut near eastern end of Balsam Lake. MoS <sub>2</sub> is fine grained and very locally disseminated.
III.	Syenite Association:
1.	fine-grained disseminated MoS <sub>2</sub> occurs locally within white diopside syenite in roadcut on Highway 62, 1.8 km east of Maple Leaf.

---

partment of Mines in 1956 by C.B. James for semiquantitative emission spectrographic analysis the results of which indicated nil to trace levels of most elements sought except Zr, which registered a general 0.5 to 5% level in one specimen. Two specimens submitted for uranium analysis revealed only nil to 0.01% U<sub>3</sub>O<sub>8</sub>. This occurrence is likely a potassic pegmatite hosted by metasedimentary migmatite. The nature of the radioactive mineralogy is not known. In August of 1955, this property was amalgamated with those of E. Dubblestein and C. Gagnon.

## SULPHIDE MINERALIZATION

Sulphide mineralization is scarce in the map area. Most of the map area is underlain by felsic to intermediate granitoid gneiss and relatively barren metasedimentary migmatitic gneiss; rock units that do not normally contain major sulphide concentrations. Local concentrations of sulphide mineralization containing scant chalcopyrite and molybdenite, however, were observed in several localities and are described below. All sulphide-enriched samples were tested for gold and silver. Neither gold nor silver were detected in 7 samples collected by field party personnel and analyzed by the Geoscience Laboratories of the Ontario Geological Survey.

### Molybdenum

Fine- to medium-grained molybdenite occurs at 5 localities in the map area. The occurrences were classified into 5 categories based upon lithologic association (Table 9). The mineralization at all occurrences is very local in extent and apparently not of present economic interest, as molybdenite contents are invariably much less than 5%.

### Copper

Minor amounts of chalcopyrite were encountered at 2 localities. In the Mitchell Lake area, a gossan-covered sulphidic amphibolite containing 5 to 10% percent pyrite and pyrrhotite combined was noted to locally have 1 to 2% chalcopyrite. Two specimens collected by field party personnel and analyzed by the Geoscience Laboratories of the Ontar-

io Geological Survey were found to contain 460 and 1020 ppm Cu and no Ni.

A second occurrence of chalcopyrite occurs in a late, zoned granitoid dike hosted in coronitic metagabbro. This mineralization is associated with pyrrhotite, pyrite and molybdenite (*see* "Molybdenum"). Two specimens collected by field party personnel and analyzed by the Geoscience Laboratories of the Ontario Geological Survey contained 1160 and 1820 ppm Cu, and 520 and 860 ppm Ni.

## ECONOMIC EVALUATION OF GRANITIC PEGMATITES

### Potassium Feldspar Geochemistry

Potassium feldspar is a useful geochemical indicator mineral in exploring for rare-element and/or ceramic-type granitic pegmatites. Potassium feldspar analyses allow a rapid economic potential classification based on diagrams devised by Gordiyenko (1976, cited in Trueman and Černý 1982). Information relating to internal geochemical fractionation patterns within specific pegmatites is another application of potassium feldspar geochemistry studies.

Potassium feldspar is an important accumulator of the large rubidium and cesium cations, and the smaller strontium and barium cations in most granitic rocks. Micaceous also contain appreciable amounts of these elements when modally abundant. Rubidium and cesium values, and K/Ba and Rb/Sr ratios, in potassium feldspar increase with magmatic and/or supercritical fluid fractionation within a given pegmatite chamber (Černý 1982). Contrastingly, K/Cs, K/Rb and Ba/Rb ratios, and concentrations of Sr and Ba generally diminish with progressing geochemical fractionation. These trends are very obvious in analyses obtained from a vertical section across the flat-lying, zoned, Dubblestein granitic pegmatite. The results are plotted on Figure 41 and also listed in Appendix 2k. Fractionation increases toward the quartz-rich core zone of the pegmatite since this zone is usually the last portion of pegmatites to crystallize and theoretically should contain the highest levels of Rb and Cs, and the lowest Sr and Ba contents, assuming that the system has remained essentially closed to external dissipation of the fluid phase.

The most significant variations are exhibited by Ba (40 to 1950 ppm) and Sr (10 to 540 ppm), and also expressed by the large variations in K/Ba (6 to 270), Rb/Sr (0.8 to 97) and  $Ba/Rb \times 10^2$  (4 to 480) ratios (see Figure 41). K/Rb ratios exhibit a more limited range of 10.7 to 26.9, but, nevertheless, indicate a high level of geochemical fractionation.

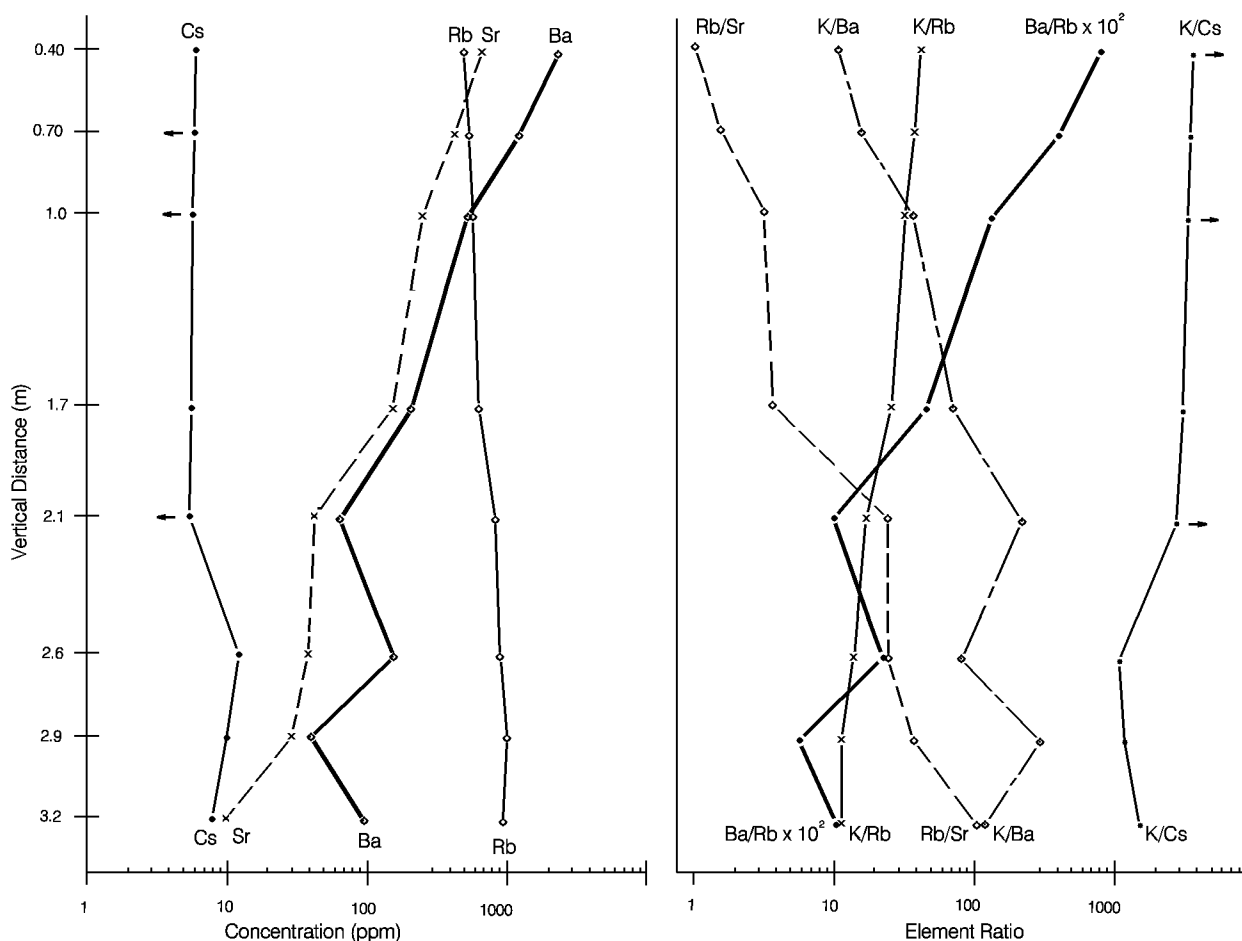
Rb/Sr ratios appear to represent a particularly useful fractionation indicator, with values rapidly increasing from 0.8 at the upper pegmatite contact, to 97 within the core zone. The fractionation pattern trending toward rapidly diminishing Sr levels is also obvious in Figure 42 and compares quite closely with the Ghost Lake batholith, an S-type granitoid mass which is the parental source of many rare-element pegmatites in the Dryden area (Breaks and Moore 1992).

Economic potential rating of a given granitic pegmatite is most readily accomplished by plotting potassium feldspar analyses on the  $Na_2O$  versus  $K/Cs$  diagram of Gordiyenko (1976, cited in Trueman and Černý 1982), which is considered by Trueman and Černý (1982, p.481) to represent the most useful diagram yet devised. Several analyses of the Dubblestein pegmatite fall within the rare-element-bearing pegmatite fields of Figure 43. In 3 analy-

ses, Cs concentrations are below the 5 ppm level of analytical sensitivity. Therefore, the K/Cs ratios based on these analyses are of a doubtful validity. Three analyses of blocky potassium feldspar crystals from the discontinuous quartz-rich core zone from the nearby Thomas uraniferous granite pegmatite are also included in Appendix 2k. The Thomas pegmatite is less fractionated as reflected by generally higher Ba (1870 to 3110 ppm) concentration, higher K/Rb and Ba/Rb ratios, lower Rb (270 to 290 ppm) concentration, and lower K/Ba and Rb/Sr ratios. Cesium concentrations all fall below 5 ppm and, thus, an economic potential rating is not possible on the Gordiyenko diagram. These potassium feldspars possibly fall into the field of micaceous-ceramic pegmatites, since rare-element-bearing oxide phases, such as euxenite, do not occur here, in contrast to the Dubblestein pegmatite. Lower  $Na_2O$  concentrations of 1.85 to 2.07% also characterize the Thomas pegmatite.

### Euxenite Mineral Geochemistry

In Appendix 2l, a partial analysis of a large 0.9 by 2.4 by 4.4 cm euhedral, relatively pure, euxenite crystal from the Dubblestein pegmatite is presented (analysis 1) and compared to selected, more complete, analyses from the literature (analyses 2 to 6). An analysis of such complex



**Figure 41.** Vertical variation of Ba, Cs, Rb, Sr and ratios  $Ba/Rb (\times 10^2)$ ,  $K/Ba$ ,  $K/Cs$ ,  $K/Rb$ ,  $Rb/Sr$  in blocky potassium feldspar from Dubblestein uraniferous granitic pegmatite.

oxide mineral phases as euxenite can provide additional input regarding geochemical characterization of pegmatites, that is, it can indicate the presence of certain metals that may be concentrated in economic amounts elsewhere in the pegmatite. Euxenite from the Dubblestein pegmatite contains the highest Nb/Ta ratio (see Appendix 21).

Thus, unless pervasive albitization has affected this pegmatite at an unexposed level, concentration of niobium should always greatly exceed tantalum and this pegmatite should be explored only if niobium is the commodity of principal interest. Euxenite in the Dubblestein pegmatite also differs from other examples in Appendix 21 by lower levels of  $Y_2O_3$ ,  $CeO_2$ , and  $TiO_2$  and relatively high  $U_3O_8$  content.

### Mineral Collecting

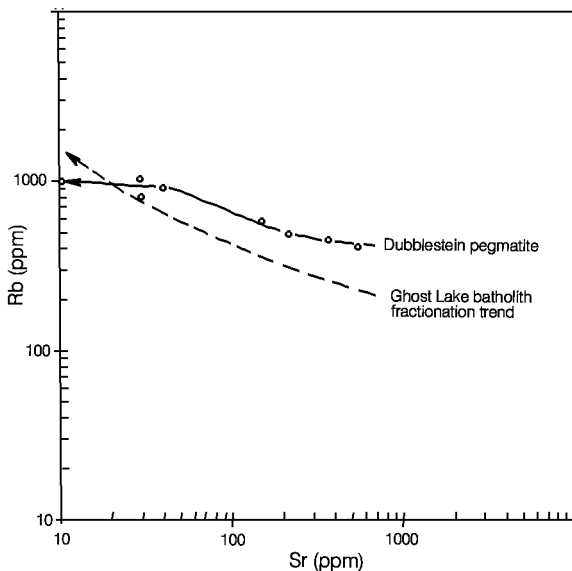
The map area has had relatively little exposure to mineral collecting as compared to the region immediately around Bancroft. At occurrences and deposits of corundum for example, the locations of which have been well documented by Hewitt (1954), one can still find good crystals of this mineral. Bronze-coloured corundum crystals can be obtained from small overgrown blast pits near the Hoover Mountain deposit. Other similar occurrences, as documented by Hewitt (1954), should also be visited if corundum crystals are desired. The possibility of obtaining better collector-quality corundum may be well worth the effort in attempting to locate overgrown minor occurrences than to visit the larger deposits such as the Burgess Mine, which have witnessed relatively intense collector traffic in recent years. Open-space fillings containing medium-

coarse-grained, euhedral, light orange, potassium feldspar may be found along certain fracture surfaces transecting some exposures within the New Carlow syenite complex. For example, excellent crystals were found by the authors at a small corundum occurrence 60 m southwest of the Hoover Mountain deposit.

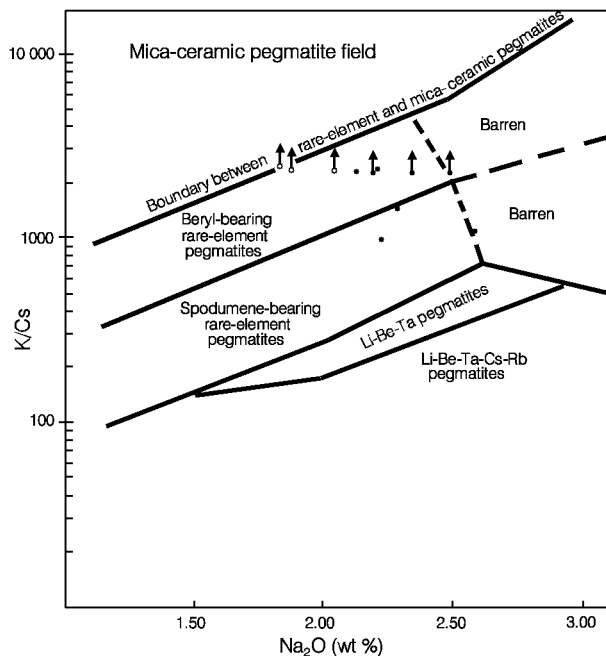
Skarn assemblages, containing well-formed, locally translucent crystals of actinolite, diopside, augite, titanite and garnet, are developed within the impure calcareous metasedimentary rocks adjacent to the New Carlow syenite complex. Calcareous enclaves within this syenite mass can also contain well-formed crystals of these minerals.

Excellent quality “micro” mineral specimens occur in the map area as late open-space fillings. For example, fine- to medium-grained euhedral spinel, chlorite, pyrite and quartz may be obtained from roadside rock cuts near the intersection of the Madawaska Highway and Little Papi-neau Lake Road. Crystals of euxenite up to 0.9 by 2.4 by 4.4 cm may be obtained from the Dubblestein granitic pegmatite on Balsam Lake. Polished slabs of graphic potassium feldspar-quartz, also from this pegmatite, are also very attractive.

There are large gravel and sand deposits with economic potential in the area, although, at present, only 2 pits are worked. These are situated near Highway 127 in Lot 2, Concession VI, McClure Township, and on Highway 62, 0.62 km northeast of its junction with the New Carlow Road. Both are utilized by the municipal government incorporation of Wicklow, Bangor, Monteagle, and Carlow townships. Many small pits that straddle all major roads in the region are used by local residents.



**Figure 42.** Sr versus Rb variation diagram for blocky potassium feldspar from the Dubblestein uraniumiferous granitic pegmatite compared to the Ghost Lake batholith in the English River Subprovince. Fractionation trend of Ghost Lake batholith is from Breaks and Moore (1992).



**Figure 43.**  $Na_2O$  versus K/Cs diagram for blocky potassium feldspar from the Dubblestein (●) and Thomas (○) pegmatite occurrences. Diagram modified from Trueman and Černý (1982, p.480, Figure 9A).

# Recommendations for Future Mineral Exploration

---

The potential for volcanogenic base metal sulphide mineralization in the Madawaska Highlands gneissic complex and the rocks of the Grenville Supergroup is low due to the absence of volcanic rocks in the area. Sulphide occurrences are only sparsely developed and, where analyzed, contain low levels of copper and nickel. Molybdenite occurrences, at present, are mainly of academic interest. Gold and silver were not encountered in any assays conducted on sulphide-bearing specimens. Ceramic potassium feldspar deposits of commercial potential may exist in the map area. At the Dubblestein radioactive pegmatite, for example, coarse, homogeneous blocky potassium feldspar crystals with diameters up to 1.36 m are virtually de-

void of mineralogical impurities. The ceramic potential of this pegmatite should be investigated further.

Mineral specimen collecting has some potential, particularly with regard to skarn assemblages developed in calcareous metasedimentary rocks situated peripherally to the New Carlow syenite complex and for bronze-coloured translucent corundum crystals occurring within the complex itself.

Some rock types encountered in the present area are very suitable for being polished. A few possible applications include their use as coverings for furniture, and exteriors and interiors of buildings.

# Appendix 1: Modal Analyses

---

- a. Modal analyses of amphibolites from the Wicklow area.
- b. Modal analyses of leucosome from amphibolite gneiss.
- c. Modal analyses of paleosome from diorite to quartz diorite gneisses.
- d. Modal analyses of stromatic leucosome and coexisting paleosome components from felsic to intermediate gneisses.
- e. Modal analyses of paleosome from various felsic to intermediate gneisses.
- f. Modal analyses of the paleosome component from metasedimentary migmatites.
- g. Modal analyses of the leucosome component from metasedimentary migmatites (metatexite).
- h. Modal analyses of various rock types from the Hoare Lake gneisses.
- i. Modal analyses of Grenville Supergroup clastic metasedimentary rocks.
- j. Modal analyses of rocks from the Little Papineau Lake plutonic complex.
- k. Modal analyses of the anorthosite suite rocks.
- l. Modal analyses of various syenitic rocks from the New Carlow syenite complex.
- m. Modal analyses of corundum-bearing syenitic rocks from Hoover Mountain.
- n. Modal analyses of metamorphosed potassic granitoid rocks.
- o. Modal analyses of generally hololeucocratic, fine-grained, muscovite-bearing metamorphosed potassic granitoid rocks.
- p. Clast and matrix modal analyses of tectonic breccia from the Wicklow granite.
- q. Modal analyses of rocks from the Indian Lake plutonic complex.
- r. Modal analyses of unmetamorphosed potassic granitoid rocks.

Appendix 1a. Modal analyses of amphibolites from the Wicklow area.

Sample No.	Common Amphibolite										Biotite Amphibolite				Diopside Amphibolite	
	1-6-4B	1-11-1B	2-7-15B	3-11-11C	5-4-4A	5-10-1B	6-1-4B	6-3-2B	6-9-35A	6-11-5C	6-13-18A	2A-2-7A	3-11-26	4A-4-25	7-2-5B	7-9-3B
Hornblende	55.4	64.4	61.1	66.9	61.0	54.9	71.6	66.0	72.2	62.3	68.4	48.6	54.0	37.4	5.0	49.1
Plagioclase	41.1	32.3	38.6	30.6	37.1	37.9	24.3	30.7	25.1	34.3	31.6	27.4	29.6	44.5	43.4	37.6
Potassium feldspar	0.9		x	x		x		x		x				x	7.7	
Quartz	1.6	1.1		1.4	0.5	3.1	2.7	1.9	0.3	x		0.6	6.3	1.2	1.9	
Biotite	0.7	1.7	0.3	x	0.7	1.4	0.5		1.0			22.9	8.1	16.2	8.2	x
Diopside	0.2		x	0.7				0.8		2.9						13.3
Titanite				x			0.7					0.6				
Carbonate								0.3								
Pyrrhotite		0.1			0.7						x		0.6	0.7		
Pyrite			x	0.2			0.2	0.3	x						0.3	
Iron oxide	x	0.3			x	2.7		x	1.5	0.6	x	1.5			3.6	x
Total	99.9	99.9	100.0	99.8	100.0	100.0	100.0	100.0	100.1	100.1	100.0	100.1	100.1	100.0	100.1	100.0
Colour Index	56.3	66.5	61.4	67.8	62.4	59.0	73.0	67.4	74.7	65.8	68.4	72.1	64.2	54.3	47.1	62.4

x = Present in trace amounts

Appendix 1b. Modal analyses of leucosome from amphibolite gneiss.

Sample No.	Common Amphibolite				Biotite Amphibolite				Diopside Amphibolite
	1-6-8B	1-14-10	2A-2-7B	4A-6-33D	4-3-ID	6-13-18A	6-13-18A	6-13-18A	
Quartz	26.4	23.1	34.6	31.5	41.7	27.8		27.8	
Plagioclase	71.3	65.7	61.0	62.9	55.7	61.3		61.3	
Potassium feldspar	x	7.5		5.6	2.6				
Biotite		3.7	2.9						
Hornblende	2.2		1.5					8.1	
Iron oxide				x				0.4	
Diopside								2.4	
Total	99.9	100.0	100.0	100.0	100.0	100.0	100.0	100.0	
Colour Index	2.2	3.7	4.4	—	—	—	—	10.9	

x = Present in trace amounts

**Appendix 1c.** Modal analyses of paleosome from diorite to quartz diorite gneisses.

Sample No.	1-6-4		1-7-2		1-8-2		1-8-3		1-14-8A		1-14-8B	
	Leuco.	Paleo.	Leuco.	Paleo.	Leuco.	Paleo.	Leuco.	Paleo.	Leuco.	Paleo.	Leuco.	Paleo.
Quartz	5.0	16.0	14.3	8.7	10.3	24.0						
Potassium feldspar	6.8	4.1	7.9	6.6	5.6	18.5						
Plagioclase	53.6	60.1	58.6	55.9	50.2	49.0						
Hornblende	23.0	7.1	12.0	16.1	17.2	4.0						
Biotite	11.7	12.7	7.1	12.2	16.7	3.5						
Iron oxide		x		0.4		1.0						
Hematite												
Total	100.1	100.0	99.9	99.9	100.0	100.0						
Colour Index	34.7	19.8	19.1	28.7	33.9	8.5						

*x = Present in trace amounts*

**Appendix 1d.** Modal analyses of stromatic leucosome and coexisting paleosome components from felsic to intermediate gneisses.

Sample No.	2-7-32B		4A-4-3		4A-4-10		4A-6-1A		4A-8-11		5-8-1A		6-8-7	
	Leuco.	Paleo.	Leuco.	Paleo.	Leuco.	Paleo.	Leuco.	Paleo.	Leuco.	Paleo.	Leuco.	Paleo.	Leuco.	Paleo.
Quartz	40.0	22.6	25.0	17.4	28.8	27.3	26.5	20.6	33.3	20.4	31.9	8.2	26.6	22.3
Plagioclase	27.1	52.3	37.1	62.5	22.7	42.1	29.7	52.8	36.7	54.7	22.1	61.4	43.5	63.6
Potassium feldspar	30.6	4.3	29.0	2.8	46.0	13.4	38.9	16.7	25.4	5.1	42.5	7.0	25.0	2.1
Biotite		6.8	8.1	15.3	1.8	15.3	4.3	6.1	3.4	18.2	1.8	11.1	4.8	6.6
Hornblende	2.4	13.6		1.4				0.6	0.6	1.5	1.8	11.7	5.0	0.4
Iron oxide	x	0.4		0.7	0.6	1.9	0.5	3.3	0.6	x		0.6		
Pyrite				0.8					x	x				
Total	100.1	100.0	100.0	100.1	99.9	100.0	99.9	100.1	100.0	99.9	100.1	100.0	99.9	100.0
Colour Index	2.4	20.8	8.9	17.4	2.4	17.2	4.8	10.0	4.6	19.7	3.6	23.4	4.8	12.0

*x = Present in trace amounts*

*Leuco. = leucosome*

*Paleo. = paleosome*

**Appendix 1e.** Modal analyses of paleosome from various felsic to intermediate gneisses.

<b>Sample No.</b>	<b>1-8-6D</b>	<b>1-8-13</b>	<b>1-8-15</b>	<b>1-10-24</b>	<b>2-7-14</b>	<b>2-7-17</b>	<b>5-4-3</b>	<b>6-5-3B</b>
Quartz	27.0	21.7	26.0	34.4	23.5	22.1	17.7	20.4
Plagioclase	44.8	56.0	52.7	55.7	52.1	39.1	46.2	51.4
Potassium feldspar	12.4	4.1	7.6		3.7	5.1	22.7	15.6
Biotite	14.6	16.8	13.7	6.3	17.0	26.9	6.7	11.5
Hornblende		1.4			2.4	6.8	6.7	1.1
Orthopyroxene				3.6				
Iron oxide	1.3				1.4			
Pyrite			x		x			x
Total	100.1	100.0	100.0	100.0	100.1	100.0	100.0	100.0
Colour Index	15.9	18.2	13.7	9.9	20.8	33.7	13.4	13.6

*x = Present in trace amounts*

**Appendix 1f.** Modal analyses of the paleosome component from metasedimentary migmatites.

Sample No.	1-11-10	1-14-11	1-14-19A	2-1-9	2-4-22	2-7-3	2-11-16	2A-1-1	2A-2-2	2A-2-4	2A-4-2	2A-5-4	2A-5-12
Quartz	13.5	35.3	17.9	11.5	17.9	40.4	23.7	25.9	14.4	20.0	18.7	24.3	21.2
Plagioclase:													
matrix	50.5	39.7	37.9	39.2	42.1	43.8	35.5	30.4	34.7	35.6	41.5	33.5	45.1
phenoblasts		2.8	2.8				8.3			9.3		6.3	2.1
Potassium feldspar:													
matrix	3.0	0.8	3.4	1.7	x	x	1.8	13.0		1.8	1.6	6.0	5.2
phenoblasts												1.8	
Biotite	32.7	20.1	36.6	42.4	38.5	8.9	21.9	30.7	40.4	20.4	33.1	22.9	26.4
Hornblende:													
matrix			1.4	4.7	0.7	1.5	7.0		5.6	3.6	5.2		4.2
phenoblasts							1.3			8.9			
Titanite											x		
Iron oxide	0.3			x	0.7	x	0.4				x	1.1	
Garnet		1.3	x			5.4			4.9				
Orthopyroxene				x									
Hematite				x									
Apatite													
Zircon											x		
Sillimanite													
Muscovite											x		
Pyrite	x			0.5	x	x				0.4		x	
Plagioclase An content				An33									
Total	100.00	100.0	100.0	100.0	99.9	100.0	99.9	100.0	100.0	100.0	100.0	100.1	100.0
Colour Index	33.0	21.4	38.0	47.1	39.9	15.8	30.6	30.7	50.9	33.3	38.3	28.2	26.4

x = Present in trace amounts

## Appendix 1f. Continued

	2A-6-1	2A-6-12	3-11-3	3-11-30	3-12-8	4A-6-21	4A-6-33A	4A-6-37	4A-8-1	4A-8-3	5-2-16	5-14-2B	5-14-9
Quartz	15.5	13.7	13.9	7.2	8.2	1.5	22.6	11.6	14.7	13.4	15.2	13.7	15.9
Plagioclase:													
matrix	33.8	35.4	38.1	55.5	35.9	39.0	23.4	48.3	46.3	53.2	48.1	42.7	48.7
phenoblasts		0.9	13.1	0.6	3.9							2.9	
Potassium feldspar:													
matrix	9.1	8.5	7.1	1.3	2.1		8.8			0.3	0.5	1.3	x
phenoblasts												0.3	
Biotite	41.6	41.2	23.8	27.1	46.3	9.7	18.7	31.4	36.2	32.4	34.0	39.1	35.3
Hornblende:										0.7	0.5		
matrix			2.4	8.4	2.8								
phenoblasts			1.2		0.7								
Titanite									x				
Iron oxide		0.3	0.4			5.1	0.3	3.9	1.3	x	1.6		x
Garnet						16.9	11.4	4.8	1.6				
Orthopyroxene						27.7							
Hematite										x			
Apatite											x		
Zircon												x	
Sillimanite							x						
Muscovite	x						14.5	x					
Pyrite	x						x						
Plagioclase An content						An35	An32	An38		An37	An30		
Total	100.0	100.0	100.0	100.1	99.9	99.9	100.0	100.0	100.1	100.0	99.9	100.0	99.9
Colour Index	42.0	41.5	27.8	35.5	49.8	59.4	30.7	40.1	39.1	33.1	36.1	39.1	35.3

x = Present in trace amounts

**Appendix 1g.** Modal analyses of the leucosome component from metasedimentary migmatites (metatexite).

Sample No.	1-14-4C	2-1-3	2-1-9	3-11-3	5-14-6	5-14-9	5-14-10
Quartz	26.6	30.8	40.3	18.8	26.5	40.2	24.9
Plagioclase	55.0	58.3	48.5	64.9	47.2	50.5	46.4
Potassium feldspar	7.1	3.4	2.1	2.1	4.6	x	7.6
Biotite		7.2	8.0	6.3	20.7	9.4	
Hornblende	3.2			7.9			20.8
Diopside	8.2						
Orthopyroxene			0.8				
Iron oxide		0.3			0.9		0.4
Hematite			0.4				
Total	100.1	100.0	100.1	100.0	99.9	100.1	100.1
Colour Index	11.4	7.5	9.2	14.2	21.6	9.4	21.2

*x = Present in trace amounts*

**Appendix 1h.** Modal analyses of various rock types from the Hoare Lake gneisses.

Unit No.	HL-5	HL-8A	HL-8B
Quartz	11.3	21.5	36.0
Plagioclase	51.2	5.1	48.9
Biotite	0.8	43.5	13.8
Garnet	1.3	29.8	1.3
Orthopyroxene	33.0		
Orthoamphibole	1.8		
Iron oxide	0.8		
Total	100.2	99.9	100.0
Colour Index	37.7	73.3	15.1

**Appendix 1i.** Modal analyses of Grenville Supergroup clastic metasedimentary rocks.

Sample No.	Pelitic Metasedimentary Rocks			Quartzite	Para-amphibolite
	6-13-16A	6-13-16B	6-11-26	6-13-28A	6-13-28B
Quartz	4.4	22.6	6.0	84.2	1.7
Plagioclase	20.4	47.8	43.8	6.5	37.1
Potassium feldspar	39.3	x	14.2	4.3	1.7
Biotite	31.1	26.9	32.6	2.9	18.1
Graphite	4.9	2.6	3.4		
Hornblende				x	39.7
Pyrite					1.7
Titanite				2.2	
Rutile				x	
Total	100.1	99.9	100.0	100.1	100.0
Colour Index	31.1	26.9	32.6	5.1	59.5

*x = Present in trace amounts*

**Appendix 1j.** Modal analyses of rocks from the Little Papineau Lake plutonic complex.

Sample No.	4-7-5	4-7-6B	4-7-7	4-7-8B	4-7-9B	4-7-11	4A-4-1A	4A-4-1B	4A-4-2B
Quartz	1.6	28.8	x	24.6	3.1	10.4	1.9	3.4	12.3
Potassium feldspar	0.4	0.6	x	1.5	1.7	5.1	1.2	1.4	2.8
Plagioclase	64.7	63.0	66.1	58.6	74.4	73.6	60.7	76.4	64.6
An content					An <sub>25</sub>			An <sub>28</sub>	
Hornblende	22.6		21.3	0.2	10.4	6.1	34.6	7.4	3.4
Biotite	9.9	7.7	12.6	15.1	7.6	4.1	1.4	10.2	16.0
Iron oxide	0.8				2.8	0.8		1.1	0.9
Titanite							0.2		
Apatite								x	
Epidote								x	
Zircon								x	
Pyrite									
Hematite									
Total	100.0	100.1	100.0	100.0	100.0	100.1	100.0	99.9	100.0
Colour Index	33.3	7.7	33.9	15.3	20.8	11.0	36	18.7	20.3
Hornblende	2.3	–	1.7	0.01	1.4	1.5	24.7	0.7	0.2
Biotite									
Sample No.	4A-4-3B	4A-4-14	4A-4-21	4A-4-19	4A-5-8	5-10-1A	5-10-5	5-10-6	5-10-7
Quartz	9.7	7.8	0.2	1.0	5.4	2.3	3.5	19.5	5.8
Potassium feldspar	0.9	1.2	1.9	0.6	1.3	0.7	0.6	6.5	0.7
Plagioclase	66.0	69.3	41.4	51.9	45.1	68.6	66.6	66.3	66.8
Hornblende	3.0	11.1	33.4	44.0	23.2	17.1	19.9		16.1
Biotite	19.1	10.7	23.0	2.5	24.6	11.2	9.3	6.5	10.1
Iron oxide	1.2	x			x	x		0.8	0.5
Titanite				x	0.5				
Apatite									
Epidote									
Zircon									
Pyrite					x				
Hematite								0.3	
Total	99.9	100.1	99.9	100.0	100.1	99.9	99.9	99.9	100.0
Colour Index	23.3	21.8	56.4	46.5	47.8	28.3	29.2	7.4	26.7
Hornblende	0.2	1.0	1.5	17.6	0.94	1.5	2.1	–	1.6
Biotite									

*x = Present in trace amounts*

**Appendix 1k.** Modal analyses of the anorthosite suite rocks.

Sample No.	1-14-14	2-3-9
Plagioclase	52.2	57.4
An content	An72	An62
Hornblende	47.9	40.3
Diopside	x	2.1
Zircon	x	
Iron oxide		0.2
Total	100.1	100.0
Colour Index	47.9	42.6

*x = Present in trace amounts*

**Appendix 1l.** Modal analyses of various syenitic rocks from the New Carlow syenite complex.

Sample No.	6-11-3C	6-11-13C	6-11-32	6-13-6	6-13-7A	6-13-10	6-13-11	6-13-13B	6-13-30	7-13-1	7-13-4	7-14-2A	7-14-2B	7-14-9	7-14-11C	7-14-12C	7A-5-7
Quartz		17.0		29.3	4.8	1.5	0.4		20.3	4.2	25.3	1.9	0.4	0.2	0.2	9.7	x
Plagioclase	81.0	15.4	19.2	37.0	38.6	44.1	22.9	20.3	42.2	22.2	27.8	44.0	29.5	29.5	39.7	19.6	25.4
An content	An28																
Potassium feldspar	0.7	63.3	53.4	32.2	42.4	48.0	71.1	73.1	28.1	67.4	43.3	14.4	55.4	60.1	52.9	66.9	71.4
Biotite	14.7	1.6	0.6	1.0				0.3	1.3			5.9		x			x
Hornblende												29.3					
Augite		2.7	19.2		13.9	5.7	4.3	5.9	0.7	4.6	1.4		13.0	8.0	7.2	3.0	3.2
Limonite								0.3						x			
Iron oxide	3.6		0.6	0.5	0.5	0.6		0.3	6.2	x	1.1	4.5		x		0.8	
Hematite		x												x			
Sphene	x	x			x		1.0	0.7	0.7	1.6	0.5	x	1.9	x	x		x
Titanite				x	x		0.2	0.3	0.3			x	x	0.2	x	x	x
Muscovite	x																
Carbonate																	
Zircon	x																
Allanite																	
Epidote											0.5			1.8			x
Total	100.0	100.0	100.1	100.0	100.2	99.9	99.9	99.9	100.1	100.0	99.9	100.0	100.2	99.8	100.0	100.0	100.0
Colour Index	18.3	4.3	20.4	1.5	14.4	6.3	4.3	6.5	8.8	4.6	2.5	39.7	13.0	8.0	7.2	3.8	3.2

*x = Present in trace amounts*

Appendix Im. Modal analyses of corundum-bearing syenitic rocks from Hoover Mountain.

Sample No.	7-14-1B	7-14-12A	7-14-12A*	7-14-12C	7-14-12C*	7-14-1	7-14-1*	7-14-1C
Plagioclase	83.6	73.3	78.0	76.5	76.0	60.6	59.9	73.8
Potassium feldspar	2.7	3.4	2.3	8.5	8.4	17.0	13.6	2.0
Biotite	4.4	0.7	2.8	3.6	4.8	3.7	5.5	18.4
Corundum	4.0	11.1	4.3	5.1	4.1	11.9	13.8	1.7
Muscovite	3.2	8.2	9.3	2.2	1.6	2.7	4.1	2.5
Iron oxide	1.9	3.4	3.5	4.1	5.2	4.1	3.1	1.7
Pyrite	0.2			x	x			
Pyrrhotite								
Titanite				x				x
Total	100.0	100.1	100.2	100.0	100.1	100.0	100.01	100.1
Colour Index	6.3	4.1	6.3	7.7	10.0	7.8	8.6	20.1

*x = Present in trace amounts*

*\* Duplicate numbers indicate modal analyses conducted on different slab surface from a large bulk sample*

Appendix In. Modal analyses of metamorphosed potassic granitoid rocks.

Sample No.	1-4-1	2-3-1B	2-7-3	2A-1-1B	4-1-1B	4A-4-11	4A-4-16	4A-6-23	4A-4-29	4A-8-6A	4A-8-12	4A-8-14	7-2-6
Quartz	28.6	18.5	23.4	31.0	20.3	31.5	27.8	32.8	31.3	29.8	27.3	34.4	29.7
Plagioclase	12.2	12.2	28.5	19.0	13.5	28.3	25.8	38.5	11.5	21.3	32.0	20.4	27.4
Potassium feldspar	55.1	62.0	45.3	45.2	60.9	31.9	41.2	26.0	52.7	43.1	30.8	43.8	38.0
Biotite	3.3	7.3	x	2.2	5.2	6.7	3.8	1.6	2.6	4.8	6.4	0.5	1.9
Hornblende											2.3	0.2	
Iron oxide	0.5			1.4		1.6	1.4	1.0	1.9	0.9	1.2	0.7	1.9
Allanite	0.2			x	x					x			1.1
Pyrite	0.2	x	0.7		x						x	x	
Hematite													
Muscovite													
Total	100.1	100.0	100.1	100.0	99.9	100.0	100.0	99.9	100.0	99.9	100.0	100.0	100.0
Colour Index	4.5	7.3	2.9	4.8	5.2	8.3	5.2	2.6	4.5	5.7	9.9	1.4	4.9

*x = Present in trace amounts*

**Appendix 1o.** Modal analyses of generally hololeucocratic, fine-grained, muscovite-bearing metamorphosed potassic granitoid rocks.

Sample No.	3-11-4B	5-4-1A	5-4-1D	5-15-7
Quartz	22.5	33.9	34.9	34.4
Plagioclase	21.3	18.2	17.0	14.8
Potassium feldspar	51.1	45.7	40.1	50.0
Biotite	3.9	1.7	6.5	0.6
Iron oxide	0.2	0.5	0.6	0.3
Allanite		x	0.9	
Muscovite	0.8	x	x	x
Hematite		x		
Pyrite				x
Total	99.8	100.0	100.0	100.1
Colour Index	4.1	2.2	8.0	0.9

*x = Present in trace amounts*

**Appendix 1p.** Clast and matrix modal analyses of tectonic breccia from the Wicklow granite.

Sample No.	Clasts + Matrix 4-3-3	Matrix					
		4-3-3	3-2-2	3-2-5	4-3-13	4-3-8	
Granite matrix	66.7	Quartz	28.1	29.6	25.8	27.3	24.1
Diorite clasts	21.8	Plagioclase	17.9	29.2	30.4	24.4	38.8
Amphibolite clasts	10.3	Potassium feldspar	50.2	28.2	31.6	42.5	28.9
Trondhjemite clasts	1.2	Biotite	2.0	10.3	12.0	4.3	x
Metasedimentary clasts	x	Hornblende	1.6	2.3			7.8
Calcite-scapolite	x	Iron oxide	0.2	0.3	0.3	1.2	0.3
diopside skarn clasts		Allanite	0.2			0.2	0.3
		Pyrite		x			
Total	100.0	Total	100.2	99.9	100.1	99.9	100.2
		Colour Index	4.0	12.9	12.3	5.7	9.4

*x = Present in trace amounts*

**Appendix 1q.** Modal analyses of rocks from the Indian Lake plutonic complex.

Sample No.	5-2-6	6-1-5A	6-1-8A	6-1-8B	7-3-10
Quartz		14.6	23.0	24.4	14.5
Potassium feldspar		1.9	0.4	2.5	2.3
Plagioclase	52.8	65.1	57.0	58.9	69.2
Hornblende	25.4	11.3	1.1		2.6
Biotite	21.8	7.1	17.0	14.2	11.4
Iron oxide			1.5		x
Pyrite					x
Total	100.0	100.0	100.0	100.0	100.0
Colour Index	47.2	18.4	19.6	14.2	14.0

*x = Present in trace amounts*

Appendix 1r: Modal analyses of unmetamorphosed potassic granitoid rocks.

Sample No.	1-2-1C	2-7-6	3-2-16	3-8-3	4-1-4	4-3-58	4A-6-39A	5-2-4A	5-6-3	5-4-4	5-8-1A	5-8-9	5-15-3B	6-1-1	6-1-1C	6-13-2
Quartz	25.4	29.2	21.5	26.7	30.5	9.7	18.8	22.1	47.1	28.9	26.7	23.2	24.4	27.9	30.5	31.3
Plagioclase	60.5	23.7	18.0	33.8	39.8	25.0	36.7	22.1	15.9	18.6	16.0	24.1	9.0	24.3	27.1	33.8
Potassium feldspar	3.5	44.3	57.8	36.0	26.2	47.2	39.3	52.3	29.6	46.6	55.7	47.6	66.0	44.7	41.4	34.5
phenocrysts	1.3															
Biotite	8.4	1.9	2.3	3.1	3.2	8.9	4.3	2.4	6.1	4.4	1.6	4.3	0.6	2.4	0.5	
Hornblende						9.3										
Iron oxide	0.3	0.6		0.2			0.9	0.6	1.3	0.9		0.6		0.2	0.5	
Titanite	0.3															
Allanite		0.4	0.3	0.2	0.4	x	x	0.6	x	0.6				0.2		0.4
Pyrite					x			x								
Hematite	0.3															
Muscovite									x			0.3		0.2	x	
Pyrite						x			x							
Chalcopyrite							x									
Apatite						x										
Total	100.0	100.1	99.9	100.0	100.1	100.1	100.0	100.1	100.0	100.0	100.0	100.1	100.0	99.9	100.0	100.0
Colour Index	9.3	2.9	2.6	3.5	3.6	18.2	5.2	3.6	7.4	5.9	1.6	5.2	0.6	2.8	1.0	0.4

x = Present in trace amounts

Appendix 1r: Continued

Sample No.	5-4-6	5-6-4	5-13-2	5-13-9	5-13-11	5-14-2A	6-8-4	6-9-27	6-9-33	6-9-37	7-2-5B	7-5-7B	7-2-1B
Quartz	27.0	27.9	22.4	32.6	23.0	27.8	19.9	22.5	24.2	36.0	27.4	37.4	14.8
Plagioclase	27.2	27.0	15.2	21.0	36.1	17.2	39.1	23.3	26.5	24.6	23.8	27.4	35.0
Potassium feldspar	42.2	36.7	55.2	44.2	32.8	43.7	25.8	43.6	45.9	38.1	46.0	34.1	38.2
Biotite	2.6	6.3	7.1	1.8	3.3	6.6	13.9	9.3	3.4	0.3	2.3	x	11.1
Hornblende					4.6	4.6							
Iron oxide	0.5	1.6		0.5	0.3		1.4	0.4		1.0	0.3	1.1	1.1
Allanite	0.5	0.6	x	x				0.4		x	0.3		
Pyrite							x	0.4					
Hematite	x												
Muscovite													
Total	100.0	100.1	99.9	100.1	100.1	99.9	100.1	99.9	100.0	100.0	100.1	100.0	100.2
Colour Index	3.6	8.5	7.1	2.3	8.2	11.2	15.3	10.5	3.4	1.3	2.9	1.1	12.2

x = Present in trace amounts

## Appendix 2: Chemical Analyses

---

- a. Chemical analyses of amphibolite from the Wicklow area.
- b. Chemical analyses of paleosome from biotite-rich mesocratic to melanocratic gneiss.
- c. Chemical analyses of metasedimentary paleosome of possible pelitic composition.
- d. Chemical analyses of metasedimentary paleosome of possible wacke composition.
- e. Chemical analyses of cordierite-gedrite-hypersthene restite, leucosome, quartz diorite and amphibolite from the Hoare Lake gneisses.
- f. Chemical analyses of dioritic rocks from the Little Papineau Lake plutonic complex.
- g. Chemical analyses of diorite and monzodiorite from the New Carlow syenite complex (unit NCS-1).
- h. Chemical analyses of augite syenite to monzonite (unit NCS-4) and quartz syenite to granite (unit NCS-6) from the New Carlow syenite complex.
- i. Chemical analyses of corundum-bearing syenites and related syenites from the Hoover Mountain corundum deposit (units NCS-7, NCS-8, NCS-9 and NCS-3).
- j. Chemical analyses, selected element ratios and Barth mesonorms for metamorphosed potassic granitoid rocks.
- k. Partial chemical analyses of blocky potassium feldspar and selected element ratios from the Dubblestein and Thomas uraniferous granitic pegmatites.
- l. Partial chemical analysis of euxenite from the Dubblestein uraniferous granite pegmatite and comparative analyses from the literature.

**Appendix 2a.** Chemical analyses of amphibolite from the Wicklow area.

Sample No.	6-11-5D	6-13-32A	7-6-5C	7-9-1A	Average <sup>1</sup>
<b>Major Oxides (wt %)</b>					
SiO <sub>2</sub>	46.6	45.5	46.2	42.0	46.9
Al <sub>2</sub> O <sub>3</sub>	14.6	13.6	13.2	11.7	13.1
Fe <sub>2</sub> O <sub>3</sub>	3.85	5.72	5.61	6.79	5.47
FeO	6.79	8.69	9.35	13.2	9.40
MgO	8.85	6.25	6.51	6.77	7.09
CaO	11.3	9.36	9.23	9.51	9.71
Na <sub>2</sub> O	3.09	3.45	2.88	1.61	1.90
K <sub>2</sub> O	0.96	1.76	1.39	0.89	0.99
TiO <sub>2</sub>	1.27	2.43	2.20	4.33	2.39
P <sub>2</sub> O <sub>5</sub>	0.30	0.32	0.25	0.31	0.25
MnO	0.14	0.25	0.27	0.32	0.26
CO <sub>2</sub>	0.10	0.27	0.14	0.36	0.20
S	0.01	0.02	0.07	0.28	0.11
H <sub>2</sub> O <sup>+</sup>	0.63	0.74	0.94	0.58	0.80
H <sub>2</sub> O <sup>-</sup>	0.05	0.05	0.08	0.04	0.05
Total	98.6	98.4	98.3	98.7	98.6
<b>Trace Elements (ppm)</b>					
Ba	140	150	140	120	138
Be	2	3	3	3	2.8
Co	37	36	43	46	41
Cr	102	86	173	8	92
Cu	8	10	25	44	22
Ga	14	14	19	19	17
Li	34	49	14	8	26
Mo	<10	<10	<10	<10	<10
Nb	9	19	16	50	24
Ni	72	30	42	13	39
Pb	<10	<10	<10	<10	<10
Rb	20	40	20	<10	<23
Sc	11	25	20	50	27
Sn	2.0	2.0	3.9	2.1	2.5
Sr	510	155	90	275	258
V	210	340	370	630	389
Y	17	47	43	54	40
Zn	120	142	195	160	154
Zr	90	105	35	25	64
La	18	22	28	18	
Ce	45	55	65	50	
Nd	20	30	30	30	
Sm	6	8	8	11	
Eu	1.6	2.3	2.2	3.3	
Gd	5	9	8	11	
Dy	4.0	9.0	8.0	10.5	
Yb	1.6	4.9	4.5	5.4	
REE	101	140	154	139	
<b>Element Ratios</b>					
K/Ba	57	97	82	62	75
K/Rb	398	365	577	>739	>520
Ba/Rb	7	4	7	>12	<0.04
Rb/Sr	0.04	0.26	0.22	>7.5	<0.14
La/Yb	7.2	2.9	4.0	2.2	4.1
Eu/Eu*	0.89	0.84	0.85	0.92	0.88

<sup>1</sup>Excluding 6-11-5D which postdates Grenville Supergroup metasedimentary rocks and syenites, and including 2 analyses from Appendix 15. See Appendix 15 for analyses of amphibolites from the Hoare Lake gneissic suite.

Eu/Eu\* = chondrite-normalized observed Eu value divided by Eu value obtained by interpolation between Sm and Gd

**Appendix 2b.** Chemical analyses of paleosome from biotite-rich mesocratic to melanocratic gneiss.

Sample No.	7-3-8	7-3-9	7-9-2
<b>Major Oxides (wt %)</b>			
SiO <sub>2</sub>	52.4	52.9	51.9
Al <sub>2</sub> O <sub>3</sub>	14.0	12.0	14.0
FeO	5.55	5.55	5.40
Fe <sub>2</sub> O <sub>3</sub>	2.48	2.12	1.95
MgO	5.52	8.46	7.58
CaO	5.67	5.34	6.41
Na <sub>2</sub> O	1.51	0.67	1.67
K <sub>2</sub> O	6.82	7.29	5.53
TiO <sub>2</sub>	2.36	1.66	1.73
P <sub>2</sub> O <sub>5</sub>	1.05	1.09	0.52
MnO	0.12	0.18	0.13
CO <sub>2</sub>	0.11	0.19	0.10
S	0.25	0.01	0.02
H <sub>2</sub> O <sup>+</sup>	0.88	1.03	0.56
H <sub>2</sub> O <sup>-</sup>	0.07	0.07	0.10
Total	98.8	98.5	97.7
<b>Trace Elements (ppm)</b>			
Ba	3550	4160	4310
Be	5	3	5
Co	25	30	30
Cr	91	361	352
Cu	50	6	5
Ga	14	24	14
Li	24	30	26
Mo	<10	<10	<10
Ni	96	220	131
Nb	15	28	18
Pb	18	<10	16
Rb	170	230	190
Sc	28	17	19
Sn	<0.8	<0.8	4.9
Sr	1390	910	1330
V	220	180	215
Y	40	30	25
Zr	105	350	220
Zn	144	160	128
<b>Element Ratios</b>			
Na <sub>2</sub> O/K <sub>2</sub> O	0.22	0.09	0.30
SiO <sub>2</sub> /Al <sub>2</sub> O <sub>3</sub>	3.74	4.41	3.71
Al <sub>2</sub> O <sub>3</sub> /Na <sub>2</sub> O	9.3	17.9	8.4
K/Ba	15.9	14.5	11
K/Rb	333	263	242
Ba/Rb	21	18	23
Ca/Sr	29	42	35
Rb/Sr	0.12	0.25	0.14
Cr/Ni	0.9	1.6	2.7

**Appendix 2c.** Chemical analyses of metasedimentary paleosome of possible pelitic composition.

Sample No.	4A-6-33A	4A-6-34	4A-6-35	7-1-9A	7-9-1C	Average
<b>Major Oxides (wt %)</b>						
SiO <sub>2</sub>	60.6	59.4	62.8	51.0	60.8	58.9
Al <sub>2</sub> O <sub>3</sub>	18.0	17.9	15.4	14.2	18.3	16.8
FeO	5.48	6.65	5.99	6.50	5.48	6.02
Fe <sub>2</sub> O <sub>3</sub>	4.18	4.06	1.69	2.65	2.31	2.98
MgO	2.64	3.08	3.24	8.18	1.88	3.80
CaO	1.57	1.96	2.23	6.61	1.37	2.75
Na <sub>2</sub> O	1.35	1.72	1.73	1.59	1.72	1.62
K <sub>2</sub> O	2.81	2.31	3.56	3.50	3.79	2.56
TiO <sub>2</sub>	1.39	1.41	1.33	1.73	1.52	1.48
P <sub>2</sub> O <sub>5</sub>	0.08	0.03	0.02	1.07	0.05	0.21
MnO	0.10	0.10	0.09	0.14	0.06	0.08
CO <sub>2</sub>	0.31	0.08	0.17	0.08	0.39	0.17
S	0.04	0.02	0.02	0.25	0.54	0.15
H <sub>2</sub> O <sup>+</sup>	0.08	0.85	0.92	0.89	1.31	0.68
H <sub>2</sub> O <sup>-</sup>	0.06	0.06	0.05	0.06	0.07	0.05
Total	98.7	99.7	99.2	98.2	99.5	98.25
<b>Trace Elements (ppm)</b>						
Ba	700	580	760	2570	550	1032
Be	1	1	2	5	1	2.4
Co	22	23	18	32	19	23
Cr	55	66	56	261	64	100
Cu	92	26	13	134	90	355
Ga	18	15	17	17	20	17
Li	12	14	16	18	34	19
Mo	<10	<10	<10	<10	10	<10
Ni	38	40	26	194	39	34
Nb	8	12	13	16	18	13
Pb	<10	<10	<10	<10	72	<22
Rb	80	80	220	150	110	128
Sc	20	21	17	17	16	18
Sn	<0.8	<0.8	2.1	2.4	2.3	<1.7
Sr	185	215	315	720	130	198
V	145	185	170	205	195	180
Y	23	20	6	21	5	15
Zr	45	35	75	265	100	104
Zn	145	165	150	160	150	154
<b>Element Ratios</b>						
Na <sub>2</sub> O/K <sub>2</sub> O	0.48	0.74	0.49	0.45	0.45	0.63
SiO <sub>2</sub> /Al <sub>2</sub> O <sub>3</sub>	3.37	3.32	4.08	3.59	3.32	3.51
Al <sub>2</sub> O <sub>3</sub> /Na <sub>2</sub> O	13.3	10.4	8.9	8.9	10.6	10.4
K/Ba	33	33	28	8	57	31
K/Rb	291	240	97	138	283	199
Ba/Rb	8.8	7.3	3.5	17	5	8.3
Ca/Sr	61	66	51	66	76	100
Rb/Sr	0.43	0.37	0.70	0.21	0.85	0.51

**Appendix 2d.** Chemical analyses of metasedimentary paleosome of possible wacke composition.

Sample No.	1-14-13	2-1-9	4A-6-33B	4A-6-37	5-2-16	6-11-13	Average
<b>Major Oxides (wt %)</b>							
SiO <sub>2</sub>	56.1	59.5	57.2	60.2	61.7	53.6	58.1
Al <sub>2</sub> O <sub>3</sub>	18.1	17.3	17.5	15.4	15.5	17.9	17.0
FeO	5.48	5.00	4.82	5.26	4.53	6.43	5.27
Fe <sub>2</sub> O <sub>3</sub>	1.74	3.31	2.84	3.44	3.00	2.78	2.85
MgO	4.04	2.72	3.28	4.24	3.66	4.33	3.71
CaO	3.44	4.02	6.43	3.76	3.17	4.79	4.27
Na <sub>2</sub> O	4.67	2.51	2.79	2.61	2.91	4.03	3.25
K <sub>2</sub> O	3.09	2.15	1.62	2.50	2.78	3.08	2.54
TiO <sub>2</sub>	1.04	1.28	0.92	1.06	1.03	1.37	1.12
P <sub>2</sub> O <sub>5</sub>	0.15	0.09	0.03	0.10	0.21	0.19	0.13
MnO	0.11	0.14	0.12	0.10	0.09	0.10	0.11
CO <sub>2</sub>	0.21	0.11	0.23	0.10	0.11	0.52	0.21
S	0.25	0.08	0.02	0.01	0.02	0.17	0.09
H <sub>2</sub> O <sup>+</sup>	0.86	1.06	0.73	0.37	0.72	0.60	0.72
H <sub>2</sub> O <sup>-</sup>	0.08	0.13	0.05	0.07	0.05	0.07	0.07
Total	99.4	99.5	98.6	99.6	99.5	100.0	99.44
<b>Trace Elements (ppm)</b>							
Ba	340	720	280	530	410	770	508
Be	2	2	2	2	2	1	1.8
Co	21	27	23	19	18	23	22
Cr	86	121	40	58	66	62	72
Cu	73	140	29	6	18	32	50
Ga	18	15	13	17	16	19	16
Li	22	10	8	13	18	17	11
Mo	<10	<10	<10	<10	<10	<10	<10
Ni	30	52	34	35	37	38	38
Nb	14	13	12	12	11	16	13
Pb	30	12	<10	<10	<10	<10	<14
Rb	150	60	40	90	100	90	88
Sc	17	20	12	12	13	14	15
Sn	2.1	1.5	1.2	1.5	1.1	1.5	1.5
Sr	270	410	335	300	220	375	318
V	180	215	175	180	185	175	185
Y	8	18	20	15	15	9	14
Zr	90	95	50	60	180	13	81
Zn	150	155	77	134	148	155	137
<b>Element Ratios</b>							
Na <sub>2</sub> O <sub>3</sub> /K <sub>2</sub> O	1.51	1.17	1.72	1.04	1.05	1.31	1.28
SiO <sub>2</sub> /Al <sub>2</sub> O <sub>3</sub>	3.1	3.44	3.27	3.93	3.98	2.99	3.42
Al <sub>2</sub> O <sub>3</sub> /Na <sub>2</sub> O	0.9	6.9	6.3	5.9	5.3	4.4	5.2
K/Ba	75	25	48	39	56	33	46
K/Rb	171	298	336	231	231	284	259
Ba/Rb	2.3	12	7	6	4.1	8.5	6.7
Ca/Sr	92	71	138	90	104	92	97
Rb/Sr	0.56	0.15	0.12	0.3	0.45	0.24	0.3

**Appendix 2e.** Chemical analyses of cordierite-gedrite-hypersthene restite, leucosome, quartz diorite and amphibolite from the Hoare Lake gneisses.

Unit No.	HL-1	HL-2A	HL-2B	HL-5	HL-10	HL-11
<b>Major Oxides (wt %)</b>						
SiO <sub>2</sub>	48.6	46.9	58.2	55.9	54.3	46.7
Al <sub>2</sub> O <sub>3</sub>	15.8	15.8	14.2	13.3	13.6	13.6
FeO	8.18	12.4	5.77	9.57	6.72	9.06
Fe <sub>2</sub> O <sub>3</sub>	6.31	2.81	7.26	5.29	3.62	5.60
MgO	17.6	17.7	10.1	7.88	7.90	8.02
CaO	0.54	0.40	1.49	4.51	9.47	11.0
Na <sub>2</sub> O	0.70	0.80	0.86	1.59	0.80	0.76
K <sub>2</sub> O	0.49	0.42	0.15	0.12	0.25	0.65
TiO <sub>2</sub>	0.54	0.69	0.29	0.85	1.06	1.95
P <sub>2</sub> O <sub>5</sub>	0.04	0.04	0.04	0.03	0.19	0.20
MnO	0.20	0.24	0.37	0.25	0.23	0.24
CO <sub>2</sub>	0.33	0.35	0.69	0.06	0.15	0.10
S	0.04	0.02	0.02	0.01	0.03	0.13
H <sub>2</sub> O <sup>+</sup>	0.67	0.69	0.58	0.17	0.85	0.87
H <sub>2</sub> O <sup>-</sup>	0.05	0.06	0.12	0.06	0.06	0.04
Total	100.0	99.2	99.9	99.6	99.2	98.9
<b>Trace Elements (ppm)</b>						
Ba	110	80	100	60	70	60
Be	2	2	1	1	1	2
Co	36	41	25	31	32	40
Cr	139	138	96	53	388	236
Cu	48	26	30	48	17	95
Ga	22	26	10	12	15	16
Li	87	108	25	18	13	12
Mo	<10	<10	<10	<10	<10	<10
Ni	62	73	24	19	94	49
Nb	14	18	30	10	16	25
Pb	<10	<10	<10	<10	<10	18
Rb	20	10	<10	20	<10	10
Sc	9	7	3	18	25	35
Sn	3.6	2.9	0.8	1.2	1.8	2.1
Sr	16	16	40	14	45	80
V	500	405	195	280	260	405
Y	4	3	5	12	12	21
Zr	11	12	6	16	45	30
Zn	350	325	160	145	180	160
La	2			2	17	9
Ce	<6			<6	40	25
Nd	<2			2	20	15
Sm	<1			<1	7	4
Eu	0.2			0.5	1.7	1.7
Gd	2			1	5	5
Dy	1.0			2.0	3.5	4.5
Yb	0.6			1.8	1.2	2.1
REE	<14.8			<16.3	95	66
<b>Element Ratios</b>						
K/Ba	37	44	12	17	29	90
K/Rb	203	349	>125	>100	>202	540
Ba/Rb	5	8	>10	3	>7	6
Rb/Sr	1.25	0.63	<0.25	1.43	<0.22	0.13
Cr/Ni	2.2	1.9	4	2.8	4.2	4.8
La/YbN	2.2			0.72	6.1	2.8
Eu/Eu*					0.87	1.2
<i>La/YbN = chondrite-normalized La/Yb ratio</i>						
<i>Eu/Eu* = chondrite-normalized observed Eu value divided by Eu value obtained by interpolation between Sm and Gd</i>						

**Appendix 2f.** Chemical analyses of dioritic rocks from the Little Papineau Lake plutonic complex.

Sample No.	4A-4-20A	4A-4-20B	4A-5-3	4-7-7	4-7-9A
<b>Major Oxides (wt %)</b>					
SiO <sub>2</sub>	62.7	55.4	47.5	54.2	54.6
Al <sub>2</sub> O <sub>3</sub>	18.4	15.9	15.8	20.1	18.6
Fe <sub>2</sub> O <sub>3</sub>	1.23	3.12	4.55	2.12	2.80
FeO	2.41	5.11	7.16	3.36	4.53
MgO	2.06	4.98	6.08	3.94	3.69
CaO	3.37	5.43	7.99	6.67	6.78
Na <sub>2</sub> O	5.36	3.89	3.07	4.59	4.10
K <sub>2</sub> O	2.07	1.97	2.28	1.43	1.70
TiO <sub>2</sub>	0.56	1.58	1.83	0.67	0.84
P <sub>2</sub> O <sub>5</sub>	0.16	0.32	0.46	0.16	0.19
MnO	0.07	0.09	0.17	0.08	0.10
CO <sub>2</sub>	0.20	0.33	0.21	0.34	0.23
S	0.01	0.01	0.23	0.01	0.01
H <sub>2</sub> O <sup>+</sup>	0.54	0.77	1.08	0.99	0.57
H <sub>2</sub> O <sup>-</sup>	0.05	0.06	0.04	0.06	0.06
Total	99.2	99.0	98.5	98.7	98.8
<b>Trace Elements (ppm)</b>					
Ba	320	260	750	570	330
Be	2	2	2	2	2
Co	9	20	31	18	24
Cr	6	74	20	18	24
Cu	7	5	20	86	10
Ga	16	15	14	17	15
Li	16	11	15	14	12
Mo	<10	<10	<10	<10	<10
Ni	18	40	20	30	27
Nb	3	10	18	6	7
Pb	30	<10	<10	32	49
Rb	100	50	60	40	30
Sc	1	14	12	5	8
Sn	2.0	2.9	2.2	1.5	1.8
Sr	390	190	660	1250	350
V	40	160	190	115	145
Y	8	38	35	8	9
Zn	73	76	145	54	78
Zr	160	100	40	30	23
La	53	32	49		
Ce	110	90	120		
Nd	35	45	50		
Sm	5	10	11		
Eu	1.3	2.4	3.0		
Gd	3	9	9		
Dy	1.8	7.5	7.0		
Yb	0.8	3.9	3.4		
REE	210	200	249		
<b>Element Ratios</b>					
Na <sub>2</sub> O/K <sub>2</sub> O	2.6	2.0	1.3	3.2	2.4
K/Ba	54	63	25	21	43
K/Rb	172	327	315	297	470
Ba/Rb	3	5	13	14	11
Ca/Sr	62	206	87	38	139
Rb/Sr	0.26	0.26	0.09	0.03	0.09
La/Yb	43.3	5.3	9.3		
Eu/Eu*	–	0.77	0.92		
4A-4-20A	<i>Massive, medium-grained, biotite-hornblende quartz diorite</i>				
4A-4-20B	<i>Massive, medium-grained, biotite-hornblende diorite</i>				
4A-5-3	<i>Massive, medium-grained, biotite-hornblende metagabbro</i>				
4-7-7	<i>Massive, medium-grained, biotite-hornblende diorite</i>				
4-7-9A	<i>Massive, medium-grained, ± biotite-hornblende diorite</i>				
<i>Eu/Eu* = chondrite-normalized observed Eu value divided by Eu value obtained by interpolation between Sm and Gd</i>					

**Appendix 2g.** Chemical analyses of diorite and monzodiorite from the New Carlow syenite complex (unit NCS-1).

Sample No.	6-13-3B	7A-5-4	7-13-3	7-14-2A	7-14-5A	7-14-8	7-14-10A	Average
<b>Major Oxides (wt %)</b>								
SiO <sub>2</sub>	61.5	50.1	46.4	48.2	50.1	46.5	49.6	
Al <sub>2</sub> O <sub>3</sub>	14.7	14.8	14.4	12.9	14.0	12.4	14.0	
Fe <sub>2</sub> O <sub>3</sub>	5.67	5.81	6.47	8.83	6.09	7.67	6.85	
FeO	3.58	5.40	8.11	7.60	5.55	6.21	5.55	
MgO	0.83	3.93	5.63	3.95	3.88	5.37	4.17	
CaO	4.23	6.41	7.92	7.03	6.86	9.28	6.60	
Na <sub>2</sub> O	3.83	3.39	3.32	4.50	4.08	2.14	3.34	
K <sub>2</sub> O	2.89	4.06	2.01	2.04	3.33	3.23	3.71	
TiO <sub>2</sub>	1.32	2.13	2.07	2.49	2.47	2.57	2.59	
P <sub>2</sub> O <sub>5</sub>	0.21	0.98	0.69	0.80	1.05	1.34	1.10	
S	0.02	0.35	0.28	0.17	0.28	0.35	0.20	
MnO	0.14	0.14	0.18	0.31	0.16	0.18	0.17	
CO <sub>2</sub>	0.28	0.19	0.63	0.20	0.69	0.49	0.33	
H <sub>2</sub> O <sup>+</sup>	0.36	0.52	0.48	0.66	0.40	0.76	0.51	
H <sub>2</sub> O <sup>-</sup>	0.07	0.07	0.05	0.10	0.08	0.08	0.08	
Total	99.7	98.3	98.7	99.8	99.0	98.6	98.8	
<b>Trace Elements (ppm)</b>								
Ba	360	6054	1790	580	3400	3460	3820	2780
Be	2	4	2	7	3	3	3	3
Co	12	10	41	20	23	33	22	23
Cr	<5	10	39	6	33	89	37	<31
Cu	8	28	48	16	31	56	29	31
Ga	19	17	16	20	16	16	18	17
Li	18	14	32	17	40	30	34	26
Mo	<10	<10	<10	<10	<10	<10	<10	<10
Nb	8	20	18	15	25	21	16	18
Ni	<5	10	65	<5	19	56	20	26
Pb	21	24	16	10	27	86	34	31
Rb	50	70	50	20	60	50	70	53
Sc	6	14	14	16	17	18	9	13
Sn	5.2	<0.8	2.1	2.4	<0.5	<0.8	<0.8	<1.7
Sr	185	2770	1330	330	2170	2080	2120	1569
V	50	240	290	210	215	245	180	204
Y	75	35	37	103	55	53	30	55
Zn	146	66	160	260	145	170	160	158
Zr	85	95	70	45	75	105	80	79
La			87	65		135		
Ce			195	145		325		
Nd			80	70		140		
Sm			15	19		30		
Eu			3.7	5.1		6.6		
Gd			11	19		20		
Dy			7.5	18.5		11.0		
Yb			3.3	9.8		4.2		
REE			403	351		672		

## Appendix 2g. Continued

Sample No.	6-13-3B	7A-5-4	7-13-3	7-14-2A	7-14-5A	7-14-8	7-14-10A	Average
<b>Element Ratios</b>								
K/Ba	66.6	5.6	9.3	29.1	8.1	7.8	8.1	19.2
K/Rb	480	481	337	847	460	536	440	512
Ba/Rb	7.2	86.5	35.8	29.0	56.7	69.2	54.6	48.4
Ca/Sr	165	16.7	42.9	153	22.8	32.1	22.4	65.0
Rb/Sr	0.27	0.03	0.04	0.06	0.03	0.02	0.03	0.07
La/Yb			17.0	4.8		20.8		
Eu/Eu*			0.89	0.83		0.82		
6-13-3B	<i>Massive, fine- to medium-grained, titanite-magnetite-biotite quartz monzodiorite</i>							
7A-5-4	<i>Massive, fine-grained, apatite-titanite-magnetite hornblende-biotite diorite</i>							
7-13-3	<i>Foliated, medium-grained, titanite-biotite-hornblende diorite</i>							
7-14-2A	<i>Foliated, medium-grained, titanite-magnetite-biotite- hornblende diorite</i>							
7-14-5A	<i>Foliated, fine- to medium-grained, apatite-titanite-magnetite-biotite-hornblende diorite</i>							
7-14-8	<i>Massive, fine- to medium-grained, apatite-titanite-magnetite-biotite-hornblende diorite</i>							
7-14-10A	<i>Massive, fine- to medium-grained, apatite-titanite-magnetite-hornblende-biotite diorite</i>							
<i>Eu/Eu* = chondrite-normalized observed Eu value divided by Eu value obtained by interpolation between Sm and Gd</i>								

**Appendix 2h.** Chemical analyses of augite syenite to monzonite (unit NCS-4) and quartz syenite to granite (unit NCS-6) from the New Carlow syenite complex.

Sample No.	6-13-10	6-13-11	6-13-6	7-13-2
<b>Major Oxides (wt %)</b>				
SiO <sub>2</sub>	64.3	64.3	72.1	65.9
Al <sub>2</sub> O <sub>3</sub>	18.0	17.4	14.4	14.6
Fe <sub>2</sub> O <sub>3</sub>	1.40	0.90	1.48	3.10
FeO	0.80	1.02	1.02	1.75
MgO	0.10	0.58	0.08	0.73
CaO	1.36	1.73	1.22	2.18
Na <sub>2</sub> O	8.46	2.94	3.92	4.45
K <sub>2</sub> O	4.26	8.60	3.95	4.31
TiO <sub>2</sub>	0.64	0.57	0.34	0.70
P <sub>2</sub> O <sub>5</sub>	0.03	0.05	0.05	0.17
S	0.01	0.02	0.02	0.03
MnO	0.06	0.05	0.03	0.07
CO <sub>2</sub>	0.24	0.66	0.55	0.42
H <sub>2</sub> O <sup>+</sup>	0.24	0.54	0.07	0.55
H <sub>2</sub> O <sup>-</sup>	0.06	0.08	0.08	0.11
Total	100.0	99.4	99.3	99.2

Sample No.	6-13-10	6-13-11	Average (unit NCS-4)	6-13-6	7-13-2	Average (unit NCS-6)
<b>Trace Elements (ppm)</b>						
Ba	560	1120	840	280	650	465
Be	2	2	2	2	4	3
Co	< 5	< 5	< 5	< 5	5	< 5
Cr	< 5	< 5	< 5	< 5	< 5	< 5
Cu	< 5	6	< 5	6	10	8
Ga	20	16	18	19	16	17
Li	10	8	9	20	10	15
Mo	11	12	11	10	16	13
Nb	25	23	24	2	35	17
Ni	< 5	< 5	< 5	< 5	< 5	< 5
Pb	20	10	15	< 10	12	< 11
Rb	80	200	140	100	120	110
Sc	1	9	5	1	11	6
Sn	6.2	3.9	5.1	4.3	5.6	5.0
Sr	320	530	425	55	335	195
V	11	12	11	10	24	17
Y	53	82	68	30	125	78
Zn	41	42	41	38	84	61
Zr	13	11	12	105	155	130
La	25	64				
Ce	80	205				
Nd	50	115				
Sm	14	30				
Eu	2.0	2.9				
Gd	13	22				
Dy	13.5	19.5				
Yb	5.4	7.0				
REE	203	465				

## Appendix 2h. Continued

Sample No.	6-13-10	6-13-11	Average (unit NCS-4)	6-13-6	7-13-2	Average (unit NCS-6)
<b>Element Ratios</b>						
K/Ba	63	64	64	117	55	86
K/Rb	442	357	400	328	298	313
Ba/Rb	7.0	5.6	6.3	2.8	5.4	4.1
Ca/Sr	31	23.5	27	160	46.9	103
Rb/Sr	0.25	0.38	0.32	1.8	0.36	1.08
La/Yb	3.0	5.9				
Eu/Eu*	0.46	0.35				
<hr/>						
6-13-10	<i>Massive, fine- to coarse-grained, augite monzonite</i>					
6-13-11	<i>Massive, coarse-grained, titanite-augite syenite</i>					
6-13-6	<i>Lineated, medium-grained, magnetite-biotite granite</i>					
7-13-2	<i>Massive, medium-grained, biotite quartz syenite</i>					
<i>Eu/Eu* = chondrite-normalized observed Eu value divided by Eu value obtained by interpolation between Sm and Gd</i>						

**Appendix 2i.** Chemical analyses of corundum-bearing syenites and related syenites from the Hoover Mountain corundum deposit (units NCS-7, NCS-8, NCS-9 and NCS-3).

Sample No.	7-14-1B	7-14-1C	7-14-12A	7-14-12C	7-14-12B	Average
<b>Major Oxides (wt %)</b>						
SiO <sub>2</sub>	53.2	53.8	51.9	49.3	56.7	
Al <sub>2</sub> O <sub>3</sub>	28.8	21.6	26.9	27.7	19.0	
Fe <sub>2</sub> O <sub>3</sub>	2.01	4.77	5.02	6.12	7.39	
FeO	1.31	4.60	2.85	2.92	2.50	
MgO	0.06	0.85	0.08	0.00	0.00	
CaO	3.03	2.72	2.05	2.28	1.36	
Na <sub>2</sub> O	8.08	6.42	6.69	7.78	10.5	
K <sub>2</sub> O	1.56	2.90	1.86	1.61	1.41	
TiO <sub>2</sub>	0.45	0.86	0.51	0.64	0.38	
P <sub>2</sub> O <sub>5</sub>	0.04	0.07	0.05	0.04	0.10	
S	0.02	0.02	0.02	0.02	0.01	
MnO	0.05	0.19	0.07	0.07	0.02	
CO <sub>2</sub>	0.16	0.10	0.72	0.64	0.26	
H <sub>2</sub> O <sup>+</sup>	0.46	0.94	0.79	0.79	0.26	
H <sub>2</sub> O <sup>-</sup>	0.05	0.04	0.05	0.05	0.06	
Total	99.3	99.9	99.6	100.0	100.0	
<b>Trace Elements (ppm)</b>						
Ba	660	500	230	210	170	354
Be	1	1	1	1	2	1
Co	5	7	< 5	< 5	< 5	< 5
Cr	< 5	29	< 5	< 5	< 5	< 10
Cu	5	6	6	6	16	8
Ga	16	18	23	23	35	23
Li	17	25	14	18	4	16
Mo	12	< 10	11	11	11	< 11
Nb	8	13	5	7	8	8
Ni	< 5	< 5	< 5	< 5	< 5	< 5
Pb	17	24	< 10	70	29	< 30
Rb	50	150	50	40	20	62
Sc	< 1	< 1	< 1	1	< 1	< 1
Sn	2.7	8.4	5.6	7.5	8.7	6.6
Sr	610	220	125	130	165	250
V	7	50	6	7	13	17
Y	4	3	2	2	5	3
Zn	50	170	78	100	70	94
Zr	23	35	15	21	370	93
La			11		8	
Ce			25		10	
Nd			7		2	
Sm			1		< 1	
Eu			0.5		0.4	
Gd			1		< 1	
Dy			0.7		0.8	
Yb			0.1		1.4	
REE			46.3		< 24.6	

## Appendix 2i. Continued

Sample No.	7-14-1B	7-14-1C	7-14-12A	7-14-12C	7-14-12B	Average
<b>Element Ratios</b>						
K/Ba	19.6	48.1	67.1	63.6	68.8	53.4
K/Rb	436	161	309	334	585	365
Ba/Rb	13.2	3.3	4.6	5.3	8.5	7.0
Ca/Sr	35.8	89.0	118	126	59	85.6
Rb/Sr	0.08	0.68	0.4	0.31	0.12	0.32
La/Yb			71.1		3.8	
Eu/Eu*			1.6			

7-14-1B *Magnetite-muscovite-corundum-biotite plagiostenite: unit NCS-9*

7-14-1C *Magnetite-corundum-muscovite-biotite plagiostenite: unit NCS-7*

7-14-12A *Biotite-magnetite-muscovite-corundum plagiostenite (typical ore from Hoover Mountain corundum deposit): unit NCS-8*

7-14-12C *Muscovite-magnetite-corundum plagiostenite (typical ore from Hoover Mountain corundum deposit): unit NCS-8*

7-14-12B *Magnetite-biotite plagiostenite ("buff" syenite of Hewitt 1954) interlayered with 7-14-12A and 7-14-12B at the Hoover Mountain corundum deposit: unit NCS-3*

*Eu/Eu\* = chondrite-normalized observed Eu value divided by Eu value obtained by interpolation between Sm and Gd*

**Appendix 2j.** Chemical analyses, selected element ratios and Barth mesonorms for metamorphosed potassic granitoid rocks.

Sample No.	3-11-4B	4-3-15B	4A-4-11	4A-7-13B	4A-8-13	5-6-4	7-2-6	7-6-4B	7-7-1
<b>Major Oxides (wt %)</b>									
SiO <sub>2</sub>	71.2	69.9	72.0	73.5	74.5	72.6	71.7	70.8	76.9
Al <sub>2</sub> O <sub>3</sub>	15.4	14.6	13.6	14.6	12.2	13.9	14.7	14.7	12.9
Fe <sub>2</sub> O <sub>3</sub>	1.04	2.30	2.54	0.90	3.08	1.47	1.53	1.85	0.26
FeO	0.66	1.61	1.61	0.73	1.31	1.17	0.80	1.31	0.66
MgO	0.28	0.55	0.64	0.23	0.33	0.44	0.21	0.61	0.34
CaO	0.78	1.41	0.93	1.15	0.71	1.11	1.38	1.22	1.19
Na <sub>2</sub> O	2.13	1.95	2.17	2.97	1.44	2.38	2.05	2.36	1.82
K <sub>2</sub> O	6.53	5.78	4.17	4.59	5.49	4.97	5.67	5.60	4.51
TiO <sub>2</sub>	0.33	0.64	0.70	0.24	0.35	0.66	0.28	0.66	0.28
P <sub>2</sub> O <sub>5</sub>	0.53	0.17	0.16	0.13	0.12	0.15	0.16	0.17	0.13
S	0.01	0.01	0.02	0.02	0.02	0.01	0.02	0.01	0.05
MnO	0.01	0.03	0.02	0.01	0.02	0.04	0.02	0.03	0.02
CO <sub>2</sub>	0.32	0.48	0.68	0.24	0.30	0.19	0.71	0.36	0.30
H <sub>2</sub> O <sup>+</sup>	0.38	0.39	0.54	0.36	0.28	0.38	0.57	0.36	0.27
H <sub>2</sub> O <sup>-</sup>	0.05	0.04	0.07	0.04	0.12	0.05	0.05	0.05	0.05
Total	99.65	99.86	99.85	99.71	100.27	99.52	99.85	100.29	99.68
<b>Trace Elements (ppm)</b>									
Ba	1710	1320	920	880	940	1050	800	1010	1210
Be	1	2	2	2	1	2	1	2	2
Co	<5	<5	<5	<5	5	5	5	5	5
Cr	<5	<5	5	<5	<5	<5	<5	<5	<5
Cu	<5	8	23	10	16	7	16	8	13
Ga	16	17	19	19	15	18	12	16	14
Li	4	13	6	6	10	10	8	12	8
Nb	<1	6	1	<1	<1	12	<1	15	<1
Ni	<5	<5	<5	<5	<5	<5	<5	<5	<5
Pb	33	38	19	15	10	11	28	17	18
Rb	170	170	80	90	130	90	130	170	110
Sc	<1	4	2	<1	1	4	<1	5	1
Sn	0.9	1.9	2.9	<0.8	1.3	1.8	1.0	2.2	1.1
Sr	440	270	170	290	230	155	260	325	300
V	21	20	25	13	65	16	20	30	13
Y	9	17	24	8	30	41	18	46	3
Zn	28	52	54	22	30	56	25	49	22
Zr	45	245	200	170	320	150	475	105	145
La	136	360	89			108	386	191	
Ce	290	790	200			260	790	395	
Nd	75	240	70			80	230	135	
Sm	10	30	12			13	29	23	
Eu	1.8	2.1	1.7			2.0	2.2	2.2	
Cd	6	16	8			10	15	16	
Dy	2.5	5.0	6.0			8.0	5.0	10.0	
Yb	0.6	1.2	2.0			4.7	1.7	3.4	
REE	522	1444	389			486	1459	776	
<b>Element Ratios</b>									
Ba/Rb	10.1	7.8	11.5	9.8	7.2	11.7	6.2	5.9	11
Ba/Sr	3.9	4.9	5.4	3.0	4.1	6.8	3.1	3.1	4.0
Ca/Sr	12.6	37.0	38.8	28.2	21.9	50.8	37.7	26.6	28.2
Ca/Y	32	36	38	43	49	39	59	46	31
K/Rb	320	282	433	423	351	458	362	273	340
Rb/Sr	0.4	0.6	0.5	0.3	0.6	0.6	0.5	0.5	0.4
Eu/Eu*	0.72	0.29	0.53			0.54	0.32	0.35	
La/YbN	148	193	29			15	53	36	

*Eu/Eu\** = chondrite-normalized observed Eu value divided by Eu value obtained by interpolation between Sm and Gd  
*La/YbN* = chondrite-normalized La/Yb ratio

## Appendix 2j. Continued

Sample No.	3-11-4B	4-3-15B	4A-4-11	4A-7-13B	4A-8-13	5-6-4	7-2-6	7-6-4B	7-7-1
<b>Barth Mesonorms</b>									
Orthoclase	38.5	33.0	23.3	26.7	32.8	28.5	33.7	31.7	26.0
Albite	19.6	18.0	20.1	27.2	13.4	22.0	18.9	21.6	16.8
Anorthite	0.0	0.3		2.4		0.9		0.1	2.1
Quartz	32.0	34.1	41.5	35.4	43.2	37.1	36.0	33.2	45.8
Apatite	0.5	0.4		0.3	0.3	0.3	0.3	0.4	0.3
Magnetite	1.1	2.5	2.7	1.0	3.1	1.6	1.6	2.0	0.3
Hematite									
Calcite	0.9	1.4	1.9	0.7	0.9	0.5	2.0	1.0	0.9
Corundum	5.4	5.6	6.2	4.3	4.4	4.8	5.8	0.2	4.8
Biotite	1.5	3.3	3.4	1.5	1.3	2.8	1.0	3.3	2.4
Sphene		1.4		0.5	0.4	1.4	0.5	1.0	0.6
Pyrite			0.1	0.1	0.1		0.1		0.1
<i>3-11-4B</i>	<i>Massive, fine-grained, hololeucocratic magnetite-muscovite granite</i>								
<i>4-3-15B</i>	<i>Massive, fine-grained biotite granite (Wicklow granite)</i>								
<i>4A-4-11</i>	<i>Well-foliated, medium-grained, magnetite-biotite granite</i>								
<i>4A-7-13B</i>	<i>Well-foliated, medium-grained, biotite granite</i>								
<i>4A-8-13</i>	<i>Well-foliated, medium-grained, biotite granite</i>								
<i>5-6-4</i>	<i>Well-foliated, medium-grained, biotite granite</i>								
<i>7-2-6</i>	<i>Lineated, medium-grained, biotite-allanite granite</i>								
<i>7-6-4B</i>	<i>Well-foliated, medium-grained, biotite granite</i>								
<i>7-7-1</i>	<i>Foliated, medium- to coarse-grained, biotite granite</i>								

**Appendix 2k.** Partial chemical analyses of blocky potassium feldspar and selected element ratios from the Dubblestein and Thomas uraniferous granitic pegmatites.<sup>1</sup>

Sample No.	K <sub>2</sub> O (wt %)	Na <sub>2</sub> O	Ba	Cs (ppm)	Rb	Sr	K/Ba	K/Cs	K/Rb	Ba/Rb	Rb/Sr
<b>Dubblestein pegmatite</b>											
40 cm	13.3	2.36	1950	<5	410	540	5.7	>2241	26.9	4.8	0.8
70 cm	13.4	2.15	1090	5	440	370	10.2	2224	25.2	2.5	1.2
1 m	13.5	2.20	440	<5	490	220	25.5	>2241	22.9	0.9	2.2
1.7 m	13.7	2.22	200	5	570	150	56.9	2274	19.9	0.35	3.8
2.1 m	13.3	2.51	60	<5	780	40	184	>2201	14.2	0.08	19.5
2.6 m	13.7	2.23	160	12	900	40	171	948	12.6	0.2	22.5
2.9 m	13.0	2.61	40	10	1010	30	270	1079	10.7	0.04	33.7
3.2 m	13.6	2.29	100	8	970	10	113	1411	11.6	0.1	97
Average	13.4	2.32	505	<7	695	175	105	>1822	15.3	1.1	22.6
<b>Thomas pegmatite</b>											
BKF-1	14.2	1.85	3110	<5	270	520	3.8	>2357	43.7	11.5	0.5
BKF-2	13.6	2.07	1870	<5	290	490	6.0	>2258	38.9	6.5	0.6
BKF-3	14.0	1.88	2280	<5	270	520	5.1	>2324	43.0	8.4	0.5
Average	13.9	1.93	2420	<5	277	510	5.0	>2313	41.9	8.8	5.3

<sup>1</sup>Analyses conducted by X-Ray Assay Laboratories Limited, Toronto.

**Appendix 2I.** Partial chemical analysis of euxenite from the Dubblestein uraniferous granite pegmatite and comparative analyses from the literature.<sup>1</sup>

	A	B	C	D	E	F
<b>Oxides (wt %)</b>						
CaO	2.56	4.86	1.92	1.08	2.03	0.85
MgO	0.41	0.13	0.03	0.06	0.07	0.08
MnO		0.59	0.28	0.16	0.19	–
PbO		0.37	1.35	0.63	1.01	0.43
K <sub>2</sub> O			0.04	0.09		
Na <sub>2</sub> O			0.17	0.18		
Al <sub>2</sub> O <sub>3</sub>		0.13	0.26	x	0.45	x
CeO <sub>2</sub>	0.02	4.34	0.44	2.20	0.87	2.45
(Y,Eu) <sub>2</sub> O <sub>3</sub>	14.0	18.22	24.31	27.73	24.95	27.32
UO <sub>2</sub>		0.67	8.61	5.83	7.25	5.64
UO <sub>3</sub>		0.04	0.20	–	1.51	–
U <sub>3</sub> O <sub>8</sub>	9.55		–	–	–	–
ThO <sub>2</sub>	2.80	4.95	3.94	3.58	2.64	4.60
SnO <sub>2</sub>		0.12	0.07	0.18	0.14	0.11
SiO <sub>2</sub>		0.07	0.09	0.17	1.08	–
Fe <sub>2</sub> O <sub>3</sub>	1.78	1.32	2.07	–	2.16	–
FeO	0.1	0.77	–	1.13	0.14	1.37
TiO <sub>2</sub>	8.89	16.39	22.96	25.68	25.04	24.43
Nb <sub>2</sub> O <sub>5</sub>	31.5	41.34	28.62	27.64	22.28	29.00
Ta <sub>2</sub> O <sub>5</sub>	0.85	3.84	2.65	1.27	5.32	11.01
H <sub>2</sub> O		1.96	2.23	2.55	2.37	–
Loss on Ignition						2.87
ZrO <sub>2</sub>		0.04	0.05	trace		
BeO					0.05	
Total	72.46	100.24	100.29	100.16	99.55	100.16

A. Euxenite from the Dubblestein granite pegmatite, this study.

B. "Lyndochite" (high calcium euxenite), Lyndoch Township, Ontario.

C. Euxenite, Sabine Township, Ontario.

D. Euxenite, Alve, Arendal, Norway.

E. Euxenite, Maberly, Ontario.

F. Euxenite, Hitterø, Norway.

<sup>1</sup> Analysis A conducted by X-Ray Assay Laboratories Limited, Toronto. All remaining analyses from Palache, Berman and Frondel (1944).

x = Present in trace amounts

## Appendix 3: Comparison with Literature

---

- a. Average amphibolite compositions from the Grenville Province.
- b. Mean bulk composition of metapelite and metawacke from the Wicklow area in comparison to similar clastic metasedimentary rocks selected from the literature.
- c. Analyses of cordierite-anthophyllite rocks, selected from the literature, associated with volcanogenic massive sulphide ore deposits.
- d. Analyses of cordierite-anthophyllite/gedrite rocks, selected from the literature, representing secondary bulk compositions, but unassociated with massive sulphide mineralization.
- e. Analyses of cordierite-bearing restite clots from advanced stage metasedimentary migmatites (diatexites), English River Subprovince, northwestern Ontario.
- f. Composition of cordierite-anthophyllite/gedrite and gedrite-bearing rocks, selected from the literature, interpreted to be unaltered, compared with selected average compositions of rocks from various metasedimentary groups.

**Appendix 3a.** Average amphibolite compositions from the Grenville Province.

	<b>A</b>	<b>B</b>	<b>C</b>	<b>D</b>	<b>E</b>
<b>Major Oxides (wt %)</b>					
SiO <sub>2</sub>	48.12	48.21	49.29	47.8	46.90
Al <sub>2</sub> O <sub>3</sub>	14.92	14.98	14.97	16.5	13.10
Fe <sub>2</sub> O <sub>3</sub>	4.06	3.57	2.28	3.53	5.47
FeO	7.97	8.95	8.06	7.88	9.40
MgO	7.36	6.82	5.94	6.76	7.09
CaO	8.84	9.23	9.51	9.76	9.71
Na <sub>2</sub> O	3.53	3.49	3.50	2.70	1.90
K <sub>2</sub> O	0.65	0.40	1.32	1.12	0.99
TiO <sub>2</sub>	1.65	1.15	1.35	1.32	2.39
P <sub>2</sub> O <sub>5</sub>	0.31	0.11	0.21	0.20	0.25
MnO	0.21	0.18	0.13	0.18	0.26
CO <sub>2</sub>	0.66	0.76	1.83	0.89	0.20
S	ND	ND	ND	ND	0.11
H <sub>2</sub> O <sup>+</sup>	1.35	ND	ND	ND	0.80
H <sub>2</sub> O <sup>-</sup>	ND	ND	ND	ND	0.05
Total	99.63	97.85	98.39	98.64	98.62

A. Average Hermon Group amphibolite (16 analyses in Jennings 1969).

B. Average orthoamphibolite, Haliburton–Madoc area (17 analyses in van de Kamp 1968).

C. Average para-amphibolite, Haliburton–Madoc area (34 analyses in van de Kamp 1968).

D. Average Tudor mafic metavolcanic rocks from the Kaladar area (10 analyses in Wolff 1982).

E. Average amphibolite from Madawaska Highlands gneissic complex (5 analyses, this study).

ND = Not determined

**Appendix 3b.** Mean bulk composition of metapelite and metawacke from the Wicklow area in comparison to similar clastic metasedimentary rocks selected from the literature.

Sample No.	A	B	C	D	E	F	G	H	I
<b>Major Oxides (wt %)</b>									
SiO <sub>2</sub>	58.1	66.73	66.75	64.43	63.66	58.9	57.42	53.26	62.6
Al <sub>2</sub> O <sub>3</sub>	17.0	15.53	13.45	15.48	14.85	16.8	19.88	20.64	15.6
FeO	5.27	3.83	3.54	ND	4.67	6.02	6.46	7.13	ND
Fe <sub>2</sub> O <sub>3</sub>	2.85	0.87	1.60	6.54	1.01	2.98	1.59	1.26	6.1
MgO	3.71	2.49	2.15	3.12	2.99	3.80	3.94	4.81	2.42
CaO	4.27	2.67	2.54	2.22	2.63	2.75	1.40	1.24	0.50
Na <sub>2</sub> O	3.25	3.35	2.93	3.74	3.14	1.62	1.96	2.20	1.4
K <sub>2</sub> O	2.54	1.94	1.99	2.44	2.30	2.56	3.57	3.53	4.65
TiO <sub>2</sub>	1.12	0.57	0.63	0.62	0.63	1.48	0.78	0.93	0.73
P <sub>2</sub> O <sub>5</sub>	0.13	0.12	0.16	ND	0.16	0.21	0.12	0.16	0.13
MnO	0.11	0.07	0.12	ND	0.12	0.08	0.09	0.09	0.06
CO <sub>2</sub>	0.21	0.12	1.24	ND	1.24	0.17	0.28	0.10	0.1
S	0.09	0.08	0.07	ND	ND	0.15	0.10	ND	0.63
H <sub>2</sub> O <sup>+</sup>	0.72	0.53	2.42	ND	2.17	0.68	1.38	4.62	3.6
H <sub>2</sub> O <sup>-</sup>	0.07	0.40	0.55	ND	ND	0.05	0.51	0.11	
Others									1.6
Total	99.44	99.83	100.23	98.59	99.99	98.25	99.48	99.98	100.12

- A. Average wacke metasediment from the Wicklow area (5 analyses, this study).  
 B. Average wacke metasediment from the Archean English River Subprovince (98 analyses, Breaks and Bond 1993).  
 C. Average of 61 greywackes of various ages (Pettijohn 1963, p.515).  
 D. Average of 25 Early Precambrian greywackes from Wyoming (Condie 1967, p.2139).  
 E. Average of 20 Archean greywackes from the Burwash Formation, Yellowknife Supergroup, Slave Province (Henderson 1972, p.890).  
 F. Average pelitic metasediment from the Wicklow area (6 analyses, this study).  
 G. Average pelitic metasediment from the Archean English River Subprovince (51 analyses, Breaks and Bond 1993).  
 H. Average mudstone from the Burwash Formation, Yellowknife Supergroup, Slave Province (3 analyses, Henderson 1972, p.890).  
 I. Average Aphebian shale from the Canadian Shield (82 analyses, Cameron and Garrels 1980, p.186-187).  
 ND = Not determined

**Appendix 3c.** Analyses of cordierite-anthophyllite rocks, selected from the literature, associated with volcanogenic massive sulphide ore deposits.

	A	B	C	D	E
<b>Major Oxides (wt %)</b>					
SiO <sub>2</sub>	30.0	53.1	44.24	48.0	67.52
Al <sub>2</sub> O <sub>3</sub>	21.41	14.9	7.46	18.62	11.45
FeO	21.22	15.48	ND	16.18	9.37
Fe <sub>2</sub> O <sub>3</sub>	7.06	3.4	27.94	1.07	1.72
MgO	11.54	7.3	9.30	11.85	7.96
CaO	–	0.35	1.10	0.64	0.19
Na <sub>2</sub> O	0.58	0.44	0.11	0.23	0.22
K <sub>2</sub> O	0.68	0.40	0.15	0.01	0.22
TiO <sub>2</sub>	0.42	0.31	ND	2.06	0.15
P <sub>2</sub> O <sub>5</sub>	0.15	0.06	ND	0.09	0.02
MnO	0.22	0.14	0.15	0.13	0.08
CO <sub>2</sub>	0.13	0.11	ND	ND	ND
S	0.56	ND	ND	ND	ND
H <sub>2</sub> O <sup>+</sup>	6.84	4.6	0.97	1.5	1.08
Total	100.81	100.59	91.37	100.38	99.98

A. "Dalmatianite" from Aulet Mine, Noranda (Wilson 1941, p.68).

B. Cordierite-anthophyllite rock from Coronation Mine, Saskatchewan (Whitmore 1969, p.42).

C. Cordierite-anthophyllite rock from Gullbridge copper deposit, Newfoundland (Upadhyay 1970).

D. Cordierite-anthophyllite rock from Traskbole, Orijarvi area, Finland (Eskola 1914).

E. Quartz-cordierite-anthophyllite rock from Falun Mine, Sweden (Larson 1932).

ND = Not determined

**Appendix 3d.** Analyses of cordierite-anthophyllite/gedrite rocks, selected from the literature, representing secondary bulk compositions, but unassociated with massive sulphide mineralization.

	A	B	C	D
<b>Major Oxides (wt %)</b>				
SiO <sub>2</sub>	59.71	61.28	60.1	48.87
Al <sub>2</sub> O <sub>3</sub>	14.28	12.11	12.6	16.71
FeO	12.14	10.78	10.5	12.85
Fe <sub>2</sub> O <sub>3</sub>	1.08	3.54	4.9	0.13
MgO	5.79	2.36	8.7	9.60
CaO	1.34	1.52	0.4	5.42
Na <sub>2</sub> O	0.97	4.22	0.9	1.61
K <sub>2</sub> O	0.19	0.12	0.3	0.27
TiO <sub>2</sub>	1.50	1.64	0.2	2.71
P <sub>2</sub> O <sub>5</sub>	0.64	0.41	ND	0.50
MnO	0.20	0.06	0.4	–
CO <sub>2</sub>	ND	–	ND	0.07
H <sub>2</sub> O <sup>+</sup>	2.03	1.74	0.9	0.99
H <sub>2</sub> O <sup>–</sup>	0.05	0.10	ND	0.07
Total	99.92	99.88	100.0	99.81

A. Cordierite-anthophyllite-quartz-almandine rock, east of Lake Katumajarvi, Aulanko area, Finland (Simonen 1948, p.24).

B. Quartz-cordierite-anthophyllite hornfels derived from amygdaloidal basalt, Yalwal, New South Wales, Australia (Vallance 1967, p.92).

C. Quartz-gedrite-cordierite-garnet-biotite gneiss, Fishtail Lake area, Ontario (Lal and Moorhouse 1969, p.157).

D. Cumingtonite-anthophyllite-cordierite-plagioclase-biotite-ilmenite greenstone hornfels, Kenidjack, Cornwall, England (Tilley 1935, p.182).

ND = Not determined

**Appendix 3e.** Analyses of cordierite-bearing restite clots from advanced stage metasedimentary migmatites (diatexites), English River Subprovince, northwestern Ontario (from Breaks and Bond 1993).

	1	2	3
<b>Major Oxides (wt %)</b>			
SiO <sub>2</sub>	69.6	72.5	74.0
Al <sub>2</sub> O <sub>3</sub>	17.2	16.4	15.6
FeO	3.46	3.49	3.66
Fe <sub>2</sub> O <sub>3</sub>	1.10	1.29	0.36
MgO	2.15	3.28	3.88
CaO	0.16	0.04	0.06
Na <sub>2</sub> O	0.00	0.25	0.19
K <sub>2</sub> O	1.11	0.94	0.25
TiO <sub>2</sub>	0.03	0.02	0.03
P <sub>2</sub> O <sub>5</sub>	0.00	0.02	0.00
MnO	0.11	0.04	0.06
CO <sub>2</sub>	1.26	0.13	0.12
S	0.02	<0.01	0.01
H <sub>2</sub> O <sup>+</sup>	2.17	1.34	0.81
H <sub>2</sub> O <sup>-</sup>	1.06	0.26	0.30
Total	99.40	100.0	99.30

**Appendix 3f.** Composition of cordierite-anthophyllite/gedrite and gedrite-bearing rocks, selected from the literature, interpreted to be unaltered, compared with selected average compositions of rocks from various metasedimentary groups.

	Cordierite-Anthophyllite/Gedrite and Gedrite-Bearing Rocks					Various Metasedimentary Groups				
	A	B	C	D	E	F	G	H	I	J
<b>Major Oxides (wt %)</b>										
SiO <sub>2</sub>	57.65	65.92	65.70	64.90	54.90	66.75	66.73	66.1	61.54	57.42
Al <sub>2</sub> O <sub>3</sub>	16.84	14.88	14.24	15.60	18.70	13.45	15.53	8.1	16.95	19.88
FeO	10.33	4.67	6.37	4.78	8.11	3.54	3.83	1.4	3.9	6.46
Fe <sub>2</sub> O <sub>3</sub>	0.85	1.68	1.51	1.64	1.11	1.60	0.87	3.8	2.56	1.59
MgO	5.30	3.52	4.89	3.18	4.50	2.15	2.49	2.4	2.52	3.94
CaO	1.28	3.22	2.39	1.85	1.75	2.54	2.67	6.2	1.76	1.40
Na <sub>2</sub> O	2.34	4.39	1.96	3.72	3.90	2.93	3.35	0.9	1.84	1.96
K <sub>2</sub> O	2.36	0.18	0.27	1.68	2.09	1.99	1.94	1.3	3.45	3.57
TiO <sub>2</sub>	1.60	0.43	0.94	0.59	0.69	0.63	0.57	0.3	0.82	0.78
P <sub>2</sub> O <sub>5</sub>	ND	0.11	0.17	ND	ND	0.16	0.12	0.1	ND	0.12
MnO	ND	0.17	0.09	0.13	0.18	0.12	0.07	0.01	ND	0.09
S	ND	ND	ND	ND	ND	0.07	0.08	ND	ND	0.10
CO <sub>2</sub>	ND	ND	ND	ND	ND	1.24	0.12	5.0	1.67	0.28
H <sub>2</sub> O <sup>+</sup>	1.08	0.69	1.60	2.10	2.46	2.42	0.53	3.6	3.47	1.38
H <sub>2</sub> O <sup>-</sup>	ND	0.09	0.13	0.10	0.12	0.55	0.40	0.7	ND	0.51
Others*		0.22	0.03							
Total	99.63	100.17	100.29	99.97	98.51	100.23	99.30	100.0	100.48	99.48

- A. Cordierite-anthophyllite gneiss, Tarklahti, Orijarvi area (Eskola 1914, p.198).
- B. Gedrite-plagioclase rock, Skato, Kragerø district, Norway (Brøgger 1934, p.218).
- C. Cordierite-anthophyllite-quartz-plagioclase-biotite rock, Trelease Mill, Lizard area, Cornwall, England (Tilley 1937, p.304).
- D. Cordierite-gedrite metagreywacke, Ross Lake area near Yellowknife, N.W.T. (Kamineni 1973, p.292).
- E. Cordierite-gedrite metagreywacke, Ross Lake area near Yellowknife, N.W.T. (Kamineni 1973, p.292).
- F. Average of 61 greywackes of various ages (Pettijohn 1963, p.515).
- G. Average of 98 wacke metasedimentary rocks from English River Subprovince (Breaks and Bond 1993).
- H. Average of 20 lithic arenites (subgreywacke) (Pettijohn 1963, p.57).
- I. Average of 155 metapelitic rocks (Shaw 1956, p.928).
- J. Average of 49 metapelitic rocks, from English River Subprovince (Breaks and Bond 1993).

ND = Not determined

\* Not identified in reference source

# References

- Adams, F.D. and Barlow, A.E. 1910. Geology of the Haliburton and Bancroft areas, Province of Ontario; Geological Survey of Canada, Memoir Number 6, 419p.
- 1913. Excursion A2—Haliburton–Bancroft area of central Ontario; *in* Excursions in the Eastern Townships of Quebec and the eastern part of Ontario, XII International Geological Congress; Geological Survey of Canada, Guidebook, no.2, p.5-98.
- Althaus, F., Nitsch, K.H., Karotke, E. and Winkler, H.G.F. 1970. An experimental re-examination of the upper stability limit of muscovite plus quartz; *Neues Jahrbuch für Mineralogie, Monatshefte*, no.7, p.325-336.
- Appleyard, E.C. 1974. Basement/cover relationships within the Grenville Province in eastern Ontario; *Canadian Journal of Earth Sciences*, v.11, p.369-379.
- Appleyard, E.C. and Stott, G.M. 1975. Grenville gneisses in the Madawaska Highlands, eastern Ontario; *in* Waterloo 1975 Field Excursions Guidebook; Geological Association of Canada–Mineralogical Association of Canada, p.26-61.
- Bailey, E.H. and Stevens, R.E. 1960. Selective staining of K-feldspar and plagioclase on rock slabs and thin sections; *American Mineralogist*, v.45, p.1020-1025.
- Barker, J.G. and Arth, F. 1976. Generation of trondhjemite-tonalite liquids and Archean bimodal trondhjemite-basalt suites; *Geology*, v.4, p.596-600.
- Barnett, P.J. and Leyland, J.G. 1981. Quaternary geology of the Bancroft area, southern Ontario; Ontario Geological Survey, Preliminary Map P.2376, scale 1:50 000.
- Barth, T.F.W. 1938. Progressive metamorphism of sparagmite rocks of southern Norway; *Norsk Geologisk Tidsskrift*, v.18, p.54-65.
- Bartlett, J.R., Brock, B.S., Moore, J.M., Jr. and Thivierge, R.H. 1984. Grenville Traverse A: cross-sections of parts of the Central Metasedimentary Belt; Geological Association of Canada–Mineralogical Association of Canada, Ottawa '86, Field Trip Guidebook 9A/10A, 63p.
- Bell, K. 1981. Will the real Grenville Orogeny please stand up; *Nature*, v.290, p.89-90.
- Bell, K. and Blenkinsop, J. 1980. Whole rock Rb-Sr studies in the Grenville Province of southeastern Ontario and western Quebec—a summary report; *in* Current Research, Part C, Geological Survey of Canada, Paper 80-1C, p.152-154.
- Best, M.G. 1966. Structural geology of Precambrian rocks south of Bancroft, Ontario; *Canadian Journal of Earth Sciences*, v.3, p.441-455.
- Binns, R.A. 1969. Hydrothermal investigations of the amphibolite-granulite facies boundary; Geological Society of Australia, Special Publication, v.2, p.341-344.
- Breaks, F.W. and Bond, W.D. 1993. The English River Subprovince—an Archean gneiss belt: geology, geochemistry, and associated mineralization; Ontario Geological Survey, Open File Report 5846, 884p.
- Breaks, F.W., Bond, W.D. and Stone, D. 1978. Preliminary geological synthesis of the English River Subprovince, northwestern Ontario and its bearing upon mineral exploration; Ontario Geological Survey, Miscellaneous Paper 72, 55p.
- Breaks, F.W. and Moore, J.M., Jr. 1992. The Ghost Lake batholith, Superior Province of northwestern Ontario: a fertile, S-type, peraluminous granite-rare element pegmatite system; *The Canadian Mineralogist*, v.30, p.835-875.
- Breaks, F.W. and Thivierge, R.H. 1983. Precambrian geology, Wicklow area, Hastings County; Ontario Geological Survey, Preliminary Map P.2614, scale 1:15 840.
- Bright, E.G. 1979. The Centre Lake area, Haliburton and Hastings counties; *in* Summary of Field Work 1979, Ontario Geological Survey, Miscellaneous Paper 90, p.86-88.
- 1980. Regional structure and stratigraphy of the Burleigh Falls area, Peterborough County; *in* Summary of Field Work 1980, Ontario Geological Survey, Miscellaneous Paper 96, p.67-69.
- Brock, B.S. 1982. Basement and Grenville Supergroup, Madawaska Highlands, Renfrew County, Ontario; abstract *in* 1982 Grenville Workshop, Ottawa–Carleton Centre for Geoscience Studies, Ottawa, Ontario, p.3.
- Brøgger, W.C. 1934. On several Archaean rocks from the south coast of Norway. I. Nodular granites from the environs of Kragerø; *Norske Videnskap-Akademi i Oslo, Skrifter I, Matematisk-Naturvidenskapelig Klasse 2, Bund 8*, 97p.
- 1935. On several Archaean rocks from the south coast of Norway. II. The south Norwegian hyperites and their metamorphism; *Norske Videnskap-Akademi i Oslo, Skrifter I, Matematisk-Naturvidenskapelig Klasse 1, Bund 1*, 421p.
- Buddington, A.F. 1939. Adirondack igneous rocks and their metamorphism; *Geological Society of America, Memoir 7*, 354p.
- Cameron, E.M. and Garrels, R.M. 1980. Geochemical composition of some Precambrian shales from the Canadian Shield; *Chemical Geology*, v.28, p.181-197.
- Carr, S.D., Easton, R.M., Jamieson, R.A. and Culshaw, N.G. 2000. Geologic transect across the Grenville Orogen of Ontario and New York; *Canadian Journal of Earth Sciences*, v.37, p.193-216.
- Carr, S.D. and McMullen, S. 2000. Geologic transect through parts of the Central Gneiss Belt (Muskoka domain), the Central Metasedimentary Belt boundary thrust zone and the Bancroft shear zone in the Barry's Bay–Bark Lake–Papineau Lake–Maynooth–Gooderham region of the Ontario Grenville; *Friends of the Grenville, Field Trip Guidebook*, Carleton University, Ottawa, Ontario, 47p.
- Carter, T.R., Colvine, A.C. and Meyn, H.D. 1980. Geology of base metal, precious metal, iron, and molybdenum deposits of the Pembroke–Renfrew area, Ontario; Ontario Geological Survey, Mineral Deposits Circular 20, 186p.
- Černý, P. 1982. Petrogenesis of granitic pegmatites; *in* Granitic pegmatites in science and industry, Mineralogical Association of Canada, Short Course Handbook, v.8, p.405-450.
- Chayes, F. 1952. The fine-grained calc-alkaline granites of New England; *Journal of Geology*, v.60, p.207-254.

- Condie, K.C. 1967. Geochemistry of early Precambrian greywackes from Wyoming; *Geochimica et Cosmochimica Acta*, v.31, p.2135-2149.
- Culshaw, N.G. 1982. Grenville L-S tectonics, Bancroft, Ontario: petrofabrics and tectonics; abstract *in* Report on the Inaugural Meeting of the Canadian Tectonics Group, *Journal of Structural Geology*, v.4, p.231-232.
- Culshaw, N.G. and Fyson, W.K. 1981. Structures associated with ductile thrusting in Grenville gneiss, Bancroft, Ontario; abstract *in* Program with Abstracts, Geological Association of Canada—Mineralogical Association of Canada, Annual Meeting 1981, v.6, p.A12.
- 1982. The SE-plunging Grenville LS tectonite, does it record NW-directed ductile thrusting? An approach using quartz microfabrics, near Bancroft, Ontario; abstract *in* 1982 Grenville Workshop, Ottawa—Carleton Centre for Geoscience Studies, Ottawa, Ontario, p.3.
- Davidson, A., Britton, J.M., Bell, K. and Blenkinsop, J. 1979. Regional synthesis of the Grenville Province of Ontario and western Quebec; *in* Current Research, Part B, Geological Survey of Canada, Paper 79-1B, p.153-172.
- Davidson, A., Culshaw, N.G. and Nadeau, L. 1982. A tectonometamorphic framework for part of the Grenville Province, Parry Sound region, Ontario; *in* Current Research, Part A, Geological Survey of Canada, Paper 82-1A, p.175-190.
- Davidson, A. and Morgan, W.C. 1980. Preliminary notes on the geology east of Georgian Bay, Grenville structural province, Ontario; *in* Current Research, Part A, Geological Survey of Canada, Paper 81-1A, p.291-298.
- de Rosen-Spence, A. 1969. Genèse des roches à cordierite-anthophyllite des gisements cupro-zincifères de la région de Rouyn—Noranda, Québec, Canada; *Canadian Journal of Earth Sciences*, v.6, p.1339-1345.
- de Waard, D. 1965. The occurrence of garnet in the granulite facies terrane of the Adirondack highlands; *Journal of Petrology*, v.6, p.165-191.
- Divi, R.R. 1972. Structural analysis of Grenville rocks near Bancroft, Ontario, Canada; unpublished PhD thesis, University of Ottawa, Ottawa, Ontario, 178p.
- Divi, R.R. and Fyson, W.K. 1973. Folds and strain in Grenville metamorphic rocks, Bancroft, Ontario, Canada; *Geological Society of America Bulletin*, v.84, p.1607-1618.
- Easton, R.M. 1992. The Grenville Province and the Proterozoic history of central and southern Ontario; *in* *Geology of Ontario*, Ontario Geological Survey, Special Volume 4, Part 2, p.715-904.
- Easton, R.M. and Davidson, A. 1994. Terrane boundaries and lithotectonic assemblages within the Grenville Province, Eastern Ontario; *Geological Association of Canada—Mineralogical Association of Canada, Waterloo '94, Guidebook A1*, 89p.
- Eskola, P.E. 1914. On the petrology of the Orijarvi region in southwestern Finland; *Bulletin de la Commission géologique de Finlande*, no.40, p.1-277.
- 1933. On the differential anatexis of rocks; *Bulletin de la Commission géologique de Finlande*, no.103, p.12-25.
- Fischer, K. and Puchelt, H. 1972. Barium; section 56 *in* *Handbook of Geochemistry*, v.II-4, Springer-Verlag, Berlin, p.56A-1 to 56O-2.
- Francoeur, D. 1975. Petrographic and structural evolution of granites and gneisses of the Grenville Province, Glamorgan and Monmouth townships, Ontario; unpublished MSc thesis, University of Ottawa, Ottawa, Ontario, 141p.
- Fraser, J.A., Heywood, W.W. and Mazurski, M.A. 1978. Metamorphic map of the Canadian Shield; Geological Survey of Canada, Map 1475A, scale 1:3 500 000.
- Froese, E. 1963. A chemical study of garnets from Stony Rapids area, Saskatchewan; *The Canadian Mineralogist*, v.7, p.698-712.
- 1969. Metamorphic rocks from the Coronation Mine and surrounding area; *in* *Symposium on Geology of the Coronation Mine, Saskatchewan*; Geological Survey of Canada, Paper 68-5, p.55-77.
- 1972. The representation of mineral assemblages coexisting with biotite on the biotite composition surface; abstract *in* *The Canadian Mineralogist*, v.11, p.573.
- 1978. The graphical representation of mineral assemblages in biotite-bearing granulites; *in* *Current Research, Part A*; Geological Survey of Canada, Paper 78-1A, p.323-325.
- Grant, J.A. 1968. Partial melting of common rocks as a possible source of cordierite-anthophyllite bearing assemblages; *American Journal of Science*, v.266, p.908-931.
- Green, D.H. and Ringwood, A.E. 1967. An experimental investigation of the gabbro-eclogite transformation and its petrological applications; *Geochimica et Cosmochimica Acta*, v.31, p.767-834.
- Greenwood, H.J. 1963. The synthesis and stability of anthophyllite; *Journal of Petrology*, v.4, p.317-351.
- Heier, K.S. 1964. Geochemistry of the nepheline syenite on Stjernoy, north Norway; *Norsk Geologisk Tidsskrift*, v.44, pt.2, p.205-215.
- 1965. A geochemical comparison of the Blue Mountain (Ontario, Canada) and Stjernoy (Finnmark, north Norway) nepheline syenites; *Norsk Geologisk Tidsskrift*, v.45, pt.1, p.41-52.
- Heitanen, A. 1959. Kyanite-garnet fedritite near Orofino, Idaho; *American Mineralogist*, v.44, p.539-564.
- Henderson, D. 1984. General geochemical properties and abundances of the rare earth elements; *in* *Rare Earth Element Geochemistry*, Elsevier, Amsterdam, p.1-32.
- Henderson, J.B. 1972. Sedimentology of Archean turbidites at Yellowknife, Northwest Territories; *Canadian Journal of Earth Sciences*, v.9, p.882-902.
- Hewitt, D.F. 1954. Geology of the Brudenell—Raglan area; Ontario Department of Mines, Annual Report for 1953, v.62, pt.5, 123p.
- 1955. Geology of Monteagle and Carlow townships; Ontario Department of Mines, Annual Report for 1954, v.63, pt.6, 78p.
- 1956. The Grenville region of Ontario; *in* *The Grenville Problem*, Royal Society of Canada, Special Publication 1, p.22-41.
- 1962. Some tectonic features of the Grenville Province of Ontario, *in* *The tectonics of the Canadian Shield*, Royal Society of Canada, Special Publication 4, p.102-117.
- Higgins, M.W. 1971. Cataclastic rocks; United States Geological Survey, Professional Paper 678, 97p.
- Hirschberg, A. and Winkler, H.G.F. 1968. Stabilitätsbeziehungen zwischen Chlorit, Cordierit und Almandin bei der Metamorphose; *Contributions to Mineralogy and Petrology*, v.18, p.17-42. [in German]

- Hobbs, B.E., Means, W.D. and Williams, P.F. 1976. An outline of structural geology; John Wiley and Sons, Inc., New York, 571p.
- Holdaway, M.J. 1971. Stability of andalusite and the aluminum silicate phase diagram; *American Journal of Science*, v.271, p.97-131.
- Irvine, T.N. and Baragar, W.R.A. 1971. A guide to the chemical classification of the common volcanic rocks; *Canadian Journal of Earth Sciences*, v.8, p.523-548.
- James, R.S., Grieve, R.A.F. and Pauk, L. 1978. The petrology of cordierite-anthophyllite gneisses and associated mafic and pelitic gneisses at Manitouwadge, Ontario; *American Journal of Science*, v.278, p.41-63.
- Jennings, D.S. 1969. Origin and metamorphism of part of the Hermon Group, near Bancroft, Ontario; unpublished PhD thesis, McMaster University, Hamilton, Ontario, 225p.
- Kamineni, D.C. 1973. Petrology and geochemistry of some Archean metamorphic rocks near Yellowknife, District of MacKenzie; unpublished PhD thesis, University of Ottawa, Ottawa, Ontario, 228p.
- Kerrick, D.M. 1972. Experimental determination of muscovite + quartz stability with  $PH_2O_{total}$ ; *American Journal of Science*, v.272, p.946-958.
- Krynine, P.D. 1950. Petrology, stratigraphy and origin of the Triassic sedimentary rocks of Connecticut; *State Geological and Natural History Survey of Connecticut, Bulletin*, v.73, 247p.
- Lal, R.K. and Moorhouse, W.W. 1969. Cordierite-gedrite rocks and associated gneisses of Fishtail Lake, Harcourt Township, Ontario; *Canadian Journal of Earth Sciences*, v.6, p.145-165.
- Larson, W. 1932. Chemical analyses of Swedish rocks; *Bulletin of the Geological Institutions of the University of Uppsala*, v.24, 47p.
- Lumbers, S.B. 1978. Southern Renfrew County; *in Summary of Field Work 1978*, Ontario Geological Survey, Miscellaneous Paper 82, p.125-127.
- 1980. Geology of Renfrew County, southern Ontario; Ontario Geological Survey, Open File Report 5282, 118p.
- 1982. Summary of metallogeny, Renfrew County area; Ontario Geological Survey, Report 212, 58p.
- Lumbers, S.B. and Vertolli, V.M. 1980. Renfrew area, western part, southern Ontario; Ontario Geological Survey, Preliminary Map P.2357, scale 1:63 360.
- Luth, W.C., Jahns, R.H. and Tuttle, O.F. 1964. The granite system at pressures of 4 to 10 kilobars; *Journal of Geophysical Research*, v.69, p.759-773.
- Masson, S.L. and Gordon, J.B. 1981. Radioactive mineral deposits of the Pembroke–Renfrew area; Ontario Geological Survey, Mineral Deposits Circular 23, 155p.
- McEachern, S.J. and van Breemen, O. 1993. Age of deformation within the Central Metasedimentary Belt boundary thrust zone, southwest Grenville Orogen: constraints on the collision of the mid–Proterozoic Elzevir terrane; *Canadian Journal of Earth Sciences*, v.30, p.1155-1165.
- McMullen, S.M. 1999. Tectonic evolution of the Bark Lake area, eastern Central Gneiss Belt, Ontario Grenville: constraints from geology, geochemistry and U–Pb geochronology; unpublished M.Sc. thesis, Carleton University, Ottawa, Ontario, 171p.
- Mehnert, K.R. 1971. Migmatites and the origin of granitic rocks; Elsevier Publishing Company, Amsterdam, 405p.
- Merrill, R.B., Robertson, J.K. and Wyllie, P.J. 1970. Melting relations in the system  $NaAlSi_3O_8$ – $KAlSi_3O_8$ – $SiO_2$ – $H_2O$  to 20 kilobars compared to results for other feldspar-quartz– $H_2O$  and rock– $H_2O$  systems; *Journal of Geology*, v.78, p.558-569.
- Miller, R.R. and Gittins, J. 1982. Geochronology and petrology of the Grenville nepheline-bearing suite: a metamorphosed rift environment; abstract *in* 1982 Grenville Workshop, Ottawa–Carleton Centre for Geoscience Studies, Ottawa, Ontario, p.7.
- Miller, W.D. 1983. Metamorphic petrography of cordierite-gedrite-orthopyroxene rocks and their associated gneisses of the Papineau Lake region, Bangor Township, Ontario; unpublished BSc thesis, Queen's University, Kingston, Ontario, 83p.
- Miyashiro, A. 1974. Volcanic rock series in island arcs and active continental margins; *American Journal of Science*, v.274, p.321-355.
- Moore, J.M., Jr. 1982. Stratigraphy and tectonics of the Grenville Orogeny in eastern Ontario; abstract *in* Grenville Workshop, Friends of the Grenville, Ottawa, Ontario, p.7.
- Moore, J.M., Jr. and Thompson, P.H. 1980. The Flinton Group: a late Precambrian metasedimentary succession in the Grenville Province of eastern Ontario; *Canadian Journal of Earth Sciences*, v.17, p.1685-1707.
- Newton, R.C., Charlu, T.V. and Kleppa, O.J. 1974. A calorimetric investigation of the stability of anhydrous magnesium cordierite with application to granulite facies metamorphism; *Contributions to Mineralogy and Petrology*, v.44, p.295-311.
- Nockolds, S.R. 1954. Average chemical composition of some igneous rocks; *Geological Society of America Bulletin*, v.65, p.1007-1032.
- Nockolds, S.R. and Allen, R. 1953. The geochemistry of some igneous rock series; *Geochimica et Cosmochimica Acta*, v.4, p.105-142.
- Palache, C., Berman, H. and Frondel, C. 1944. The system of mineralogy of J.W. Dana and E.S. Dana, v. I (Elements, sulfides, sulfosalts, oxides), 7th ed.; John Wiley and Sons, New York, 834p.
- Park, R.G. 1969. Foundations of structural geology; Blackie, Glasgow, 135p.
- Paulter, J.M. 1980. Alteration and mineralization of a pegmatite dyke in the Pembroke–Renfrew area; unpublished BSc thesis, Laurentian University, Sudbury, Ontario, 41p.
- Peck, W.H. and Valley, J. 2000. Genesis of cordierite–gedrite gneisses, Central Metasedimentary Belt boundary thrust zone, Grenville Province, Ontario, Canada; *The Canadian Mineralogist*, v.38, p.511-524.
- Pettijohn, F.J. 1957. Sedimentary rocks, 2nd ed.; Harper, New York, 718p.
- 1963. Chemical composition of sandstones—excluding carbonate and volcanic sands; *in* Data of Geochemistry, 6th ed., United States Geological Survey, Professional Paper 440-5, p.S1-S21.
- Pettijohn F.J., Potter, P.E. and Siever, R. 1972. Sand and sandstone; Springer-Verlag, New York, 618p.
- Rheinhardt, E.W. 1968. Phase relations in cordierite-bearing gneisses from the Gananogue area, Ontario; *Canadian Journal of Earth Sciences*, v.5, p.455-482.

- Rheinhardt, E.W. and Skippen, G.B. 1970. Petrochemical study of Grenville granulites; *in* Report of Activities, Part B, Geological Survey of Canada, Paper 70-1B, p.48-54.
- Robinson, P. and Jaffe, H.W. 1969. Aluminous enclaves in gedrite-cordierite gneiss from southwestern New Hampshire; *American Journal of Science*, v.267, p.389-421.
- Schreyer, W. and Yoder, H.S. 1964. The system Mg-cordierite-H<sub>2</sub>O and related rocks; *Neues Jahrbuch für Mineralogie, Abhandlungen*, v.101, p.271-342.
- Schwerdtner, W.M. and Mawer, C.K. 1982. Geology of the Gravenhurst region, Grenville structural province, Ontario; *in* Current Research, Part B, Geological Survey of Canada, Paper 82-1B, p.195-207.
- Shaw, D.M. 1956. Geochemistry of pelitic rocks. Part III: major elements and general geochemistry; *Geological Society of America Bulletin*, v.67, p.919-934.
- Silver, L.T. and Lumbers, S.B. 1966. Geochronological studies in the Bancroft-Madoc area of the Grenville Province, Ontario, Canada; abstract *in* Geological Society of America, Special Publication 87, p.156.
- Simonen, A. 1948. On the petrology of the Aulanko area in southwestern Finland; *Bulletin de la Commission géologique de Finlande*, v.143, 66p.
- Simonen, A. and Kuovo, O. 1951. Archean varved schists north of Tampere in Finland; *Société géologique de Finlande, Compte Rendus*, v.24, p.93-117.
- Spry, A. 1969. *Metamorphic textures*; Pergamon Press, Oxford, 350p.
- Storey, C.C. and Vos, M.A. 1981. Industrial minerals of the Renfrew-Pembroke area, part 2; *Ontario Geological Survey, Mineral Deposits Circular* 22, 214p.
- Storre, B. and Karotke, E. 1971. An experimental determination of the upper stability limit of muscovite + quartz in the range 7-20 kbar water pressure; *Neues Jahrbuch für Mineralogie, Monatshefte*, v.49, p.56-58.
- Streckeisen, A. 1976. To each plutonic rock its proper name; *Earth Science Reviews*, v.12, p.1-33.
- Taylor, S.R. 1965. The application of trace-element data to problems in petrology; *Physics and Chemistry of the Earth*, v.6, no.2, p.133-214.
- Thivierge, R.H. 1982. Structural relationships of Grenville gneisses in Bangor Township, southeastern Ontario—a preliminary evaluation; abstract *in* 1982 Grenville Workshop, Ottawa-Carleton Centre for Geoscience Studies, Ottawa, Ontario, p.9.
- Thompson, J.B., Jr. 1957. The graphical analysis of mineral assemblages in pelitic schists; *American Mineralogist*, v.42, p.842-859.
- Tilley, C.E. 1935. Metasomatism associated with greenstone-hornfels of Kenidjack and Botallack; *Mineralogical Magazine*, v.24, p.181-202.
- 1937. Anthophyllite-cordierite granulites of the Lizard; *Geological Magazine*, v.74, p.300-309.
- Trueman, D.L. and Černý, P. 1982. Exploration for rare-element granitic pegmatites; *in* Granitic pegmatites in science and industry, Mineralogical Association of Canada, Short Course Handbook, v.8, p.463-493.
- Turekian, K.K. and Kulp, J.L. 1956. The geochemistry of strontium; *Geochimica et Cosmochimica Acta*, v.10, p.245-296.
- Turekian, K.K. and Wedepohl, K.H. 1961. Distribution of the elements in some major units of the Earth's crust; *Geological Society of America Bulletin*, v.72, p.175-192.
- Tuttle, O.F. and Bowen, N.F. 1958. Origin of granite in the light of experimental studies in the system NaAlSi<sub>3</sub>O<sub>8</sub>-KAlSi<sub>3</sub>O<sub>8</sub>-SiO<sub>2</sub>-H<sub>2</sub>O; *Geological Society of America, Memoir* 74, 153p.
- Upadhyay, H.D. 1970. Geology of the Gullbridge copper deposit, central Newfoundland; unpublished MSc thesis, Memorial University of Newfoundland, St. John's, Newfoundland, 134p.
- Upadhyay, H.D. and Smitheringale, W.G. 1972. Geology of the Gullbridge copper deposit, Newfoundland: volcanogenic sulfides in cordierite-anthophyllite rocks; *Canadian Journal of Earth Sciences*, v.9, p.1061-1073.
- Vallance, T.G. 1967. Mafic rock alteration and isochemical development of some cordierite-anthophyllite rocks; *Journal of Petrology*, v.8, no.1, p.84-96.
- van de Kamp, P.C. 1968. Geochemistry and origin of metasediments in the Haliburton-Madoc area, southeastern Ontario; *Canadian Journal of Earth Sciences*, v.5, p.1337-1372.
- van de Kamp, P.C., Leake, B.E. and Senior, A. 1976. The petrography and geochemistry of some Californian arkoses with application to identifying gneisses of metasedimentary origin; *Journal of Geology*, v.84, p.195-212.
- Vernon, R.H. 1972. Reactions involving hydration of cordierite and hypersthene; *Contributions to Mineralogy and Petrology*, v.35, p.125-137.
- Wakita, H., Rey, P. and Schmitt, R.A. 1971. Abundances of the 14 rare-earth elements and 12 other trace elements in Apollo 12 samples: five igneous and one breccia rocks and four soils; *Proceedings of the Second Lunar Science Conference*, p.1319-1329.
- White, D., Forsyth, D.A., Asudeh, I., Carr, S.D., Wu, H., Easton, R.M. and Mereu, R.F. 2000. A seismic-based cross-section of the Grenville Orogen in Ontario and western Quebec; *Canadian Journal of Earth Sciences*, v.37, p.183-192.
- Whitmore, D.R.E. 1969. Geology of the Coronation copper deposit; *in* Symposium on the Geology of the Coronation Mine, Saskatchewan, Geological Survey of Canada, Paper 68-5, p.37-53.
- Wilson, M.E. 1941. *Noranda District, Quebec*; Canada Department of Mines and Resources, Geological Survey, Memoir 229, 162p.
- Winkler, H.G.F. 1979. *Petrogenesis of metamorphic rocks*, 5th ed.; Springer-Verlag, New York, 348p.
- Wolff, J.M. 1982. Geology of the Kaladar area, Lennox, Addington and Frontenac counties; *Ontario Geological Survey, Geological Report* 215, 94p.
- Wynne-Edwards, H.R. 1972. The Grenville Province; *in* Variations in tectonic styles in Canada, Geological Association of Canada, Special Paper 11, p.263-334.

# Metric Conversion Table

Conversion from SI to Imperial			Conversion from Imperial to SI		
SI Unit	Multiplied by	Gives	Imperial Unit	Multiplied by	Gives
LENGTH					
1 mm	0.039 37	inches	1 inch	<b>25.4</b>	mm
1 cm	0.393 70	inches	1 inch	<b>2.54</b>	cm
1 m	3.280 84	feet	1 foot	<b>0.304 8</b>	m
1 m	0.049 709	chains	1 chain	20.116 8	m
1 km	0.621 371	miles (statute)	1 mile (statute)	<b>1.609 344</b>	km
AREA					
1 cm <sup>2</sup>	0.155 0	square inches	1 square inch	<b>6.451 6</b>	cm <sup>2</sup>
1 m <sup>2</sup>	10.763 9	square feet	1 square foot	<b>0.092 903 04</b>	m <sup>2</sup>
1 km <sup>2</sup>	0.386 10	square miles	1 square mile	2.589 988	km <sup>2</sup>
1 ha	2.471 054	acres	1 acre	0.404 685 6	ha
VOLUME					
1 cm <sup>3</sup>	0.061 023	cubic inches	1 cubic inch	<b>16.387 064</b>	cm <sup>3</sup>
1 m <sup>3</sup>	35.314 7	cubic feet	1 cubic foot	0.028 316 85	m <sup>3</sup>
1 m <sup>3</sup>	1.307 951	cubic yards	1 cubic yard	0.764 554 86	m <sup>3</sup>
CAPACITY					
1 L	1.759 755	pints	1 pint	0.568 261	L
1 L	0.879 877	quarts	1 quart	1.136 522	L
1 L	0.219 969	gallons	1 gallon	<b>4.546 090</b>	L
MASS					
1 g	0.035 273 962	ounces (avdp)	1 ounce (avdp)	28.349 523	g
1 g	0.032 150 747	ounces (troy)	1 ounce (troy)	<b>31.103 476 8</b>	g
1 kg	2.204 622 6	pounds (avdp)	1 pound (avdp)	<b>0.453 592 37</b>	kg
1 kg	0.001 102 3	tons (short)	1 ton (short)	<b>907.184 74</b>	kg
1 t	1.102 311 3	tons (short)	1 ton (short)	<b>0.907 184 74</b>	t
1 kg	0.000 984 21	tons (long)	1 ton (long)	<b>1016.046 908 8</b>	kg
1 t	0.984 206 5	tons (long)	1 ton (long)	<b>1.016 046 90</b>	t
CONCENTRATION					
1 g/t	0.029 166 6	ounce (troy)/ ton (short)	1 ounce (troy)/ ton (short)	34.285 714 2	g/t
1 g/t	0.583 333 33	pennyweights/ ton (short)	1 pennyweight/ ton (short)	1.714 285 7	g/t

## OTHER USEFUL CONVERSION FACTORS

	Multiplied by	
1 ounce (troy) per ton (short)	31.103 477	grams per ton (short)
1 gram per ton (short)	0.032 151	ounces (troy) per ton (short)
1 ounce (troy) per ton (short)	20.0	pennyweights per ton (short)
1 pennyweight per ton (short)	0.05	ounces (troy) per ton (short)

*Note: Conversion factors which are in bold type are exact. The conversion factors have been taken from or have been derived from factors given in the Metric Practice Guide for the Canadian Mining and Metallurgical Industries, published by the Mining Association of Canada in co-operation with the Coal Association of Canada.*





**ISSN 0704-2582**  
**ISBN 0-7729-9514-1**

# Chart A

Figure 34. Map of structural trend surfaces in the Wicklow and adjacent areas. The area delineated by the inset box represents the area of the Wicklow map (Map 2550).

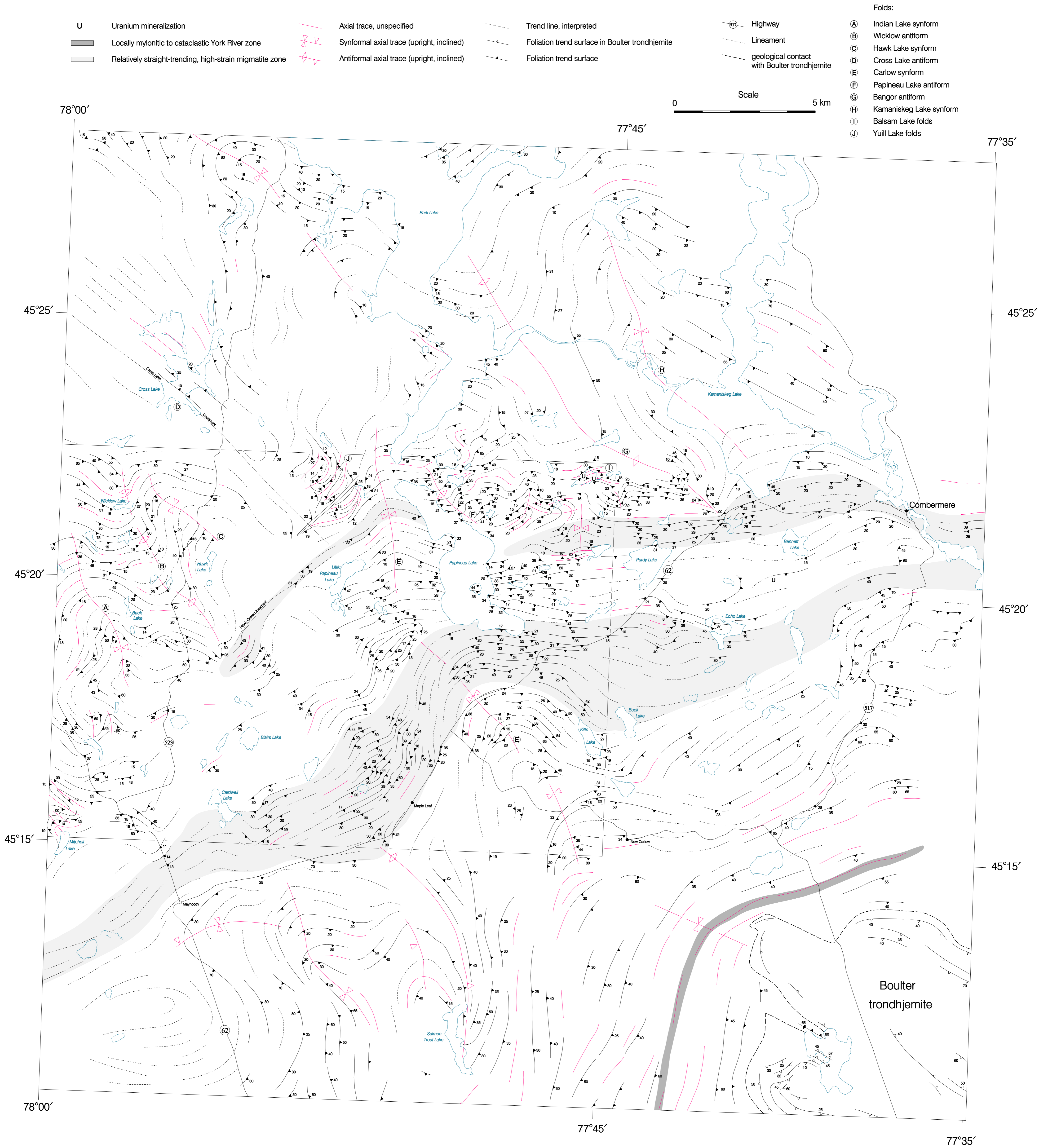
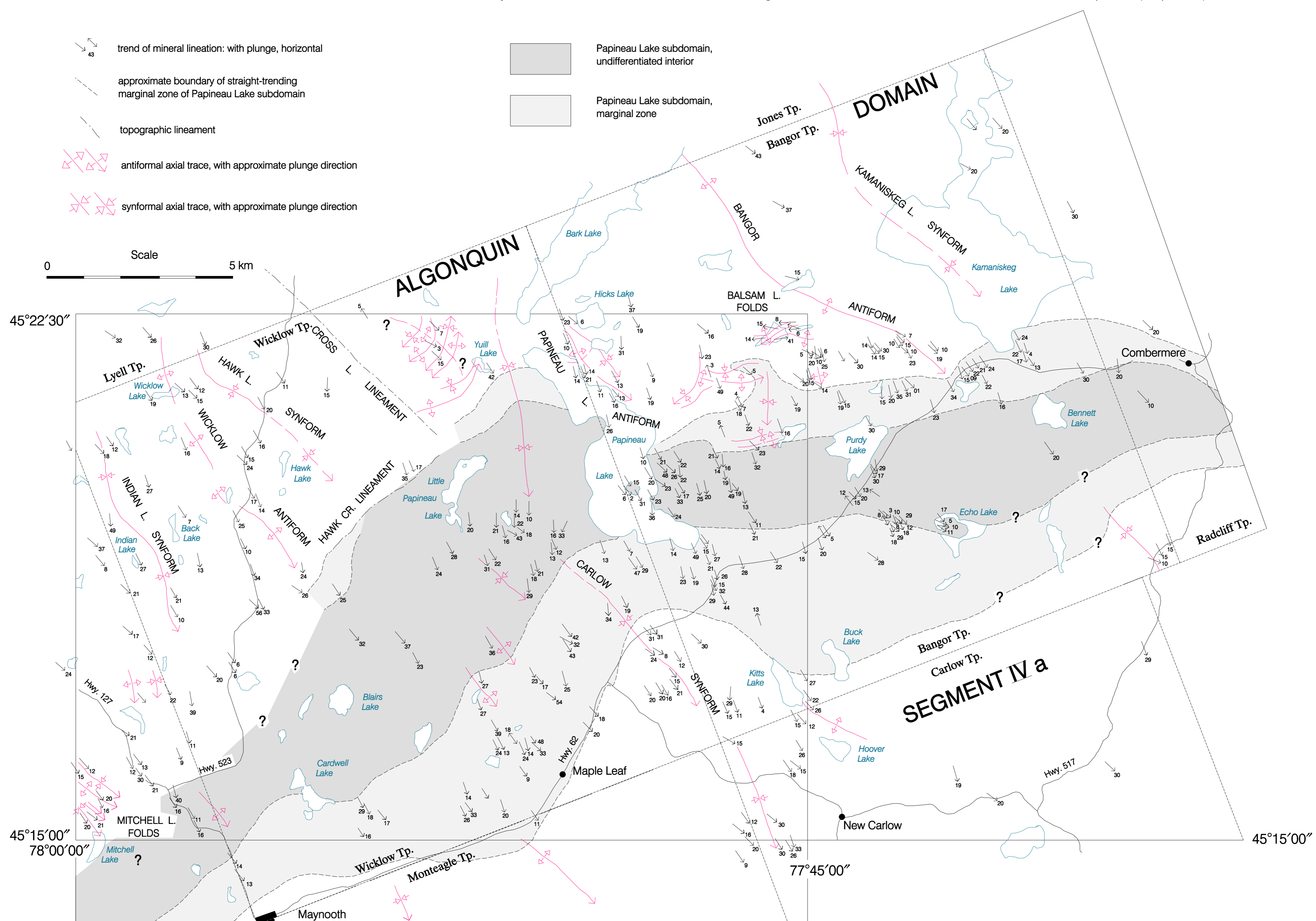







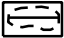
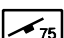
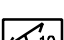
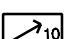


Figure 35. Mineral lineation patterns in the Wicklow area, in relation to structural domains, and  $F_3$  and later folds. The Papineau Lake subdomain is stippled; the marginal zones are distinguished from undifferentiated rocks of the interior of the subdomain. The area bounded by latitudes 45°15'N and 45°22'30"N and longitudes 77°45'W and 78°00'W outlines the Wicklow map area (Map 2550).



# LEGEND

-  Magnetite amphibole biotite syenite, equigranular, foliated
-  Actinolite-diopside syenite, coarse grained, massive; associated scapolite-sphene-actinolite-diopside skarn
-  Muscovite-magnetite-biotite-corundum syenite, coarse grained, massive
-  Muscovite-corundum-biotite syenite, medium to coarse grained, massive
-  ±Muscovite ± corundum - biotite syenite, medium grained, massive to foliated
-  Pit outline
-  Outcrop
-  Geological contact (observed)
-  Joint, with dip
-  Foliation, with dip
-  Lineation, with plunge

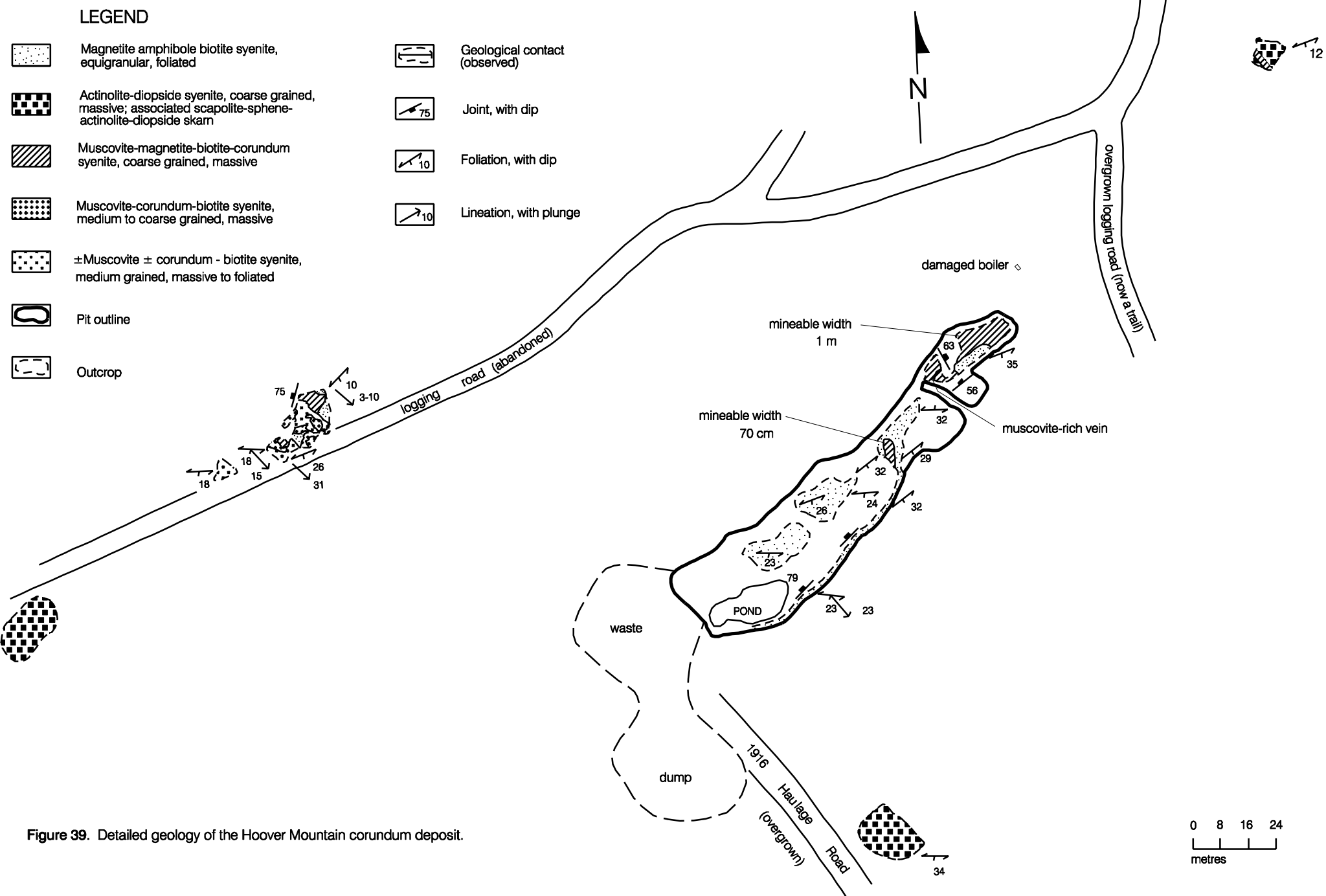


Figure 39. Detailed geology of the Hoover Mountain corundum deposit.

